Plant cell walls as barriers to lipid bioaccesibility in model lipid-rich plant food (almond)

Grundy, Myriam Marie-Louise

Awarding institution:
King's College London

Plant cell walls as barriers to lipid bioaccessibility in model lipid-rich plant food (almond)

Myriam Marie-Louise Grundy B.Sc. (Hons), M.Sc.

A thesis submitted to King's College London for the degree of Doctor of Philosophy in Nutritional Science and Biochemistry

Division of Diabetes and Nutritional Sciences

School of Medicine

King's College London

September 2014

In loving memory of my dad

PREFACE

This thesis was submitted to King's College London for the degree of Doctor of Philosophy. The work presented herein was undertaken in the Division of Diabetes and Nutritional Sciences (previously the Nutritional Sciences Research Division), King's College London, from October 2010 to September 2014.

ABSTRACT

It is generally assumed that most of the nutrients contained in a food are released (bioaccessible) during digestion and potentially available for absorption. However, the structure of plant food such as almonds, in particular the cell walls ('dietary fibre'), may encapsulate intracellular nutrients, thereby limiting their bioaccessibility. The main aim of the studies described in this thesis was to investigate the role played by almond cell walls in the regulation of lipid bioaccessibility and digestion kinetics using a combination of *in vivo*, *in vitro* and *in silico* methods.

The particle size distributions of masticated whole raw and roasted almonds collected from 15 volunteers were used to predict lipid bioaccessibility from a mathematical model. Predicted values were compared with experimental measurements of lipid release in the same almond samples. Samples of masticated almonds were then loaded into a dynamic gastric model followed by a static duodenal model to determine lipid loss in these compartments. The rate and extent of lipolysis were measured by pH-stat titration and gas liquid chromatography of released fatty acids on almond materials with different degrees of bioaccessibility under simulated duodenal digestion conditions. The effect of processing on lipid losses and almond microstructure was also determined in ileostomy subjects who consumed two almond meals varying in lipid bioaccessibility. Finally, the potential penetration of lipase(s) through the cell wall matrix was investigated using notably confocal microscopy.

The findings of this project indicated that following mastication and gastrointestinal digestion of whole almonds, only a small proportion of lipid was released from ruptured cells. Depending on the almond structure and degree of processing, the amount of lipid released from the food matrix and fatty acids produced from lipolysis varied substantially. This work has provided further evidence that cell walls act as a physical barrier that limits nutrient digestion.

ACKNOWLEDGEMENTS

I would firstly like to thank my supervisors, Prof Peter Ellis, Dr Peter Butterworth and Dr Sarah Berry, as well as Dr Jeremy Sanderson for their invaluable guidance and support throughout my PhD. Secondly the Diet and Health Research Industry Club (DRINC) of the Biotechnology and Biological Sciences Research Council (BBSRC), who financed my PhD (BBSRC studentship award no. BB/H531994/1), and Karen Lapsley from the Almond Board of California for providing the almonds.

I would like to thank all the members of the Biopolymers group, past and present: Dr Frederic Warren for his support during the early stages of my project, Hamung Patel, Daphne Vasilopoulou and Dr Terri Grassby; also all the undergraduate project students we have had in the lab, in particular Bérengère Bayart for her contribution on the lipase and cell wall permeability work. Special thanks go to Cathrina Edwards who assisted me in many ways throughout those 4 years.

Some of the work reported in this thesis was undertaken in collaboration with different institutes and universities, in particular the Institute of Food Research (IFR) in Norwich. My special thanks go to Dr Giusy Mandalari, Prof Keith Waldron and Richard Faulk for their assistance on the design and running of the DGM/SDM work, and Dr Mary Parker who provided advice on microscopy techniques. I am also deeply grateful to Prof Peter Wilde and Dr Alan Mackie for sharing with me their knowledge on interface, emulsion and lipid digestion, and coping with my endless questions.

I would also like to thank Prof Frédéric Carrière for giving me the opportunity of visiting, in two occasions, the Laboratory of Enzymology at Interfaces and Physiology of Lipolysis (EIPL) in the Centre National de la Recherche Scientifique (CNRS) in Marseille. I am highly grateful for his advice and supervision on the enzymology of lipolysis and lipases aspects of my work, and for the excellent discussions and ideas for this part of the project. Many thanks to Dr Sawsan Amara, Dr Hélène Gaussier and Eduardo Mateos for helping me with the lipase experiments. Thanks also to the EIPL team for making me feel so welcome in their lab.

Many thanks to Dr David Gray and his team at the University of Nottingham who contributed to the work presented in this thesis and kindly offered their expertise on oil bodies.

Thank you to the dedicated staff at the Clinical Research Facility at St Thomas' Hospital especially Dana Navaie. Many thanks to Dr Shuvra Ray, Paula Darroch and the volunteers for their enthusiastic contribution and effort in the Biogut study, Dr Tracy Nelson and GSTS pathology for blood analyses.

I am very grateful to the technical team at King's College London, David Lincoln, Anne-Catherine Perz, Mary-Jo Searle, Robert Gray, Rosie Calokatsia and David Gondi for their fantastic work at sorting out all the details that were essential for the smooth progression of my PhD.

There are many others notably Prof Willats and his group from the University of Copenhagen who very kindly did the analysis of the almond cell wall using antibodies; Dr Trevor Blackall for letting me use the Malvern Mastersizer 2000® at the Geology department at King's College London; Dr Gema Vizcay-Barrena and Leanne Glover from the Centre for Ultrastructural Imaging as well as Dr Jan Soetaert from the Nikon Imaging Centre at King's College London for their help with some of the microscopy; and Dr Peter Milligan for his aid with statistical analysis.

Finally, I would like to thank my mum, David, Caroline and the Grundies/Cotons, who supported me from day one and developed a surprising interest in almonds despite not always understanding what I was doing with them.

MEETINGS ATTENDED, PRESENTATIONS AND AWARDS

Oral presentations

(i) 21st and 22nd of June 2012, Science and Technology of Food Emulsions, London, UK. "Role of cell walls during *in vitro* duodenal digestion of almond lipids"

(ii) 1st to 5th of July 2012, Food Oral Processing, Beaune, France. "The role of mastication in determining macronutrient bioaccessibility using almonds as a model food". Obtained a Conference Fund Grant from King's College London Graduate School (£300).

(iii) 10th and 11th of September 2012, Nutrition Society Postgraduate Conference, Newcastle, UK. "Role of cell walls during *in vitro* duodenal digestion of almond lipids"

(iv) 8th of May 2013, Biosciences KTN Early Careers Researchers Event, London, UK. "Role of cell walls during *in vitro* duodenal digestion of almond lipids"

(v) 24th to 26th of June 2013, Dream conference - From Model Foods to Food Models, Nantes, France. "Plant cell walls as barriers to lipid bioaccessibility in a model lipid-rich plant food". Selected among the 25 best PhD student papers and awarded with free participation at the conference and reimbursement of travel cost.

(vi) 15th to 18th of July 2013, Nutrition Society Conference within the BBSRC (DRINC) satellite session, Newcastle, UK. "The role of plant cell walls in regulating lipid bioaccessibility"

(vii) 11th to 14th of March 2014, 3rd International Conference on Food Digestion, Wageningen, the Netherland. "Investigating the permeability of almond cell walls to digestive enzymes". Obtained a Travel Grant from the Nutrition Society (£350).

Poster presentations

(i) 11th of March 2011, Kings College London Diabetes and Nutritional Sciences Research Division annual symposium. "The role of plant cell walls in regulating lipid bioaccessibility"

(ii) 13th and 14th of April 2011, 6th DRINC Dissemination Event, Bristol, UK. "The role of plant cell walls in regulating lipid bioaccessibility"

(iii) 17th of June 2011, Kings College London Medicine School Showcase. "The role of plant cell walls in regulating lipid bioaccessibility"

(iv) 12th and 13th of October 2011, 7th DRINC Dissemination Event, Manchester, UK. "Lipid bioaccessibility of almonds: the influence of mastication and simulated digestion"

(v) 15th and 16th of May 2012, 8th DRINC Dissemination Event, Leeds, UK. "Role of cell walls during *in vitro* duodenal digestion of almond lipids"

(vi) 5th and 6th of February 2013, 9th DRINC Dissemination Event, Bristol, UK. "*In vitro* duodenal digestion of raw and roasted almond lipids". **Winner of first prize for PhD poster presentations**.

(vii) 5th to 8th of March 2013, 2nd International Conference on Food Digestion, Madrid, Spain. Poster and 4 minutes presentation (PhD contest) "Role of food structure during *in vitro* duodenal digestion of raw and roasted almond lipids". Obtained a General Travel Grant from the Biochemical Society (£348).

Other awards

(i) 22nd to 26th of April 2013, Selected to attend the **PhD Training School on "Food Digestion and Human Health"** in Gdansk, Poland organised by InfoGest COST Action.

(ii) October 2013, One month **Short-Term Scientific Mission** (STSM) awarded by InfoGest COST Action (2500 Euros). Worked with Prof Frédéric Carrière for a month in the Laboratory of Enzymology at Interfaces and Physiology of Lipolysis (EIPL) in the Centre National de la Recherche Scientifique (CNRS) in Marseille.

(iii) 6th of June 2014, Shortlisted for the **Young Lipid Scientist Award** organised by the lipid group AGM of the Society of Chemical Industry (SCI) at the University of Reading. I gave a 15 min presentation summarising the work performed during my PhD: "Plant cell walls as barriers to lipid bioaccessibility in a model lipid-rich plant food".

PUBLICATIONS

(i) Grassby, T., Edwards, C., **Grundy, M.** and Ellis, P.R. (2012) Functional components and mechanisms of action of 'dietary fibre' in the upper gastrointestinal tract: implications for health, Chapter 4 in *Stability of Complex Carbohydrate Structures: Biofuels, Foods, Vaccines and Shipwrecks*, Cambridge: Royal Society of Chemistry.

(ii) Mandalari, G., **Grundy, M.M.-L.**, Grassby, T., Parker, M. L., Cross, K.L., Chessa, S., Bisignano, C., Barreca, D., Bellocco, E., Lagana, G., Butterworth, P. J., Faulks, R.M., Wilde, P.J., Ellis, P.R. and Waldron, K. W. (2014) The effects of processing and mastication on almond lipid bioaccessibility using novel methods of *in vitro* digestion modelling and micro-structural analysis, *British Journal of Nutrition*, 112: 1521-1529.

(iii) Makkhunab, S., Khoslab, A., Foster, T., McClements, D.J., **Grundy, M.M.-L.** and Gray, D.A. (2014) Impact of extraneous proteins on the gastrointestinal fate of sunflower seed (Helianthus annuus) oil bodies: A simulated gastrointestinal tract study, *Food & Function*, 6: 124-33.

(iv) **Grundy, M.M.-L.**, Grassby, T., Mandalari, G., Parker, M.L., Waldron, K.W., Butterworth, P.J., Berry, S.E.E. and Ellis, P.R. (2015) Effect of mastication on lipid bioaccessibility of almonds in human subjects and its implications for digestion kinetics, metabolizable energy and postprandial lipemia, *American Journal of Clinical Nutrition*, 101: 25-33.

(v) **Grundy, M.M.-L.**, Wilde, P.J., Butterworth, P.J., Gray, R. and Ellis, P.R. (2015) Impact of almond structure in lipid bioaccessibility and lipolysis during *in vitro* duodenal digestion, *Food Chemistry* (Submitted for publication)

(vi) Edwards, C.H., **Grundy, M.M.-L.**, Grassby, T., Vasilopoulou, D., Frost, G.S., Butterworth, P.J., Berry, S.E.E., Sanderson, J. and Ellis, P.R. (2015) Manipulation of starch bioaccessibility in wheat endosperm to regulate starch digestion, postprandial glycemia, insulinemia and gut hormone responses: A randomized controlled trial in healthy ileostomy participants, *American Journal of Clinical Nutrition* (Submitted for publication)

TABLE OF CONTENTS

LIST OF FIGURES

LIST OF TABLES

LIST OF EQUATIONS

LIST OF ABBREVIATIONS

AA	Arachidonic acid
ACW	Antrum contraction waves
AF	Muffin containing almond flour
AGP	Arabinogalactan protein
ALA	α-linolenic acid
AP	Muffin containing almond macroparticles
APS	Ammonium persulphate
BBSRC	Biotechnology and Biological Sciences Research Council
BCA	Bicinchoninic acid
BMI	Body mass index
BS	Bile salts
BSA	Bovine serum albumin
CCK	Cholecystokinin
CDTA	Cyclohexanediamine tetraacetic acid
CEH	Carboxyl ester hydrolase
CLSM	Confocal laser scanning microscopy
CMC	Critical micelle concentration
CNRS	Centre National de la Recherche Scientifique
CRF	Clinical Research Facility
CS	Combined samples
CUI	Centre for Ultrastructural Imaging
CVD	Cardiovascular disease
CW	Cell wall
$d_{3,2}$	Surface-weighted average diameter
$d_{4,3}$	Volume average diameter
DA	Degree of acetylation
DAG	Diacylglycerol
DE	Degree of methyl-esterification
DGM	Dynamic gastric model
DHA	Docosahexaenoic acid
DF	Dietary fibre
DRINC	Diet and Health Research Industry Club

EFA	Essential fatty acids
EPA	Eicosapentaenoic acid
EIPL	Laboratory of Enzymology at Interfaces and Physiology of Lipolysis
FAME	Fatty acid methyl esters
FFA	Free fatty acid
FID	Flame ionization detector
FTIC	Fluorescein isothiocyanate
FSA	Food Standards Agency
GIT	Gastrointestinal tract
GIP	Glucose dependent insulinotropic peptide
GLC	Gas liquid chromatography
GLP-1	Glucagon-like peptide 1
GPLRP2	Guinea pig pancreatic lipase-related protein 2
HG	Homogalacturonan
HGL	Human gastric lipase
HPL	Human pancreatic lipase
HPLRP	Human pancreatic lipase related-protein
iAUC	Incremental area under the curve
IFR	Institute of Food Research
IS	Internal standard
LA	Linoleic acid
LDL	Low-density lipoprotein
LM	Light microscopy
MAG	Monoacylglycerol
MTT	Mean transit time
MUFA	Monounsaturated fatty acids
MW	Molecular weight
N	Number of chews
NA	Raw almond
NaTC	Sodium taurocholate
NaTDC	Sodium taurodeoxycholate
NaGDC	Sodium glycodeoxycholate
NDNS	National Diet and Nutrition Survey
NEFA	Non-esterified fatty acids

OB	Oil body
PA	Phosphatidic acid
PC	Phosphatidylcholine
PE	Phosphatidylethanolamine
PI	Phosphatidylinositol
PL	Pancreatic lipase
PLRP2	Pancreatic lipase-related protein 2
PPL	Porcine pancreatic lipase
PPE	Porcine pancreatic extract
PS	Portion (28 g) samples
PSD	Particle size distribution
PUFA	Polyunsaturated fatty acids
PYY	Peptide YY
RA	Roasted almond
R_g	Radius of gyration
RGE	Rabbit gastric extract
RS	Resistant Starch
SA	Specific activity
SCFA	Short chain fatty acids
SDM	Static duodenal model
SDS	Sodium dodecyl sulphate
SEM	Scanning electron microscopy
SFA	Saturated fatty acids
sPLA2	Pancreatic phospholipase A2
T	Duration of mastication sequence
TAG	Triacylglycerol
TEM	Transmission electron microscopy
TLC	Thin layer chromatography
Tris	Tris(hydroxymethyl)aminomethane
VLDL	Very-low-density lipoprotein
β-Lg	Beta-lactoglobulin

CHAPTER 1

INTRODUCTION AND LITERATURE REVIEW

1.1 Background and project overview

Diets containing foods high in fat are considered to have detrimental health effects, but studies have shown that the consumption of almond seeds, a lipid-rich food (Yada *et al.*, 2011), is associated with a beneficial effect on postprandial glycaemia, oxidative damage and risk factors for cardiovascular disease (CVD), particularly in individuals with type 2 diabetes mellitus (Cohen and Johnston, 2011; Jenkins *et al.*, 2002a; Li *et al.*, 2011a; Spiller *et al.*, 2003). One possible explanation for this paradox is the limited bioaccessibility (release) and rate and extent of digestion almond lipids.

The effect of dietary fibre (DF) on postprandial nutrient and hormone responses have been studied previously, but none of these investigations have explored the mechanisms by which DF affects postprandial metabolism, especially in relation to postprandial lipaemia (Cara *et al.*, 1992; Gemen *et al.*, 2011; Redard *et al.*, 1990). The major sources of DF are plant cell walls (CWs). The role of the CW matrix, more specifically its composition and structure, on nutrient release has rarely been studied (Ellis *et al.*, 2004; Mandalari *et al.*, 2008a).

The overall objective of the current project were to (a) determine the extent to which lipids contained in almond seeds are released (bioaccessible) during mastication and on the subsequent stages of the digestion process and (b) understand the role played by CW in influencing the bioaccessibility and digestion of almond lipid. To address this question, a multidisciplinary approach was used, involving a novel combination of *in vivo*, *in vitro* and *in silico* methods to study lipid bioaccessibility and digestion kinetics in almond seeds. This project was part of a larger programme of research, funded by the BBSRC (BB/H004866/1) to investigate the role of plant CWs in regulating lipid, but also starch bioaccessibility from plant foods.

1.2 Lipids and health

1.2.1 Classification and general structures of dietary lipids

Lipids are a large and heterogeneous group of compounds that includes notably triacylglycerols (TAGs), phospholipids, steroids (i.e. cholesterol), waxes and fat soluble vitamins. A common property is their insolubility in water. The main dietary form of fatty acids (92-96%) are esters of a single glycerol and three fatty acids: TAG (Figure 1.1) (Carey and Hernell, 1992).

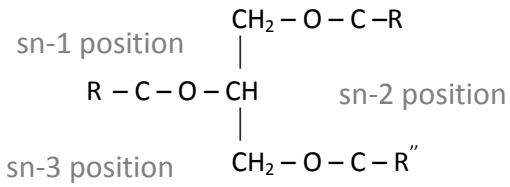

Figure 1.1 Stereochemical structure of triacylglycerol molecule (Carey and Hernell, 1992)

Fatty acids can be classified according to the number of double bonds they contain: saturated (none, SFA), monounsaturated (one, MUFA) or polyunsaturated (two or more, PUFA) fatty acids. Essential fatty acids (EFA) belong to the PUFA category; they are fatty acids that cannot be synthesised by the human body; EFA should therefore be provided from the diet. They include two families: the omega-3 such as α-linolenic acid (ALA) and its derivatives eicosapentaenoic acid (EPA) and docosahexaenoic acid (DHA), and the omega-6 such as linoleic acid (LA) a precursor of arachidonic acid (AA).

Dietary fats are obtained from both animal and plant sources. Animal fats are generally solid at room temperature and contain predominantly SFA and MUFA, i.e. meat, milk, dairy products, egg yolks and their derivatives; whereas fats in plants contain a wider variety of fatty acids and thus tend to be liquid at room temperature, i.e. oils from seeds, nuts and their oils. Exceptions to this generalisation are fish fats that are rich in PUFA especially oily fish such as salmon or fresh tuna, and coconut and palm oils that are high in saturated fats (Chow, 2000).

1.2.2 The physiological and clinical significance of lipids

According to the current recommendations from the UK Food Standards Agency (FSA), the dietary lipids should not exceed 35% of the total energy intake for total fat, of which approximately 11% from saturated fat, 13% from monounsaturated fat, 6.5% is from polyunsaturated fat and 2% is obtained from trans-fat (Food Standards Agency, 2013). The latest National Diet and Nutrition Survey (NDNS) report published in 2003 revealed that in British adults, aged 19 to 64, total fat intake accounts on average for 35.8 % of the total energy intake of men and 34.9% of women (Henderson *et al.*, 2003). Furthermore, in approximately 13.4% of men and 13.2% of women, the total energy intake is derived from saturated fat. Lipid intakes, especially saturated fats, are therefore above the UK dietary reference values. An overconsumption of fats can lead to hyperlipidaemia, elevated levels of lipids and cholesterol in the blood (Grundy and Denke, 1990), which is an important risk factor for atherosclerosis and therefore CVD (Kris-Etherton *et al.*, 1988; Stone, 1990; Temple, 1994). Elevated plasma fatty acids has also been associated with insulin resistance (Boden, 1997; Shulman, 2000) and obesity (Bray *et al.*, 2004).

Despite these adverse effects, lipids have incontestable nutritional values. Firstly, lipid stored in adipose tissue is a source of energy during times of food restriction. The yield from the complete oxidation of fatty acids is about 9 kcal/g (or 38 kJ/g) which is superior to proteins and carbohydrates, both with energy yields of approximately 4 kcal/g (17 kJ/g). Secondly, regular consumption of fish, seeds and nuts provides EFA. EPA, DHA and AA can thereby be directly supplied from those foods or synthesised from their precursors, ALA and LA. However, the fractional conversion of ALA to DHA and EPA are limited, in that they are approximately 4 to 9% and 0.3 to 21% respectively, depending on gender (Arterburn *et al.*, 2006; Burdge and Wootton, 2002; Harnack *et al.*, 2009). Thus, it is recommended that they are obtained from the diet in order to meet the body's requirements. The omega-3 fatty acids (i.e. EPA, DHA and ALA) are involved in the synthesis of eicosanoids that are important metabolites in inflammatory processes (Calder, 2010; Simopoulos, 2002) and neuronal functions (Bourre, 2006; Lavialle and Laye, 2010; Wainwright, 2002).

Furthermore, fatty acids are structural components of cell membranes and subcellular organelles, mainly as phospholipids arranged into a bilayer. The nervous system, including the brain, has the largest membrane surface areas compared with other organs; 40 to 60 percent of the brain's dry weight consists of lipids, 35% of which are PUFA (Lauritzen *et al.*, 2001; Yehuda *et al.*, 1999). The quality of fatty acids consumed, in particular the degree of unsaturation (i.e. PUFA), has therefore an impact on brain structure and function (Haag, 2003). PUFA are able to modulate the 3-dimensional structure of membranes and thereby their fluidity. Indeed, unsaturated fatty acids provide more flexibility to the membrane than saturated ones do, due to bends in the fatty acid chain created by the double bonds. Optimal fluidity is essential to permit neurotransmitters to bind to membrane receptors and the propagation of the electrical information within the cell. Dietary lipids are also required for the transport and absorption of fat soluble vitamins (A, D, E and K) and they are the precursors of steroid hormones (oestrogens, testosterone, adrenal hormones) (Gurr *et al.*, 2002). Finally, from an organoleptic point of view, lipids provide palatability to the food by contributing to its texture (mouthfeel) and also have the capacity to carry aromatic compounds (Lucca and Tepper, 1994).

1.3 Lipid digestion

The lipids present in plant foods are found mainly as TAGs enclosed in oil bodies (OBs), but they are also constitutive components of cell membranes, i.e. phospholipids in plasma, vacuole, mitochondria and plastid membranes (Buchanan *et al.*, 2002). Lipid digestion is a complex process which leads to the release of TAGs from the food matrix and their transformation into smaller absorbable lipids (Figure 1.2). Unlike cholesterol, TAG cannot be directly absorbed by the enterocytes and must first be hydrolysed. The four main steps of that process are: 1) lipid release from the food matrix and its dispersion into emulsion droplets; 2) enzymic hydrolysis of TAGs in the stomach and small intestine;

3) Removal of lipolytic products from the interface and formation of micelles; and 4) absorption of the hydrolysed products at the enterocytes brush-border.

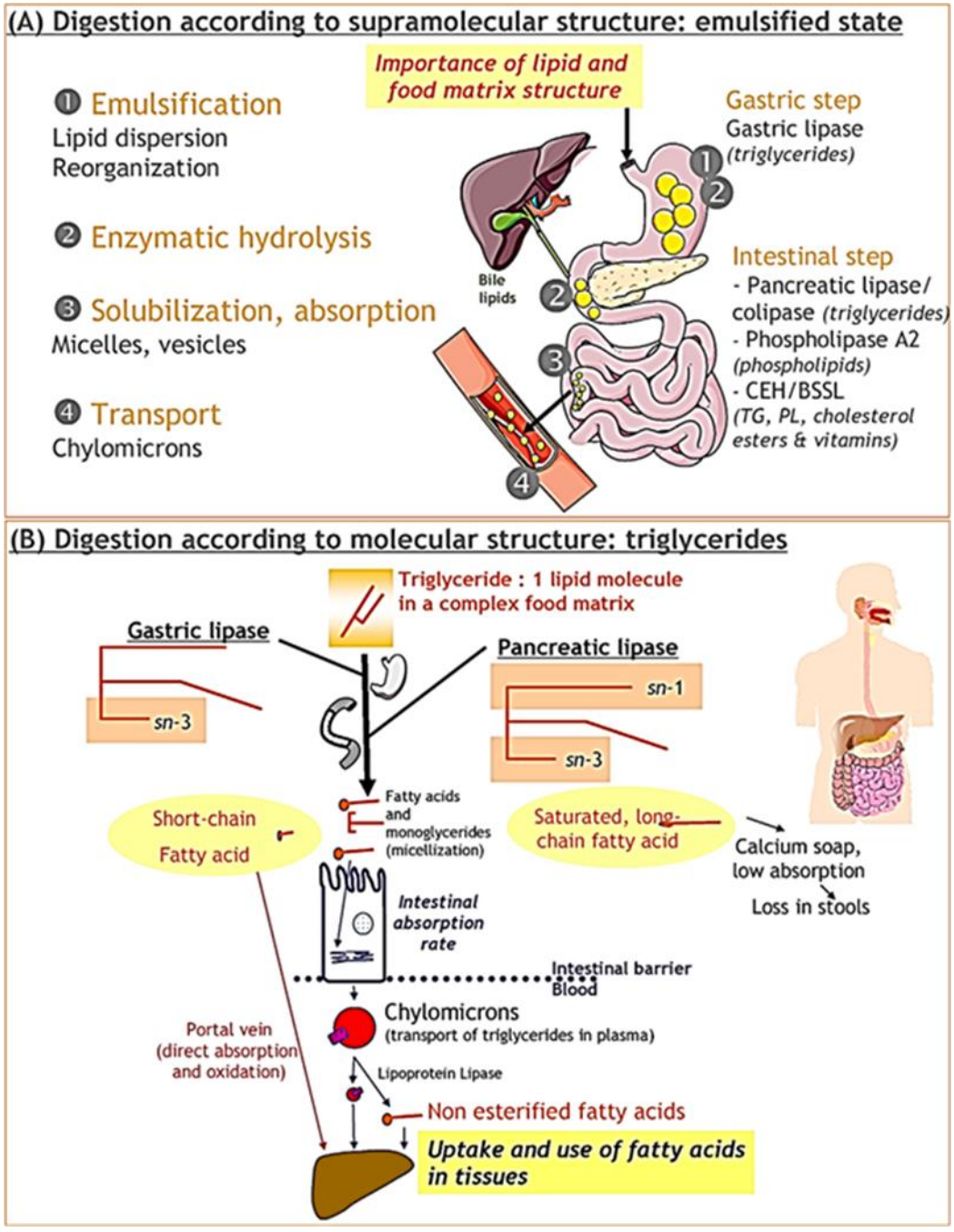

Figure 1.2 Principal events occurring during lipid digestion and absorption on supramolecular (A) and molecular (B) scales (Michalski et al., 2013).

Abbreviations: BSSL, bile-salt stimulated lipase; CEH, cholesterol ester hydrolase; PL, phospholipids; TG, triglycerides.

1.3.1 The mouth

Mastication is the first stage of the digestion process and consists of breaking down the food ingested into smaller particles as well as lubricating it with saliva in order to facilitate its progression through the oesophagus. However, this process is not as simple as it may first appear as demonstrated by the Hiiemae model (Hiiemae, 2004). Indeed, the mastication process consists of crushing, partitioning, lubrication including moisture uptake by the food, lingual transport of the food to different teeth, formation of a bolus and finally swallowing (Heath, 2002). A complex sensory feedback mechanism occurs during mastication to continuously adapt the jaw movements and saliva secretion together with the bolus properties (Woda *et al.*, 2006a).

During mastication, the food matrix is greatly transformed where its surface area is increased and a bolus formed. Various amounts of nutrients are released from the food according to its physico-chemical properties. The mixing of saliva with food containing lipids has an effect on the structure and properties of the food and individual nutrients including lipid. Saliva is a biological fluid made up of water; mucins, proteins, such as amylase, lysozyme, and peroxidase; it also contains electrolytes, including Ca^{2+}, Na^{+}, K^{+} and Mg^{2+}, and urea (Humphrey and Williamson, 2001; Levine, 1993). These molecules fulfil different functional roles which include control of pH, cleaning action, mineralization regulation of tooth enamel and antibacterial activity. Emulsions presents in the oral cavity can flocculate, coalesce and undergo phase inversion (e.g. oil in water emulsion becomes a water in oil emulsion) due to saliva, mixing forces produced by mastication and mouth temperature (Malone *et al.*, 2003; Vingerhoeds *et al.*, 2005). Indeed, saliva, and the mucins it contains, can induce flocculation of the oil droplets due to a depletion or bridging mechanism, which in turn has an effect on their subsequent digestibility in the digestive tract (McClements *et al.*, 2009; Silletti *et al.*, 2007).

Lingual lipase probably initiates the lipid digestion in human infants and rodents; however its role, and even its actual presence, is less clear for human adults (Bernback *et al.*, 1990; DeNigris *et al.*, 1988; Hamosh and Scow, 1973; Hamosh, 1984; Kulkarni and Mattes, 2014; Stewart *et al.*, 2010).

The journey of the food in the mouth finishes with the deglutition and its descent into the oesophagus.

1.3.2 The stomach

Once swallowed, the bolus rapidly passes down the oesophagus and enters into the stomach where it is submitted to mechanical and biochemical digestion by mixing with digestive juices. The gastric juice contains various substances and enzymes, especially gastric acid, pepsin, mucus (containing the glycoproteins mucins) and water. HCl, the main gastric acid, contributes to the digestion of protein notably by activating pepsin. The gastric pH varies between 1 and 3 during a fasting state and between 5.5 and 7 after food ingestion, although those values greatly fluctuate between individuals and depend on the food eaten in terms of quantity and type (Kong and Singh, 2008; N'Goma *et al.*, 2012). The lining of the stomach is covered with columnar epithelial cells tightly joined together as well as mucus that protects the mucosa from acid secretion and pepsin digestion (Smith and Morton, 2001).

At this stage the lipids released from the food are integrated into large droplets (a mixture of TAG, phospholipids, cholesterol, free fatty acids and surface proteins). Armand and colleagues showed that only a small proportion of the lipids present in the stomach are not emulsified (Armand *et al.*, 1994). The size of the lipid droplets (70 to 100 µm diameter) were reduced to generate fine droplets (1 to 10 µm diameter) thus increasing the total surface area. Therefore, lipid droplets that had a size larger than 10 to 20 µm were broken down whereas when their size was smaller, they tended to coalesce. However, protein-coated droplets remained small as the proteins protect them from coalescence. Lipolysis, occurring during the first hour of digestion, is initiated by gastric lipase and results in the partial hydrolysis of TAG into diacylglycerol (DAG) and free fatty acids (FFAs). The

lipolytic products are then integrated into the droplets, which, at the end of the gastric digestion have a median diameter of about 20 to 40 µm (Armand *et al.*, 1994).

Human gastric lipase (HGL) is synthesised in the fundic gastric mucosae, and secreted from the chief cells located in the gastric glands (Moreau *et al.*, 1989). Cholinergic mechanisms have been shown to increase HGL output however neither cholecystokinin (CCK) or secretin has an impact on its secretion (Borovicka *et al.*, 1997). Measuring HGL output accurately, however, has been reported to be challenging because of the great fluctuations observed, because HGL stability tends to decrease with pH levels below 1.5 (Lengsfeld *et al.*, 2004). HGL accounts for 5 to 40% of the lipid hydrolysis in the stomach to which is added 7.5% occurring in the duodenum (Armand, 2007).

1.3.3 The small intestine

Emulsified lipids are subsequently released into the duodenum where pancreatic juices and bile are secreted, the principal digestive agents being bile salts (BS, an emulsifier), pancreatic lipase (enzyme) and colipase (overcomes the inhibitory effect of BS on the activity of pancreatic lipase) (Carey and Hernell, 1992). Most of the TAG hydrolysis is considered to occur at this stage leading to the formation of DAG, monoacylglycerol (MAG), and FFAs. During optimal hydrolysis, TAG is transformed into one MAG molecule and two FFAs. It was revealed that following the ingestion of coarsely emulsified test meals, the greatest fraction of lipids (> 90%) in the duodenum was present as emulsified droplets of 1 to 100 µm (Armand *et al.*, 1996). After 1 h digestion, the median oil droplet diameter dropped from about 55 to 20 µm; the large droplets having disappeared and the small droplets having a diameter of 1 to 50 µm.

The hydrolysis provides a continuous source of digested lipids for absorption at the brush-border membrane of the enterocytes by either simple passive diffusion or active transport (Carey and Hernell, 1992). Short- and medium chain fatty acids (chain length < 12 carbon atoms) are fairly

soluble in water and pass into the enterocytes by passive diffusion. Long chain fatty acids (> 12 carbon atoms), in particular those that are partially ionized, are required to be solubilised by BS and transported as mixed micelles (Hernell *et al.*, 1990). The mixed micelles can then be absorbed through the intestinal microvilli into the mucosal enterocytes. Once inside the cells, the digested products are re-esterified in the endoplasmic reticulum to form TAG. The newly synthesised TAG as well as the digested cholesterol and phospholipids molecules are then coated with proteins to form chylomicrons in order to enter the lymphatic vessels (Carey *et al.*, 1983; Iqbal and Hussain, 2009). However, FFAs can be transported either via the portal vein or the lymphatic vessel depending on their chain-length and degree of unsaturation (Mu and Hoy, 2004). Thus, short and medium chain FFAs, which are more water-soluble than the long chain FFAs, are absorbed directly into the portal blood.

Pancreatic enzymes, including human pancreatic lipase (HPL), are synthesised and secreted by the acinar cells. These enzymes are stored in zymogen granules within the apical pole of the acinar cells. The secretion of the digestive enzymes from the zymogen granules is stimulated by a wide range of secretagogues in particular CCK (Borovicka *et al.*, 1997; Lengsfeld *et al.*, 2004), which is released by the duodenal and jejunal I cells in response to the presence of lipids in the duodenum (Wu *et al.*, 2013). The hormone stimulates gall bladder contractions and thereby causes the release of BS via the common bile duct into the duodenum. It is also responsible for the stimulation of pancreatic juice secretion. A complex feedback mechanism takes place where on the one hand CCK modulates the secretion of the lipases and on the other hand lipolytic products stimulate the secretion of CCK (Hildebrand *et al.*, 1998). Furthermore, CCK has been shown to be more strongly stimulated by unsaturated fatty acids, as found in almonds, than by saturated fatty acids (Beardshall *et al.*, 1989). Adrenaline and secretin work in synergy with CCK in the regulation of pancreatic enzyme secretion from acinar cells.

Pancreatic lipase outputs vary depending on the feeding state: between 100 to 400 U/mL during fasting and 500 to 1500 U/mL postprandially (Keller and Layer, 2005). These values can also fluctuate depending on the lipid content of the ingested meal. The presence of other lipases has also been detected in the duodenum: pancreatic lipase related-protein 1 and 2 (HPLRP1 and HPLRP2) (Giller *et al.*, 1992), cholesterol ester lipase, and bile-salt dependent lipase (Armand, 2007) (for more details see *Chapter 7*).

1.3.4 The colon

The material that is not absorbed within the small intestine reaches the colon, the main site of water and electrolytes uptake. Short chain fatty acids (SCFA; acetic, propionic and butyric acids) are produced in the colon from the fermentation by bacteria of dietary carbohydrates that have escaped the digestion and absorption in the upper gastrointestinal tract (GIT) (Cummings, 1981). Most of these SCFA get reabsorbed. On the other hand, ingested SCFA are released from TAG and absorbed by passive diffusion in the upper GIT, then transported in the portal vein to the liver (Carey *et al.*, 1983). BS and cholesterol that enter the colon can either be reabsorbed at this site or degraded and excreted in faeces (Owen, 1986; Thompson, 1986).

Since the digestion of lipids is a highly efficient process, it is assumed that the majority of dietary lipids are hydrolysed and absorbed within the small intestine (Carey *et al.*, 1983). The presence of excess, undigested lipid in faeces, steatorrhea, is generally observed in individuals suffering from pancreatic or gastrointestinal diseases (i.e. bile acids insufficiency) (Davenport, 1982), or in patients who has been administrated lipase inhibitors such as the ones prescribed for weight management (i.e. tetrahydrolipstatin, generic drug name orlistat) (Hvizdos and Markham, 1999). However, depending on the structure of the ingested plant foods (i.e. encapsulated by DF as intact CWs or surrounded by an indigestible coating) a significant proportion of lipids, and lipophilic nutrients such

as carotenoid, may pass from the ileum to the colon in healthy subjects (Ellis *et al.*, 2004; Hoad *et al.*, 2011; Mandalari *et al.*, 2008a; Mandalari *et al.*, 2013; Tydeman *et al.*, 2010). Thus, when lipid-containing foods that are incompletely digested are consumed it is important to also consider the processes occurring in the colon (i.e. fermentation and nutrient degradation by colonic bacteria).

1.3.5 Physiological response to fat consumption

The dietary components of a food and the sensory cues resulting from its ingestion influence the individual feeding behaviour in particular in the short term (French, 1999). Evidence has demonstrated that humans are able to detect the presence of fat in the mouth not only due to the food texture or viscosity but also as a result of olfactory and taste mechanisms possibly via taste bud cells (CD36) (Degrace-Passilly and Besnard, 2012; Mattes, 2005). This oral detection of lipids leads to the release of stored TAG from the adipose tissue thus increasing blood lipid concentration as well as promoting their absorption (Mattes, 2002). The amount of nutrient released at that stage has an impact on the digestion as a whole: gut signalling, mechanical processes and absorption (Frecka *et al.*, 2008). Mastication stimulates cephalic phase responses and may promote the release of numerous gut hormones, notably ghrelin, glucagon-like peptide 1 (GLP-1) and CCK which subsequently has an effect on energy intake.

The motility of the GIT is controlled by a complex feedback system involving neural networks as well as gut peptides released from the enteroendocrine cells (K and I cells located in the upper small intestine, L cells in the ileum and the colon) (Wu *et al.*, 2013). The entry of TAG in the small intestine stimulates the release of CCK and other gastrointestinal peptides such as peptide YY (PYY) and GLP-1. These hormones induce slowing down of gastric emptying and gastrointestinal mobility as well as pancreatic and biliary secretions, which inhibits hunger and thereby food ingestion (Chaudhri *et al.*, 2006). The generated satiety signals rely on the physicochemical properties of lipids, especially chain

length and degree of unsaturation (Feltrin *et al.*, 2004; Samra, 2010). In the ileum, the presence of lipid activates the ileal brake, a series of negative feedback mechanisms that aim to reduce food intake by inhibiting gastric emptying and intestinal motility (Maljaars *et al.*, 2008; Van Citters and Lin, 1999; Van Citters and Lin, 2006). Glucose dependent insulinotropic peptide (GIP), similarly to CCK, is secreted from K cells in response to duodenal distension. Its main action is to increase insulin secretion but it also stimulates lipoprotein lipase activity (McIntosh *et al.*, 2009). Moreover, a high fat diet has an effect on the microbial flora of the large bowel, with notable increases in the *Bacteroides* species (Borriello, 1986).

The rate and extent of starch digestion (amylolysis) is an important determinant of the glycaemic response, and a number of *in vitro* systems (e.g. the hydrolysis index, Englyst system, and, more recently LOS analysis) have been used to predict glycaemia without necessity for always performing human studies (Butterworth *et al.*, 2012; Englyst *et al.*, 1992; Goni *et al.*, 1997). However, equivalent systems are not available for lipids despite a recent attempt (Ooi *et al.*, 2011). The only approach to evaluate the metabolic response of the consumption of food containing lipids is to obtain postprandial blood lipid profiles. Knowing the complexity of the lipid metabolism as described above, it is clear that TAG and cholesterol concentrations in peripheral blood will not directly reflect the absorption of nutrients.

Postprandial lipaemia is defined as an elevated level of circulating TAG within an hour of meal ingestion (Lairon *et al.*, 2007b). The TAGs are transported in the bloodstream within lipoprotein particles, such as chylomicrons and very-low-density lipoprotein (VLDL), provided by the liver and the small intestine. This marked elevation lasts between 5 to 8 h for a meal consisting of 30 to 60 g of lipids. To obtain a measurable postprandial lipaemia the lipid intake has to exceed 15 g; 40 to 50 g are in fact necessary to observe a significant increase in healthy adults (Dubois *et al.*, 1998). Given that individuals in Western countries have high lipid intake, with an average daily intake between 80 and 164 g depending on the country (FAOSTAT, 2009), and eat every 3 to 5 h, much of the waking

hours are spent in the postprandial state. In the post-absorptive state (about 4 h after meal ingestion), non-esterified fatty acids (NEFA) constitute a substantial source of energy and their blood levels reflect the mobilisation of fat from body stores (Frayn, 2010). NEFA are released from the hydrolysis, by lipoprotein lipase, of TAGs stored in adipose tissues in response to negative energy balance that cannot be restored by carbohydrate metabolism.

The regulation of the circulating TAG levels is highly individual and reflects metabolic efficiency. The postprandial response is influenced by the meal composition (e.g. size, and quantity and type of macronutrients including the type of fatty acids), overall dietary habits, lifestyle (e.g. physical activity and alcohol consumption), health status (e.g. cardiovascular risks, dyslipidaemia, obesity, diabetes and metabolic syndrome), age and gender (e.g. elevated postprandial lipaemia in older subject and post-menopausal women), and genotype (Lairon *et al.*, 2007b; Sanders, 2003).

1.4 Lipases and lipolysis

1.4.1 Lipases structure and functional analysis

1.4.1.1 Gastric and pancreatic lipases active structure

HGL and HPL have an apparent molecular weight of about 45 and 50 kDa with 379 and 449 amino acid residues, respectively (Figure 1.3) (Canaan *et al.*, 1999; Lowe, 1997). HPL is a glycoprotein composed of two main structural domains; a large N-terminal domain that comprises the active site (hydrophobic), and a smaller C-terminal domain. The active site is covered with by an α-helical area forming a loop (lid) inaccessible for the substrate (Canaan *et al.*, 1999; Winkler *et al.*, 1990). HGL also lacks an active site freely accessible to TAG. A lid formed of complex folding moieties prevents the direct binding of a lipidic substrate molecule to the enzyme (Miled *et al.*, 2000). Van der Waals'

forces occurring between two domains, β5 (i.e. residues 75 to 84) and β9 (i.e. residues 203 to 223) loops, maintain the closed conformation of the enzyme (Brownlee *et al.*, 2010). Because of the difference in overall polarity between enzyme and substrate, the enzyme reaction occurs at the lipid-water interface. The lipase has then an open conformation where its lid allows the binding of its hydrophobic patch to the interface (Figure 1.4) (van Tilbeurgh *et al.*, 1999).

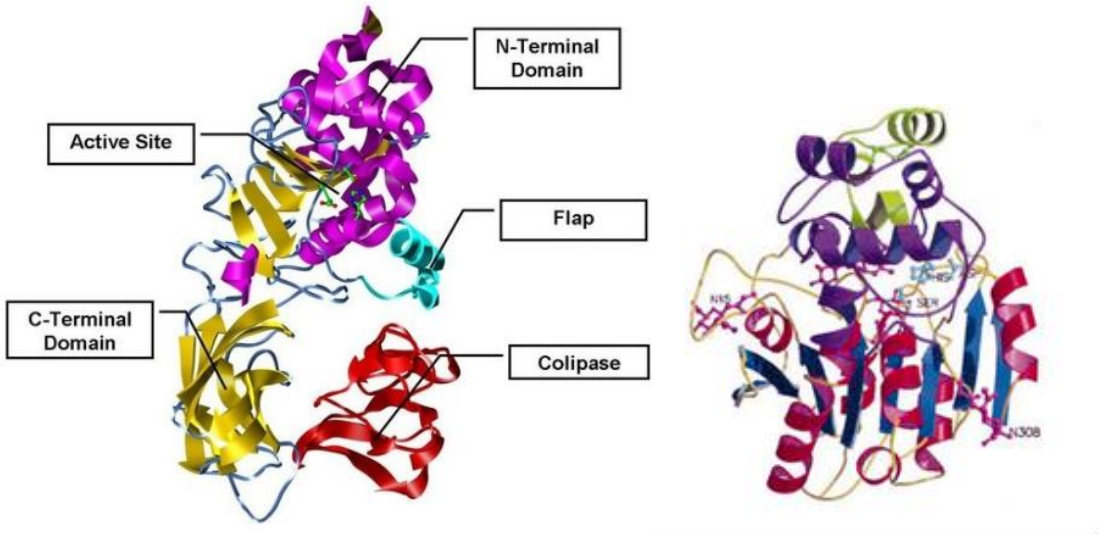

Figure 1.3 Representation of pancreatic (Fromer and Merolla, 2012) and gastric (Canaan et al., 1999) lipases.

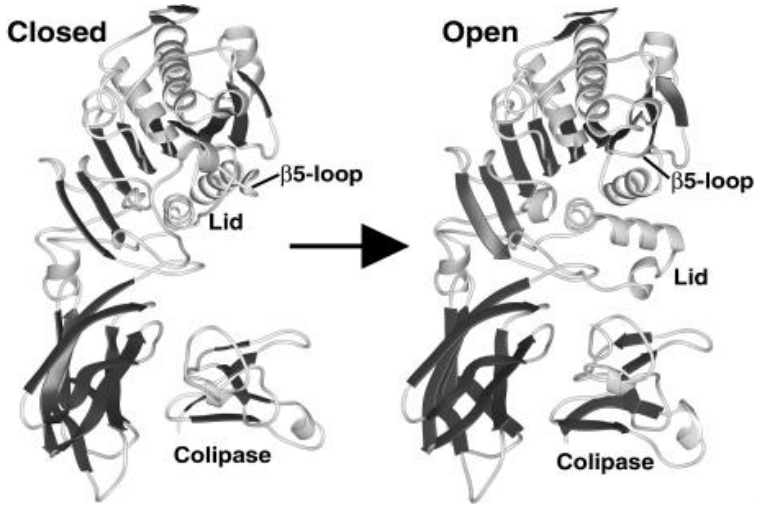

Figure 1.4 Representation of pancreatic lipase, closed and open conformation (Lowe, 2002).

Pancreatic lipase requires the presence of **colipase** or its precursor, procolipase, for the lipolysis to occur (Chapus *et al.*, 1975). Colipase is a small non-enzymic protein (≈10-12 kDa), that is fairly flat, and composed of 112 amino acid residues. The activated form is shorter than the procolipase from which five amino acids have been removed by trypsin (Lowe, 1997). This pentapeptide is called enterostatin and it is believed to play a role in satiety regulation and fat intake (Bauer *et al.*, 2005). Previous models indicate that colipase binds exclusively to the C-terminal β-sheet domain, extending over more than 50 Å and thus generating a hydrophobic plateau (Figure 1.5) (Miled *et al.*, 2000; van Tilbeurgh *et al.*, 1992). This association engenders a shift of the lid and β5-loop, so that the hydrophobic β9-loop open and the oxyanion hole[1] is created (Cygler and Schrag, 1997). The catalytic N-terminal domain is brought in close contact with the lipid-water interface, the active site thus becoming exposed to lipolytic substrates. The hydrophobic plateau ensures a strong interaction between the lipase-colipase complex and the lipid-water interface. However, the conformation change is not induced in the absence of an interface.

Colipase therefore reduces the competition for the interface with other substances (e.g. BS and proteins), in favour of HPL, by expanding the hydrophobic area of the latter (Wilde and Chu, 2011). Brockman's work goes further by showing evidence of the colipase ability to reorganize the interface and thus to concentrate lipolysis reactants in its vicinity (Brockman, 2002).

[1]During the transition-state (enzyme-substrate intermediate, see Figure 1.5), certain amino acids, located in the active site, have a single bond on their carbonyl group creating a negative charge on the oxygen atom (an oxyanion (Egloff *et al.*, 1995; Miled *et al.*, 2000). The latter forms hydrogen bonds to amide chains on other amino acids thus stabilizing the intermediate linked together by hydrogen bonds. The binding site is called the **oxyanion hole**. The **catalytic triad** is formed of serine, histidine and aspartate or glutamate residues.

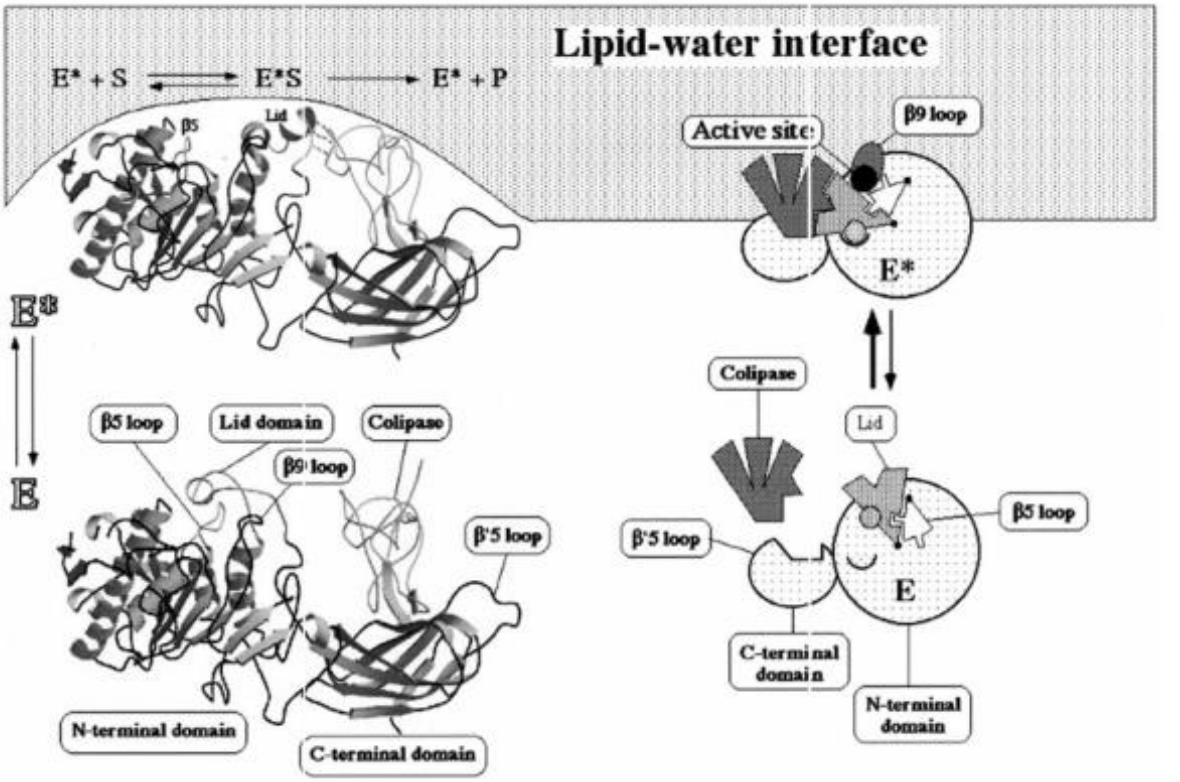

Figure 1.5 Structure of the pancreatic lipase-colipase complex (left) and reaction scheme on lipid-water interface of a lipid droplet (right), where E is the closed form of the complex, E is the active lipase at the interface (open form generated by conformational changes in the lid and the β5-loop unmasking the hydrophobic β9-loop) (van Tilbeurgh et al., 1999).*

1.4.1.2 Effect of bile salts and calcium on lipases activity

Bile is a complex mixture of organic and inorganic components, made up of water, BS (~25-35% of the solid content), phospholipids (mainly lecithin), cholesterol (about 4% of the solid content), pigments such as bilirubin (~2% of the solid content), and inorganic salts (Johnson, 1991). BS, synthesised in the liver from cholesterol, are delivered into the duodenum after having been stored in the gall bladder. BS are natural surfactants, amphiphilic molecules with an unusual structure composed of a lipophilic and a hydrophilic face (Figure 1.6). The most abundant are cholate, deoxycholate and chenodeoxycholate conjugated with either glycine (75%) or taurine (25%) (Maldonado-Valderrama *et al.*, 2011). They position themselves at the interface by projecting their

hydrophilic face into the water and the hydrophobic one into the TAGs (Figure 1.7) (Carey and Hernell, 1992).

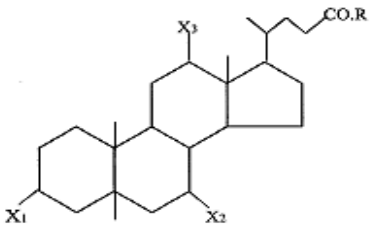

Bile salt	X1	X2	X3	Proportion found in human bile (%)
Glycocholate	α-OH	α-OH	α-OH	29.8
Glycochenodeoxycholate	α-OH	α-OH	H	24.5
Glycodeoxycholate	H	α-OH	α-OH	11.9
Taurocholate	α-OH	α-OH	α-OH	12.6
Taurochenodeoxycholate	α-OH	α-OH	H	13.6
Taurodeoxycholate	α-OH	H	α-OH	7.6
Glyco-conjugated BS		**R** → $NHCH_2CH_2CO_2Na$		
Tauro-conjugated BS		**R** → $NHCH_2CH_2SO_3Na$		

Figure 1.6 Molecular structure of bile salts and their organisation, adapted from (Gargouri et al., 1986a; Madenci and Egelhaaf, 2010; Wickham et al., 1998).

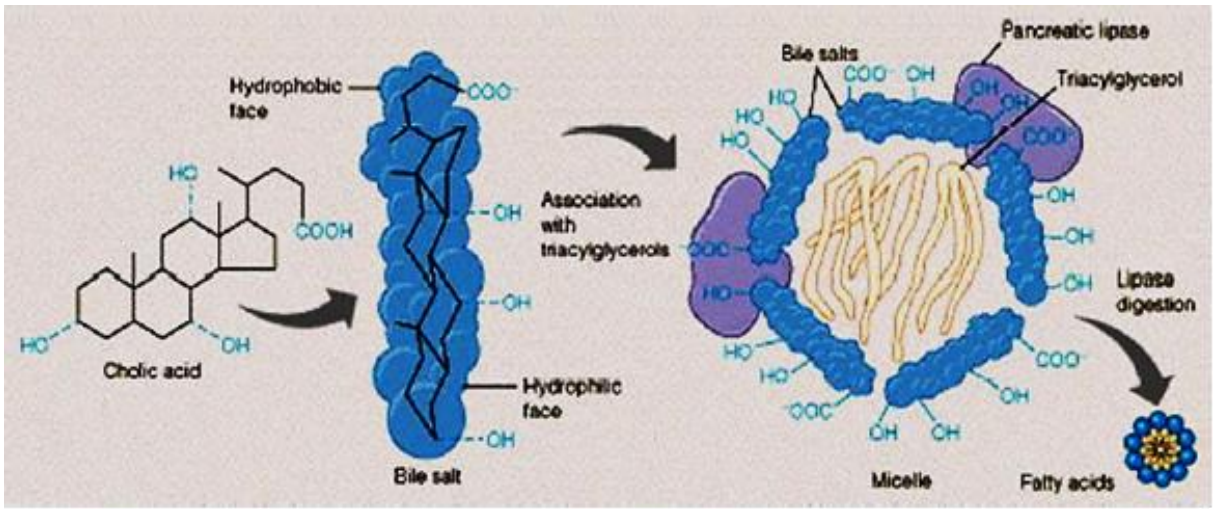

Figure 1.7 Structure of bile salts and their arrangement on the surface of a micelle (Mathews et al., 2000).

The accumulation of BS at the interface gives a negative charge to the oil droplets which directs the adsorption of colipase, and also reduces the surface tension of the droplets making the anchoring possible (Lowe, 2002). Additionally, BS have a 'cleaning' role as they remove from the interface other amphiphile molecules such as proteins and lipolytic products, this action being due to their high surface tension-active property (Maldonado-Valderrama *et al.*, 2011). BS are also involved in solubilizing the products of the lipolysis and, with the simultaneous action of phospholipids, integrating them into micelles. Recent work (Parker *et al.*, 2014) revealed that different BS have contrasting roles; the structure on the BS, mainly the unconjugated part (cholates versus deoxycholates and chenodeoxycholates), influences their behaviour on the interface and their interaction with colipase. The results supported the idea that cooperative absorption occurs between BS (sodium taurocholate, NaTC) and colipase. They also showed that sodium glycodeoxycholate (NaGDC), because of its reduced interfacial residence time, may facilitate the displacement of lipolytic products.

For the catalytic reaction to be feasible, the BS should reach the critical micelle concentration (CMC) that corresponds to the concentration, generally expressed in millimolar (mM), above which micelles form spontaneously and BS self-assemble (Maldonado-Valderrama *et al.*, 2011). Surfactants and other molecules present at the interface are thus displaced and the HPL-colipase complex can then bind to the emulsion. CMC values, determined experimentally, vary from one BS to another, ranging from around 1 to greater than 250 mM (Bauer *et al.*, 2005; Roda *et al.*, 1983), but they are usually around 2 to 4 mM which is rather high (Maldonado-Valderrama *et al.*, 2011). In the small intestine, however, BS concentrations exceed the CMC; so that in the duodenum the BS concentration is ~6-15 mM, in the jejunum it is ~10 mM and in the ileum < 4 mM (McClements and Li, 2010). CMC is contingent on factors associated with the reaction environment, which includes the presence of endogenous MAGs and phospholipids, temperature, pH and ionic strength of the solution, as well as on the structural characteristics of the salt such as length of side chain, moieties present (e.g. hydroxyl and carbonyl) and hydrophobicity (Borgström, 1977; Roda *et al.*, 1983; Simonovic and

Momirovic, 1997). The presence of BS may also inhibit the lipase activity if its concentration is too low – so that the removal of products and other surface-active molecules is impaired; or if the concentration of these molecules is too high – the anchoring of the lipase-colipase complex onto the interface is prevented (Gargouri *et al.*, 1983).

Finally, HPL is not fully active if the complex does not contain calcium ions (Benzonana, 1968). Calcium seems to bind to the lipase itself probably to counteract the electrostatic repulsion existing at the interface between the lipase and BS. The cation is also involved in the removal of long chain FFAs from the surface of lipid droplets and hereby preventing product inhibition.

To summarise, the pancreatic lipase action can occur in a simplified way, involving three essential events when it is in contact with a lipolytic substrate: a change of conformation, an adsorption (with the intervention of colipase for HPL) and a catalysic process (Figure 1.8).

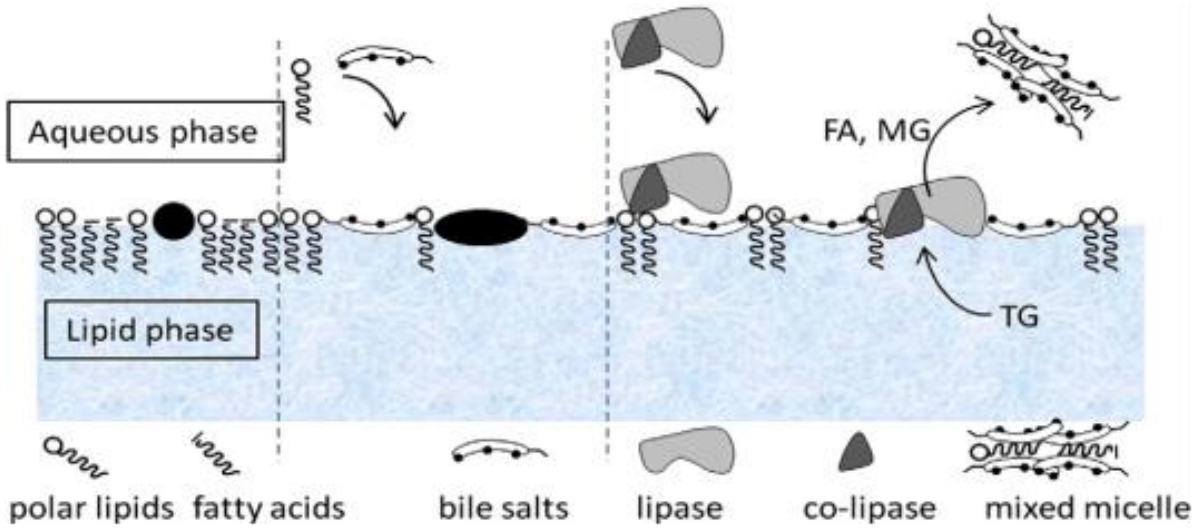

Figure 1.8 Schematic representation of duodenal lipolysis. Left: lipid-water interface is coated by surface active material surviving stomach such as polar lipids, fatty acids, emulsifiers etc. Centre: bile salts and phospholipids secreted into the duodenum adsorb onto lipid interface. Right: pancreatic lipase and colipase adsorb, aided by the interaction with BS and hydrolyse TAG, which are 'solubilised' by BS into mixed micelles (Wilde and Chu, 2011).

1.4.1.3 Roles of the gastric lipase

The mode of action of HGL is much less documented than that of HPL, although it has been demonstrated that it can digest milk fat on its own (Carey and Hernell, 1992). In contrast to HPL, HGL has the capacity to bind to the lipid droplet interface even though BS are present. In fact BS seem to prevent the inhibition of the enzyme (Borel *et al.*, 1994).

HGL contributes quantitatively to the lipid hydrolysis but more importantly qualitatively (Fave *et al.*, 2007). Indeed, HGL modifies the lipid-water interface by generating surface-active products and also stabilises the granulometry of the lipid droplets, which range in size of between 2 and 20 µm, since emulsification does not occur in the lower part of the GIT. The lipolytic products, MAG and FFA, are some of the surface-active molecules that act to promote emulsification.

Finally, the long-chain fatty acids released in the stomach stimulate the secretion of CCK thus slowing down the gastric emptying, and also reduce the lag-time preceding the activation of the HPL-colipase complex (Armand, 2007).

1.4.2 The lipolytic hydrolysis

The major distinction of lipases compared with other enzymes is that they act on insoluble substrate, and they have the ability to adsorb at the lipid-water interface. The conformation change occurring during the adsorption may explain why the HPL and HGL are synthesised and secreted in their potentially active forms rather than as proenzymes as most other digestive enzymes seem to be (Miled *et al.*, 2000).

Lipases hydrolyse ester bonds on the glycerol backbone of TAG. *In vivo* HGL selectively acts at the *sn*-3 position of TAG, generating *sn*-1,2-DAG residues (Carriere *et al.*, 1993). However, *in vitro* HGL has been shown to be able to hydrolyse fatty acids on both *sn*-3 and *sn*-1 positions (Carriere *et al.*, 1991).

Even though the enzyme can hydrolyse long-chain fatty acids, it acts preferentially on short- and medium-chain fatty acids that can be easily absorbed by the stomach mucosae. Pancreatic lipase hydrolyses ester bonds in position 1 or 3 of the TAG leading to the production of *sn*-1,2-diacylglycerol (DAG), *sn*-2-monoacylglycerol (MAG) and FFAs (Carriere *et al.*, 1993). The complete degradation of the TAGs into one glycerol and three FFAs can occur when the fatty acid in the *sn*-2 position of the DAG molecule reconfigures into *sn*-1,3-DAG but only a small proportion of the molecules undergo this acyl migration (Small, 1991). Efficient intestinal absorption is achieved for MAG and FFA (Gurr *et al.*, 2002); the complete absorption of fat occurs when at least 66% of the TAGs contained in the meal have been hydrolysed, with HGL activity accounting for 1 hydrolysed acyl chain out of 4.

The lipolysis reaction follows a Michaelis-Menten model only when lipases and substrates are present in the same phase (interface) and the products generated are soluble (short- or medium-chain lipids) and consequently do not accumulate (Panaiotov and Verger, 2000). Since lipase partitions between a two-phase system (i.e. aqueous phase and lipid-water interface) the usual Michaelis-Menten model no longer applies. The simplest model describing the interfacial mechanisms of lipase hydrolysis has been proposed by Verger and his team (Verger *et al.*, 1973) (Figure 1.9 A):

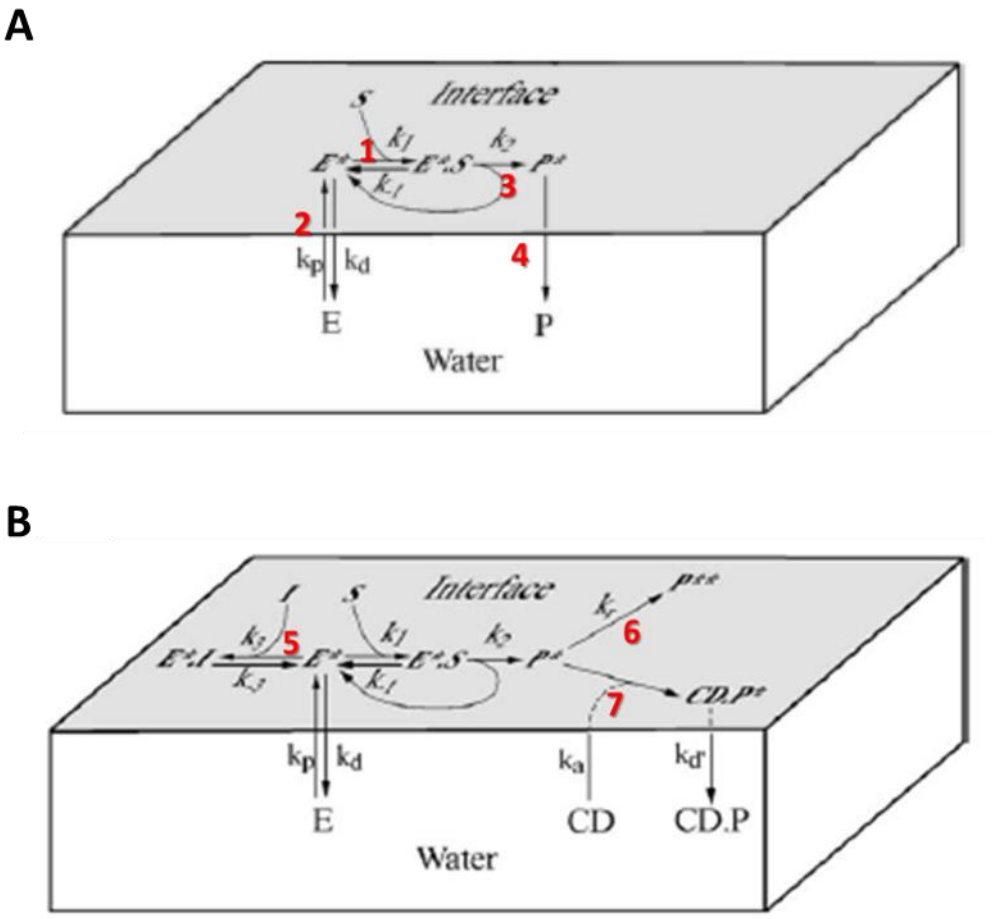

Figure 1.9 Michaelis-Menten kinetic model adapted to interfacial enzymic lipolysis of short- and medium-chain lipids (A) (Verger and de Haas, 1973), and general scheme of interfacial catalysis (B) (Panaiotov et al., 1997); where E is the lipase, E is the active lipase at the interface, S is the TAGs, E*S is the lipase-substrate complex, P* is soluble products, P** is insoluble products and the ks are rate constants for the different reaction steps.*

1: Binding of the lipase to the interface; 2: Confromational change of the lipase; 3: Formation of lipolytic products (DAG, MAG and FFA); 4: Diffusion of the soluble products into the aqueous environment; 5: Competitive inhibition of the interface; 6: Accumulation, reorganisation and segregation of the DAG, MAG and FFA generated; and 7: Solubilisation of lipolytic products in the presence of an acceptor, here CD (cyclodextrin), which is a non-surface-active molecule that forms a complex with the lipolytic products (CD-P and CD-P). In vivo, BS solubilise the lipolytic products, combine with them to form micelles thereby promoting their uptake by the enterocytes.*

Benzonana and Desnuelle demonstrated that K_m and V_{max} were meaningless with insoluble substrate notably because K_m is influenced by the size of the emulsion droplets (Benzonana and Desnuelle,

1965). To obtain some meaningful kinetic parameters, it would be necessary to accurately determine the surface area of these droplets which is a difficult task. Contrary to a soluble substrate, increase in lipid concentration does not lead to an increase in the quantity of available molecules as the interface exposes a relatively constant number of substrate molecules per area unit (Sarda and Desnuelle, 1958). Moreover, the kinetics of the lipolysis fluctuates with the specific colloidal structure of the system. As a result, the model presented in Figure 1.9 A has been further developed to be applied to various interfacial structures (Figure 1.9 B).

The amount of substrate available for hydrolysis has been estimated at 2 to 5 mole percent of the interface surface (Bauer *et al.*, 2005). During the digestion of a test meal, the HPL output was approximately 250 mg with a liquid meal and 203 mg with a solid meal, while HGL output was about 22 mg regardless of the meal. The HPL production was maximal at the beginning of the digestion and then decreased progressively, whereas HGL appeared to be constant overtime although this is contingent on the rate of gastric emptying (Carriere *et al.*, 1993). The amount of lipase secreted however increases with the lipid content of the meal (Lengsfeld *et al.*, 2004). The turnover number for HPL is high and corresponds to the production of 500 000 molecules of FFAs per minute.

The activity of the lipases depends on the structure of the food and lipid studied. The specific activity (SA) values obtained from *in vitro* studies performed on almond oil emulsions were 2865 ± 269 U/mg for HPL and 202 ± 21 U/mg for HGL (Beisson *et al.*, 2001a). The maximum SA of HPL using tributyrin as substrate has been reported to be 12000 U/mg at pH 8 (Miled *et al.*, 2000).

The requirement for lipase to catalyse lipid hydrolysis at a lipid-water interface along with the involvement of various mediators can result in the appearance of a lag time in the catalytic activity especially for long-chain lipid substrates. This unusual lag phase was observed with hydrolysis of OBs (Gallier and Singh, 2012) but not at low surface pressure or for emulsion systems (Borgström *et al.*, 1979; Wieloch *et al.*, 1982). The rate-limiting step could therefore be the interfacial binding which regulates the concentration of lipase at the lipid-water interface: the smaller the interface, the fewer

colipase-lipase complexes bind to the surface and the slower the reaction rate. Subsequent to the lag-time, a rapid hydrolysis of TAG is observed.

1.4.3 Parameters affecting the hydrolysis reaction process

The hydrolysis of TAG is a highly complicated reaction that relies on the composition of the environment especially the lipid-water interface. As for any enzyme, the rate at which lipases work depends on the initial quantity of substrate (surface area of the interface), the accumulation of hydrolysed products, the temperature, the pH (i.e. the optimum pH for HGL activity is between 4 and 6, and for HPL 6.5 and 9), and the presence/absence of other elements in the catalytic environment. In other words, hydrolysis can be affected by environmental conditions and compounds that can alter the structure and/or the integrity of the interface (e.g. colipase, digestion products and surface-active molecules such as proteins, BS and phospholipids) (Carriere *et al.*, 1991; Embleton and Pouton, 1997).

1.4.3.1 Substrate characteristics

The 'quality' of the interface affects the enzymic lipolysis, in particular the structure and mode of organisation of the colloidal system (e.g. micelles, emulsions and liposomes) that have direct implication on the area/volume ratio of the oil droplet (Carey *et al.*, 1983; Panaiotov and Verger, 2000; Verger and de Haas, 1976). An increase in **surface area** and decrease in droplet size, will lead to an increase in TAG availability. Emulsification, the dispersion of oil in water by creating a suspension of oil droplets, is an essential step in lipid digestion that produces a drastic rise in the ratio of surface area to droplet volume. Since emulsions are intrinsically unstable, to prevent the occurrence of instability processes, such as breaking, creaming or flocculation, they require molecules that reduce their **surface tension** – i.e. surfactant or emulsifier (Sherman, 1968).

Phospholipids (i.e. lecithin) and BS are surface-active compounds that form a layer that surrounds oil droplets to reduce the interfacial tension and thus promote effective hydrolysis (Brockman, 1984). Other surface-active molecules include surfactants such as whey proteins, in particular beta-lactoglobulin (β-Lg); casein and polysorbate 20 (tween 20). All those compounds are amphiphile molecules. The structure and the properties of the emulsion, and its interface, strongly depend on the type of emulsifier used (Hur *et al.*, 2009).

The core of oil droplets are composed of TAGs, the *sn*-2 fatty acids being orientated in the opposite direction to the *sn*-1 and *sn*-3 fatty acids (Carey *et al.*, 1983). Esterified cholesterol and fat-soluble vitamins are also often contained in these droplets. The TAGs located at the interface and therefore readily available to the lipase are digested first. Then, once the lipolytic products have been removed, other TAGs replace the initial substrates and become reoriented, ready to be broken down (Carey and Hernell, 1992). Reorganisation and segregation occur throughout the lipolysis reaction thereby affecting the quality of the lipid-water interface. As the TAGs get digested, the size of the oil droplets progressively decreases and their surface area increases, thereby accelerating the rate of lipolysis (Boron and Boulpaep, 2009).

The ultrastructure of the emulsion and the **size** of its droplets also regulate lipase activity (Marangoni, 1994; Singh *et al.*, 2009). According to the **type of fatty acids** present on the glycerol molecule backbone, in particular positions *sn*-1 and *sn*-3, the droplet size, and consequently the lipolysis rate, will be different (Jandacek *et al.*, 1987). Furthermore, lipolytic products are removed at different rates from the interface depending on the water solubility of the fatty acids constituting the TAG. For instance long-chain fatty acids can accumulate at the interface and inhibit the lipase. A maximum lipolysis rate was obtained for emulsions of medium-chain TAG compared with long-chain and mixed medium-and long-chain TAG (Armand *et al.*, 1992). It has also been demonstrated that both gastric (Borel *et al.*, 1994) and pancreatic (Armand *et al.*, 1999) lipase activities were greater on fine lipid droplets than coarse ones; the size of the droplets decreasing as the digestion progresses

but to a greater extent in the stomach. Subsequently, TAGs were mostly present in larger droplets, their concentration decreasing with the droplet size, while DAGs were found in medium size droplets, and MAGs and FFAs in the pellet (Armand *et al.*, 1996). As expected, the amount of TAG is inversely proportional to the digestion progress whereas the opposite is observed for DAG, MAG and FFA, the reduction in size of the lipid droplets being caused by the degradation of TAG and DAG. Nevertheless, the size and the aggregation state of the lipid droplets fluctuate greatly throughout the digestion due to the various mechanical forces generated - mastication, churning in the stomach and peristaltic movements in the intestine. If the surface tension of the interface is not strong enough the droplets coalesce leading to a greater mean particle size. On the other hand, the digestion of TAG and the movement of the digestion products to the aqueous phase results in smaller lipid droplets (McClements and Li, 2010).

The initial form of the lipid phase within a food may impact on its subsequent digestion and absorption (Hur *et al.*, 2009). For instance, an investigation done on almond OBs showed a slower lipolysis compared with almond oil emulsions (Beisson *et al.*, 2001a). In this study, the SA of HPL with colipase was 2865 ± 269 µmol/min/mg with the emulsion and 1079 ± 98 µmol/min/mg with OBs, and for HGL the activity values were 202 ± 21 and 71 ± 3 µmol/min/mg for the emulsion and OBs, respectively. The authors concluded that the layer of phospholipids and embedded oleosins was a rate-limiting parameter in OBs, nevertheless the hydrolysis could not occur without preliminary degradation of that layer, for instance by phospholipases.

Furthermore, lipids that are embedded within a protein-coated droplet or a DF (CW) matrix may prevent the access of the enzyme to the substrate. In certain conditions, the activity of BS may not be sufficient and other enzymes may be required such as proteases, glycosidases and amylases to remove other substrates that are co-located with the lipid (McClements and Li, 2010). The rate of lipase activity would be dependent on the catalytic rates of these molecules.

1.4.3.2 Lipid-water interface and surface tension

For the lipid hydrolysis to occur, the lipase needs to come in proximity to the interface and adsorbs to the surface. The interfacial surface tension of oil droplets is minimized by partitioning. The presence of amphiphiles, such as BS, lowers the surface tension as well as stabilises the droplets by expelling the water from the interface (Brockman, 2002). Consequently, pure TAGs in water have a surface tension of 15 to 20 mN/m whereas BS decreases these values to 8-13 mN/m (Carey and Hernell, 1992; Gargouri *et al.*, 1986b). This interfacial tension explains the induced irreversible denaturation (unfolding) of lipase observed during its adsorption onto the interface which becomes possible thanks to BS (Borel *et al.*, 1994). Throughout the digestion interfacial active components such as lipolytic products, intermediates and BS, have an effect on the surface tension which in turn influences the lipase activation (Reis *et al.*, 2009). Therefore, during digestion, the interfacial properties of the lipid droplets may be altered, the molecules present at the interface can be digested (e.g. proteins by proteases and phospholipids by phospholipases) or removed by other surface-active components (McClements and Li, 2010).

1.4.3.3 pH variations

Both HGL and HPL activities rely highly on pH. HGL is stable for a broad range of pH – from 3 to 6, whereas HPL loses its activity below 5 and has an optimal pH of 6.5-9 (Carriere *et al.*, 1993). HGL thus remains active in parts of the duodenum, particularly when HPL is present (Gargouri *et al.*, 1986a). Furthermore, in the stomach, the pH varies greatly between fasted and fed states as well as among the types of food ingested. As a result gastric pH can reach values as high as 6-7 (Lengsfeld *et al.*, 2004). When half of the stomach is full, its pH is close to 5 while after digestion, containing mainly only gastric juice, the pH is low (1-2). In contrast, the pH within the duodenum does not fluctuate to a great extent, and it is generally between 5 and 7 (N'Goma *et al.*, 2012).

1.4.3.4 Other parameters

Overall, HPL has a higher SA than HGL (6 fold greater), which for both enzymes decreases with increase in the chain length of the TAG, DAG also being a more appropriate substrate than TAG (Canaan *et al.*, 1999). The lipolytic hydrolysis starts in the stomach with the action of HGL, and the products thus formed (DAG and FFAs) facilitate the subsequent hydrolysis by HPL, which results in a faster rate of reaction (Armand *et al.*, 1999). A low quantity of substrate at the interface will also inhibit the lipolysis (Brockman, 2002).

The products of the hydrolysis are not directly partitioned into mixed bile salt micelles and may accumulate in the interface, at least at the beginning of the reaction due to a reaction rate exceeding the capacity of incorporating the products into micelles (Carey and Hernell, 1992). However, the greater polarity of FFA and MAG compared with TAG facilitates their transport to the aqueous phase. Once they are incorporated into micelles the lipase inhibition by its products is prevented as well as the competition for the interface (Maldonado-Valderrama *et al.*, 2011). The partitioning is enhanced by the gradual increase in pH within the intestine as well as by the dispersion effect of BS. Since neither HPL nor HGL has the capacity to hydrolyse 2-*sn*-MAGs the rate of lipolysis is reduced if these products are not removed from the interface area (Bauer *et al.*, 2005).

1.5 Plant cell walls as a source of dietary fibre

The definition of DF has been the subject of great debate and controversy. DF is a generic term for a chemically diverse group of carbohydrates that are resistant to endogenous enzymes present in the human digestive tract, and includes the remnants of plant cells, individual polysaccharides, lignin and associated substances resistant to hydrolysis (Cummings and Overduin, 2007). Table 1.1 summarises some of the DF components often found listed in the literature.

Non-starch polysaccharides are the main components of plant CW which can be divided into the following categories: cellulose, hemicelluloses and pectic compounds. Hemicelluloses and pectins can be further classified according to their monomeric composition and glycosidic linkages (see *Section 1.5.2*). Starch that is resistant to digestion has also been included in the DF definition by some researchers. Resistant starch (RS) is the fraction of starch that is not digested and absorbed in the small intestine (Champ *et al.*, 2003). RS can be either starch that is encapsulated within the food matrix and inaccessible for digestion (RS1); raw or undercooked starch resistant to amylolysis (RS2); starch that re-associates and recrystallizes following thermal processing, i.e., retrograded starch (RS3); or starch that has been chemically modified to resist digestion (RS4). Short chain carbohydrates are oligosaccharides containing between 3 and 10 monosaccharide residues (Cummings and Overduin, 2007). Certain short chain carbohydrates, in addition to RS and other forms of CW carbohydrates, stimulate the growth of colonic bacteria and are called 'prebiotics'. Finally, plant gums and mucilages produced by the epidermis of the seeds of certain species, including psyllium or ispaghula, can also be categorised as DF (Harris and Smith, 2006). The chemical composition and structure (e.g. the conformation of polysaccharide chains) of DF influences their fermentability and solubility; as an example RS, pectins, guar gum are fermentable whereas cellulose tends to be resistant to microbial fermentation (Champ *et al.*, 2003).

The major components of DF are plant CWs, which are supramolecular structures, composed of complex heterogeneous networks of cellulose, hemicelluloses and pectic substances. The amounts and relative proportions of these polysaccharides vary depending on the type and maturity of the plant tissue. In terms of the sensory and nutritional properties, CWs give texture to the food and also have important effects on human health since there is now a large body of evidence to indicate that DF has the potential to reduce the risk of various non-infectious diseases or conditions (e.g. irritable bowel syndrome, type 2 diabetes, obesity, CVD and certain cancers especially colon cancer) (Anderson *et al.*, 2009; Brownlee, 2011; Kendall *et al.*, 2010; Mann and Cummings, 2009).

Table 1.1 Types of dietary fibre, with selected examples, adapted from (Grassby et al., 2013).

Non-starch polysaccharides	**Resistant Starch**	**Short-chain carbohydrates**
Cell walls	RS1 – Physically	Galacto-oligosaccharides
Cellulose	Inaccessible	Fructo-oligosaccharides
Hemicelluloses	(encapsulated)	Inulin
Xylan	Starch	Raffinose
Xyloglucan	RS2 – Native starch	Polydextrose
Arabinoxylan	RS3 – Retrograded	Stachyose
Mannan	Starch	Maltodextrins
Glucomannan	RS4 – Modified	
Galactomannan	Starches	
β-glucan		
Callose		
Pectins		
Homogalacturonan		
Rhamnogalacturonan I		
Rhamnogalacturonan II		
Arabinan		
Galactan		
Arabinogalactan I		
Arabinogalactan II		
Storage		
Guar* (galactomannan)		
Other		
Psyllium seed husk mucilage (arabinoxylan)		

*Located mainly in CWs

1.5.1 Plant food matrix and cell wall

Plant cells differ in many ways to animal cells, one of the main differences being the presence of CWs in the former. Indeed, plant cells contain this rigid wall that surrounds the plasma membrane and provides, *inter alia,* mechanical support for the cell (Figure 1.10).

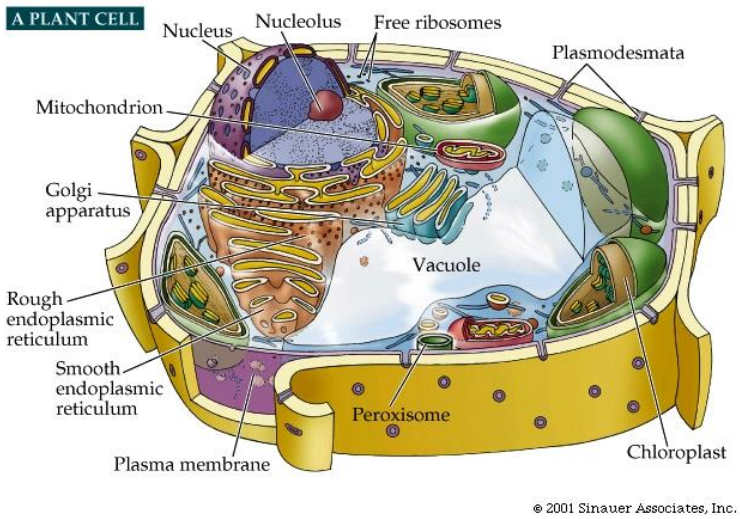

Figure 1.10 Schematic representation of a plant cell.

The constitutive cells of a plant tissue react differently when submitted to physical disruption (mastication or mechanical trituration), they can either separate or rupture depending on the cross-links holding the CWs together (Brett and Waldron, 1996). This behaviour is responsible for the different textural properties of plant foods. A food with cells that rupture will have a crunchy texture, as it is the case for raw almonds, which are relatively hard and brittle, whereas cells that separate result in a softer texture of the plant food (Figure 1.11). In crunchy foods, the cells fracture because the cell-cell bonding is stronger than the forces holding the CW together, resulting in the release of the cell contents. Alternatively, in soft foods, such as very ripe fruit and many cooked vegetables, cells separate along the plane of the middle lamella and their content is not available as the CWs remain intact (Waldron *et al.*, 1997). Empirical evidence has demonstrated that ripening or processing, such as fermentation and/or cooking, decrease cell adhesion and increase cell separation, but due to different processes. For instance, the depolymerisation of pectic polysaccharides is thought to be one of the causes of reduced cell-cell adhesion (Waldron *et al.*, 1997). Thermally stable diferulic acid that crosslinks between polysaccharides, has a central role in the thermal stability of cell adhesion and a good example of this is the crisp texture of hydrothermally-treated Chinese water-chestnut (Parker *et al.*, 2003).

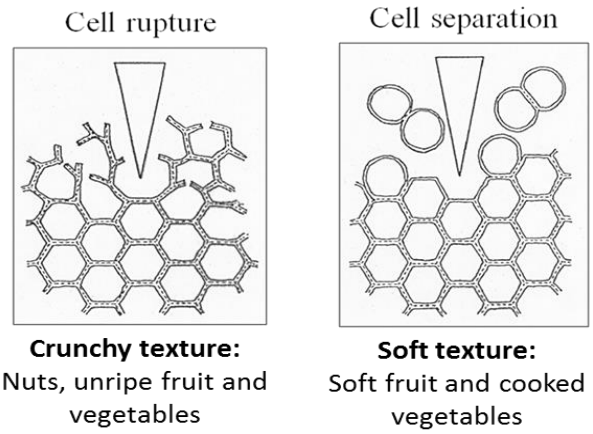

Figure 1.11 Cell behaviour after physical disruption in relation to the food texture, adapted from (Brett and Waldron, 1996).

1.5.2 Cell wall

During cell division a new CW is synthesised, the latter consists of three layers. The first, outer layer is the middle lamella that is shared between adjacent cells. This layer is composed of pectic compounds and proteins, and it is relatively thin apart from the cells corner regions. The second layer is the primary CW. This is a dynamic structure, the spatial arrangement of the polymer network and molecular composition is modified during growth and by attack from pathogens. It has various functions including maintenance of cell shape and ultimately plant physiology, through control of cell expansion and cell signalling notably via plasmodesmata (Brett and Waldron, 1996; Kendall *et al.*, 2010). The secondary CW, which is closest to the plasma membrane, is synthesised when the cell has ceased to enlarge (Zhong and Ye, 2009) and is composed of cellulose, hemicelluloses, and lignin. Contrary to the primary CW, the secondary CW is predominantly present in specific cells, sclerenchyma cells, which are found in tracheary elements (in vascular plant) as well as fibres of wood. The secondary CW is a rigid layer that provides mechanical support and defence against pathogens to the plant; the sclerenchyma cells also permit the transport of water. Pear and

asparagus are two examples of edible plant materials that contain secondary CWs (Harris and Smith, 2006). Certain plants such as cotton seed, possess non-lignified secondary CWs.

1.5.2.1 Cell wall composition

The composition and structure of the CW matrix is specific to the plant as well as to the tissue, since it is associated to the particular role of the cell within the tissue and its stage of development (McDougall *et al.*, 1996). At the cellular level, heterogeneity is also observed (Burton *et al.*, 2010). In spite of this, three main polysaccharide constituents of primary CW are normally present, i.e. cellulose, hemicelluloses and pectins (Figure 1.12).

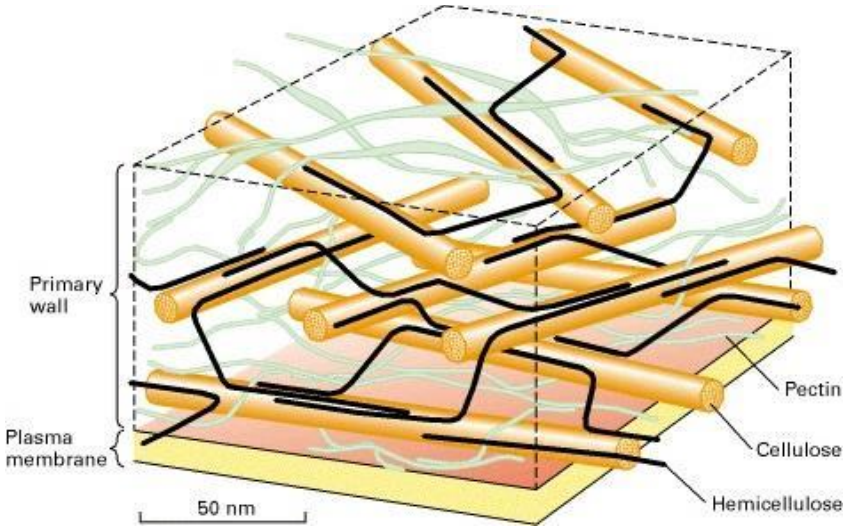

Figure 1.12 Structure of cell wall (onion) (McCann et al., 1992).

1.5.2.1.1 Cellulose

Cellulose is a polymer of **β-1,4-linked glucan chains** (homopolymer of β-D-glucose), comprising 3 to 35% of the primary CWs depending on the CW type (Brett and Waldron, 1996; Selvendran, 1984).

Cellulose consists of several thousands of glucose residues and is organised into microfibrils that are crystalline in structure. The glucan chains are bound together by non-covalent bonds, i.e. hydrogen bonding as well as van der Waals forces (Fry, 1986; Somerville *et al.*, 2004). Microfibrils located in the same layer of CW tend to have the same alignment, but each layer has a different alignment to its neighbours. The microfibrils network formed by the unbranched glucan chains makes cellulose an extremely strong structure. Because of this unique spatial organisation, cellulose is more resistant to mechanical, chemical and microbial degradation than any other polysaccharide found in CW (Brett and Waldron, 1996).

1.5.2.1.2 Hemicelluloses

Hemicelluloses consist of **β-1,4-linked** backbone (hexoses or pentoses) with a range of side-chains (Scheller and Ulvskov, 2010). Hemicelluloses have a semi-rigid, amorphous structure and are alkali-soluble, and in some cases soluble in water at room temperature (e.g. galactomannan of the guar seed). Examples of these polymers include:

-**Xyloglucans**: backbone of glucan (β-1,4 glucose) and short side chains containing predominantly xylose

-**Xylans**: backbone of β-1,4-linked xylose residues with substitutions on C2 of some xylose residues by α-linked 4-O-methylglucuronic acid, on C2 or C3 by α-linked arabinose and on C2 or C3 by acetyl ester

-**Mannans**: linear polymer of mannose

-**Galactomannans**: backbone of β-1,4-linked mannose residues with galactose side-chains

-**Glucomannans**: backbone consisting of mannose and glucose residues arranged in a non-repetitive pattern

-**β-1,3, β-1,4 glucans (β-glucan)**: mixed-link glucans.

Strong hydrogen bonds can exist between certain sections of the hemicellulose chains (xyloglucan and arabinoxylan) and the cellulose microfibrils (Scheller and Ulvskov, 2010).

1.5.2.1.3 Pectins

Pectins are the major component of land plant CW accounting for up to 35% of primary CW with the highest concentration being found in the middle lamella. Pectins are well-known for its gelling properties hence they utilisation for making jam and as thickening agent. The most prevalent pectic polysaccharides, homogalacturonans (HGs), have a galacturonic acid (**1,4-linked α-D-galacturonic acid**) backbone with different degree of esterification, either methyl-esterification (DE) or acetylation (DA) (Willats *et al.*, 2006). Both DE and DA determine the properties of pectin (e.g. gelling capacity). When DE is > 50% the pectins are identified as high methyl but when DE is < 50% they are classified as low methyl (Thakur *et al.*, 1997). High methyl pectins form gels with sugars and acids (i.e. acid gels), whereas bivalent cations such as calcium induce gelation of low methyl pectins (i.e. calcium gels). On the other hand, acetylation prevents pectin gelation but increases the pectin stability and emulsification ability. DE of pectin directly influences the firmness and adhesion of CWs, as for instance in ripening fruit where DE decreases (de-esterification by pectin methyl esterases) leading to pectin degradation and cell separation (Willats *et al.*, 2001).

Pectins also contain rhamnose, arabinose and galactose residues. Common pectic polysaccharides are included in the following list (Brett and Waldron, 1996; Caffall and Mohnen, 2009):

-**Homogalacturonan**: made of α-1,4-linked galacturonic acid

-**Rhamnogalacturonan I**: backbone of α-1,4-linked galacturonic acid and α-1,2-linked rhamnose, and side-chains principally of arabinose and galactose attached to the C4 of rhamnose

-**Rhamnogalacturonan II**: has a complex structure made of galacturonic acid, rhamnose, arabinose, galactose and apiose (in parsley and aquatic plant such as duckweed)

-**Arabinan**: made of a backbone of α-1,5-linked arabinose and single arabinose side chains α--linked to C2 or C3

-**Galactan**: made of a β-1,4-linked galactose backbone with, in some cases, 1,6-linked galactose residues

-**Arabinogalactan I**: made of a β-1,4-linked galactose backbone with α-1,5-linked arabinose side-chains attached at C3 of galactose.

CWs also contain non-polysaccharide components, including glycoproteins such as extensin and arabinogalactan proteins (AGPs), phenolic compounds, all of which can have marked effects on the properties of the CW even though they are present in relatively small quantities. For instance phenolic compounds, in particular ferulic acid, promote the thermal stability of cell adhesion thereby limiting dissolution of CW polysaccharides when cooked (Waldron *et al.*, 2003). Also, AGPs are complex molecules (highly glycosylated proteins rich in hydroxyproline) found in the plasma membrane and in the CW and seem to be involved in the development and growth of plants as well as in cell adhesion and signalling (Showalter, 2001).

1.5.2.2 Cell wall structure

Primary CW can be classified as type I or II (Figure 1.13) based on their polysaccharide compositions (Carpita and Gibeaut, 1993). Dicotyledons (i.e. most fruit and vegetables), non-commelinid monocotyledons (e.g. asparagus and onion), and conifers have a type I CW. In addition to cellulose, the most abundant polysaccharides in type I cell walls are xyloglucans, main interlocking polysaccharides, and pectic polysaccharides (Selvendran, 1984). Type II CW are found in cereals and grasses, and contain a high proportion of cellulose as well as arabinoxylan (hemicellulose), but only negligible amounts of pectic polysaccharides and proteins. Great differences exist between the

composition of cereal endosperm and cereal bran, in particular in the amount of cellulose and hemicellulose (Brett and Waldron, 1996).

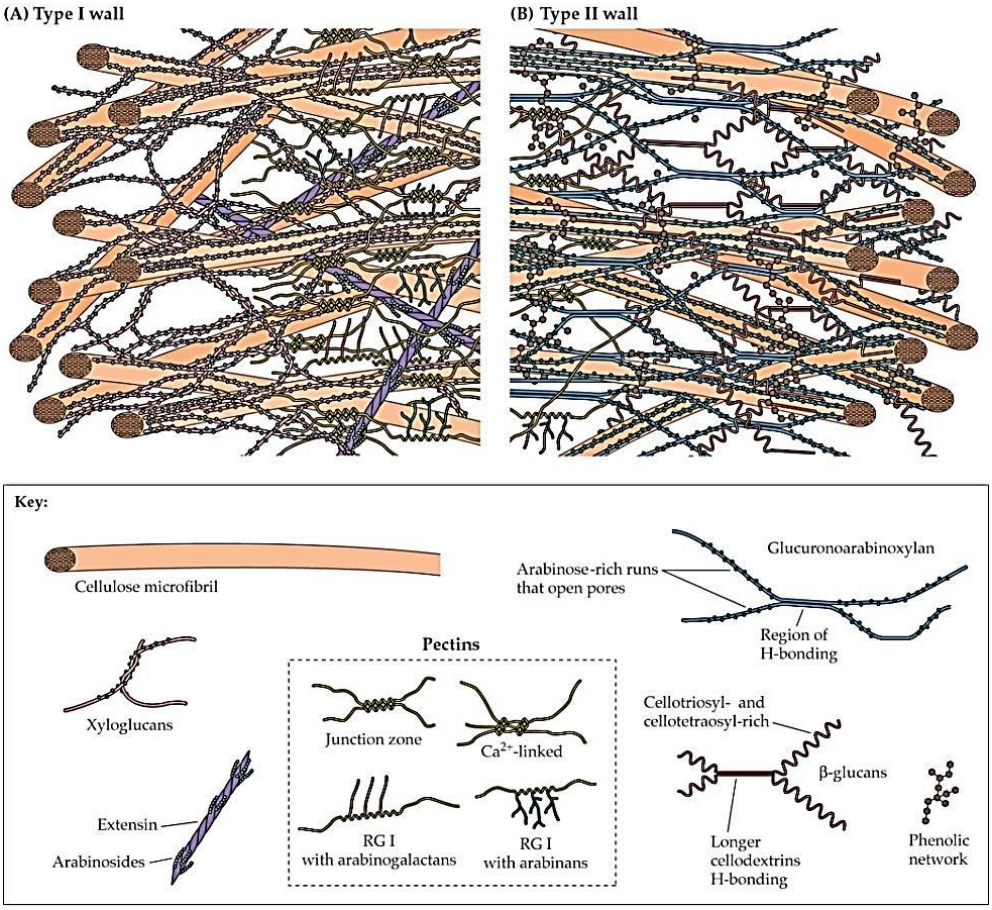

Figure 1.13 Illustration of the potential interactions between components of the primary cell wall for type I and type II cell walls (Buchanan et al., 2002).

1.5.2.3 Cell wall porosity

The CW of plant foods behaves as a filter that regulates the exchange of molecules between the intra and extracellular compartments. However, it is not an impermeable barrier and communication between the cell and the outside environment is assured notably through pores such as plasmodesmata creating an opening at the cell surface. Only molecules with a diameter smaller than the pores, the size of which is specific to the plant food studied (limiting Stokes' diameters of about 4 to 5 nm; 4.6 nm corresponds to a 41 kDa fluorescein-derivatized dextran), would have the ability

to permeate the plasma membrane (Baron-Epel *et al.*, 1988; Carpita *et al.*, 1979; Ehwald *et al.*, 1992). The diffusion of a molecule through the CW not only depends on the size of the pore but also on its conformation and flexibility.

In vitro experiments using alginate gel beads revealed that the pore size modulates the diffusion of pancreatic lipase inside the beads and consequently the rate of lipid digestion (Cheirsilp *et al.*, 2009; Li *et al.*, 2011b). When the beads were placed under gastric conditions they shrank, thus reducing the size of the pores, which in turn retarded the penetration of enzymes inside the beads and slowed down the digestion process, whereas under conditions identical to the ones found in the small intestine, the beads swelled and therefore increased their porosity. However, Li and co-workers demonstrated that the pore diameter of calcium alginate beads decreased when the pH rose (Li *et al.*, 2011b).

The organisation of the pectin molecules within the CW, in particular the network they form by covalent and cross-linkages, is an essential factor affecting its porosity (Baron-Epel *et al.*, 1988; Rondeau-Mouro *et al.*, 2008). Indeed, the removal of pectins in onion CW seems to enlarge the pore, which was originally approximately 10 nm, to 30-40 nm with a maximum of 60 nm (McCann *et al.*, 1990). The spacing between cellulose microfibrils maintained by hemicellulosic cross-links also plays a significant role.

1.5.2.4 Cell wall digestion

Because of the complexity of CW in terms of its constituents and more importantly, the inter- and intra-polymer chain linkages, it is difficult to digest it in the upper GIT of humans. For instance, mammals, including humans, lack the enzymes (e.g. cellulases) necessary to hydrolyse certain polysaccharides such as cellulose into its constituent monosaccharides (Beguin and Aubert, 1994). Human digestive enzymes (i.e. α-amylase and disaccharidases) can only hydrolyse α-1,4 glucan

bonds, even though the tight packing of cellulose microfibrils would obstruct the access of enzymes to the linkages (Brett and Waldron, 1996).

The undegraded CW material from the small intestine arrives in the colon where water-soluble polysaccharide components of the CW are more susceptible to being fermented by the microflora into SCFA, whereas most of the cellulose and hemicelluloses as well as cross-linked pectin remain intact (McDougall *et al.*, 1996). The SCFA are then absorbed and reach the bloodstream. Some CW can also be found undisturbed in the faeces (Ellis *et al.*, 2004). The differences in the extent of fermentation observed between different CW are likely to be due to their composition and the inter-polymer cross-links between soluble polymers since tissues with similar matrices but different linkage show different degrees of degradation (Fry, 1986).

1.6 Nutrient bioaccessibility in plant food

Bioaccessibility refers to the amount of nutrients or any other substance (i.e. phytochemicals) released from the food matrix and potentially available for absorption in the intestine (Parada and Aguilera, 2007). This term differs from **bioavailability,** which incorporates absorption, metabolism, tissue distribution and biological action of the nutrient (Fernandez-Garcia *et al.*, 2009). The definition of bioaccessibility could also include nutrients that are still enclosed within the cell but are available to digestive enzymes, as it is the case in plant foods with permeable CW such as durum wheat (Edwards, 2014).

Bioaccessibility is an important parameter since decreased macronutrient digestion and absorption may present some advantages for individuals who aim at reducing their calories consumption, but becomes problematic for those suffering from undernourishment in particular premature babies and

the elderly, and patients with diseases that require additional energy intake (e.g. certain cancers and HIV).

It is well established that not all the nutrients contained within a food are available for absorption; however consumers, scientists and health care providers often rely on the nutrient composition to assess the 'healthiness' of a food, as the information and understanding of nutrient availability in most foods is limited. This can lead to misconceptions about the health properties of a food. For instance, on the basis of nutrient composition information, almonds contain what may generally be considered to be an excessive amount of calories and lipid, however only a proportion of that lipid may actually be absorbed (Novotny *et al.*, 2012). Furthermore, almonds contain phytochemicals and other nutrients (Yada *et al.*, 2011), that have potential health benefits in relation to heart disease, diabetes and obesity, and may therefore be healthier than what is conveyed on the nutrition label.

Accumulating evidence shows that the structure and properties of plant foods (e.g. legumes, cereals and nuts), particularly of CWs, play an important role in regulating the release/availability of nutrients (i.e. lipid and starch) from plants foods during mastication and digestion (Berry *et al.*, 2008; Butterworth *et al.*, 2012; Ellis *et al.*, 2004; Lemmens *et al.*, 2010; Mandalari *et al.*, 2008a; Tydeman *et al.*, 2010; Waldron *et al.*, 2003). In order to be digested, the nutrients have to be released from the food matrix and thereby available for digestion at the appropriate site of the GIT (upper segments of the small intestine for lipid). However, a significant proportion of CW may remain intact despite mastication and other phases of the digestion process, thus affecting the rate and extent of nutrient digestion and the postprandial blood response (e.g. postprandial glycaemia and insulinaemia).

As an example, in an early study, the consumption of bread containing coarse particles in which starch was encapsulated by CWs was found to attenuate the rise of blood glucose and insulin, compared with the blood glucose response observed after consumption of an identical bread in which the CW were disturbed by the milling process (Holm and Bjorck, 1992). Such studies highlight the importance of physical encapsulation of starch by CWs, but rarely provided any profound insight

of the behaviour of CWs. More recently, faecal analysis showed that after ingestion of almonds a significant proportion of lipid remains enclosed inside the parenchyma cells of almond cotyledon (Ellis *et al.*, 2004). Moreover, the amount of fat recovered in the faeces of individuals who consumed whole peanut was greater that when they ate either peanut butter, peanut flour or peanut oil (Traoret *et al.*, 2007).

1.7 Almond as a model

1.7.1 Health and almond consumption

Almond seeds have been selected as a 'food model' for studying lipid release because of their high lipid content (Yada *et al.*, 2011) and widespread consumption in the UK and worldwide (Almond Board of California, 2013). Almonds are consumed predominantly in the raw, sliced or roasted forms, although marzipan as well as almond butter and milk are also commonly found. They are principally eaten as a snack but they also contribute to the composition of various sweet (cakes, biscuits, etc.) and savoury (e.g. salads, curries and tajines) dishes. According to the Food and Agriculture Organization (FAO), the annual world production of almond has been estimated to be about 2,300,000 metric tons of shelled product in 2009 (Food and Agriculture Organization of the United Nations, 2009). The main producing countries are USA (California), Spain, Syria and Italy.

Also, a reason for choosing almond as food model is that there is an interest in the effects of its consumption on postprandial metabolism and long term health, notably cardiovascular risk reduction (Berry *et al.*, 2008; Ellis *et al.*, 2004; Mandalari *et al.*, 2008a). Human studies have shown that almonds decreased fasting plasma low-density lipoprotein (LDL) and oxidised-LDL cholesterol, postprandial glycaemia and insulinaemia, and oxidative damage (Cohen and Johnston, 2011; Jenkins *et al.*, 2006; Spiller *et al.*, 2003). The consumption of nuts and almond seeds was associated with a

beneficial effect on risk factors for a number of conditions such as obesity, CVD and type 2 diabetes (Joice *et al.*, 2008; Sabate and Ang, 2009). Some of these benefits, in particular counteraction of oxidative damage, could be attributed to the polyphenol and antioxidants present in the almond skin (Bolling *et al.*, 2010). On the other hand, the type of lipids constitutive of almonds and more importantly their potentially limited bioaccessibility are likely to promote lower postprandial lipidemia (Berry *et al.*, 2008; Mandalari *et al.*, 2008a), and thereby reduce the symptoms of CVD (Hu and Stampfer, 1999; Jenkins *et al.*, 2002a). The physical properties of almonds in limiting nutrient release, the possible effects of masticated almonds on gastric emptying and the presence of phenolic from the skins may also contribute to the explanation of why almonds improve glycaemic control and type 2 diabetes (Li *et al.*, 2011a; Lovejoy *et al.*, 2002).

1.7.2 Almond anatomy and composition

1.7.2.1 Macroscopic structure

The sweet almond *(Amygdalus communis* L.) belongs to the *Rosaceae* family. Almond is a drupe[2] of which the only edible part is the kernel (seed) (Vaughan, 1970). The latter is composed of an embryo (two cotyledons), surrounded by a skin also called testa or seed coat. The pericarp, which encloses the seed, contains a green fleshy hull and a hard pitted shell (Figure 1.14). The Nonpareil variety used in this project has a soft shell, light in colour and with a high suture opening. The almond (i.e. kernel) has a medium size, flat shape and smooth surface.

[2]Fruit that possesses simultaneously fleshy (mesocarp or hull) and stony (endocarp or shell) layers surrounding the seed (Armstrong, 2009).

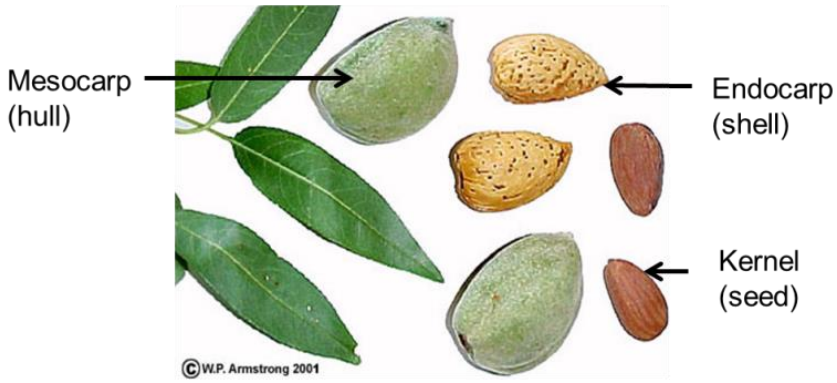

Figure 1.14 Almond (Amygdalus communis L.) anatomy (Armstrong, 2009).

1.7.2.2 Microscopic structure

The cotyledons (i.e. the white lipid-bearing tissue) are made of rounded cells, principally parenchymal, with a relatively thin CW (about 0.1 µm) (Figure 1.15). Pigmented sclerenchyma (outer layer) and parenchyma cells as well as xylem tissue compose the testa (Mandalari *et al.*, 2010a). The testa cells possess a secondary CW which is confirmed by the presence of a significant amount of lignin (Femenia *et al.*, 2001). A layer of aleurone cells, containing globoid crystals as well as protein and lipid bodies, forms the endosperm that separates the testa (spermoderm and perisperm) from the cotyledon (Winton and Winton, 1932).

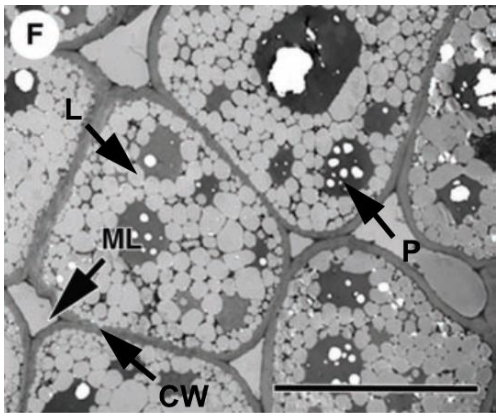

Figure 1.15 Transmission electron micrographs of cross section of parenchymal cells of almond cotyledon. L: oil body, P: protein body, CW: cell wall, ML: middle lamella. Scale bar: 20 µm (Ellis et al., 2004).

1.7.2.3 Nutritional composition

Brown pigments are found in the testa while the cotyledons contain intracellular oil bodies (OBs, transparent droplets of approximately 1 to 5 μm of diameter) as well as darker, larger inclusions enclosing proteins (Figure 1.15). The major storage protein found in almond, sometimes called amandin or almond major protein, belongs to the legumin class of seed proteins, itself part of the globulin family (Kshirsagar *et al.*, 2011; Osborne and Campbell, 1896). Globulin proteins are classified according to their sedimentation coefficient, with the legumin type being 11S. Amandin accounts for about 70% of the total soluble proteins. Along with 2S albumin, conglutin and profilin, the protein is responsible for the food allergy reactions observed in certain individuals (Alasalvar and Shahidi, 2009). It has a hexameric structure and each of the six subunits is composed of two polypeptides (α-chain of about 45 kDa and β-chain of about 20 kDa) linked by a disulphide bridge, giving the molecule a molecular weight (MW) of approximately 450 kDa (Sathe *et al.*, 2002).

Lipids, predominantly triacylglycerol, are assembled into OBs. These organelles are delimited by a monolayer of phospholipids in which oleosins, integral proteins, are embedded (Beisson *et al.*, 2001b; Tzen *et al.*, 1993) (see *Chapter 7* for more details). Depending on the harvest and variety, the kernel is made of approximately 50% of lipids of which 70-80% is oleic acid, 15% linoleic acid and 5% palmitic acid (Yada *et al.*, 2011). Compared to other tree nuts, almond has a low amount of total and saturated fatty acids, but nonetheless a significant proportion of PUFA and MUFA acids, with oleic acid being the predominant fatty acid (United States Department of Agriculture, 2010).

Almond seed carbohydrate (e.g. sugars and starch) and DF (mainly non-polysaccharides) contents are about 5.5% and 11.8%, respectively (Ellis *et al.*, 2004). Almond is also rich in micronutrients, mainly manganese, magnesium, copper, phosphorus and vitamin E. The mineral reserves of the seed are present in the form of crystals such as calcium oxalate (Dourado *et al.*, 2004). The almond seed coat or skin also contains a significant amount of lipid, protein and DF as well as phenolic

compounds, such as *p*-hydroxybenzoic acid, catechin and quercetin, which potentially contribute to the skin's antioxidant properties (Mandalari *et al.*, 2010b; Milbury *et al.*, 2006).

1.7.2.4 Roasting of almonds

The roasted almonds used in this project were roasted by the Almond Board of California using a two-steps standard procedure of hot air roasting with typical temperatures ranging from ~130 to 154°C. The first step employed an intermediate temperature to stabilize the nut microstructure, and the second step was performed at a higher temperature in order to generate the distinctive roasted flavour and brown colour of the cotyledon. Thus, during roasting, moisture evaporates, and the Maillard reaction takes place which is a complex reaction between reducing sugars and amino acids and is responsible for the brown colour.

This process was shown to lead to very little weight variation in whole almond; most of the loss being attributed to water evaporation (Perren and Escher, 2013). However, the OBs and the endoplasmic network were destroyed, and the volume of extracellular pores enlarged. Roasting can therefore greatly affect the structure of almond cells, CW as well as OBs as demonstrated elsewhere (Pascual-Albero *et al.*, 1998). In Pascual-Albero study, OBs appeared to coalesce to form larger oil droplets than the ones observed in raw almond cells.

1.7.3 Existing evidence on almond and lipid bioaccessibility

Our group previously showed that only the first outer layers of cells of almond particles fracture by mechanical trituration or chewing, so that most of the parenchyma cells of almonds remain intact and therefore contain encapsulated lipid (Ellis *et al.*, 2004). However, in a subsequent study in ileostomy volunteers, the lipids present in the intact cells located underneath the fractured layers,

appeared to 'leach' from the intact cells, but only after a prolonged incubation in the upper GIT (Mandalari *et al.*, 2008a). Indeed, almonds collected in ileostomy volunteers after 12 h digestion showed cells with a thicker (swollen) CW (~1.2 µm) than after 2 h digestion (~0.6 µm) and undigested cells (0.1-0.2 µm) (Figure 1.16). This swelling of the CW may explain why intact cells lose lipid after longer retention time, suggesting that lipase, colipase and BS could diffuse into the intracellular compartment and proceed with the lipids digestion. It has been suggested that the CW swelling is mainly attributed to the degradation and solubilisation of pectic compounds present in the CW and middle lamella (Baron-Epel *et al.*, 1988; Femenia *et al.*, 2001; Waldron *et al.*, 2003). Nonetheless, it remains unclear to what extent lipolysis occurs inside those cells and whether the lipids are able to leave the cells as TAG molecules or hydrolysed products. Regardless of the pathway used, the rate of digestion of the lipids present in those unfractured cells is likely to be reduced given that they are less accessible to emulsification and digestion by the lipases.

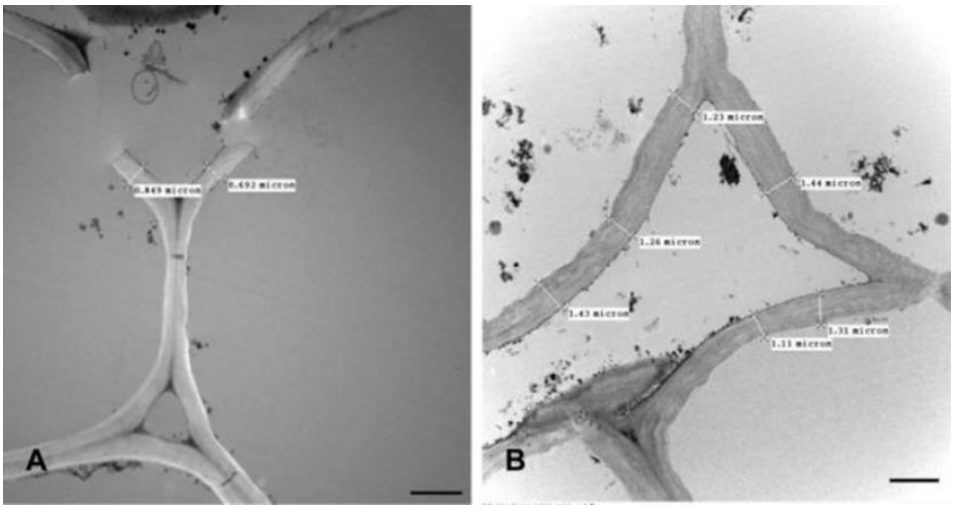

Figure 1.16 Sections of digested almond tissues recovered from ileostomy volunteers visualised by transmission electron microscopy after 2 h (A) and 12 h (B) of digestion. Scale bars: 2 µm (Mandalari et al., 2008a).

The released lipids seem to coalesce and form droplets (size ~10-40 µm) at the surface of the ruptured cells, thus becoming available for lipolysis by the lipases. The study by our group also showed that the cells of the almond cotyledon behave in a fairly predictable way as they fracture

rather than separate after chewing (Ellis *et al.*, 2004), most likely due to their strong cell-cell adhesion (Waldron *et al.*, 2003).

Collection of faeces after ingestion of almond revealed the presence of significant amounts of almond tissues (cotyledon and testa) (Ellis *et al.*, 2004) (Figure 1.17). Some of the cells were found intact, whereas others contained bacteria that seemed to be utilising (i.e. fermenting) both intracellular nutrients (including lipid) and CW polysaccharides (notably pectic substances). Indeed, the erosion of CWs, the presence of virtually empty cells (i.e. no intracellular nutrients) and bacterial replication provide some evidence for the potential role of almonds as a source of nutrients for the gut microflora. Also, Mandalari and colleagues have confirmed the prebiotic role of almonds and that the lipid components of almonds are susceptible to fermentation (Mandalari *et al.*, 2008b). Moreover, since the lipids provide most of the energy contained in the almond, undigested lipids excreted in the faeces could facilitate body weight management. This hypothesis has been confirmed by the measurement of metabolisable energy content of almond (Novotny *et al.*, 2012). The findings indicated that the energy values of raw almond calculated using the conventional Atwater factor overestimate the actual energy absorbed by about 32%.

A digestion model simulating the gastric environment provided contradictory information on the behaviour of almond particles in the digestive tract (Kong and Singh, 2009a). Almond cells appeared to separate following the acidic hydrolysis of the middle lamella, which lessened the cell-cell adhesion. The authors also detected the presence of breach and breakage in CW causing the release of nutrients into the extracellular environment and/or the penetration of enzyme and digestive material into the cells. However, there are serious doubts about the quality of the micrograph images and the microscopy methods used to produce them (Dr Mary Parker, Personal Communication). Also it is unsure that the model used reproduced accurately/appropriately the physical and chemical processes occurring in the stomach. Clearly this is an area that requires further investigation.

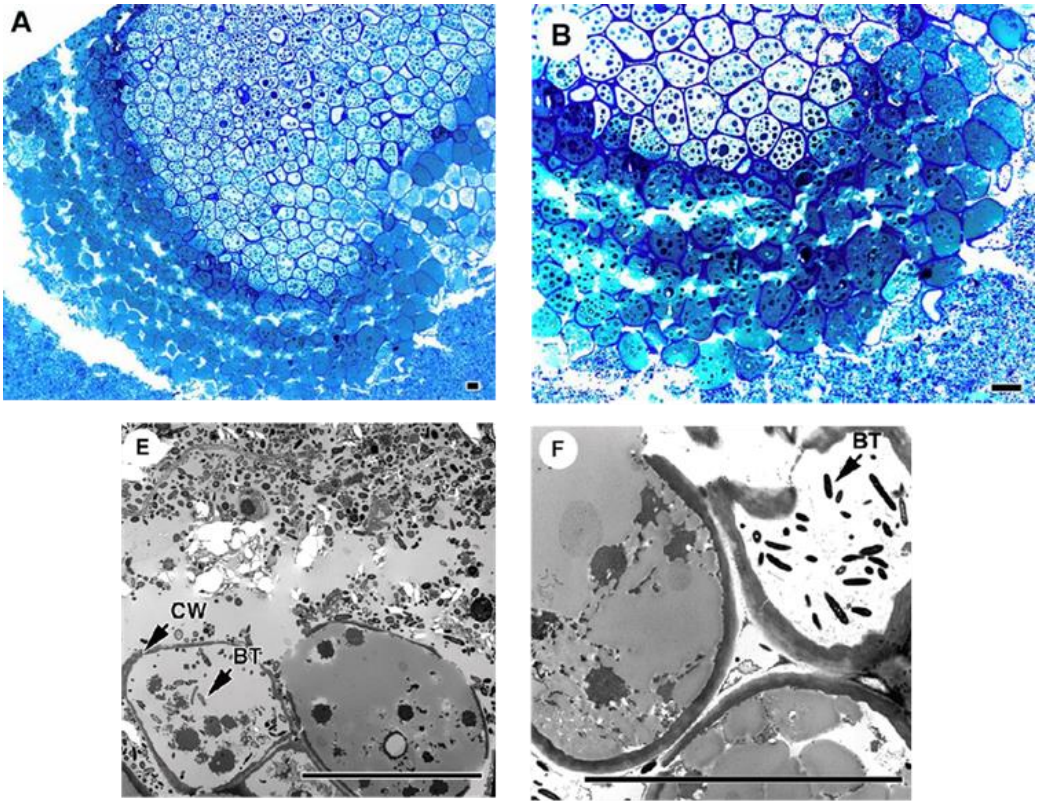

Figure 1.17 Sections of almond tissues recovered from human faeces visualised by light (A and B) and transmission electron (E and F) microscopy. CW: cell wall; BT: bacteria. Scale bars: 20 µm (Ellis et al., 2004).

In vitro (Mandalari *et al.*, 2008a) and *in vivo* (Berry *et al.*, 2008) studies revealed variations in lipolysis rates and postprandial blood TAG concentrations between meals containing different forms of almond (whole natural, blanched, milled flour, free oil, etc.), which were mainly attributed to differences in lipid release (bioaccessibility). In the oil form, lipids were highly available and therefore fully digested (leading to a high concentration of TAG in the blood), whereas encapsulated nutrients (whole almonds) did not lead to a postprandial response as rapid and strong as the almond oil (Berry *et al.*, 2008). These results strengthen the assumption that by increasing the number of fractured cells through either processing or mastication, the bioaccessibility of nutrients, especially lipids, is improved.

However, little is known about the exact structural organisation of the almond CW since this structure has not been investigated specifically and, as highlighted by McDougall and colleagues (McDougall *et al.*, 1996), each cell type has a distinct wall composition. For instance, the plasmodesmata have been identified in different tissues of angiosperms (flowering plants) especially parenchyma cells (Esau, 1977), but it is not clear that they are present in seeds. Furthermore, the precise molecular composition and spatial arrangement of the polysaccharides constitutive of the CW has not been completely delineated. Nevertheless, almond CWs may have a structure and composition similar to onion (dicotyledon) (McCann *et al.*, 1992), the main difference being in the water content. Dourado *et al*, 2004 established that the CW of the seed, testa excluded, was mainly pectin (Dourado *et al.*, 2004). Other studies have found that the CWs of almond seed cotyledon are rich in arabinose, uronic acid, glucose, xylose and galactose, which implies that the CW is composed of arabinose-rich polysaccharides (Ellis *et al.*, 2004; Femenia *et al.*, 2001). The CW of almond testa also contained arabinose, galacturonic acid, glucose, xylose and galactose, but their proportion are different and mannose, rhamnose and fucose are also part of their constitution (Mandalari *et al.*, 2010a). Quantitative and qualitative analysis of the carbohydrates that comprise the CWs of digested (*in vitro*), finely ground almonds revealed that they were not degraded during digestion; however, the intracellular contents, mainly lipid and protein, were degraded by the microorganisms originating from the human large intestine (Mandalari *et al.*, 2008b). By comparing the growth of faecal bacteria cultures between almond seeds with normal lipid content and defatted ones, they also confirm the assumption made by Ellis and colleagues that bacteria utilise almond lipids as a source of energy for growth and maintenance.

1.8 Project aims and objectives

It was hypothesised that CW of the parenchyma cells of almond cotyledon fracture when masticated and therefore liberate the intracellular content, whereas intact CW structures would delay or prevent the release of intracellular lipids and their digestion and absorption in the intestine.

The main objectives of this project were to:

(a) Assess the effect of mastication on CW integrity and lipid content from fractured and intact cells by factoring in particle size data into a theoretical model previously developed to predict lipid release (**Chapter 3**);

(b) Assess the effect of digestion on lipid release and CW permeability using two digestibility models, i.e. static and dynamic processes using the Dynamic Gastric Model (DGM) developed by our collaborators at the Institute of Food Research (IFR) in Norwich (**Chapter 4**);

(c) Determine the rate and extent of the kinetics of lipid digestion on raw and roasted almond materials with various degrees of bioaccessibility using a simple duodenal digestion model (**Chapter 5**)

(d) Quantify lipid losses during the gastrointestinal digestion (i.e. DGM and an ileostomy volunteer) of two almond meals of different bioaccessibility and examine the microstructure of the recovered almond tissue (**Chapter 6**);

(e) Investigate the potential penetration of lipases through the CW matrix of almond seeds (**Chapter 7**).

CHAPTER 2

MATERIALS AND METHODS

2.1 Introduction

The approach employed for this project was multidisciplinary and combined the use of various *in vitro* and *in vivo* methods in order to improve our understanding of the mechanisms by which nutrients are released during digestion and in particular the role played by plant CWs. In order to successfully estimate the degradation/digestion of almonds within the different compartments of the GIT, while employing consistent and well-controlled conditions, a combination of *in vitro* models were used which included dynamic and static gastrointestinal models.

The mastication study, a randomised cross-over design, was used to compare the effects of mastication on the particle size and microstructure of raw and roasted almonds (*Chapter 3*). Some of the masticated almond samples were loaded onto the dynamic gastric (DGM) and static duodenal (SDM) models (*Chapter 4*). The DGM and SDM, which were developed at the IFR (Norwich), were designed to simulate the biochemical as well as biomechanical processes occurring during digestion in the human stomach and small intestine (Wickham *et al.*, 2009). The digested almond samples were also analysed for particle size and for changes in microstructure to compare the effects of *in vitro* digestion to those in humans. Lipid losses were determined using both the traditional AOAC method (Soxhlet) and the theoretical model developed by our group (Grassby *et al.*, 2014). Information on the particle size distribution (PSD), based on the number of particles of each size, for masticated and digested almonds were required in order to calculate the amount of lipid released in a more realistic situation. The measurement of monosaccharides of hydrolysed CW polysaccharides was performed at the IFR using a standard method of sugars analysis, and also by Prof William Willats and his team at the University of Copenhagen, who used a number of polysaccharide specific antibodies to determine the polysaccharide composition.

Alongside these analyses, the kinetics of lipid digestion was studied on various materials - emulsions, almond cells and almond particles of various sizes, using the pH-stat and gas liquid chromatography

(GLC) (*Chapter 5*). These methods permitted the monitoring of the rate and extent of lipolysis of almond samples that varied in structural complexity (e.g. pure oil versus separated cells) and particle size, and therefore the amount of encapsulated lipid in almond tissue. Microscopy was also used to characterise the structural changes in almond samples following digestion.

A second human study was carried out in ileostomy volunteers, the Biogut study (*Chapter 6*), with the aim of quantifying nutrient loss (lipid or starch) at the terminal ileum from meals (almond or wheat) predicted to have high and low bioaccessibility values, and then comparing these values to subsequent blood glucose or lipid responses. Effluents and blood were collected at different time points. In this study, the amount of lipid (Study 1) or starch (Study 2) lost from the ruptured cells (i.e. potentially bioaccessible) were quantified using Soxhlet extraction for lipid and standard chemical methods of analysis for starch (a modified version of total starch assay procedure from Megazyme). Effluent samples were examined by light and transmission electron microscopy. The structural examination focused on CW integrity and providing evidence of lipid/starch loss from ruptured and intact cells. Postprandial blood concentration of glucose, TAG, NEFA, insulin, and C-peptide were measured after eating the test meal as well as the gut hormones PYY, CCK, GLP-1 and GIP.

Finally, the potential diffusion of various digestive lipases through almond CWs was investigated (*Chapter 7*). By comparing the extent of lipolytic hydrolysis between encapsulated (almond cells) and accessible lipid bodies (OBs), it was possible to obtain a better insight of the role of the CW in nutrient digestion. This work was performed in collaboration with Dr David Gray from the University of Nottingham (UoN), Prof Frédéric Carrière from the Laboratory of Enzymology at Interfaces and Physiology of Lipolysis (EIPL) in the Centre National de la Recherche Scientifique (CNRS) in Marseille as part of the InfoGest Short-Term Scientific Missions (STSM), and also Dr Alan Mackie from the IFR.

2.2 Materials

2.2.1 Almond materials and emulsion preparations

2.2.1.1 Almond and almond particles

Raw and roasted almond kernels were kindly provided by the Almond Board of California (*Amygdalus communis L.*; variety, Nonpareil). The average nutrient content of the raw and roasted almonds used in this project was provided by the Almond Board of California (Table 2.1). The DF value is a reflection of the CW content, mostly non-starch polysaccharides, of the almond seeds.

Table 2.1 Nutritional composition of raw and roasted almonds, performed by Covance Laboratories Inc. (Madison, United States) on behalf of the Almond Board of California.

	Raw	**Roasted**
Proximates		
Energy (Kcal/100g)	617	625
Protein (%)[1]	20.1	20.7
Lipid (%)[2]	**51.7**	**52.4**
Carbohydrate (%)	22.4	23.4
Sugar (%)	4.6	4.8
Dietary fibre (%)	11.0	10.6
Moisture (%)	5.1	2.7
Ash (%)	2.7	3.4
Fatty acids		
Saturated (%)	**4.0**	**3.8**
16:0 Palmitic	*3.3*	
18:0 Stearic	*0.6*	
Monounsaturated (%)	**34.6**	**32.9**
18:1 Oleic	*33.5*	
Polyunsaturated (%)	**11.1**	**10.9**
18:2 Linoleic	*11.1*	

[1]Dumas method (N x 1.58). [2]Soxhlet method

Almond particles of different sizes (Figure 2.2) were obtained by grinding almonds in a coffee blender (Lloytron PLC, Lancashire, UK) before sieving and collecting the particles from the sieves of 1000, 500

and 250 µm aperture as well as a sieve base (size < 250 µm). For the ileostomy study, two size ranges of particles were used to make the muffins: 1700 to 2000 µm and < 450 µm. The large particles were obtained by grinding the raw almonds and using two sieves (1700 and 2000 µm apertures). Flour provided by the Almond Board of California was sieved using a 450 µm sieve. The original flour was generated from the same variety of almond (*Amygdalus communis* L; variety, Nonpareil) with a commercial grinder (Maseto Technologies, Alicante, Spain). This process permitted the production of particles of sufficiently small sizes and also prevented their aggregation.

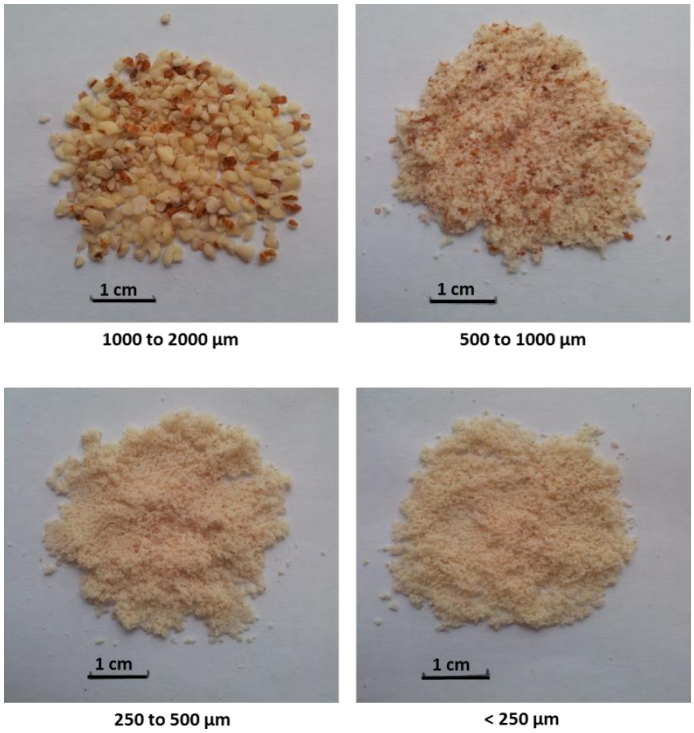

Figure 2.1 Photographs of particles with the different size ranges used (1000 to 2000, 500 to 1000, 250 to 500, and < 250 µm). Scale bars = 1 cm.

2.2.1.2 Separated almond cells

Almond particles (about 2-3 mm^3) were left for 4 weeks with rotation in a solution of 50 mM cyclohexanediamine tetraacetic acid (CDTA) and a preservative (5 mM sodium metabisulphite, $Na_2S_2O_5$) at pH 7 (Jarvis, 1982; Mandalari *et al.*, 2014). The particles were briefly rinsed and then

mashed using a mortar and pestle to a paste consistency. The sample was loaded on a stack of 3 sieves - apertures 90, 63 and 53 µm and a 20 µm nylon mesh, with a base to collect the liquid. After elimination of most of the water, the material present on the nylon mesh was then transferred into a dialysis membrane (Float-A-Lyzer G2 10 mL, 3.5-5Kd). The membrane was placed in phosphate buffer (10 mM, pH 7) for about 4 h; the operation was repeated 4 times as recommended by the manufacturer. The dialysis permitted the removal of CDTA from the separated cells, since CDTA is known to inhibit lipase activity (Weaber *et al.*, 1971). Even though the majority of almond cells obtained in this way were intact, the preparation always contained a small proportion of damaged cells, with their intracellular content missing (Figures 5.5 and 7.2).

2.2.1.3 Emulsions

Powdered β-Lg was donated by Davisco Foods International (Lot # JE 002-8-415, Le Sueur, MN, USA). Almond oil from *Amygdalus communis L.*, glyceryl tributyrate (99%) and glyceryl trioleate (65%) were obtained from Sigma (Poole, Dorset, UK) and roasted almond oil from Huilerie Croix Verte (Neuillé, France). β-Lg solution was prepared by dissolving 1% w/w of powdered β-Lg into 10 mM Phosphate buffer and stirring for at least 2 h. Emulsions were made from either synthetic lipids commonly used to assess lipase activity, tributyrin and triolein, or from raw and roasted almond oils. Tributyrin is composed of butyric acid and triolein of oleic acid. Raw and roasted almond oils contained approximately 64.1 and 63.1% of oleic acid, 26.1 and 25.9% of linoleic acid and 6.8 and 7.2% of palmitic acid, respectively (fatty acid analysis was performed by GLC as described in *Section 2.3.1.2.2*). Almond emulsions (Figure 2.2) were obtained by pre-emulsifying 1.6% w/w of oil in β-Lg solution using a homogeniser (Ultra-Turrax T25, IKA® Werke, from Fisher Scientific Ltd) for 1 min at 11 000 rpm. The pre-emulsion was then sonicated using an ultrasonic processor (Vibracell, Sonics & Materials Inc, Newtown, USA) equipped with a 6 mm high grade titanium alloy probe at 70% amplitude for 2 min.

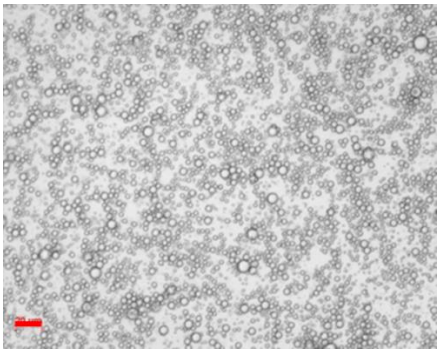

Figure 2.2 Light micrograph of almond oil emulsion. Scale bar = 20 µm.

2.2.1.4 Oil bodies

OBs (Figure 2.3) were isolated from raw almond seeds using a method previously described (White *et al.*, 2009). Briefly, almond seeds were homogenised (Moulinex, Masterchef 650 duotronic, Windsor, UK) in water (ratio 1:4) with 2-3 drops of azide (0.2%, w/v) at full power for 2 min. The slurry was filtered through three layers of cheesecloth to remove almond particles and cell fragments. The filtrate was then centrifuged (Beckman J2-21 centrifuge; fixed rotor JA-10) at 9936 g, 4°C for 20 min. The upper layer (creamy white pad) of each sample was removed with a fork and transferred into a bijou bottle, this pad is referred to as the **crude OBs**. **Washed OBs** were obtained by re-suspending the pad of crude OBs in either a 9 M urea or 0.1 M sodium bicarbonate ($NaHCO_3$) solution at a ratio of 1:4 (OB: washing solution). The dispersion was vortexed and then centrifuged (Beckman J2-21 centrifuge; fixed rotor JS-7.5) at 9936 g, 4°C for 20 min. The creamy upper layer was removed and placed into new tubes. The operation was repeated three more times with water.

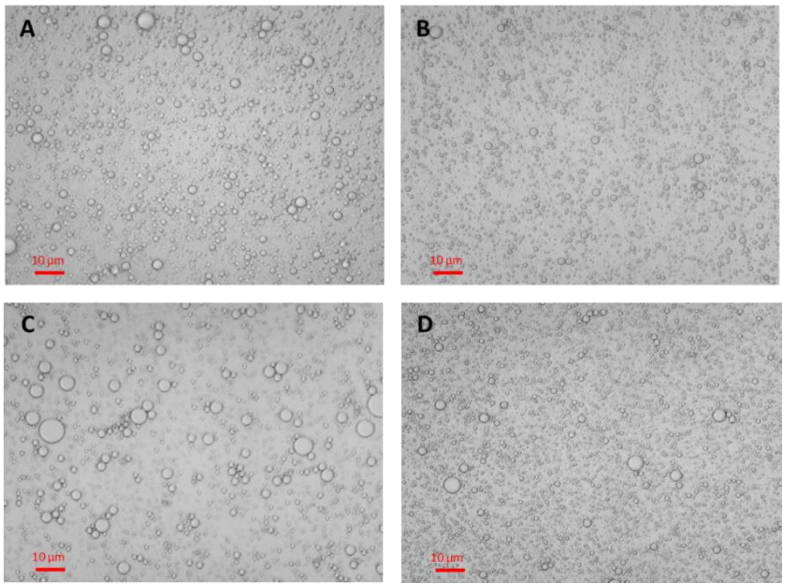

Figure 2.3 Light micrographs of crude raw (A) and roasted (B) almond oil bodies (10% v/v in water), urea-washed (C) and $NaHCO_3$-washed (D) raw almond OBs (10% v/v in water). Scale bars = 10 µm.

2.2.2 Chemicals

NaH_2PO_4 (99%), Na_2HPO_4 (99%), CDTA (98.5%), $Na_2S_2O_5$ (98-100.5%), Tris(hydroxymethyl)aminomethane (Tris, ≥ 99.9% TLC), NaCl (99.5%), $CaCl_2$ (93%), sodium taurodeoxycholate (NaTDC, ≥ 95% TLC), NaGDC (≥ 97% TLC), sodium dodecyl sulphate (SDS, ≥ 98.5% GC) and lipase from porcine pancreas type II (No. L3126, lipase activity 53 units/mg powder, where 1 unit corresponds to 1 µmol of butyric acid released from tributyrin per minute at 37°C, pH 8.0) were purchased from Sigma. NaTC (≥ 97% TLC) was obtained from Alpha Aesar. Rabbit gastric extract (RGE), porcine pancreatic extract (PPE), porcine pancreatic lipase (PPL), guinea pig pancreatic lipase-related protein 2 (GPLRP2), were gifts from Prof Frédéric Carrière (Director of the Laboratory of Interfacial Enzymology and Physiology of Lipolysis, Marseille, France). The internal standard for GLC analysis, C15:0 (pentadecanoic acid), was purchased from Nu-Chek-Prep, Inc (Elysian, USA).

2.3 Methods

2.3.1 Chemical characterisation

2.3.1.1 Moisture content

Samples were weighed into an appropriate container (aluminium dish for large samples or microtubes for OBs) and dried either by using a vacuum oven (Gallenkamp Vacuum Oven, Fistreem International Ltd, Loughborough, UK) or a bench-top freeze dryer (Model LP3, Jouan S.A., Saint-Herblain, France). They were then weighed for a second time to calculate the moisture content by difference. Approximately 200 mg of OBs were placed into microtubes in the vacuum oven at 40°C for 48 h. Freeze dried samples required to be frozen at -40°C beforehand, and then left in the freeze drier for about 3 days.

2.3.1.2 Lipid content

2.3.1.2.1 Crude lipids

The analysis of total lipid content done on **masticated** and ***in vitro* digested samples** (masticated raw and roasted almonds as well as almond muffins) was performed in Italy by Dr David Barreca and his team from the Dipartimento di Scienze Chimiche, University of Messina with an automated Soxhlet (Soxtec 2050) extraction using n-hexane as solvent (Mondello *et al.*, 2000). Following centrifugation of the samples (3800 g for 15 min), the liquid phase of the collected sample was removed; the remaining particles were then dried, weighed and analysed. Each sample was analysed in duplicate. Lipid loss was estimated by calculating the difference between the total lipid content of the original almond samples and the lipid content of the almonds post-mastication/post-digestion, but appropriately adjusted to account for the loss of almonds in the mouth. The results of lipid content were expressed as a percentage of dry weight.

The lipid content of **effluent samples** collected during the Ileostomy study was measured in our laboratory at KCL using the Soxhlet method with hexane as a solvent. Two to three grams of ground, freeze-dried effluent were placed in pre-weighed porous cellulose thimbles. After 24 h (non-consecutive) extraction, the thimbles where left in the fume cupboard for the hexane to evaporate. They were then dried overnight in a forced-air oven at 55°C. The mass of lipid extracted was determined by weight difference of the thimbles before and after the extraction, the results expressed as percentage of dry weight.

The lipids from the OBs were extracted by adding 500 µL of isooctane into 0.20 g of dried OBs. The tubes were homogenised into a FastPrep®-24 Instrument (MP Biomedicals, Cambridge, UK) for 30 seconds and microcentrifuged (MSE Micro Centaur, Sanyo, London, UK) at 13 000 g for 5 min. A known volume of the supernatant was pipetted and transferred into labelled Eppendorf tubes. The extraction was repeated 3 times. One millilitre of the pooled supernatant was poured into a bijou bottle and dried in a vacuum oven for a few hours. The isooctane remaining in the tubes was evaporated *in vacuo* and the pellet stored in the freezer at -20°C for protein analysis.

2.3.1.2.2 Fatty acids composition by gas liquid chromatography

Lipids present in the samples were first extracted using the Folch method then separated by fractionation. The recovered lipids underwent GLC separation in order to identify their constitutive FFA. The conversion of FFAs into apolar derivatives, fatty acid methyl esters (FAME), permitted their migration along the column using gas as mobile phase. The FFAs were eluted at different times depending on their polarity (chain length and degree of saturation) and boiling point, the fatty acids with the lowest boiling point and/or the most polar had the shortest retention time. The FFAs were then identified by comparing their retention times with those obtained from standards.

Folch extraction

In a 50 mL glass tube, 25 mL of chloroform/methanol (2:1, v/v) solution were added to 5 mL of sample (Folch *et al.*, 1957), plus 1 mL of 1 M HCl to terminate lipolysis and 80 µL of internal standard (IS) solution. IS was used to quantify the absolute amounts for all lipid species. The mixture was then frozen at -20°C until further analysis. The IS were weighed to four decimal place accuracy, and the exact weight recorded. For a reaction involving 300 mg of lipids and knowing that about 25% of IS are required, it was necessary to add 6.2 mg of pentadecanoic acid to 1 mL of chloroform. For each sample, 400 µL of the chloroform layer were collected and transferred into a glass tube. The samples were then evaporated to dryness in a heated centrifugal evaporator (Genevac SF50, Genevac Ltd., Ipswich, UK) connected to a pump (Büchi Vac® V-500, Büchi Labortechnik AG, Flawil, Switzerland) for about 45 min to 1 h. The dried extracts were dissolved in 50 µL chloroform and FFA from neutral lipids (TAG, DAG and MAG) separated by solid phase extraction based on a method previously described (Ruiz *et al.*, 2004).

Solid phase extraction

The separation of the lipids into their different classes was performed using a 20-port vacuum manifold coupled to a vacuum pump and LRC cartridges (Agilent HF Bond Elut LRC-NH2, Agilent Technologies UK Ltd., Wokingham, UK). All neutral lipids were eluted with 2 x 2 mL of chloroform/isopropanol (2:1, v/v) solution, and the FFA with a chloroform/methanol/acetic acid (100:2:2, v/v) solution. Each fraction was evaporated to dryness in the heated centrifugal evaporator.

Gas liquid chromatography

FAME were obtained by dissolving each sample into 1.8 mL of acidic methanol and toluene (80:20). The tubes were placed in the incubator at 60°C for 2 h (or 40°C overnight). $NaHCO_3$ was dissolved in

deioinsed water to obtain a 6% solution, 5 mL of the solution were then added in each tube. After 10 min centrifugation at 4°C, for each tube the toluene layer containing the FAME was pipetted into gas chromatography vials. FAME were quantified using GLC (7890A, Agilent Technologies UK Ltd, Wokingham, UK) equipped with a column injector port 25 m x 0.22 mm (i.d.), 25 µm film thickness (BPX70, SGE Europe Ltd, Cat no. 054602, Milton Keynes, UK), an auto-injector, EPC split inlet and a flame ionization detector (FID). The capillary column was operated with the following parameters:

-Injection volume:	1 µL
-Injection mode:	Split (ratio 50:1)
-Inlet temperature:	240°C
-Detector temperature:	250°C
-Carrier gas:	Hydrogen
-Hydrogen detector gas flow:	30 mL/min
-Air detector gas flow:	400 mL/min
-Combined flow:	35 mL/min
-Make up flow:	On
-Make up gas:	Nitrogen
-Oven program:	Initial temperature 160°C for 4 min, increased to 200°C in 1 min, hold that temperature for 6 min, increased to 240°C in 1 min with a final hold time of 5 min. The total run time was 29 min.

The fatty acids were identified by comparing their relative retention time with those of standards (Sigma Aldrich, Cat no. 1891-1AMP, Dorset, UK). The quantity of FFA was determined using the C15 IS and were expressed in micromoles (µmol):

$$n_i = \left(\left(\frac{A_i}{A_{IS}} \right) \times w_{IS} \right) \div M_i \qquad \text{(Eq. 2.1)}$$

where n_i is the number of moles of the fatty acid, A_i the area under the curve for the fatty acid, A_{IS} the area under the curve of the IS, w_{IS} the weight of the IS and M_i the MW of the fatty acid. The total amount of FFA was obtained by summation of the n values.

2.3.1.2.3 Fatty acids composition by thin layer chromatography (TLC)

Lipids were extracted by Folch extraction as described above. Standards and samples (15 µL) were spotted on thin layer silica gel 60 plates (10×20 cm from Merck) using a Linomat IV apparatus (Camag, Muttenz, Switzerland) equipped with a 100 µL dosage syringe (Camag, Muttenz, Switzerland). The plate was then placed into a tank containing a mixture of heptane/diethyl ether/formic acid (40:36:1, v/v/v) for the separation of neutral lipids, or methyl acetate/1-propanol/chloroform/methanol/0.25% potassium chloride (25:25:25:10:7, v/v/v/v/v) for the separation of phospholipids, and left to migrate for about 10 min. Once dried, the plate was sprayed with a saturated aqueous solution of cupric acetate with 85% phosphoric acid (1:1, v/v). The liquid was left to evaporate for 10 min and the plate placed in the oven at 180°C for 10 min.

2.3.1.3 Protein analysis

2.3.1.3.1 Protein content

Determination of the protein content was performed using a bicinchoninic acid (BCA) assay (Sigma's kit Product # BCA1-1KT). Similar to the Lowry method, the BCA assay is based on the reaction of Cu^{2+} with protein in an alkaline environment, so that cysteine, cystine, tryptophan, tyrosine, and the peptide bond reduce Cu^{2+} to Cu^{1+} (Wiechelman *et al.*, 1988). The amount of Cu^{2+} that reacted with proteins can then be monitored with the use of bicinchoninic acid (Smith *et al.*, 1985). When bound

to Cu^{1+}, the reagent has an intense purple colour; the amount of reduction, or intensity of the colour, is proportional to the protein present. The method presents the advantages of being easy to use, having great sensitivity and less interference by other substances compared with other procedures such as the popular Lowry or Bradford methods.

The assay was prepared according to Sigma's protocol (No. BCA1). Sixteen millilitre of Reagent A (BCA, sodium carbonate, sodium tartrate, and sodium bicarbonate in 0.1 M NaOH) was combined with 0.32 mL of reagent B (4% w/v, copper (II) sulphate pentahydrate) to obtain the BCA working reagent. One part of protein solution (standard or sample) was added to 20 parts of working reagent, and then left to incubate for 30 min in a water bath set to 37°C. A standard curve was obtained with known concentrations (ranging from 200 to 1 000 µg/mL) of Bovine Serum Albumin (BSA). The absorbance was then read for each sample relative to a reagent blank at 562 nm on a spectrophotometer (CE 2041, Cecil instruments, Cambridge, UK). The protein content present in the samples was calculated from the standard curve. Each sample analysis was performed in triplicate.

Before being analysed with this BCA method, the protein layer from the defatted OB samples (*Section 2.3.1.2.1*) was sonicated for ~1 min and 1 mL of 2% (w/v) SDS added to it. The samples were heated at 60°C for 30 min, vortexed for 1 min and centrifuged at 13 000 g for 3 min. The supernatant was collected and diluted 100 fold with 2% SDS.

2.3.1.3.2 SDS-PAGE

Proteins were separated by SDS-PAGE using 12% (w/v) polyacrylamide resolving gel made by mixing together 4.9 mL of deionised water, 6.0 mL 30% (w/v) Bis-acrylamide, 3.8 mL separating gel buffer (1.5 M Tris-buffer, pH 8.8), 0.15 mL 10% (w/v) SDS, 0.15 mL ammonium persulphate (APS, 10% (w/v)) and 8 µl TEMED. The gel was pipetted between 2 glass plates hold together by a casting frame, water

added to the top, and left to polymerize for 20 min. Once formed, the water was removed from the plates, a stacking gel containing 4.1 mL of deionised water, 1.0 mL of 30% (w/v) Bis-acrylamide, 0.75 mL stacking gel buffer (0.5 M Tris-HCl buffer, pH 6.8), 0.60 mL 10% SDS, 0.60 mL APS and 5 µl TEMED, was poured on the top of the separating gel, a comb inserted to make the wells and left to set for another 20 min. Meantime, the samples were prepared by adding 3 mg of dried OBs into 200 µL of IPG buffer (2 M thiourea, 7 M urea, 2% (w/v) CHAPS and 0.0125% (v/v) bromophenol blue), the mixture was then diluted 1/10 into Laemmli buffer (450 µL of laemmli solution, 50 µL of β-mercaptoethanol and 350 µL of water) and heated for 10 min at 95°C. The samples and marker (Precision Plus Protein™ unstained standards, #161-0363, from Biorad) were loaded onto the gel. The plates were placed into the inner chamber assembly of the SDS-PAGE electrophoresis (Bio-Rad mini-protean tetra cell SDS), which was then transferred into the mini-tank filled with running buffer (25 mM Tris, 250 mM Glycine, 0.1% (w/v) SDS, pH 8.3). After electrophoresis (120 V for 1 h 20 min), the gel was stained (1 h) with Coomassie brilliant blue R-250 and destained (overnight) with destaining solution (Bio-Rad Coomassie Brilliant Blue R-250 destaining solution). The gel was imaged using a BIO-RAD GS-800 densitometer and images were processed using PDQuest Quantity-one (Bio-Rad, Hercules, USA).

2.3.2 Particle size analysis

The dimension of the particle is an important parameter that influences the physical properties (dissolution, stabilities of dispersion, etc.) of a material such as that used in the current study where size and shape are likely to affect the bioaccessibility of the nutrients (lipids) contained in the food (almonds). The sphere is the only particle shape that can be described with a unique number, hence its choice for most particle size analysis (Figure 2.4). Since many materials have particles of irregular shape (non-spherical), a common way of defining particle size is to use an **equivalent sphere diameter** the definition of which varies depending on the technique used (Washington, 1992). It can

be expressed, for instance, in term of sieve aperture, volume or surface area, which refers to the measure of the diameter of the sphere that either passes through the same sieve aperture, has the same volume or the same surface area as the particle (Figure 2.5). The **distribution** of particle sizes describes the dimensions of a large number of particles within an analysed sample.

In the current project, particles sizing has been used to describe the size of particles consisting of masticated (mechanical sieving and Malvern Mastersizer 2000®) and digested (Malvern Mastersizer 2000®) almond samples, emulsions (Beckman Coulter LS13320®), as well as separated almond cells (Beckman Coulter Multisizer 3 Coulter Counter®).

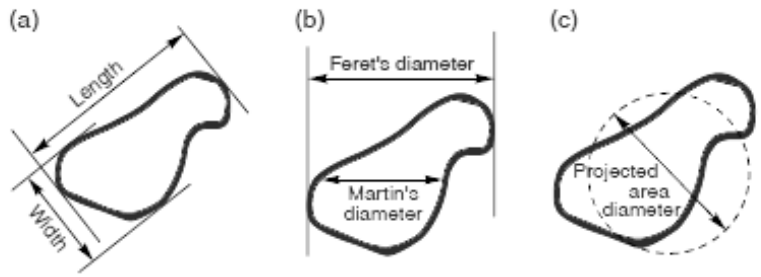

Figure 2.4 Commonly used descriptors for particle size (Brittain, 2001).

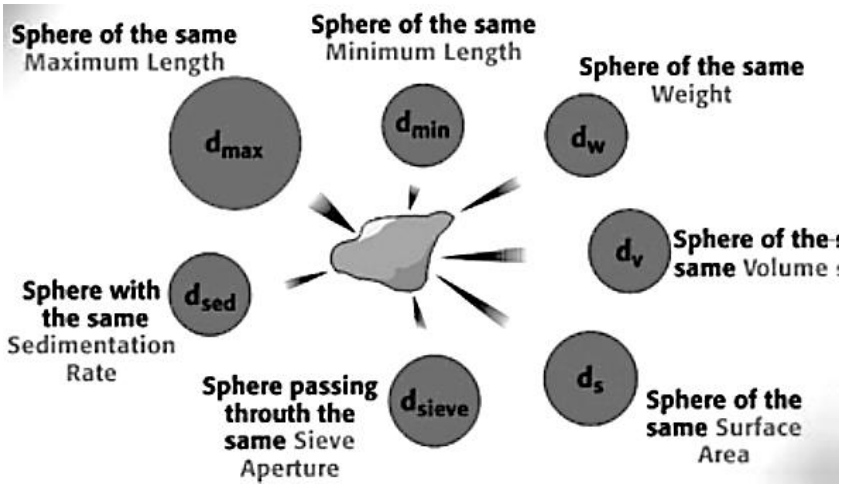

Figure 2.5 Equivalent diameter for irregular shapes (Malvern, 2011a).

2.3.2.1 Mechanical sieving

Sieve analysis is a technique that allows the particle size distribution of a sample to be obtained by separating these particles using sieves. Each sieve is made of a mesh with a specific size that corresponds to the number of wires per inch (Figure 2.6 A). The sieves were placed on top of each other in order of decreasing size with the coarsest sieve to the uppermost, and a base for collecting the finest particles. The sample to be analysed was fed onto the sieve with the largest opening, the undersize particles pass through to the sieves below until all particles become separated into their various size fractions. Sieve shakers facilitated the sieving process by applying vibrations (Figure 2.6 B). In this project, the sieve stack was left to shake for a fixed period of 15 min, small rubber balls were added in each sieve to accelerate the separation. The maximum number of sieves that could be stacked in the shaker was 10 including the base, the mesh sizes ranging from 5 to over 240 (from 3350 to 32 µm aperture). The masticated almond samples were washed with deionised water before and after the sample were shaken to facilitate separation of the particles.

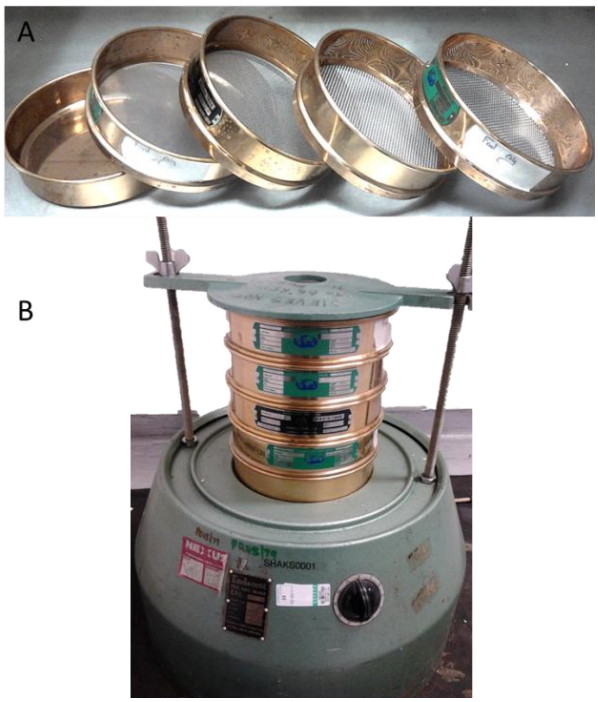

Figure 2.6 Example of sieves used - woven wire, 200 mm diameter (A), the same sieves on the vibratory sieve shaker (B) (Endecott test sieve shaker, Endecotts Ltd, London SW19, UK).

The fraction of particles present on a sieve of specific aperture was calculated by subtracting the weight of the dried sieve (without any particle) to its weight after the analysis (with the particles). The proportion of sample retained on each sieve, expressed as a percentage of the sample total weight, was calculated as following:

$$\text{Percentage weight retained} = \frac{W_S}{W_T} \times 100 \qquad \text{(Eq. 2.2)}$$

where W_s is the weight of sample present on a sieve of a specific aperture and W_t the total weight of the sample.

2.3.2.2 Malvern's laser diffraction analyser

Malvern laser diffraction particle sizer 2000® (Malvern Instruments Ltd, Worcestershire, UK) consists of an optical unit containing the measurement cell into which the sample continuously circulate (Figure 2.7). The laser diffraction sizer was connected to a sampling dispersion system for wet samples, Hydro 2000G, which contains a suspension unit of 800 mL capacity provided with an adjustable ultrasonicator, stirrer and pump.

Laser diffraction measurements are based on the principle that particles, depending on their size, scatter light at different angles and intensity. The device measures the **diffraction pattern** of the particles present in a sample with a size range of 0.02 to 2000 µm. Two laser light sources produce a red and a blue beam of light which then illuminate the measurement cell where the particles are suspended in a suitable solvent (Figure 2.8). Each particle, when submitted to the light beam, scatters the light at its external surface. Also, some of the light passes through the particle and interfere with the light that goes around the particle, thus creating a range of interferences characteristic of the scattering pattern of that particle. Particles with different sizes scatter the light at different angles: small particles scatter light at a low intensity and a wide angle whereas large ones at a small angle.

The instrument is composed of a multi-element detector including forward scatter detectors that measure light scattered at less than 90° and backscatter detectors for light scattered at angles greater than 90°. Beforehand, the scattered light is focused by a Fourier lens that assures that two particles of the same size scatter light to the same detector regardless of their location in the beam and the speed at which they are travelling.

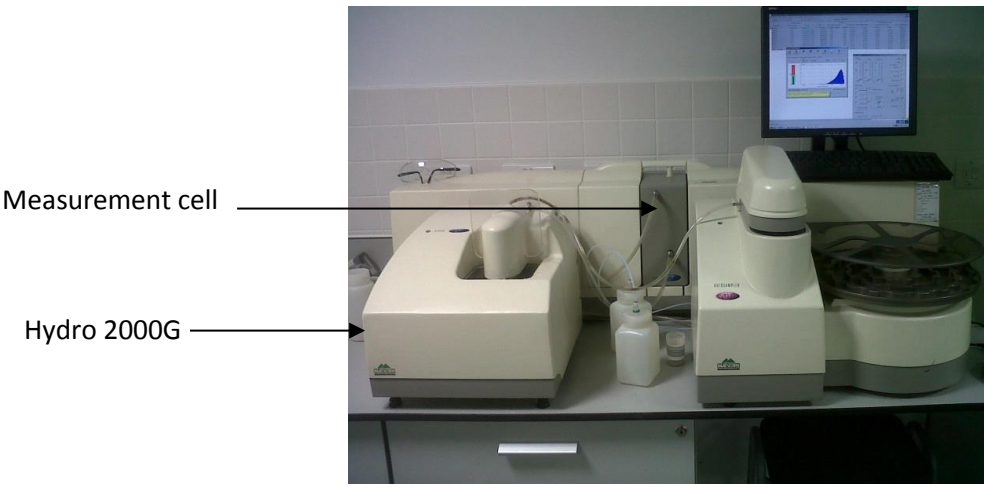

Figure 2.7 Malvern laser diffraction particle sizer 2000® equipped with a Hydro 2000G.

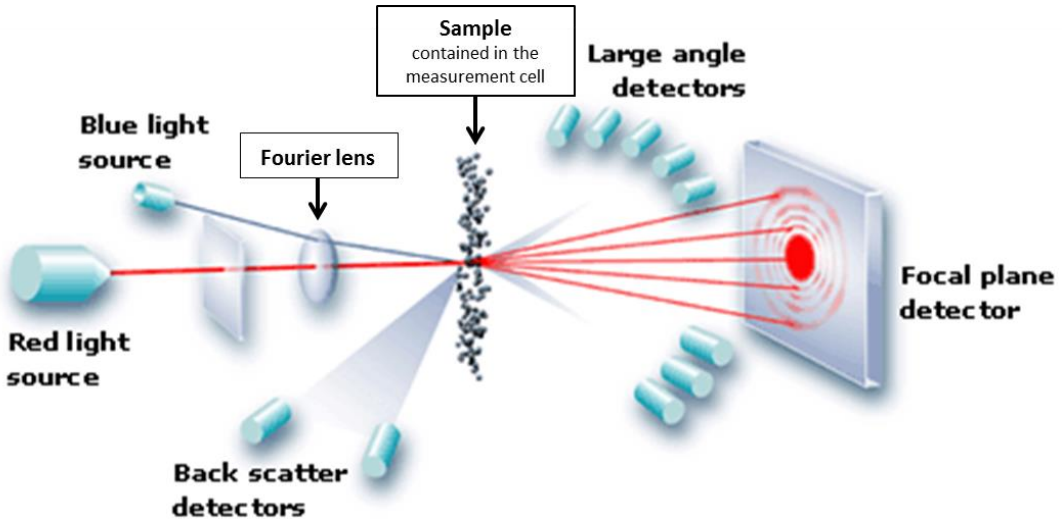

Figure 2.8 Schematic representation of Malvern laser diffraction particle sizer 2000® (Malvern, 2011b).

The particle size distribution is a combination of the scattering patterns of all the particles present in the analysed sample. A computer then performs the digital integration over a suitable period of time to convert the diffraction pattern into a size distribution expressed by volume. The technique assumes that the particles are perfect spheres. The results are therefore presented as equivalent sphere diameters.

For the calculation of the PSD from light intensity distribution, there is an option of using two theories, namely Fraunhofer and Mie (Malvern, 2011a). The Fraunhofer theory makes the assumption that the particles are totally opaque and therefore the optical properties of the sample are not required. However, the theory is an approximation and does not give an accurate estimate of the number of fine particles. On the other hand, with the Mie theory, the amount of fine material in the sample is determined correctly, but it requires the refractive index of both the studied material and the solvent to be known. Because of the wide range of particle sizes the Mie theory was applied in our study; water has a refractive index of 1.330 and almond oil of 1.471. The latter was measured using a refractometer (Rhino Brix90 Handheld Refractometer, Reichert, Inc., New York, USA).

2.3.2.3 Beckman Coulter

The size of the **emulsions oil droplets** and the **OBs** were measured using a Beckman Coulter LS13320® (Beckman Coulter Ltd., High Wycombe, UK). PSD of emulsified lipids and OBs is presented, and similarly to almond particles, as a PSD curve but also as surface-weighted ($d_{3,2}$) and volume ($d_{4,3}$) mean diameters:

$$d_{3,2} = \frac{\sum n_i d_i^3}{\sum n_i d_i^2} \quad \text{(Eq. 2.3)}$$

$$d_{4,3} = \frac{\sum n_i d_i^4}{\sum n_i d_i^3} \quad \text{(Eq. 2.4)}$$

where n_i is the number of droplets and d_i their diameters.

Particle size analysis and quantification (number) of **separated cells** was performed using a Beckman Multisizer™ 3 Coulter Counter® (Beckman Coulter Ltd, High Wycombe, UK) fitted with a 140 µm orifice tube (size range between 2.8 and 84 µm). A small amount (≈ 0.1 mL) of diluted cells was dispersed in 100 mL of 0.9% saline (Fresenius Kabi, Steriflex®). A 2 mL volume was used for each analysis. The instrument was calibrated with Coulter counter standard L10 polystyrene latex (mode diameter 9.92 µm).

2.3.3 Microscopy

2.3.3.1 Light microscopy

Some samples could be visualised 'as is', whereas some others (i.e. particles with size > 500 µm) required specific preparation (e.g. fixing). The protocol was adapted from previous work (Ellis *et al.*, 2004), with the assistance of Dr Mary Parker (the IFR, Norwich). Almond samples were placed into glass vials containing 2.5% (v/v) glutaraldehyde fixative in 0.1 M sodium cacodylate buffer (pH 7.2) and placed in the refrigerator at 4°C. After at least 2 days in the fixative, the almonds particles were washed 3 times in 0.1 M sodium cacodylate buffer for 30 min each.

The samples were then post-fixed in 2% (v/v) osmium tetroxide in 0.1 M sodium cacodylate buffer (pH 7.2) for 4 h before performing 3 washes of 30 min each in sodium cacodylate buffer washes and dehydration in a graded ethanol series (10, 20, 30, 40, 50, 60, 70, 80, 90, 100%) with 1 h between ethanol changes. The final ethanol change was repeated twice more with 100% ethanol.

The almond particles were placed in a solution containing propylene oxide and 100% ethanol (1:1) for at least 20 min. They were washed 3 times in 100% propylene oxide for 10 min. The propylene oxide was then replaced with a 1:2 mix of Spurr Low viscosity resin (London Resin Company Ltd, Reading, UK) to 100% propylene oxide and put on a rotator for a few hours. This was followed by a 1:1 and a 2:1 mix of Spurr resin to 100% oxide propylene and finally 100% resin, with at least 1 h on

the rotator between each change. After 1 h in 100%, the resin was changed twice more with fresh 100% resin with periods of at least 8 hours on the rotator between changes. Four particles from each sample were put into BEEM® flat embedding capsules (Agar Scientific, No. G3654) with fresh resin and polymerised overnight at 70°C.

Samples were then brought to the Centre for Ultrastructural Imaging (CUI), King's College London, where they were stained and sectioned. Semi-thin (0.5 µm) sections were cut using a diamond knife (Diatome Diamond knife ultra, Leica Microsystems Ltd, Milton Keynes, UK). The sections were transferred onto a drop of water on a glass slide and dried in a hot plate. They were then stained with 1% (w/v) toluidine blue in 1% (w/v) sodium borate for only a few seconds and then rinsed with water before being dried again on the hot plate. The slides were viewed under the optical Zeiss Axioskop 2 mot plus microscope (Carl Zeiss Ltd, United Kingdom). Images were captured with a Zeiss AxioCam HRc and AxioVision v3.1 microscope software (Carl Zeiss, UK).

Nile red (1 mg/mL in dimethyl sulphoxide) was also used on fresh particles (size ≤ 500 µm) of almond samples, either masticated (*Chapter 3*) or following digestion (*Chapter 6*), to identify lipids. The samples were examined immediately on the light microscope with Zeiss Filter Set 14 (excitation around 510-560 nm and emission around 590 nm).

2.3.3.2 Electron microscopy

Samples intended for examination by scanning electron microscope (SEM) were fixed and post-fixed as described above and then critical point dried in a Polaron E3000 CP Drier (Quorum Technologies, Newhaven, United Kingdom). At the CUI, the samples were mounted on stubs, coated with gold in a Polaron E5100 sputter coating unit to make the specimen conductive, and viewed in a Hitachi S-3500N scanning electron microscope (FEI Company, Cambridge, United Kingdom).

Samples for transmission electron microscopy (TEM) were prepared using the same protocol as that for light microscopy (LM). Thin sections of 70 nm were cut with the diamond knife mounted on a ultramicrotome, stained in toluidine blue and visualised by TEM (Tecnai™ T12, FEI Europe, Eindhoven, Netherland) fitted with an AMT camera system.

2.3.3.3 Confocal microscopy

The microstructure of almond cells and OBs before and after digestion was studied using an inverted confocal laser scanning microscope (CLSM at King's College London; Leica TCS SP2, DMIRE2 inverted, Milton Keynes, UK) or SP1 or SP5 CLSM (at the IFR; Leica Microsystems, Mannheim, Germany). Images were captured using both 40x (N.A. 1.25) and 63x (N.A. 1.32) oil immersion objective lenses. Nile red (1 mg/mL in dimethyl sulphoxide) and calcofluor white were used to detect lipids and CW, respectively. The samples were excited using an argon laser at 488 nm for Nile red and Alexa Fluor 488, and 405 nm for calcofluor white. The fluorescence emitted by the samples was detected at 630 to 680 nm (Nile red), 505 to 550 nm (Alexa Fluor 488) and 406 to 460 nm (calcofluor white).

2.3.4 Cell wall analysis

2.3.4.1 Gas liquid chromatography method

The CW analyses of natural (raw) and roasted almonds before and after mastication and digestion using a common method, as previously described (Parker and Waldron, 1995), were performed at the IFR. Once the CW materials were prepared, sugar and uronic acid contents in the almond samples were measured.

2.3.4.1.1 Preparation of cell wall material

CW material was prepared from both masticated and digested samples. The first step of the preparation consisted of extracting the lipid using the Soxhlet method. The raw and roasted almonds were ground using a coffee blender (Lloytron PLC, Lancashire, UK). The duodenal and gastric samples were centrifuged, and the supernatant pipetted to remove most of the liquid. Five grams of samples were placed into Soxhlet thimbles and then in the apparatus. The Soxhlet extraction was ran for 4 h to de-fat the material using 250 mL of hexane as an extraction solvent. Once the hexane evaporated, the defatted ground almonds were weighed (about 2.5 g).

To each sample, 100 mL of 1.5% (w/v) of SDS solution containing 5 mM of metabisulphate were added in order to remove the proteins present. The mixtures were homogenised with an Ultra-Turrax homogeniser (T25 basic, IKA® Werke, from Essex Scientific Laboratory, Benfleet, UK) for 5 min, 30 s at a time, at power 1 (11000 rpm). If required, a few drops of octanol were added to reduce foaming. The samples were filtered through a 50 µm nylon mesh supported by a Buchner funnel and flask, and then they were washed with 100 mL of 0.5% (w/v) SDS solution containing 3 mM of $Na_2S_2O_5$ and sufficient water to reduce foaming. The residue was ball-milled at 4°C in 80 or 95 mL of 0.5% (w/v) SDS, depending on the sample, at about 60 rpm for 4 h. Each ball was then washed with water and filtered through a 50 µm nylon mesh. After several washes with water the CW material was allowed to dry overnight in acetone in the fume cupboard.

2.3.4.1.2 Sugar analysis

The sugar composition of the samples was determined by GLC (Perkin-Elmer Autosystem XL, Waltham, USA) equipped with FID using a method adapted from Blakeney *et al.* (Blakeney *et al.*, 1983). Briefly, the polysaccharides were first hydrolysed with 72% (w/w) sulphuric acid at 100°C for

2.5 h, followed by reduction with 3 M ammonia containing 150 mg/mL of sodium borohydride, and then acetylation to alditol acetates using 1-methylimidazole and acetic anhydride.

2.3.4.1.3 Uronic acids analysis

Uronic acid is found in both pectins (i.e. galacturonic acid) and hemicelluloses (e.g. glucuronic acid as found in xylans). Its measurement provides additional information about the composition of the CW. Some of the hydrolysates generated for GLC analysis were kept for the measurement of uronic acids by a colorimetric method (Blumenkrantz and Asboe-Hansen, 1973). The hydrolysates were added to sodium tetraborate reagent (25 mM in concentrated sulphuric acid) and heated at 100°C for 10 min. Then 0.15% (w/v) of 3-phenyl phenol in 0.5% NaOH were added to the samples and then after leaving the samples in the dark for about 30 min, the absorbance was read at 520 nm using a spectrophotometer. A set of glucuronic acid standards, from 5, 15, 25 and 35 µg/mL, were simultaneously assayed; the concentrations of uronic acids present in the samples were calculated from this standard curve.

2.3.4.2 Method using antibodies

Prof Willats and his team performed CW analysis using oligosaccharides microarrays (Pedersen *et al.*, 2012). This highly specific technique provided semi-quantitative data on CW composition of raw, roasted, and blanched almonds, and of almond skin, as well as digested almonds (raw only). The monoclonal antibodies used in the microarrays are powerful tools that facilitate the characterisation of CW in addition to giving more detailed information about CW composition and structure than that produced by GLC analysis. This method permitted the identification of individual oligosaccharides namely:

-Pectic polysaccharides: HG with various degrees of methyl esterification, xylogalacturonan, arabinan and (1→4)-β-D-galactan;

-Hemicellulose compounds: xyloglucan, xylan, arabinoxylan, mannan, gluco- and galactomannan; and

-Some proteins: extensin and AGP.

The details of the methodology used can be found elsewhere (Pedersen *et al.*, 2012). Briefly, CW material was prepared using an alcohol insoluble residue (AIR) method. The almond homogenate was added to an excess of 70% ethanol, the sample centrifuged (1352 g for 10 min), and the supernatant discarded. The procedure was repeated 5 times, then 100% acetone was used instead of ethanol once more before air drying the pellet. Ten mg of the preparation were extracted with CDTA followed by 4 M NaOH for 2 h each. Similarly to cell separation, CDTA permitted removal of the ionic bonding stabilised by calcium and thus extraction of the pectin without degradation of the galacturonan chains (Jarvis, 1982). NaOH extracted the remaining polysaccharides apart from cellulose. Each sample (4 replicates and 3 dilutions, resulting in 12 spots for each sample) was then spotted onto nitrocellulose membrane (Whatman, Maidstone, UK). Each spot was analysed and assigned a value based on antibody signal intensity. The output from the analysis was presented as heat maps, each being an average of the 12 values with the highest signal indexed to 100. Weak signals with values below 5 were disregarded.

2.4 Gastric and duodenal *in vitro* models

2.4.1 Lipase characteristics

Lipases (triacylglycerol acylhydrolases EC 3.1.1.3) are a group of enzymes that catalyses the hydrolysis of TAGs. As shown in Figure 2.9, TAGs are stepwise converted into DAG and MAG

accompanied at each step by the release of one FFA. The two main lipases involved in lipid digestion in human are HGL and HPL, each having a positional specificity. Consequently, HGL hydrolyses the ester bond of the fatty acid located in *sn*-3 position of the TAG leading to the production of DAG and one FFA, whereas HPL hydrolyses in *sn*-1 or 3 positions thus generating DAG, MAG and FFAs.

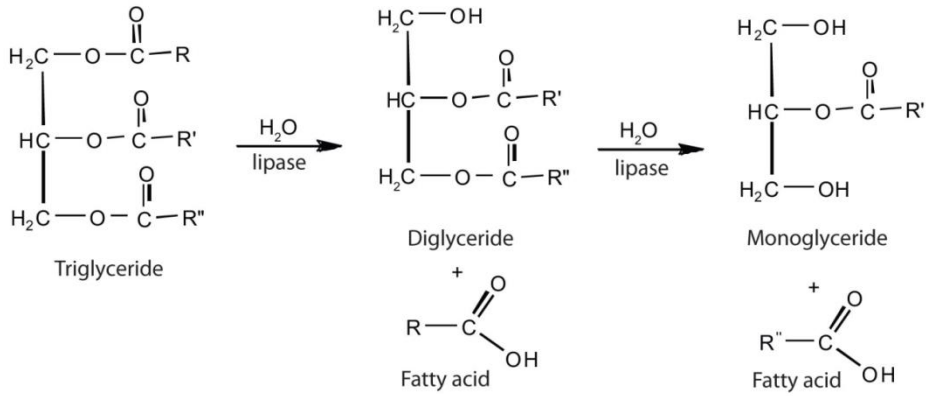

Figure 2.9 Schematic representation of TAG hydrolysis.

Since lipase is water soluble and the substrate is not, lipolysis is a heterogeneous reaction that takes place at the lipid-water interface. Its activity depends on the amount of substrate present at the interface (often expressed as specific surface area in cm^2/mL of emulsion) and the quality of the latter. Unlike esterase, lipase cannot act on a monomeric solution of ester (Verger, 1997). Some common interfacial structures are oil in water (o/w) emulsions, micelles, liposomes and monolayer films (Jurado *et al.*, 2006).

In the current project, several types of lipases were used, namely: lipase type II which is similar in constitution to porcine pancreatin and contains lipases but also proteases and amylase (Figure 2.10), RGE, PPE, PPL and GPLRP2. GPLRP2 is a recombinant enzyme produced in the yeast *Pichia pastoris* that has a MW of 47.6 kDa (as determined by mass spectrometry by Eduardo Mateos, PhD student from Prof Carriere's group). The protein content and composition of the lipases solutions were measured using the BCA and SDS-page methods described above.

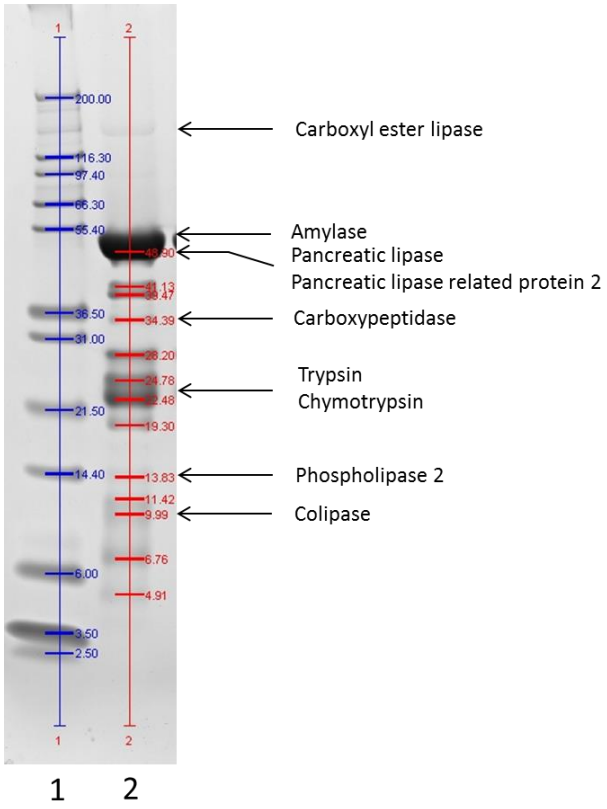

Figure 2.10 Protein composition of lipase type II (SDS-page performed by Neil Rigby from Dr Alan Mackie's group at the IFR). Lane 1 M_w marker and lane 2 lipase type II.

2.4.2 Lipase activity measurement using the pH-stat

Numerous methods have been developed for measuring lipase activity and lipid digestion often based on the quantification of fatty acids released (Beisson *et al.*, 2000; Hasan *et al.*, 2009). The most common techniques that have been used are titration using the pH-stat (Armand *et al.*, 1992; Li *et al.*, 2011c; Mun *et al.*, 2006), and spectrophotometric analysis using *ρ*-nitrophenyl laurate as a substrate (Pinsirodom and Parkin, 2001). GLC combined with the pH-stat has been shown to monitor accurately the course of the lipolysis while also providing data on the proportion of lipolytic products generated (Helbig *et al.*, 2012; Zhu *et al.*, 2013). The criteria to consider when choosing a method are sensitivity, continuous or discontinuous measurements, and ease of procedure. The assays mentioned above are continuous and can therefore be used to study the kinetics of lipase activity.

However, colorimetric and fluorometric assays give higher sensitivity. In the present project, both GLC and pH-stat were used to estimate the amount of FFAs released by lipolysis of masticated and ground almonds, separated almond cells and almond oil emulsions (*Chapter 6*). More sophisticated digestion models such as the DGM are described in more details in *Chapter 4*.

2.4.2.1 Principle

A convenient and well-known method to measure the activity of lipase is the pH-stat titration (848 Titrino plus Metrohm Ltd., Herisau, Switzerland) (Beisson *et al.*, 2000) (Figure 2.11). The device consists of a mechanically-stirred reaction vessel connected to an electrode that monitors the pH and an autoburette for the addition of NaOH. The temperature of the reaction system is maintained constant (37°C) via a water bath.

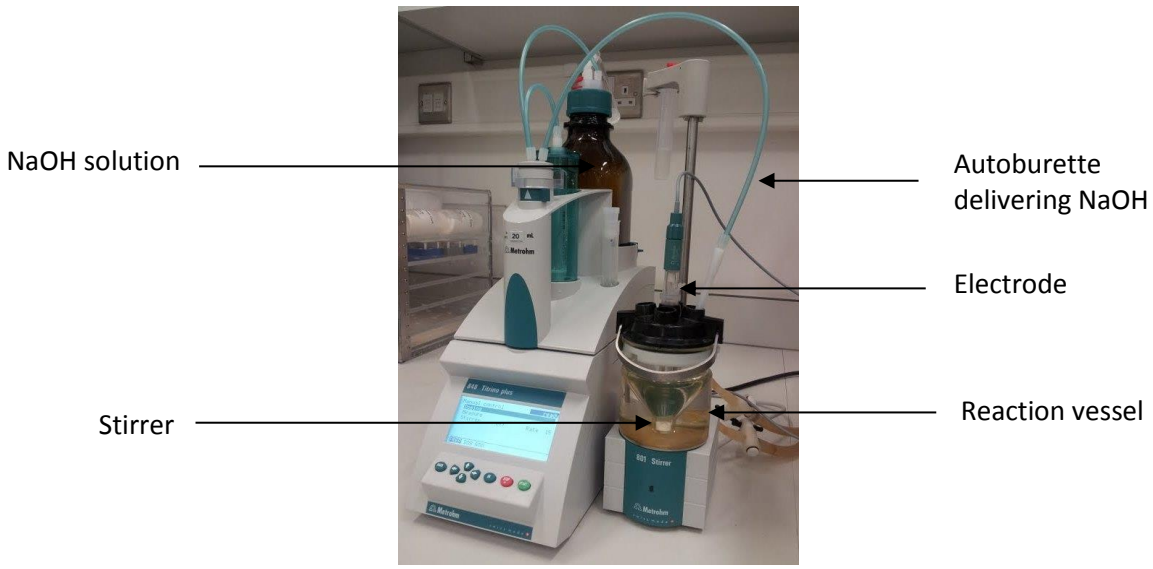

Figure 2.11 Metrohm 848 Tritrino plus (pH-stat).

The production of FFAs following TAG hydrolysis results in a decrease in the pH of the solution. Fatty acids are weak acids whose pK_a increases with their chain length and degree of unsaturation, for

instance short chain fatty acids have a pK_a of approximately 4.7 and 4.9, oleic acid between 7.7 to 8.9 and linoleic acid has a pK_a 7.9 (Pinsirodom and Parkin, 2001). However, these values correspond to apparent pK_a and are likely to fluctuate according to the reaction environment, e.g. buffer, presence of BS and other fatty acids; and besides, under physiological conditions (pH ≈ 7) ~99% of fatty acids are ionised (Mead *et al.*, 1986). The release of FFAs can be monitored at a constant pH value by automated addition of NaOH once the pH value is shifted down from the pH endpoint. The amount of NaOH (µmoles) added as a function of time to keep the pH constant are equivalent to the amount of FFAs released due to the lipase activity. If a large excess of substrate is used and if the enzyme is stable under the selected experimental conditions, the FFA release shows a linear relationship overtime. This activity can be expressed in international units: **1 U = 1 µmole of FFAs released per min**.

The titration in itself is not restricted to FFAs, therefore for the procedure to measure FFA generated from TAG lipolysis, it has to be performed with settings specific to the reaction measured (pH, temperature and initial conditions) (Kanicky and Shah, 2002; Pinsirodom and Parkin, 2001). As lipid hydrolysis depends on the reaction conditions such as temperature and pH, they were rigorously monitored before and during the experiments in order to standardise the digestion assays.

The pH endpoint corresponds to the pH value at which the enzyme displays its maximum activity. The pH endpoints of the assays performed in the gastric compartment was set at 5 and at 7 for the duodenal phase. Back titrations are often required in order to avoid underestimation of the FFAs formed because some of the FFAs, in particular oleic acid would not be totally protonated at pH 7. In this project, back titration was not performed for the duodenal phase as lipids were conjointly analysed by GLC. The rates of lipolysis were continuously measured by titration of released FFAs with 0.15 M NaOH at 37°C and an endpoint of pH 7.0. The pH fluctuation of the assay mixture alone (substrate included) was determined by running the titration without any enzyme; the volume obtained was then deduced from the volume data produced from the subsequent sample. This step

of the titration ensures the accurate quantification of newly formed FFAs from the test samples. Each digestion reaction was repeated in triplicate.

Preliminary measurements of the lipases activity were done using a standard assay method with tributyrin as a substrate (Lowe, 1999). The assay mixture consisted of 0.5 mL of tributyrin and 14.5 mL of assay buffer:

-For gastric lipase (RGE): NaCl 150 mM, NaTDC 2 mM, BSA 0.1 g/L, pH 5.5.

-For pancreatic lipase (lipase type II, PPE and PPL) and GLRP2: Tris 2 mM, NaCl 150 mM, $CaCl_2$ 2 mM, NaTDC 4 mM, pH 8. Colipase was added in lipolysis with PPL at a 2 to 1 excess molar ratio.

After leaving the substrate to emulsify in the reaction vessel at 37°C, colipase was added. The reaction was run for 20 min using 0.1 M NaOH as titrant.

The phospholipase activity of GLRP2 was tested using 5 mL of substrate solution (one egg yolk in 100 mL of 4 mM $CaCl_2$) and 10 mL of 20 mM deoxycholate, pH 8.0 (Thirstrup *et al.*, 1994).

2.4.2.2 Intestinal conditions

Each assay was performed over 1 h in a mechanically-stirred reaction vessel of a pH-stat. The *in vitro* duodenal digestion model used was adapted from previous studies (Li and McClements, 2010; Li *et al.*, 2011c): (i) 19.0 mL of sample containing 300 mg of lipids, either emulsion, separated almond cells or almond particles in β-Lg solution; (ii) 15.0 mL of bile salt solution (31.25 mM of NaTC and NaGDC in 10 mM phosphate buffer, pH 7.0, 37.0°C); and (iii) 1 mL of NaCl (5.625 M in deionised water) and 1 mL of $CaCl_2$ (0.375 M in deionised water). The lipolysis of unemulsified oils (raw and roasted almond oil as seen in Results section of *Chapter 5, Table 5.1*) was performed by adding the oils directly into the reaction vessel without preliminary preparation. The system was adjusted to pH 7 and then 1.5 mL of freshly prepared lipase solution was added (40 mg/mL in 10 mM phosphate buffer). The final volume of the reaction system in the vessel was 37.5 mL and its composition was therefore 0.8% lipid, 12.5 mM BS, 2.4 mg/mL lipase, 150 mM NaCl and 10 mM $CaCl_2$. Phosphate buffer (prepared by

mixing together 10 mM solutions of NaH_2PO_4 and Na_2HPO_4, pH 7) was used as its buffering capacity covers the optimal pH of pancreatic lipase (6.3 to 8.1).

The volume of NaOH (in mL) added as a function of time to keep the pH constant is equivalent to the amount of FFA released. Also, since the hydrolysis of TAG leads to one molecule of MAG and 2 FFAs, the percentage of FFA released can be calculated as follows:

$$\% \text{ FAA} = 100 \times \left(\frac{V_{NaOH} \times m_{NaOH} \times M_{lipid}}{w_{lipid} \times 2}\right) \quad \text{(Eq. 2.5)}$$

where V_{NaOH} corresponds to the volume of NaOH required to neutralise the FFAs produced, m_{NaOH} is the concentration of the NaOH solution used (in M), w_{lipid} is the total mass of TAG initially present in the reaction vessel (in g), and M_{lipid} is the molecular mass of oil (in g/mol) (Li and McClements, 2010).

The MW of almond oil was estimated to be **878 g/mol**; this value was calculated from the TAG composition of the oil and the occurrence of the FFAs (oleic, linoleic and palmitic acids) within these TAGs (from the analysis performed by the Almond board of California) as shown in Table 2.2.

Table 2.2 Main fatty acids present in almond oil and their MW.

Fatty acid	MW (g/mol)	Proportion in almond oil (%)
Oleic acid (18:1n-9)	282.5	66.8
Linoleic acid (18:2n-6)	280.5	23.4
Palmitic acid (16:0)	256.4	6.8
Palmitoleic acid (16:1)	254.4	1.2
Stearic acid (18:0)	284.5	0.5

The lipid content of the almonds studied here was about 51.7% for raw and 52.4% for roasted almonds (see Table 2.1). The initial rates of lipolysis were calculated from the slopes of the product concentration (in µmol/mL) versus time (in min).

2.4.3 Dynamic gastric model and static duodenal model

The following protocol was developed in collaboration with the IFR to study the *in vitro* digestion, under gastric (DGM) and duodenal (SDM) conditions, of masticated almond samples obtained from the Mastication study (*Chapter 3*) (Mandalari *et al.*, 2008a; Pitino *et al.*, 2010). For each type of almond, raw and roasted, two different sets of samples were loaded into the DGM: a combined sample of fifteen (one from each participant, 15 x 4 to 5 g) and four 28 g individual samples (*Chapter 4*). Furthermore, masticated muffins, containing either 1700 to 2000 μm almond particles or almond flour (~187 μm), underwent *in vitro* digestion with the DGM and SDM (*Chapter 6*).

2.4.3.1 Description of the apparatus

The DGM was developed in collaboration with the IFR and validated using both echo planar magnetic resonance imaging on healthy volunteers and ileostomy studies (Wickham *et al.*, 2009). A number of food and pharmaceutical products have been tested with this model, in particular muffins containing pistachio nuts (Mandalari *et al.*, 2013). This *in vitro* model stimulates the human stomach by mimicking the biochemical and mechanical processes, including forces and fluid flow, leading to the formation of a chyme (Wickham et al., 2012). It is composed of the main body - simulating the fundus, in which gastric juices of similar composition to that of the *in vivo* secretion, are dynamically added (Figure 2.12). The lower part of this stomach model consists of a piston and a barrel simulating the antrum, and it is connected to the main body by a valve that generates reflux of material between those two compartments. By analogy to the human stomach, the bolus is subjected to gentle shear forces (pulsatile contractions) in the main body as well as powerful breaking forces in the antrum allowing churning, inhomogeneous mixing with gastric juice, variable emptying regimes and preferential sieving of the foods.

A feedback mechanism controls the addition of acid via a pH meter whereas the rate of enzyme deliveries is set up by the operator depending on the food/material loaded into the DGM (i.e. size, calorie content, solid or liquid, and viscosity). The expulsion of the chyme from the machine occurred at defined timed intervals and differed in composition in a way that simulated the *in vivo* process.

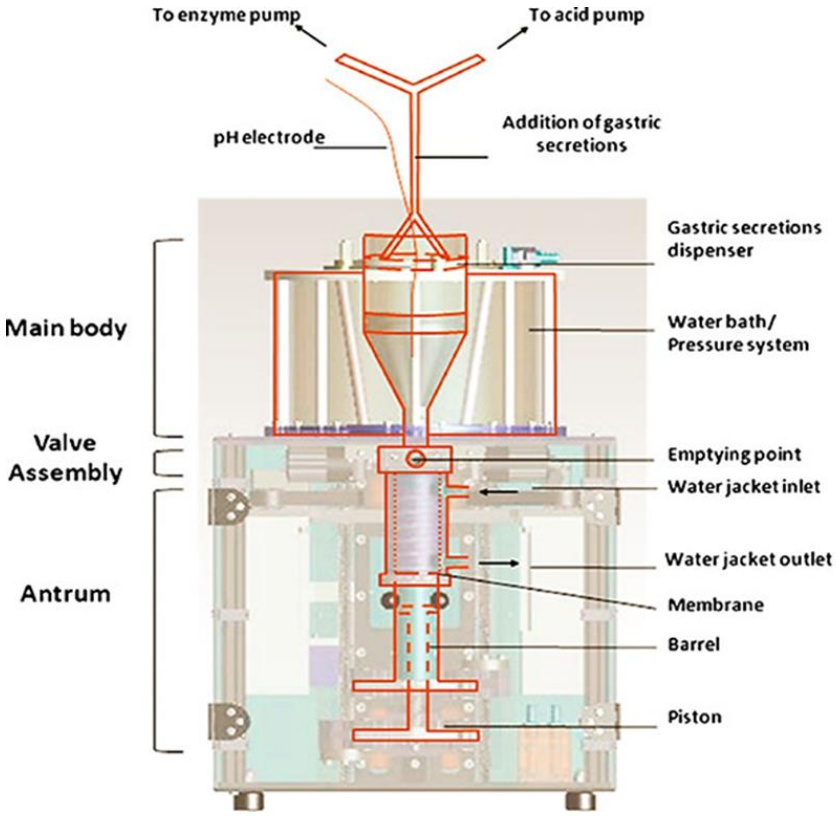

Figure 2.12 Schematic representation of the dynamic gastric model, adapted from (Vardakou et al., 2011).

2.4.3.2 Protocol

2.4.3.2.1 Gastric digestion

Solution preparation

A solution of single shelled lecithin liposomes (grade 1, Lipid Products, Surrey, UK) was prepared using a method as previously described (Mandalari *et al.*, 2008a). A 0.299 mL aliquot of lecithin stock

solution (63.5 mM in chloroform/methanol) was dried under nitrogen flow. The samples were placed in a vacuum oven, purged three times with nitrogen at room temperature, and dried under vacuum overnight. The solvent was removed from a 0.94 mL aliquot of phospholipid stock solution (63.5 mM in chloroform), under rotary evaporation with vacuum at 5°C. Any residual solvent was removed at room temperature under vacuum overnight after purging three times with nitrogen. The resulting film of phospholipids was then suspended in 12.2 mL of warmed simulated gastric buffer (0.15 M NaCl, pH 2.5, at 37°C), and sonicated to produce single-shelled liposomes. The sonication system consisted of a sonication probe (Status US 200; Avestin) operated at 5°C in a coolant-jacketed vessel, with a pulsed cycle of 30% full power on for 0.9 s and off for 0.1 s. Liposomes were then filtered through a Nalgene 0.22 mL nylon syringe filter (Nalgene, United Kingdom) to remove any titanium deposited by the sonicator. The liposomes were then put back in the shaking incubator (170 rpm) for 20 min to equilibrate at 37°C.

The fasted state was replicated by priming the DGM with 20 mL of acid solution, which was composed of a mixture of NaCl (58 mM), $CaCl_2$ (0.5 mM), NaH_2PO_4 (0.864 mM), KCl (30 mM) and HCl (10 mM).

The simulated gastric enzyme solution was prepared by dissolving porcine gastric mucosa pepsin (activity 4220 U/mg of protein calculated using haemoglobin as substrate, Sigma, Poole, UK) and a gastric lipase analogue from Rhizopus oryzae (F-AP15, activity ~150 U/mg of powder, Amano Enzyme Inc. Nagoya, Japan) in a simulated gastric solution containing 58 mM NaCl, 0.5 mM $CaCl_2$, 0.864 mM NaH_2PO_4 and 30 mM KCl at the final concentrations of 9000 U/mL and 60 U/mL for pepsin and lipase, respectively. The simulated gastric acid solution had the same composition as the simulated gastric solution apart from the acid (200 mM HCl).

The lecithin liposomes solution was suspended in 50 mL of the simulated gastric enzyme solution. The mixture was placed in the incubator (Innova 4200, New Brunswick Scientific, Edison USA) with an

internal shaker table (set at 37°C, 170 rpm) for approximately 20 min to bring to the incubator temperature and then filtered (0.22 μm).

Digestion procedure

The acid and enzyme pumps were calibrated as well as the pH detector, and the new pumps parameters entered into the computer software. The recipe was entered into the DGM software according to calculations done previously corresponding to the meal (Wickham *et al.*, 2012). The samples were then poured into the aperture of the DGM and the starting pH was recorded. Throughout the digestion, the gastric enzyme and acid solutions were added at a physiological rate via a loop (i.e. 'Addition of gastric secretions' in Figure 2.12), thus ensuring a homogeneous secretion of both enzyme and acid similar to the *in vivo* process. A defined number of digesta samples (aliquots) were collected throughout the gastric digestion according to the experimental protocol (6 samples for the eight individual 28 g masticated almonds, 11 samples for the 15 pooled masticated almonds, and 7 for the masticated muffins). Each aliquot was weighed and neutralised (pH 6.8) by adding NaOH (0.1 M).

2.4.3.2.2 Duodenal digestion

Solution preparation

A salt solution was made of NaCl (146.0 mM), $CaCl_2$ (2.6 mM), and KCl (4.8 mM). The solution of lecithin liposome was prepared as previously described. Then 33.5 mg NaTC and 25.0 mg NaGDC were weighed into a previously cleaned vial (final composition of the simulated bile solution: 4 mM cholesterol, 12.5 mM NaTC and 12.5 mM NaGDC)**.** The BS were suspended in 5 mL of the salt solution, and the vial was gently mixed by hand until the BS were dissolved. This hepatic solution was placed in the incubator with an internal shaker table (set at 37°C, 170 rpm) until it became clear.

To 19 mL of pancreatic mix solution (125.0 mM NaCl, 0.6 mM $CaCl_2$, 0.3 mM $MgCl_2$, 4.1 µM $ZnSO_4.7H_2O$), 0.118 mL of porcine pancreatic lipase (type VI-S, 590 U/mL) stock solution, 4 mg of porcine colipase (3.2 µg/mL), 0.0159 mg of porcine trypsin (type IX-S, 11 U/mL), 5.7 mg of bovine α-chymotrypsin (type II, 24 U/mL) and 0.600 g of porcine α-amylase (type VI-B, 300 U/mL) were added (pancreatic enzyme solution). The pH of the resulting solution was adjusted to 6.8.

Digestion procedure

The gastric samples were collected from the DGM at different time points determined by the software and then pooled followed by addition of the hepatic and pancreatic enzymatic solutions, the quantities of which depended on the size and type of meal. The mixture was then placed in the incubator (37^{o}C, 200 rpm) for 2 h. Each pooled gastric and pooled duodenal samples were centrifuged at 3700 rpm for 15 min (7°C) to separate the soluble fraction from the residue. All samples were immediately snap-frozen in liquid nitrogen and retained for analyses.

2.5 *In vivo* studies

2.5.1 Mastication study

Further details about this study can be found in *Chapter 3*. Briefly, a randomised cross-over design was used to compare mastication effects on raw and roasted almonds. The volunteers (n=15) were asked to masticate four almonds until they felt the urge to swallow, at which stage they expectorated the contents of their mouth and rinsed it into a container. Some of the collected samples were then loaded on the gastric (DGM) and duodenal (SDM) models.

PSD were measured using two methods, for comparative purposes, mechanical sieving and laser diffraction. The microstructure of masticated almond tissue was examined using a range of microscopy techniques. Lipid bioaccessibility was determined using both the Soxhlet method and the mathematical model, which is based on the particle size of masticated almond particles and almond cell dimensions (Grassby *et al.*, 2014). The model calculates the amount of lipid released from the ruptured cells of almond cubes of defined size. Information on the PSD, number of particles of each size, for masticated almond was required in order to calculate the amount of lipid released in a more realistic situation. The measurement of monosaccharides of hydrolysed CW polysaccharides was performed at the IFR laboratory using a standard sugars analysis as described in *Section 2.3.4.1*.

2.5.2 Ileostomy study

Further details about this study can be found in *Chapter 6.* Briefly, two single-blinded, randomised, cross-over design studies (Study 1 for lipid and Study 2 for starch) were conducted in 9 male and female ileostomy individuals, aged 20-75 years, involving 2 to 4 test meals. Volunteers were given test foods specifically designed to vary in nutrient bioaccessibility, which predominantly consisted of either lipid (almond muffin) or starch (wheat porridge).

Following consumption of the test meal, ileal effluents and blood were collected at regular intervals. Effluents were divided for subsequent analyses of lipid 'losses' and the physical state (microscopy) of the tissue entering the large bowel at each time point. Blood samples were analysed for changes in lipid, glucose, insulin, C-peptide, and gut hormones concentrations.

CHAPTER 3

EFFECT OF MASTICATION ON LIPID RELEASE FROM ALMOND SEEDS

3.1 Introduction

Mastication is the initial step of digestion and includes comminution, the breaking of solid food such as almond to form smaller particles, and lubrication with saliva. One mastication sequence is initiated by the insertion of food in the mouth (ingestion) and ends with the passage of the bolus into the oesophagus (deglutition). The appearance and characteristics of the bolus formed depends on the teeth, bite force, which is structure and properties of the jaw muscles, the cheek, and the tongue; and also saliva production (van der Bilt *et al.*, 2006).

Oral processing has a significant effect on bioaccessibility since the mechanical damage occurring to the tissue makes the release of nutrients more likely. The size and microstructural characteristics of the resulting particles also have a significant impact on digestion kinetics and other physiological processes in the GIT. Indeed, it is well known that when mechanical stress is applied to edible plant tissue during chewing the nutrient-rich cells can behave differently by either rupturing or separating (Brett and Waldron, 1996). This behaviour has implications on nutrient bioaccessibility, which relies on the proportion of ruptured cells, which in turn is determined by the degree of mastication. The structure of the food matrix itself, emulsion or encapsulated lipids inside intact cells, affects the accessibility of lipids to digestive enzymes and other components involved in digestion.

Almonds are an energy dense food typically containing 50% of lipids, so such food would be expected to generate a high postprandial lipaemic response when ingested. Almond cells rupture rather than separate when milled or masticated, so their contents of mainly lipid and protein become potentially available for digestion (Ellis *et al.*, 2004). Previous studies have shown however that a high proportion of almond lipid remains encapsulated by CWs in the parenchyma cells and is therefore unavailable for digestion, producing a low lipaemic response (Berry *et al.*, 2008; Ellis *et al.*, 2004).

The size of the particles resulting from oral processing as well as the changes occurring as these particles pass through the GIT have therefore an impact on the rate and extent of lipid digestion (McClements and Li, 2010). The degree of mastication has been linked to the rate of starch digestion in rice (Ranawana *et al.*, 2010) and an early study highlighted the importance of mastication in influencing post-prandial glycaemia (Shimoyama *et al.*, 2007), but little is known about lipid bioaccessibility in almond following chewing.

There is indeed a need to quantify the release of lipids because it is still unclear how and to what extent mastication affects lipid bioaccessibility. The relationship between the particle size of masticated plant food, which closely reflects the proportion of ruptured cells in the plant tissue, and nutrient bioaccessibility have received little attention, with the notable exception of food such as carrots (Knockaert *et al.*, 2012; Lemmens *et al.*, 2010; Stinco *et al.*, 2012). Therefore, it is still unclear to what extent mastication affects lipid bioaccessibility in almond. By quantifying the changes in the particle size distribution, lipid release and CW composition before and after mastication of almonds, we will be able to have a better understanding of the mechanisms involved in lipid bioaccessibility. The theoretical model developed by our group (Grassby *et al.*, 2014) has been used in the current study to predict the proportion of lipid released from almonds, based on the size of the almond particles present in the bolus. Another objective of the present study was to determine PSDs for masticated raw and roasted almonds, from which predictions of lipid loss from masticated almond tissue could be made, and validated against experimental values. Studies of this kind are urgently required as the mechanisms of nutrient bioaccessibility during mastication are poorly understood, in particular, the relationship between the disassembly of ingested foods and nutrient release in the mouth and GIT. The current work also sought to compare two particle sizing techniques, mechanical sieving and laser diffraction, for quantifying particle size distribution of masticated almonds.

3.2 Aims

The objectives of the current work were to:

(a) Quantify the PSD of masticated raw and roasted almond particles;

(b) Determine changes in lipid content and CW polysaccharide composition due to mastication in healthy human volunteers;

(c) Examine the microstructural changes in almond tissue following oral processing; and

(d) Factor particle size data obtained from masticated almonds into a theoretical model previously developed to predict lipid release.

It was hypothesised that the CW of almond cells would fracture when masticated and liberate their contents, whereas intact cells would delay or prevent the release of lipids.

3.3 Materials and methods

3.3.1 Subjects and location

All mastication sessions took place in the metabolic unit facilities at King's College London. Fifteen healthy adults (11 females, 4 males) recruited among staff and students of King's College London, University of London (Figure 3.1), were included in the study (mean age of 25.4 ± 5.8 years, and body mass index (BMI) of 21.6 ± 3.7 kg/m^2). Previous studies investigating PSD under similar conditions have reported statistically significant differences in 10-13 subjects (Cassady *et al.*, 2009; Frecka *et al.*, 2008; Peyron *et al.*, 2004). Therefore, on this basis, the number of volunteers recruited was 17 to allow for a 15 to 20% drop out. Exclusion criteria were:

-Allergy to almonds or related allergens (other tree nuts, celery, pears, apples, cherries, peaches or parsley);

-Incomplete dentition, other than unerupted wisdom teeth any dental treatment in the last three months, except check-ups;

-Current infectious disease

None of the volunteers included in the study showed any evidence of malocclusion and masticatory malfunction.

After having received a full explanation of the study aims and procedure, each participant signed a consent form. The protocol was accepted by the Research Ethic Committee of the North London's National Research Ethics Service (reference no. 10/H0717/096) and the Research and Development office at Guy's and St Thomas Hospital (reference no. RJ111/N032). This trial was registered at isrctn.org as ISRCTN58438021. Each participant was assigned an identification number at screening. Confidential information was kept in a secure locker and on a password protected encrypted hard drive, and was only accessible to designated researchers working on the trial (in accordance with the Data Protection Act 1988).

3.3.2 Test foods

Raw and roasted almond (*Amygdalus communis L.*; variety, Nonpareil) kernels with the skin were provided by the Almond Board of California. The nutrient content (percentage by weight of edible portion) of the raw and roasted almonds were as follows: moisture 5.1 and 2.7%, ash (total minerals) 2.7 and 3.4%, protein 20.1 and 20.7% (total N x 5.18), lipid 51.7 and 52.4% (Soxhlet, hexane), available carbohydrates (mainly sugars), 4.6 and 4.8%; and DF 11.0 and 10.6% respectively (AOAC method). The compositional analysis was performed by Covance Laboratories Inc. (Madison, United States) on behalf of the Almond Board of California. The DF value is a reflection of the CW content (mostly non-starch polysaccharides) of the almond seeds.

3.3.3 Experimental protocol

Each subject attended a total of four mastication sessions, two per type of almond, NA and RA, with at least 1 week between each session. The almond types were masticated in random order over the four sessions. Each subject was asked to masticate each almond sample (4-5 g) on ten different occasions during each chewing session (i.e. 10 replicates, each mastication occasion separated by a rest period of 2 min and rinsing of the mouth with water). For the first two samples, the participants chewed and swallowed as normal, the number of chews (counted cycles = N) as well as the mastication duration (duration of sequences = T) were recorded and averaged. The mastication frequencies were then calculated by dividing N by T. These values were used as guides for the subsequent expectorations (eight replicates). During these tests, the participants chewed the sample until they reached the number of chews previously recorded (N), at which stage they expectorated the content of their mouth into individual pre-weighed plastic containers. They then rinsed their mouth with about 25 g of water and emptied it in the container previously used to maximise recovery of the chewed almond samples. The samples were analysed soon after collection except those used for lipid analysis, for which the almond boluses were stored at -20°C before being processed.

3.3.4 Particle sizing

In the present study, mechanical sieving and laser diffraction were compared and subsequently combined to cover the whole PSD (Figure 3.1). These methods were selected to cover the broad range of the PSDs of almond boluses and also to facilitate comparison with published data from other research groups that have employed similar techniques (Cassady *et al.*, 2009; Frecka *et al.*, 2008; Jalabert-Malbos *et al.*, 2007). Each type of almond, collected on different days, was measured twice, immediately after collection, for each participant by both sizing methods.

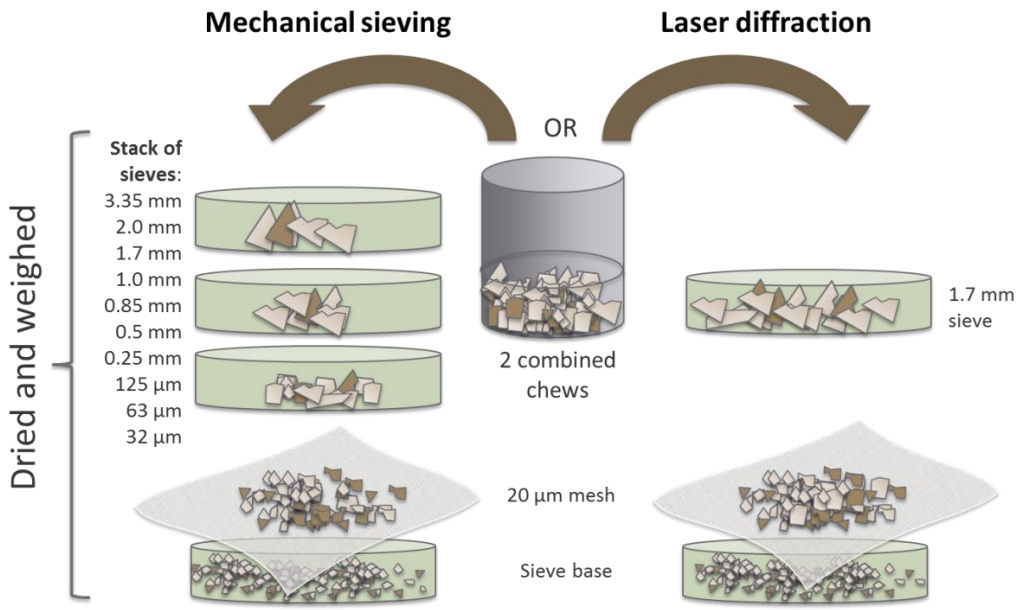

Figure 3.1 Overview of the methodology employed for particle sizing.

3.3.4.1 Mechanical sieving

Two masticated samples, approximately 10 g, collected from each participant were loaded on a stack of sieves with 10 aperture sizes: 3350, 2000, 1700, 1000, 850, 500, 250, 125, 63 and 32 µm (Endecott test sieve shaker, Endecotts Ltd, London SW19, UK). A nylon mesh of 20 µm was also placed between the base and the 32 µm sieve to allow comparison with the laser diffraction. The expectorated samples were washed with deionized water, shaken for 15 min, and washed again; thus ensuring that the particles were properly sieved. They were then dried in a forced-air oven at 56°C for 6 h as previously described (Cassady *et al.*, 2009; Frecka *et al.*, 2008). The bases were left to dry at 100°C overnight (about 15 h), which permitted the total evaporation of the water. The sieves were weighed before loading the sample and then again after having been dried in the oven. The dried fractions retained on each sieve and the base were expressed as a percentage of the weight of almonds before mastication.

3.3.4.2 Laser diffraction

The sample preparation was similar to the process already described for mechanical sieving. Thus, two of the masticated samples (replicates) were combined and loaded onto a sieve of 1700 µm aperture. The sieve was placed on top of a sieve base covered with a nylon mesh (aperture of 20 µm) and washed with deionized water. Once the water passed through the mesh, the remaining particles were collected into a 250 mL glass bottle by washing them off the mesh with deionised water. Removing particles of sizes > 1700 µm and < 20 µm prevented, for the former, obstruction of the instrument (upper size limit between 1500 and 2000 µm depending on the particles shape) and, for the latter, interference with the measurements, since particles of these sizes correspond only to cell/CW fragments and intracellular contents (e.g. oil droplets). These materials were examined by LM and there was no evidence of intact cells (*data not shown*).

The samples were then loaded into the Malvern 2000® laser diffraction particle sizer (Malvern Instruments Ltd, Worcestershire, UK) connected to a dispersant unit (Hydro 2000G) filled with water. The protocol used for the particle size measurements was adapted from previous work (Jalabert-Malbos *et al.*, 2007). Before loading, each sample was divided into several relatively equal quantities and consecutive ten-second measurements were taken for each one of these sub-samples. The set of measurements thus obtained was averaged to give the PSD for the whole sample. The almond oil and water have a refractive index of 1.471 and 1.330, respectively (see *Chapter 2, Section 2.3.2.2*). The absorption of almond particles was 0.1. The speeds of the stirrer and the pump were 700 and 1175 rpm, respectively. These settings were selected because under these conditions, the samples were well dispersed into water, showed no aggregation and consistently low intra and inter-sample variation (i.e. the variation in relative standard deviation of the average particle size was < 1%). The diffraction data were analysed using the Mie diffraction method respectively (see *Chapter 2, Section 2.3.2.2*), which is used to accurately measure the light scattering behaviour of spherical particles over a large size range (0.02 to 2000 µm). The particle sizes were

obtained as volume percentage of the total volume of all particles in the distribution. The d(0.1), d(0.2), d(0.5), d(0.8) and d(0.9) values were sometimes used as they allowed a simple characterisation of the PSD. They correspond to the centiles, in other words the size in µm of a particle below which 10, 20, 50, 80 and 90% of the sample lies.

3.3.5 Determination of lipid bioaccessibility

3.3.5.1 Predictions from the theoretical model

A mathematical model was developed to predict lipid bioaccessibility based on homogeneous, geometrically-defined particles (i.e. cubes) (Grassby *et al.*, 2014). For the current study, this model was adapted to allow predictions of bioaccessibility using heterogeneous particle sizes of masticated raw and roasted almond boluses. The original model predicts the fraction of lipid released from particles of almond cotyledon tissue with a specific particle edge length (particle size, *p*), and average cell diameter (*d*); *d* being approximately 35 µm for almond parenchyma cells (Equation 3.1) (Grassby *et al.*, 2014).

$$\mathrm{L}_R(\%) = \frac{1}{2}\left[\frac{64}{\pi^2}\left(\frac{d}{p}\right) - 8\left(\frac{d}{p}\right)^2 + \frac{4}{3}\pi\left(\frac{d}{p}\right)^3\right] \times 100 \qquad \text{(Eq. 3.1)}$$

where L_R is the percentage of lipid release, *d* is the average diameter of cells and *p* is a specific particle size.

The initial model was constructed on the basis that the almond particles were cubes for two reasons, first that it simplified the development of the model, and second that cubes were used in our previous *in vitro* and *in vivo* digestibility studies (Mandalari *et al.*, 2008a). To predict lipid release values from the mastication size data using Equation 3.1, it was necessary to transform this data into particle edge lengths. However, the laser diffraction method generated particle size values expressed as volume equivalent sphere diameter, which is the diameter of a sphere with the same

volume as the particle. The sphere diameters (*D*) were therefore converted into particle edge lengths (*p*) using the equation below:

$$p = \sqrt[3]{\frac{4}{3}\pi\left(\frac{D}{2}\right)^3} \qquad \text{(Eq. 3.2)}$$

It was also assumed that only the cells through which the fracture plane passes were ruptured (i.e. the surface of ruptured cells created by fracturing the almond), and therefore released their contents, as observed previously (Ellis *et al.*, 2004). The sieve particle sizes were also converted into particle edge lengths using Equation 3.2. The mathematical model was used to calculate lipid bioaccessibility for each *p* value, and then multiplied by the weight percentage of that particle size fraction in the complete bolus to give lipid bioaccessibility for the bolus, as reported in *Appendix B*.

The weight percentages of four fractions, with particle size ranges of 20 to 1700 µm, 1700 to 2000 µm, 2000 to 3350 µm and > 3350 µm, were calculated relative to the total weight retained by the sieves. The percentage weight values of the different sub-fractions within the 20 to 1700 µm size range were estimated using the laser diffraction data. The values for each fraction were then combined to give the predicted lipid release, expressed as a percentage, for each bolus (L_T) produced by the volunteers. The details of the calculation used and an example are presented in *Appendix B*.

3.3.5.2 Bioaccessibility analysis by solvent extraction method

The lipid content of the original raw and roasted almonds and the corresponding masticated almonds was determined to obtain the amount of lipid that had been released during the chewing process. We asked four volunteers to masticate a typical portion size of almond (28 g) and expectorate it in a similar manner to that described above. The lipids were then extracted as described in *Section 2.3.1.2.1*. Results of lipid content were expressed as a percentage of dry weight. These data were then compared to the theoretical values, of the same four volunteers, obtained with the mathematical model.

3.3.6 Composition of cell-wall polysaccharides

CW analyses for masticated samples were performed at the IFR as described in *Chapter 2*.

3.3.7 Microstructural analysis

Masticated samples were prepared for light, scanning and transmission electron microscopy as indicated in *Chapter 2*. Nile red was also used on fresh almond samples.

3.3.8 Statistical analysis

The data were analysed using SPSS version 20.0. For all tests, the significance level was set at $P < 0.05$ (2 tailed). All data were normally distributed (analysed using Shapiro-Wilk test and Normal Q-Q plots); they are expressed as mean ± SEM. Repeated measures ANOVA was used to assess the differences between replicates (i.e. visit 1 and 2) and almond form and also differences in lipid release between the two methods (i.e. Soxhlet and mathematical model). Differences in masticatory parameters, particle size and lipid release between the almond forms were tested by Student's paired *t*-test. Finally, a Pearson correlation test was also performed to explore the link between the number of chews and the particle sizes. To simplify the latter analysis the d values (0.1, 0.2, 0.5, 0.8 and 0.9) were used.

3.4 Results

3.4.1 Mastication parameters

A total of 15 subjects attended the four mastication sessions (Figure 3.2). In previous studies the investigation of mastication function and efficiency, the measure of mastication sequences, cycles and frequency provide information on the individual chewing behaviour (Hiiemae *et al.*, 1996; Jalabert-Malbos *et al.*, 2007; Woda *et al.*, 2006b). Depending on the individual as well as the food and its physical properties, those basic parameters are expected to vary (Kohyama *et al.*, 2008; Lassauzay *et al.*, 2000; Proschel and Hofmann, 1988; Woda *et al.*, 2006a). The masticatory parameters for raw and roasted almonds are presented in Table 3.1. The results showed no statistically significant difference in the number of mastication cycles (34.4 ± 3.90 vs. 33.1 ± 3.64, NA and RA respectively) and mastication frequency (1.4 ± 0.05 s^{-1}, for both type of almonds) between the two forms of almond. Only the duration of the mastication sequences was statistically different ($P < 0.05$) between the almond forms, although this difference was relatively small, as seen by the mean values 25.4 ± 2.72 s vs. 23.3 ± 2.40 s, for NA and RA, respectively.

Table 3.1 Masticatory parameters for raw and roasted almonds (n=15, means ± SEM).

	Number of cycles	**Sequence duration (s)**	**Mastication frequency (s^{-1})**
Raw almonds	34.4 ± 3.90	25.4 ± 2.72[1]	1.4 ± 0.05
Roasted almonds	33.1 ± 3.64	23.3 ± 2.40[1]	1.4 ± 0.05

[1]Significant difference between almond forms ($P < 0.05$) as calculated by Student's paired *t*-test.

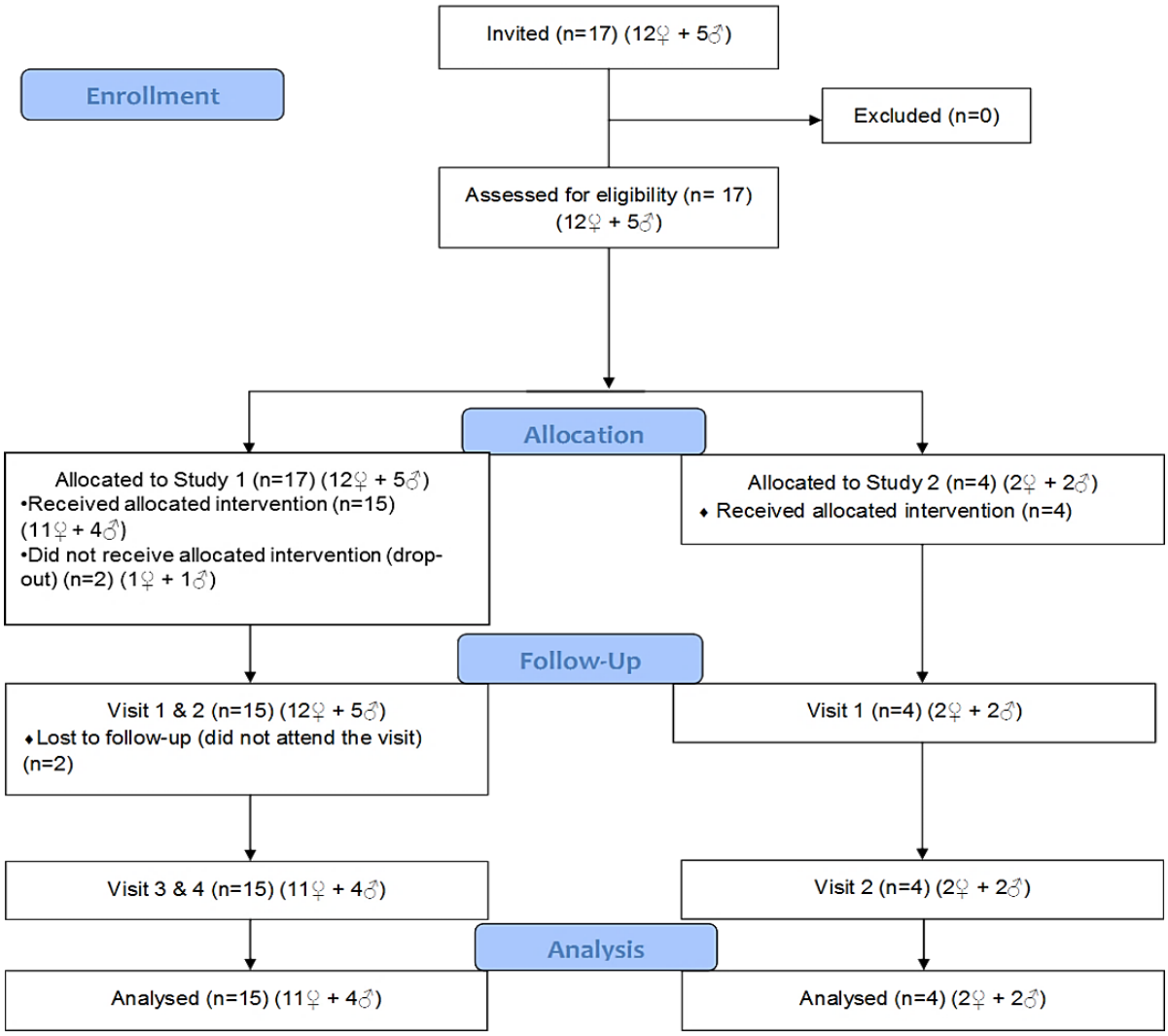

Figure 3.2 CONSORT diagram of subject flow throughout the study. Fifteen subjects completed Study 1 and 4 completed Study 2. Study 1: 4 visits of 10 mastication sessions and Study 2: 2 visits of the mastication of a 28 g portion of almonds (see Chapter 4).

3.4.2 Particle sizing of the masticated samples

Each form of almond, collected on different days, was measured for each participant by both sizing methods, each of which has some methodological limitations. We observed that, compared with mechanical sieving, laser diffraction was more efficient, reproducible (as shown by the small error bars in Figure 3.4) and a less time-consuming method. One advantage of mechanical sieving is that it provided a size distribution over a wider range of sizes compared with the laser method, albeit with

poorer size resolution. Problems of sieve damage (especially at low aperture size) and particle aggregation were also experienced with mechanical sieving, whereas laser diffraction was not affected by such deficiencies.

3.4.2.1 Mechanical sieving

Raw and roasted almond had a total percent recovery of 45.6 ± 1.66% and 53.3 ± 1.84 %, respectively. When the content of the sieve bases (i.e. containing the water used to rinse the sieves, fragments of cells and CWs and isolated intracellular components such as oil droplets), collected and dried, was included, the percentage recovery values were 85.4 ± 1.47 % for raw and 89.5 ± 1.50 % for roasted almond samples which were relatively high compared to other studies. The reported recovery values previously reported for almonds by other groups are approximately 44% of almonds (Frecka *et al.*, 2008) and 62% of almonds (Cassady *et al.*, 2009). As suggested by the authors, the good recoveries obtained for the current study was attributable to the fact that the cells fragments and released nutrients produced from the mastication were collected. After evaporation of water in the saliva, the solid content of saliva would be very low, would have made a negligible contribution to the recorded mass of almond nutrients.

The weight of masticated almond retained on the sieves, presented as a percentage of the original weight of the pre-masticated almond, was plotted against the aperture size of each sieve. The average PSD for raw and roasted almond is shown in Figure 3.3. Sieve PSDs are usually measured using a systematic mathematical progression in sieve aperture size; therefore the fractions from the 1700 and 2000 µm sieves were combined, as were those from the 850 and 1000 µm sieves, so that aperture size roughly doubled at each step. Repeated measures ANOVA, with size as a factor, revealed significant differences in PSDs between the raw and roasted almonds ($P < 0.05$). Student's paired *t*-test showed significant differences ($P < 0.001$) in particle size at all the size fractions

between the raw and roasted almonds, except at size fractions 850 and 1000 µm where the two curves overlapped. Therefore, the proportion of large particles (1700 to > 3350 µm) was found to be greater for raw than roasted almond, whereas the opposite was observed for small particles (20 to < 1700 µm), so the masticated roasted samples contained a higher proportion of smaller particles. This result is in agreement with data from a recent chewing study that used a similar sieving method (Cassady *et al.*, 2009; Frecka *et al.*, 2008); in our study ~60 and 24% of the particles from raw almonds, obtained with mechanical sieving, were found to have particle sizes < 500 µm and > 1700 µm, respectively (Table 3.2). Similar results were obtained for roasted almonds, with 64% of particles < 500 µm and 20% > 1700 µm.

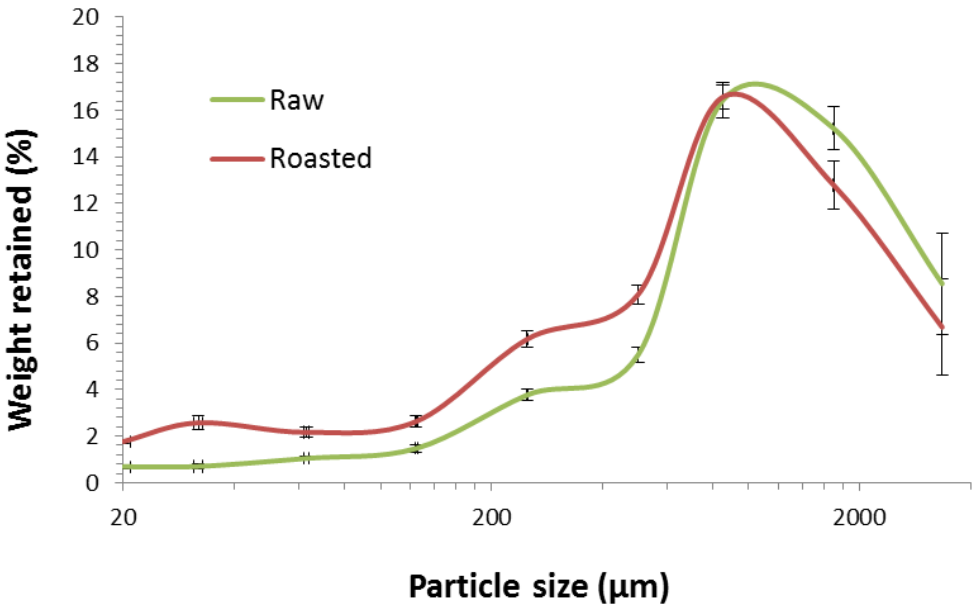

Figure 3.3 Particle size distributions by mechanical sieving of raw and roasted almond boluses (n=15, means ± SEM). Significant differences found between raw and roasted were calculated by Student's paired t-test (P < 0.001).

Table 3.2 Percentage weight of almond particles retained on the sieves by size ranges (n=15, means and cumulative percentages) from the present study as well as others (Cassady et al., 2009; Frecka et al., 2008).

	Present study				Frecka *et al.*				Cassady *et al.*	
	Raw		**Roasted**		**Raw**		**Roasted**		**Raw 40 chews**	
	MEAN	Cumulative %	MEAN	Cumulative %	MEAN	Cumulative %	MEAN	Cumulative %	MEAN	Cumulative %
< 20 µm	46.6	46.6	40.4	40.4					38.0	38.0
20 to 32 µm	0.7	47.3	1.8	42.2						
32 to 63 µm	0.7	48.0	2.6	44.8	56.1	56.1	55.0	55.0	1.0	39.0
63 to 125 µm	1.0	49.1	2.2	46.9					4.0	43.0
125 to 250 µm	1.5	50.5	2.6	49.6					3.0	46.0
250 to 500 µm	3.8	54.3	6.2	55.8	4.9	61.0	7.3	62.2	5.0	51.0
500 to 850 µm	5.5	59.8	8.1	63.8	11.2	72.3	12.6	74.8	10.0	61.0
850 to 1000 µm	5.2	65.0	6.0	69.8						
1000 to 1700 µm	11.3	76.2	10.6	80.4	15.4	87.6	14.8	89.7	17.0	78.0
1700 to 2000 µm	8.9	85.1	7.5	87.9						
2000 to 3500 µm	6.4	91.4	5.2	93.2	8.6	96.2	7.5	97.2	10.0	88.0
> 3350 µm	8.6	100.0	6.7	100.0	3.8	100.0	2.8	100.0	12.0	100.0

3.4.2.2 Laser diffraction

Figure 3.4 shows the average PSD of raw and roasted almond obtained by laser diffraction. All the PSDs were multimodal and broad and are similar to the distributions obtained by mechanical sieving, except that the laser method does not include sizes at the high end of the distribution due to an upper size limit between 1500 and 2000 µm. Inter-subject variation was relatively small (i.e. pooled CVs were 12% for NA and 9% RA). Student's paired *t*-test indicated significant differences ($P < 0.001$) in particle size at all the size fractions of the distributions between the two almond forms, apart from the size fractions 141, 159, 178 and 200 µm where the two curves overlapped.

The data indicate that 47 and 56% of the NA and RA particles, respectively, have a size < 500 µm. However, the laser measurements did not include particles > 1700 µm due to size limits, as explained in the *Materials and methods section*. In view of the reliability of the particle size data obtained from the mastication study, using the two different sizing methods, we were justified in incorporating this data into the theoretical model for predicting lipid bioaccessibility.

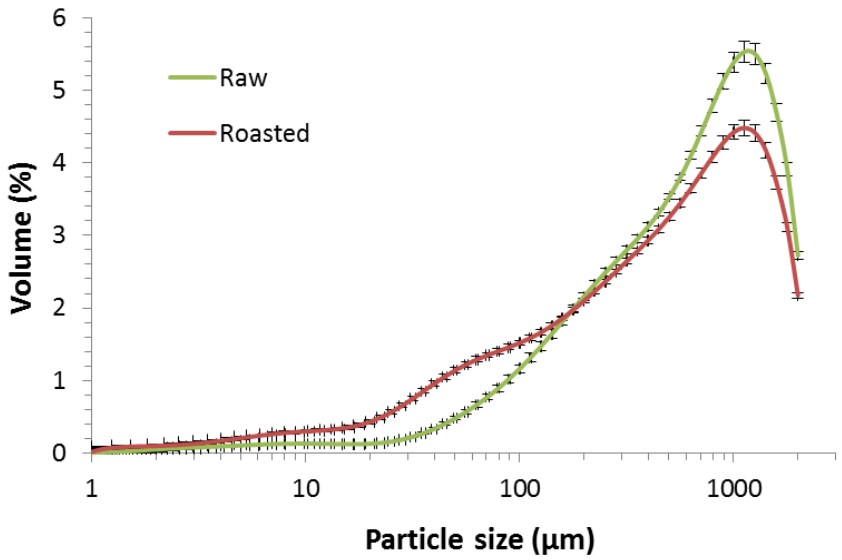

Figure 3.4 Particle size distributions by laser diffraction of raw and roasted almond boluses (n=15, means ± SEM). Significant differences found between raw and roasted were calculated by Student's paired t-test (P < 0.001).

Comparison between studies is challenging as each researcher group use different number of chews and also different sieve aperture size for determining PSD (Al-Ali *et al.*, 1999; Cassady *et al.*, 2009; Frecka *et al.*, 2008; Mowlana *et al.*, 1994; Peyron *et al.*, 2004; Yurkstas and Manly, 1950). Therefore, any future mastication protocols employed to predict nutrient bioaccessibility will need to be standardised.

3.4.3 Correlation between particle size and number of chews

For this part, the d(0.1), d(0.2), d(0.5), d(0.8) values were used to facilitate the comparison between the particle size and the number of chews. As previously explained, these parameters indicate the percentage of the sample that lies below a specific size. As an example, the d(0.8) of raw almonds corresponds to 1076 ± 15.2 µm which means that 80% of the particles constitutive of the samples had a size inferior to approximately 1076 µm (Table 3.3). The number of chews was correlated with the smaller particles sizes (d(0.1) and d(0.2), d(0.5) for raw almond only). This suggests, as previously demonstrated (Buschang *et al.*, 1997; Frecka *et al.*, 2008), that the spreading of the PSD is highly dependent on masticatory parameters. Few mastication cycles produce a lower proportion of the smallest particles.

Table 3.3 Centile (d) values (n=15) of particle sizes (µm) and correlation coefficient (r) between number of chews and particle size for raw and roasted almonds (means ± SEM).

	Raw almonds		**Roasted almonds**	
		r		*r*
d(0.1)	97 ± 4.3[1]	0.83[1]	39 ± 2.4[1]	0.66[1]
d(0.2)	185 ± 8.2[1]	0.83[1]	95 ± 5.3[1]	0.67[1]
d(0.5)	553 ± 16.3[1]	0.60[1]	417 ± 13.9[1]	0.51
d(0.8)	1076 ± 15.2[1]	0.41	958 ± 13.8[1]	0.26
d(0.9)	1347 ± 12.8[1]	0.36	1253 ± 12.0[1]	0.20

[1]Significant difference between almond forms ($P < 0.05$) as calculated by Student's paired *t*-test.

3.4.4 Lipid bioaccessibility determined by the theoretical model and solvent extraction

The predicted and measured percentages of lipid released from masticated almonds by 4 volunteers (28 g almond portion) are presented in Table 3.4. The average values obtained by both methods are in close agreement with about 8% of lipid released for raw and 11% for roasted almonds. Similar predictions (8.4 ± 0.3% for raw almond and 11.1 ± 0.3% for roasted almond) were obtained for the overall group of volunteers (n=15) when they masticated only 4 almonds Tables 3.5; statistically significant differences were found between these two almond forms ($P < 0.001$). The predicted lipid bioaccessibility ranges were 6.4-9.9% for raw, and 8.6-12.5% for roasted almond, reflecting the slightly increased proportion of small particles in the particle size distribution of the RA type.

The model indicated a threshold value of *p*, approximately 55 μm for almond, which is the point at which no more intact cells are present in the cube (particle), based on an average cell size of 35 μm (according to measurements by Beckman Multisizer™ 3 Coulter Counter® and microscopy observations, almond cell sizes range from 20 to 50 μm). Therefore, to obtain 100% release, all the particles would have to be 55 μm or smaller. This is obviously not the case in masticated almonds, and even almond flour (average particle size 250 μm) has a predicted lipid release of ~40% (see *Appendix B)*.

Table 3.4 Percentage of lipid release estimated either measured by the Soxhlet or estimated by the mathematical model using particle size data or measured (n=4, means ± SEM).

	Soxhlet		**Mathematical model**	
Volunteer	Raw	Roasted	Raw	Roasted
1	5.9	11.1	9.4	11.2
2	8.6	12.9	7.5	11.7
3	7.8	12.5	7.2	10.9
4	9.1	8.1	9.9	11.4
MEAN[1]	**7.9 ± 0.7**	**11.1 ± 1.1**	**8.5 ± 0.7**	**11.3 ± 0.2**

[1]Significant difference between the two almond forms ($P < 0.05$) as calculated by Student's paired *t*-test were found, but no differences were found between the experimental and theoretical methods (repeated measures ANOVA).

Table 3.5 Percentage of lipid release predicted by the mathematical model (n=15) for raw (A) and roasted (B) almonds.

A-Raw almonds

Volunteer		**1**	**2**	**3**	**4**	**5**	**6**	**7**	**8**	**9**	**10**	**11**	**12**	**13**	**14**	**15**	**Mean**
Sizes from laser diffraction (µm)	*d(0.1)*	113	104	139	103	104	77	92	86	100	105	82	88	95	96	70	**97**
	d(0.2)	222	197	268	200	199	154	176	160	184	196	168	167	178	176	132	**185**
	d(0.5)	670	587	672	576	591	507	510	521	543	562	567	524	523	521	425	**553**
	d(0.8)	1182	1108	1152	1097	1122	1043	1017	1063	1064	1074	1114	1047	1056	1062	933	**1076**
	d(0.9)	1434	1374	1404	1366	1387	1323	1297	1339	1339	1345	1383	1322	1334	1341	1221	**1347**
Predicted lipid loss		**6.4**	**6.9**	**7.1**	**7.2**	**7.5**	**7.5**	**8.3**	**8.3**	**9.4**	**9.4**	**9.4**	**9.5**	**9.8**	**9.9**	**9.9**	**8.4**

B-Roasted almonds

Volunteer		**1**	**2**	**3**	**4**	**5**	**6**	**7**	**8**	**9**	**10**	**11**	**12**	**13**	**14**	**15**	**Mean**
Sizes from laser diffraction (µm)	*d(0.1)*	46	59	43	42	36	46	39	43	43	46	36	26	24	29	33	**39**
	d(0.2)	118	142	103	98	88	102	93	98	109	102	96	67	64	65	82	**95**
	d(0.5)	504	516	439	431	419	412	398	417	456	407	448	324	349	348	381	**417**
	d(0.8)	1053	1024	990	982	992	939	914	961	985	952	983	845	882	942	929	**958**
	d(0.9)	1332	1304	1281	1278	1287	1233	1207	1255	1274	1253	1270	1149	1188	1253	1232	**1253**
Predicted lipid loss		**9.3**	**10.1**	**8.6**	**10.9**	**11.7**	**11.8**	**12.2**	**12.52**	**11.6**	**9.7**	**11.2**	**11.5**	**12.0**	**11.7**	**11.4**	**11.1**

3.4.5 Composition of cell-wall polysaccharides

The sugar composition of the CW of masticated almonds is presented in Figure 3.5. Almond seed CW are mainly composed of arabinose-rich polysaccharides, including pectic substances, encasing the cellulose microfibrils. Indeed, arabinose, glucose and galacturonic acids were the major sugars found in masticated raw and roasted almond CW, with GLC analysis showing sugar concentrations of 37.9 and 31.1%, 19.0 and 24.3%, and 23.2 and 24.5%, respectively. These values are in close agreement with the ones obtained for whole almonds (before mastication): arabinose, glucose and galacturonic acids concentrations were 35.7 and 38.3%, 20.3 and 20.0%, and 27.8 and 23.5% for raw and roasted almonds, respectively (Ellis *et al.*, 2004). Therefore, no major modifcation in the composition of the CW appears to have occured after mastication compaired with the original non masticated samples, as previously reported (Ellis *et al.*, 2004; Femenia *et al.*, 2001).

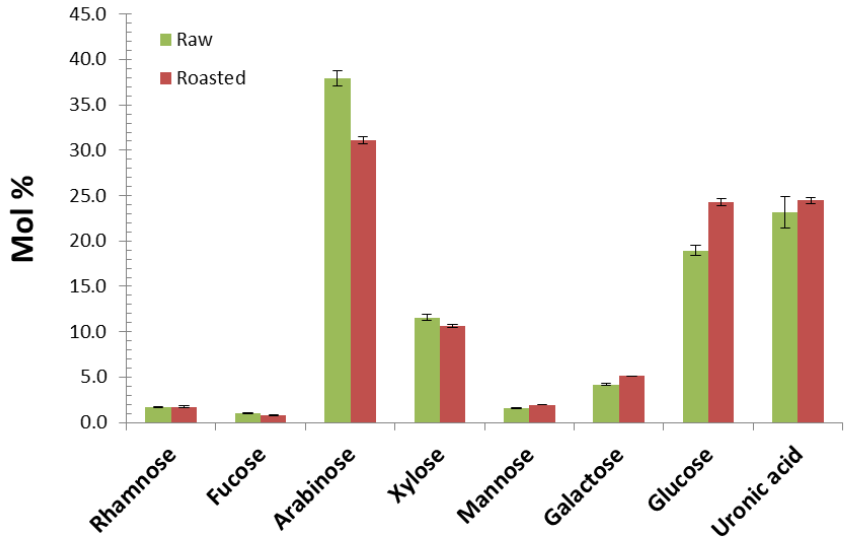

Figure 3.5 Monosaccharide composition (mol%) of raw and roasted almond boluses. Values are mean ± SEM (triplicates).

3.4.6 Microstructure of the masticated almonds

The microstructural characteristics of masticated almonds (Figure 3.6) show that the lipid-rich parenchyma cells appear to remain largely intact, not just in the centre of the particle, but also as

previously shown (Ellis *et al.*, 2004) a few layers of cells beneath the surface. Thus, extensive cell breakage was observed mainly at the fractured surfaces of relatively large particles (e.g. sizes ~1200 µm and 500 µm in Figure 3.6 A and B). Moreover, there was little or no evidence of cell separation in these masticated particles. However, in particles of smaller size (approximately 250 µm), there was evidence of significant levels of cell distortion and rupture in all areas of the almond particle, not just at the fractured surface (Figure 3.6 C).

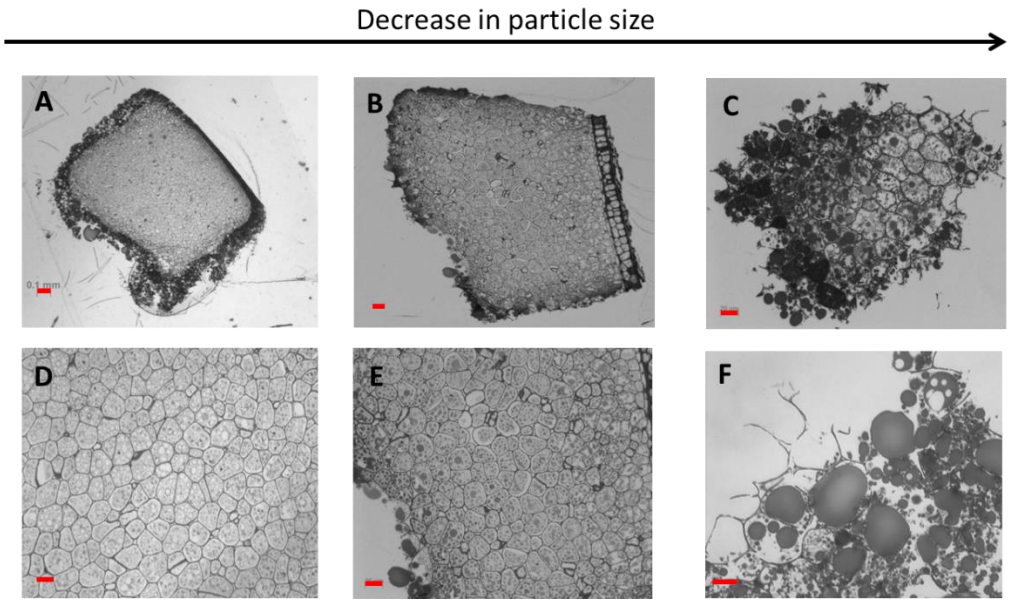

Figure 3.6 LM images of masticated raw almond seed: whole particle of decreasing size (A, B and C); parenchyma cells located in the centre of the particles (D and E); cells situated at the edge of the particles (F, G and H); note the presence of coalesced lipid droplets (images C, E and F). Scale bars: A = 100 µm; B = 50 µm, C-E = 20 µm, and F = 20 µm. Approximate size: A: 1200 µm, B: 500 µm, and C: 250 µm.

SEM images provide further evidence of the apparent greater damage caused by chewing in the smaller almond particles (Figure 3.7). One possible explanation of this is that small particles may have received a larger number of deformations (chews) during mastication, potentially leading to greater structural damage to the cellular tissue. The lipid-rich parenchyma cells were found to be tightly packed together, but much less so for some of the small particles, thus creating a compact tissue matrix that makes the diffusion of molecules (e.g. lipase) and fluid extremely difficult, as

illustrated by the centres of the particles remaining unstained with osmium tetroxide (Figure 3.6). The micrographs (Figures 3.6 and 3.8) clearly show that the majority of the nutrients remained encapsulated in their original form inside the cells. These intracellular inclusions are mainly lipid bodies as demonstrated by Nile red staining (Figure 3.9). The relatively uniform ('spherical') microstructure of the OBs can be distinctly seen in TEM images in Figure 3.8 A and B.

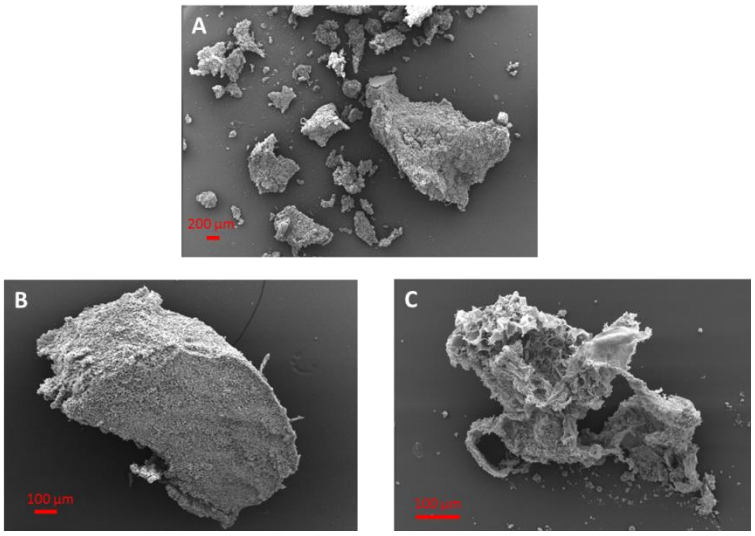

Figure 3.7 SEM of particles from masticated raw almond seed. Scale bars: A and B = 200 µm; and C = 100 µm. Approximate sizes of raw almond particles: B, 2000 µm; and C, 550 µm.

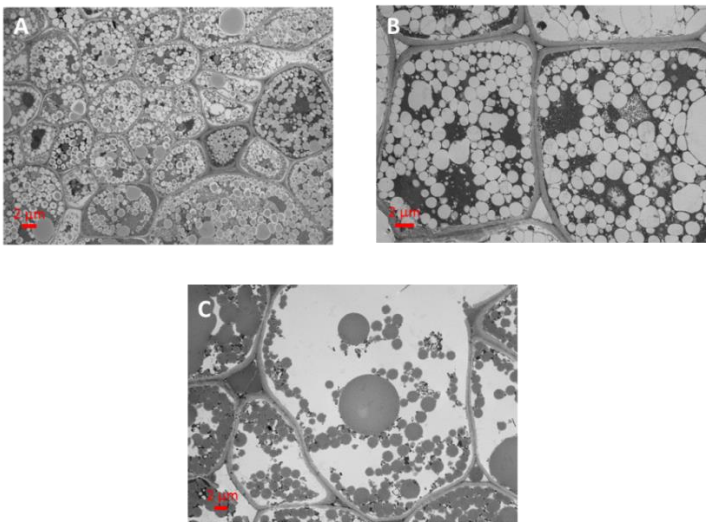

Figure 3.8 TEM images (A and B) of masticated raw almond seed (A and B) showing intact cells and their content. TEM image (C) of ruptured cells at the surface of the masticated raw almond particle; note the coalesced oil bodies. Scale bars: A = 6 µm; B and C = 5 µm.

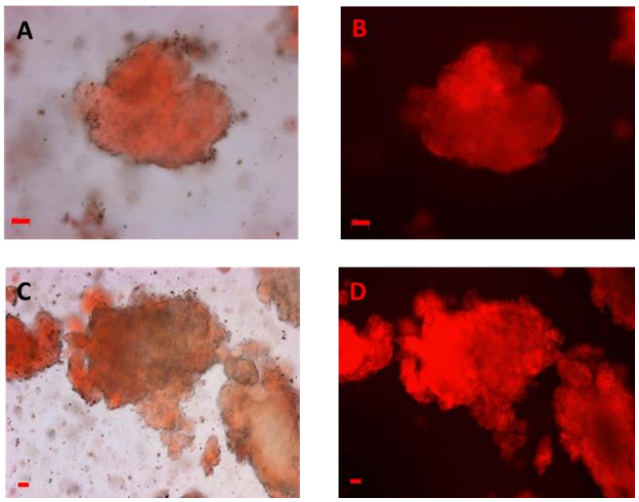

Figure 3.9 LM images of masticated raw almond seed stained with Nile red; images A and B are ~140 µm and images C and D are ~375 µm particles. Scale bars: A-D = 20 µm.

As previously demonstrated (Ellis *et al.*, 2004), the cells located at the surface of the particles were ruptured, and intracellular contents exposed to the external environment, although some of the nutrients, including lipids, were still present and thus not removed by saliva at the fractured surface (Figure 3.10). However, when masticated, tissue rupture appears to occur unevenly within the almond particle and fissures running from the fractured surface of almond particles into the underlying core tissue were observed (Figure 3.6 C and F); some of these fissures created new particles that were eroded from the particle surface (Figure 3.6 F). These fissures seemed to be more frequent in the small particles relative to large ones.

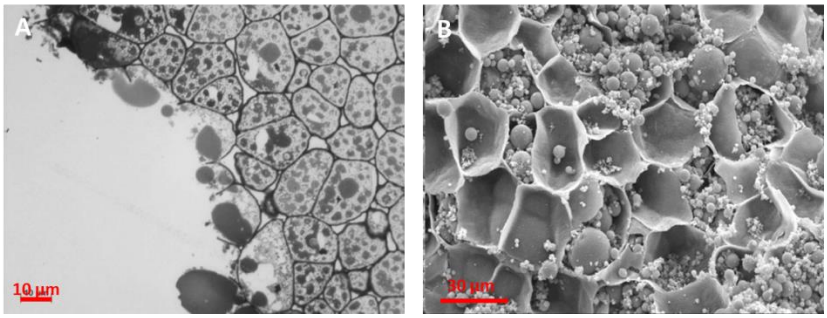

Figure 3.10 LM (A) and SEM (B) images of the surface of masticated almond particles. Scale bars = 10 µm and 30 µm for images A and B, respectively.

3.5 Discussion

The accumulation of evidence from epidemiological and human metabolic studies has shown that the consumption of nuts such as almonds reduces a number of risk factors associated with non-infective disease, such as type 2 diabetes, cardiovascular disease (CVD) and obesity (Bao *et al.*, 2013; Jenkins *et al.*, 2006; Joice *et al.*, 2008; Sabate and Ang, 2009). The behaviour of almonds in the GIT may explain why almonds have these potential health benefits, notably a slow rate and limited extent of digestion of almond lipid and other macronutrients post-mastication (Berry *et al.*, 2008; Ellis *et al.*, 2004; Mandalari *et al.*, 2008a). These effects are strongly linked to the structure and properties of almonds, particularly the structural integrity of their CW. Almond seeds are an energy-dense food, typically containing ~50% of lipid, so they would be expected to elicit a relatively high postprandial lipaemic response when ingested. However, previous work has revealed that a high proportion of lipid remains encapsulated in the cells of almond tissue and is therefore less available for digestion (Ellis *et al.*, 2004), leading to reduced energy absorption (Cassady *et al.*, 2009; Novotny *et al.*, 2012) and a low postprandial lipaemic response (Berry *et al.*, 2008). These findings are reinforced by a recent study showing that the Atwater factors, used for estimating the metabolisable energy content of foods, overestimates the energy content of almonds by as much as ~32%, relative to the empirically-derived value in humans (Novotny *et al.*, 2012).

One crucial aspect previously overlooked in many nutrition studies is the complex behaviour of food materials in the GIT. It is now well recognized that changes in the structure and physicochemical properties of plant food matrices significantly affect the rate and extent of nutrient digestibility; e.g. CW encapsulation (Ellis *et al.*, 2004; Noah *et al.*, 1998). For instance, to be optimally digested, lipids must be released from the cells of almond tissue and emulsified (Michalski *et al.*, 2013). However, in the present study we have shown that the proportion of lipid released from the almonds following mastication is severely limited. Thus, lipid bioaccessibility values predicted by the theoretical model

or determined experimentally were very low, within the range of 8 to 11% for almonds, but with the roasted form being slightly higher at the top end of this range.

Particle size of boluses of two types of almonds, raw and roasted, were measured using mechanical sieving and laser diffraction. Little difference in the PSDs was found between raw and roasted almonds; however, a higher proportion of small particles were observed in the roasted almond boluses. For both almond forms an important proportion of the boluses' particles, ~35 to 40%, had a size > 500 µm. Individuals therefore tend to swallow large particles, with low bioaccessibility, when eating almonds. We also found that depending on the size of the generated particles the degree of damages varied (Figure 3.7). For large almond particles (size > 500 µm), the cells on the surface were mostly ruptured by mastication, whereas the structural integrity of cells in the central part of the particles were preserved. On the other hand, smaller particles showed damages even in the cells located in the core of the particles. The relatively high proportion of large particles in the masticated samples explains why chewed almonds have such a low lipid bioaccessibility. This observation is consistent with the results of a digestibility study showing that lipid digestion in raw almonds, albeit in 2 mm cubes rather than masticated samples, is restricted to ~10% in the early stages of digestion (≤ 3 h) in the gastric and duodenal phases (Mandalari *et al.*, 2008a). Restricted bioaccessibility and digestion of lipid post-mastication, caused by encapsulation of lipid by the CW in almond seeds, also plays a crucial role in determining postprandial lipaemia (Berry *et al.*, 2008). Moreover, these findings may provide some explanation of why the consumption of whole almonds suppresses hunger and desire to eat, as recently reported by the Mattes group (Tan and Mattes, 2013). The same group had previously demonstrated the importance of chewing in relation to gut hormone signalling, and the effect on satiety (Cassady *et al.*, 2009). Also, a bolus composed of particles that are large (size > 1000 to 2000 µm) and hard delays gastric emptying as they cannot pass through the pylorus (i.e. related to the so-called 'sieving effect') (Kong and Singh, 2008), inducing a feeling of fullness, which may contribute to lower subsequent energy intake (Mattes and Dreher, 2010).

However, no attempt has been made previously to characterise masticated almonds to allow quantification of lipid potentially available for digestion, including the early stages of digestion, which is a key determinant of postprandial lipaemia (Berry *et al.*, 2008), and other metabolic responses (Jenkins *et al.*, 2006).

As reported previously (Mishellany *et al.*, 2006; Peyron *et al.*, 2004), an almond bolus before swallowing consists of particles of various sizes, which is consistent with the multimodal PSDs obtained for both almond forms seen in the current study. The initiation of swallowing has been suggested to rely on a particle size threshold (Prinz and Lucas, 1995). The ready-to-swallow bolus must also be cohesive to prevent particles getting into the airways. Texture and lubrication are also essential criteria for swallowing to occur, and are generally consistent between individuals (Drago *et al.*, 2011). The sensory signals received by the mouth receptors trigger deglutition, based notably on the insalivation and the rheology (i.e. viscosity) of the bolus (Flynn *et al.*, 2011; Lucas and Luke, 1986; Peyron *et al.*, 2004; Yurkstas, 1965). The absence of intra- and inter-individual variability in our data confirms the hypothesis that the almond bolus has to reach a specific consistency, which seems similar between individuals, before being swallowed (Prinz and Lucas, 1997). Despite the fact that mastication is highly individual, PSD per almond type is similar among subjects, which is in agreement with other studies (Hiiemae, 2004; Jalabert-Malbos *et al.*, 2007; Jiffry, 1981; Mishellany *et al.*, 2006; Peyron *et al.*, 2004). As explained by Hiiemae (Hiiemae, 2004), the masticatory parameters, such as number of chews, their strength and frequency, is specific to the individual, but the end product (bolus) is similar. Masticatory behaviour differs depending on the food properties and the transformations occurring to it when chewed (Woda *et al.*, 2006b). Hard foods such as tree nuts require more mastication cycles and chewing for longer than softer food (i.e. carrot or cauliflower), producing a bolus containing more particles of a smaller size. Moreover, a single chew could break foods into various numbers of particles according to the physicochemical properties of that particular food, notably water content as well as DF (cell wall) content and structure. For

instance, tree nuts such as almonds, appear to produce more small particles per chew than carrots (Jalabert-Malbos *et al.*, 2007; Lucas and Luke, 1986; Mowlana *et al.*, 1994; Varela *et al.*, 2008a).

One explanation for the wide size range of particles comprising the almond bolus has been expressed by Flynn and colleagues (Flynn *et al.*, 2011). They suggested that the mouth contains several compartments where food fracture differs. Thus, during mastication some particles are broken into several smaller fragments, while others are retained in 'non-mastication' compartments of the oral cavity inaccessible to the crushing or grinding action of the teeth. The adhesion of the compressed particles to the contact surfaces of the teeth while masticating probably amplifies this phenomenon and, as such, almond material adhering to teeth surfaces will be more easily fractured than freely moving particles (Woda *et al.*, 2006b). This may also explain the greater damage that occurred to the smaller almond particles (Figure 3.7), which has a significant bearing on lipid bioaccessibility. Indeed, a greater number of fissures in the almond tissue below the fractured surface results in an increase in the accessibility of lipid substrate to digestive fluids containing lipase and BS.

The mastication parameters obtained for the two types of almonds were very similar despite the differences in their PSDs. The greater number of small particles in the roasted almond boluses is probably related to the reduced water content of the CW. In the CW, water can act as a plasticiser, so when it is removed, the CW as well as the whole almond tissue become more brittle (Blahovec, 2007). The roasting process also affects the integrity of almond CW microstructure and induces coalescence of the lipid bodies to produce large lipid droplets that are less susceptible to be digested (i.e. reduced surface area to volume ratio) (Agrawal *et al.*, 1997; Pascual-Albero *et al.*, 1998; Varela *et al.*, 2006).

A wide range of techniques are available to measure the size of particles, for nuts and almond in particular, and mechanical sieving is the technique that is most commonly used. In previous studies, mechanical sieving, laser diffraction, image analysis and optical scanning methods have been used on natural (Hoebler *et al.*, 2000; Jalabert-Malbos *et al.*, 2007; Lemmens *et al.*, 2010; Schneider and Senger, 2001; Wang *et al.*, 2006) as well as artificial foods (Buschang *et al.*, 1997; Olthoff *et al.*, 1984; van der Bilt *et al.*, 1993), usually in order to evaluate masticatory efficiency. As far as almonds are concerned, the method predominantly employed has been mechanical sieving (Al-Ali *et al.*, 1999; Cassady *et al.*, 2009; Frecka *et al.*, 2008; Ow *et al.*, 1998; Peyron *et al.*, 2004). Masticated almond samples have been described as a mixture of medium size (200 to 4000 µm) and fine (< 200 µm) particles; 35 µm being the approximate size of a single almond cell and 4000 µm the largest particle found (Cassady *et al.*, 2009; Frecka *et al.*, 2008; Peyron *et al.*, 2004). Medium size particles can be analysed with mechanical sieving however this technique has been described as inaccurate for fine particles because the separation is frequently incomplete, especially in lipid-rich material such as almond (Lauer, 1966). In the present study, mechanical sieving and laser diffraction were used. This choice was justified by the heterogeneity, as well as the broadness, of the particle size distribution of the almond bolus.

The main difficulty encountered with the particle sizing related to the complexity and behaviour of the material studied here. For example, masticated almond particles tend to aggregate due to the lipid release occurring during the mastication process. Nevertheless, the almond seed has been described as a suitable material to use for particle sizing studies as it is easily comminuted, it is not humid or stringy, it does not break up into smaller fragments during the sizing process as a result of the sieves vibrations, it does not disperse or solubilise in water and saliva, and it is possible to weigh it after chewing (Schneider and Senger, 2001). Another major advantage is that almond is often consumed raw and non-processed, the present measurements are therefore likely to be representative of almonds consumed in a typical diet.

Mechanical sieving is an economic and easy method to measure the particle size of dry/semi-dry and non-cohesive materials. The use of a sieve shaker permits researchers to obtain more accurate and reproducible data than hand sieving as the vibrations are consistent in intensity during and between measurements. Washing the sieves with deionised water before and after shaking them permitted the satisfactory separation of the almond particles. One advantage of the Malvern 2000® laser diffraction particle sizer is that it allows a broad size range of particle, from 0.02 to 2000 μm, to be determined. However, sieve analysis can also be performed on larger particles (covering the largest particles contained in almond boluses, ~4 mm), although finer particles can reduce sieving efficiency (Allen, 1997). The sieves of small apertures get easily damaged when used regularly especially with lipidic material such as almonds. The laser diffraction method gives continuous measurements of particle sizes as opposed to the sieving method, which is limited in the number of sieve sizes that could be used; thus only 8-10 sieves can be loaded on the shaker. Despite the slightly narrower size range of particles measured by laser diffraction (limited to sizes below 2000 μm), the technique gave a good estimation of the overall distribution. Another advantage of using the laser diffraction in the current study was that, once the instrument was set up for analysis, it allowed the operator to obtain accurate and reproducible results quickly without having to calibrate against a standard. It was clearly less time consuming than using mechanical sieving as it took approximately 2 h for preparing and measuring the samples for the laser diffraction as opposed to approximately 10 h for mechanical sieving. However, identifying the machine parameters characteristic of the analysed material required a good understanding of both the principle of the laser diffraction and the physicochemical properties of the material. Malvern 2000® laser diffraction particle sizer is therefore the recommended method to determine particle size distribution of almonds and other nuts. Nonetheless, in the current study a combination of laser diffraction and sieving was required to generate detailed information on masticated almonds so that reliable nutrient release values could be predicted from the mathematical model. Using this method to produce a complete PSD, we would anticipate that the model could be applied to other foods relatively simply. For example, we

would expect foods with similar physical and structural properties to almonds to be particularly amenable to this approach. To be applied, the model requires that the majority of cells rupture rather than separate during chewing, that they are roughly spherical, and that an average diameter is available.

Therefore, the present study demonstrated that after mastication only a small proportion of lipid was released from the ruptured cells located on the fractured surfaces of masticated almonds (Figures 3.6 to 3.10). The cells underneath these layers remained intact (i.e. integrity preserved as showed on the micrographs and CW composition analysis), and retained their content. The mathematical model estimates how much lipid is released from the fractured layer of ruptured cells. In almond tissue, particle size is therefore the key parameter that affects lipid release. The more the almonds are chewed the more the particle sizes contained in the bolus are reduced and the more ruptured cells are produced. The smaller the particles the greater the lipids released. Lipid release increases rapidly as particle size decreases, until the point at which all the cells are ruptured.

As discussed above, laser diffraction provided a reliable and efficient method for obtaining size information on almonds masticated by human volunteers. Compared with sieving, laser diffraction generated much more data from narrower size intervals. However, for applying size data to the theoretical model for predicting bioaccessibility, additional information on the largest masticated particles (≥ 1700 µm), using the sieving method, was required. Given the importance of mastication in influencing bioaccessibility, digestion kinetics, postprandial lipemia and energy metabolism (Berry *et al.*, 2008; Cassady *et al.*, 2009; Ellis *et al.*, 2004; Mandalari *et al.*, 2008a; Mattes, 2005; Novotny *et al.*, 2012; Waldron *et al.*, 2003), this novel approach of combining *in vitro* and *in vivo* methods with mathematical modelling has potential for the future. For instance, this approach could be applied to other nutrients (e.g. starch and vitamin E) (Butterworth *et al.*, 2012; Mandalari *et al.*, 2008a) found in plant foods in which CW rupture is the predominant mechanism of nutrient release (Berry *et al.*,

2008; Ellis *et al.*, 2004; Mandalari *et al.*, 2008a), including nuts and seeds with similar properties to almonds.

In conclusion, we have developed a new methodology for determining lipid bioaccessibility of masticated almonds, showing that the majority of lipid (about 88%) is retained within the tissue matrix (i.e. as intracellular lipid). As previously shown, this encapsulated lipid severely reduces the amount of substrate available for lipase action in the stomach and small intestine (Mandalari *et al.*, 2008a) and also attenuates lipaemia in human subjects (Berry *et al.*, 2008). An encapsulated lipid mechanism also provides a plausible explanation of why almonds elicit a low postprandial lipaemia and have a low metabolisable energy content despite its status as a high energy density food (Cassady *et al.*, 2009).

CHAPTER 4

IN VITRO GASTROINTESTINAL DIGESTION OF WHOLE ALMOND SEEDS

4.1 Introduction

In vitro gastrointestinal models can potentially overcome many of the difficulties associated with human studies as the latter are often costly, time-consuming and depending on the design of study and food tested, some ethical issues may also arise. However, the GIT is a complex system that relies on a range of physical and biochemical processes (i.e. gastric emptying, secretion of enzymes and digestive fluids, and motility) contingent on the individual, his/her body requirements and the food consumed. An efficient model has to simulate the dynamic conditions of the different digestive compartments while keeping them consistent and well monitored in order to measure the variable of interest (e.g. nutrient release) (Venema *et al.*, 2009).

This chapter describes in more details the physiological events occurring in the stomach and the intestine during digestion as well as some of the current *in vitro* models. The DGM and SDM were used to study the digestion of masticated raw and roasted almonds results of which are presented here.

4.1.1 Physiological activity in the stomach

The food coming from the mouth arrives in the stomach via the oesophagus where its disintegration into smaller particles continues. The stomach also acts as a short-term storage reservoir and thus controls the delivery of chyme[3] to the duodenum. It consists of 4 regions which are the fundus, body, antrum, and pylorus (Figure 4.1). The fundus and body are 'storage locations' for undigested material and are responsible for the emptying of liquids (Johnson, 1991; Kong and Singh, 2008; Schulze, 2006). The antrum assures the mechanical digestion, which involves churning, mixing with gastric juice and sieving of solid foods by powerful contractions. Chemical and mechanical processes

[3]Semi-liquid food mixture resulting from the digestion occurring in the stomach (Guyton and Hall, 2010)

perform simultaneously to reduce the meal into digestible particles. In order to achieve a completed gastric digestion, the food ingested should therefore be transformed into particles that are diluted into the gastric juice, and with a surface area that allows the penetration of the elements essential to the digestion, such as enzymes (i.e. pepsin and gastric lipase) and salts.

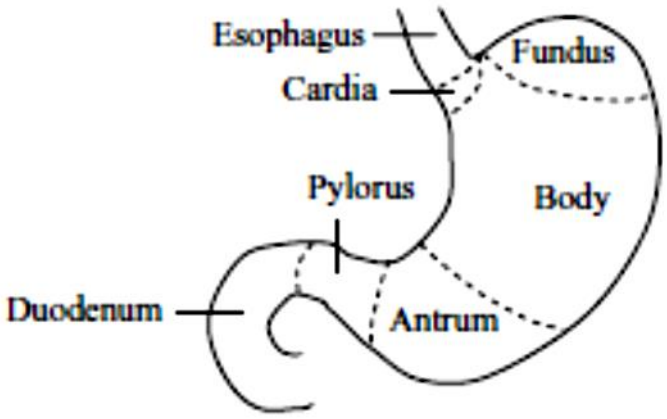

Figure 4.1 Anatomy of the stomach with its different compartments (Kong and Singh, 2008).

During digestion, two types of contractions are generated in the stomach: slow volume-reducing (fundus) and peristaltic (antrum contraction waves, ACW) contractions (Pal *et al.*, 2007). The weak contractions of the fundus ensure the transport of the bolus from the top to the bottom of the stomach thus driving gastric emptying (Figure 4.2), whereas the waves engendered by the antrum's peristaltic contractions disintegrate the bolus and mix it with gastric juice. These mechanical and hydrodynamic forces result from the peristaltic waves initiated by the stomach wall. The way the contractions are produced vary between fed state, when continuous movements are propagated, and fasting state, when the contractions follow a 4 phases, cyclic pattern. The food contained in the fundus progresses to the antrum once the pyloric sphincter opens to deliver the chyme, and thus the antrum continually empties its content into the duodenum.

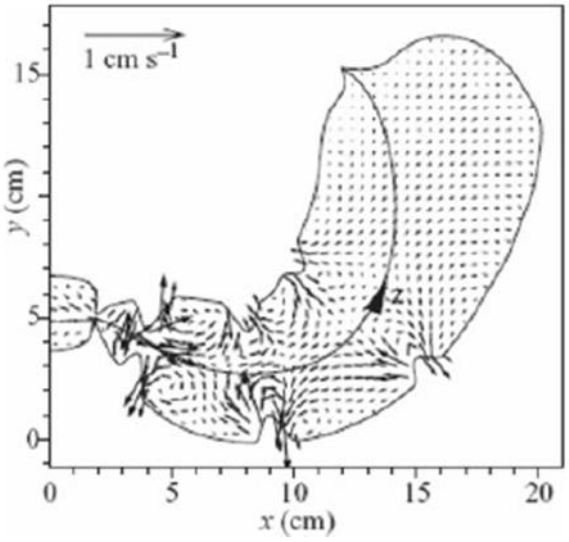

Figure 4.2 Predicted flow patterns produced by propagating ACW (Pal et al., 2007).

However, according to the computer model developed by Pal and colleagues, the gastric emptying appears to be much more complex than this traditional description. The chyme located in the region that the authors called 'stomach road' (or 'Magenstrasse'[4]) is initially emptied, followed, sometimes much later, by the remaining digesta that has been deposited into the antrum. Therefore, two flow paths might exist: a rapid one, for which the chyme (liquid phase) travels from the fundus to the duodenum within 10 min; and a slower trajectory for the solid phase of the chyme. A sieving mechanism takes place where liquids and small particles take the rapid path (during digestive motility), whereas larger and heavier debris are collected into the antrum (during the fasting motility), lipids forming a floating layer on the top of the bolus (Schulze, 2006). Retropulsion, which corresponds to the 'return' of the chyme into the stomach after having been propulsed and grinded in the distal stomach area, also occurs (Figure 4.3). This mechanism is generated by the strong contraction at the terminal antral area (Bilecen *et al.*, 2000).

[4]Gastric canal along the lesser curvature from the cardia to the antrum (Pal *et al.*, 2007)

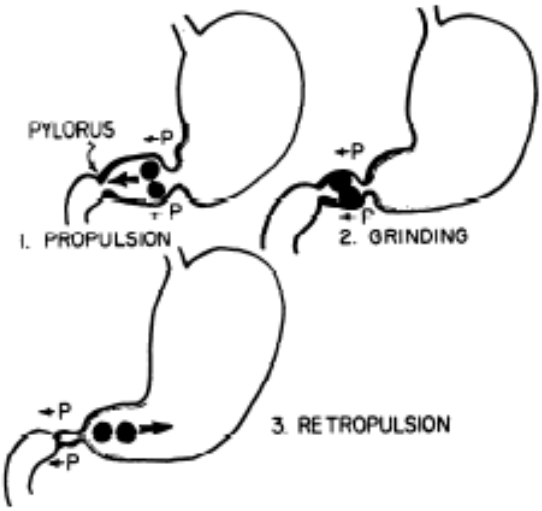

Figure 4.3 Propulsion, grinding and retropulsion of solid food in the stomach (Kelly, 1980).

A study done by Marciani and co-workers using echo-planar magnetic resonance imaging revealed that the gastric secretions penetrate slowly into the bolus, starting with the outer part then attaining the inner one (Marciani *et al.*, 2001). The extent to which gastric secretions spread into the bolus appears to rely on the viscosity of the meal ingested. Contrary to the conventional opinion, the latter remains heterogeneous for a long period of time thus preventing the gastric secretions from reaching the centre of the bolus. Furthermore, the most diluted part of the bolus, the one that contains the greater amount of gastric secretions, is the first to leave the stomach to enter the duodenum which is in accordance with Schulze's theory (Schulze, 2006).

The gastric emptying rate influences the food disintegration which also regulates the rate of nutrients absorption. The different functional attributes of the stomach rely on the chemical composition and physical nature as well as the amount of the food ingested. The proportion of liquid and solid in the meal affects the time required to digest it. Larger size particles, denser and/or harder food delay the gastric emptying rate. The same occurs in the presence of lipid in the meal either because of the phase separation in the chyme or as lipids enter the duodenum cholecystokinin is released and pyloric contractions altered (Heddle *et al.*, 1989; Marciani *et al.*, 2001). Viscosity and calorie content of the food are additional crucial regulators of gastric emptying (Marciani *et al.*, 2000)

as the force of contraction of the stomach walls adjusts appropriately (Marciani *et al.*, 2001). For instance, guar gum, a galactomannan-rich legume flour (a form of 'soluble fibre') was reported to induce a change in hydrodynamic factors (e.g. alter flow patterns by raising viscosity) and disrupt gastric sieving (Meyer *et al.*, 1986; Meyer and Doty, 1988). Stomach emptying appears also to depend on the mastication, in other words if the food has been broke down into small particles to a great extent the digestion taking place in the stomach will be facilitated, as the surface area for digestion will be increased (Pera *et al.*, 2002). Also, a number of other factors especially nervous reflexes and hormonal signals (e.g. gastrin, CCK and GIP), themselves related to the properties of the meal ingested, modulate the amount of chyme entering the duodenum (Crawley and Corwin, 1994; Heddle *et al.*, 1989; Horowitz *et al.*, 1994; Meyer *et al.*, 1989; Tougas *et al.*, 1992).

4.1.2 Physiological activity in the small intestine

The small intestine consists of 3 parts: the duodenum, jejunum and ileum. Its main function is the digestion and absorption of nutrients, most of it occurring in the upper portion of the small intestine (duodenum). To fulfil this role, intestinal enzymes, BS and various electrolytes (i.e. Na, Cl and K) are required. The absorption of nutrients is maximised by the large absorptive area of the intestine. Its inner wall, or mucosa, is folded, each fold being covered with villi, which in turn are lined with microvilli.

The chyme that reaches the small intestine undergoes a longitudinal mixing and breaking down by peristalsis and segmentation (Figure 4.4). Segmentation contractions are of various types (i.e. regular/irregular and isolated/spaced) and are responsible for the motility of the chyme in both directions, thereby churning and fragmenting the digestive material. As for peristaltic contractions, they propel the chyme along the length of the small intestine.

The extent of the chyme mixing and propagation along the intestinal tract is determined by its rheological properties (i.e. viscosity) which affect release and absorption of nutrients.

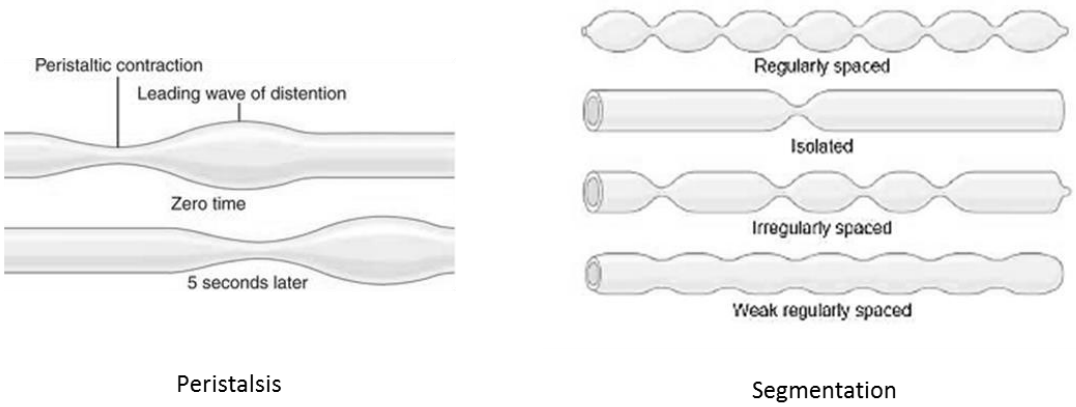

Figure 4.4 Schematic representation of the peristalsis and segmentation contractions occurring in the small intestine, adapted from (Guyton and Hall, 2010).

4.1.3 Transformation occurring to digesta and emulsion in the GIT

The digesta is a suspension of particulates the composition of which changes as it progressively transits in the GIT (Lentle and Janssen, 2008). As a result of the secretion of gastrointestinal juices and the absorption of nutrients and water, the concentration, shape and size of the particulates is altered thereby affecting the physicochemical properties of the digesta. The lipids released from the food matrix are emulsified first in the stomach.

The intensity of the contractions within the GIT fluctuates greatly. The ACW are relatively weak and leads to a surface mixing, whereas the contractions generated by the pylorus are much stronger thus ensuring a effective size reduction of the lipid droplets (Armand *et al.*, 1996; Lentle and Janssen, 2008; Schwizer *et al.*, 2006). Moreover, the stability of the emulsions decreases when exposed to the acidic components of the gastric juice and the low pH of the stomach since these parameters induce changes in interfacial composition. Indeed, if the pH is close to the isoelectric point of the proteins

stabilising the emulsion, their tertiary and quaternary structure is altered and so is their adsorption onto the interface (Dalgleish, 1997). In addition to the reorganisation of their interface, the average emulsion size decreases to about 20 to 40 µm due to the stomach contractions and the retropulsion phenomenon (Armand *et al.*, 1994). TAG emulsification susceptibility increases with the chain length and degree of unsaturation of the fatty acids in the TAG molecule (Kimura *et al.*, 1994). Therefore the nature of the lipids ingested could presumably influence the characteristics of the emulsion generated (i.e. variability in droplet sizes) and correspondingly their digestibility (see *Chapter 5*). The emulsification and lipolysis occurring in the stomach are essential steps that facilitate the subsequent intestinal digestion of lipids.

Surface-active molecules are secreted in the intestine, i.e. BS and lecithin, which also has an effect on the emulsification process and consequently the lipolysis. These biosurfactants appear to 'clean' the surface of the oil droplets by removing existing molecules present on the interface (Wilde and Chu, 2011). The generated lipolytic products are then solubilised in the form of mixed micelles and vesicles. The products of lipid digestion need to be removed from the lipid-water interface to prevent lipase inhibition, in particular long chain fatty acids (Lairon, 2009).

The fate and characteristics of the undigested food particulates is rarely mentioned in the literature, since it is often assumed that they are fully disintegrated and dispersed in the aqueous phase of the digesta. Many different forms of DF have been extensively studied as isolated molecules (e.g. galactomannanns) or as extracted particulates (e.g. wheat bran) on gut function and digestion, but studies of intact plant tissues, such as the structural matrix of CW, has received very little attention. Our research group has however previously highlighted the importance of such work by showing that tissue particles of hard plant foods (e.g. nuts) are only partially digested, some of which are recovered in the faeces (Ellis *et al.*, 2004; Mandalari *et al.*, 2008a).

4.1.4 Methods for studying digestion

Various methods have been employed to simulate the digestion process (from the mouth to the anus) and study food disintegration (Guerra *et al.*, 2012; Venema *et al.*, 2009). *In vivo* procedures include the design of feeding studies using intubation (Heddle *et al.*, 1989; Marciani *et al.*, 2000), scintigraphic and ultrasonographic methods, echo-planar MRI (De Schepper *et al.*, 2004; Kwiatek *et al.*, 2006; Marciani *et al.*, 2000; Marciani *et al.*, 2001), and other indirect methods such as blood and breath tests (Choe *et al.*, 2001; Klein, 2001). However, *in vivo* methods have the disadvantage of being often fairly invasive, time-consuming, inaccurate and/or expensive, whereas *in vitro* systems may not realistically simulate the biological processes. Indeed, one of the major difficulties faced by using laboratory models is to reproduce the variable gastric residence time specific to a particular food/meal and the hormonal responses induced by the ingestion of that food. Sampling is often challenging in studies involving humans; the digesta may simply not be accessible without invasive procedure (i.e. intestinal digesta) and it may not be homogeneous. Moreover, the measurement of certain parameters may not be possible (i.e. pH). In order to overcome these issues, *in vitro* models have been developed and according to Prof Alric and her team these models need to be flexible, accurate and reproducible (Guerra *et al.*, 2012).

The most basic *in vitro* digestion assays are called **static** models (or biochemical) where only the biochemical mechanisms occurring in the stomach and/or the intestine are mimicked and the products of digestion remain during the whole digestion process (Wickham *et al.*, 2009), unless simple models employing dialysis bags are used. On the other hand, in **dynamic models** the pH, enzyme secretion and shear stress conditions vary over time to simulate physiological conditions.

Some *in vitro* models have been designed to simulate one compartment of the GIT (*Appendix C*). These include the mouth model known as the **chewing simulator** (Salles *et al.*, 2007), and the stomach models, for example, human gastric simulator (**HGS**) from UC Davis (Kong and Singh, 2010)

and the **DGM** at the IFR, Norwich (Wickham *et al.*, 2012). Other models are multicompartmental, which model all the main sites of the gut: the stomach, duodenum, jejunum and ileum. A well-known example of this is the dynamic computer-controlled upper GIT model (**TIM-1** and **TIM-2** digestion model from TNO Nutrition and food research in the Netherlands)(Krul *et al.*, 2000). TIM is considered to be a realistic model used to simulate the digestive tract of adult and young humans and also other mammalian guts such as that of the dog. TIM was developed to mimic the physiological conditions (i.e. digestive juices secretion, pH changes, body temperature and transit) and it is also equipped with a dialysis system that simulates the absorption of the digestion products as well as water. A more ambitious gut model is the one developed by the University of Ghent, the Simulator of the Human Intestinal Model Ecosystem (**SHIME**), that comprises the stomach, duodenum, jejunum, ileum, caecum and ascending colon (De Boever *et al.*, 2000). The SHIME not only simulates the entire GIT, but also possesses a stable, *in vitro*-adapted microbial community.

In the present project, the DGM coupled with a static duodenal model (SDM) was used to investigate the gastrointestinal digestion of masticated almonds (Figure 4.5). The DGM reproduces the peristaltic movements occurring in the stomach and controls different parameters such as emptying cycles, shear forces and the quantity of enzymes and acids delivered to the system, consistent with the meal content (see *Chapter 2* for more details). Therefore the limitations of GIT models previously identified such as fluctuation of the chyme composition throughout the digestion process, transit and motility including sieving activity, and anticipation of the body response have been addressed in this model (Venema *et al.*, 2009; Wickham *et al.*, 2009; Wickham *et al.*, 2012). However, the model is monocompartmental, hence the requirement of the SDM. The SDM is a very simple model that does not mimic the mechanical processes (segmentation contraction and peristalsis) that occur in the human duodenum. It consists of an Erlenmeyer flask containing the digested samples collected from the DGM and the simulated pancreatic juice that is left to incubate at 37°C usually for 1 h.

A more simplified static model of gastric and duodenal digestion involving the pH-stat has also been used in this project to study the mechanisms of digestion of oils and a range of almond materials that have been manipulated to produce different levels of lipid bioaccessibility (see *Chapter 5*).

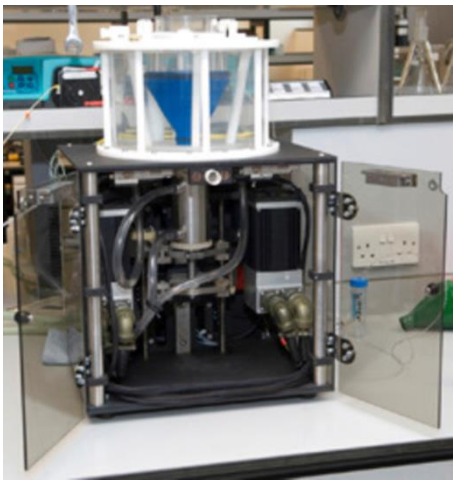

Figure 4.5 Image of the dynamic gastric model.

4.2 Aims

The main objectives for these experiments were to determine:

(a) The microstructural changes occurring to masticated almond during the gastric and intestinal phases (particle size and CW composition); and

(b) The amount of lipid released from the almond particles.

Some of the experiments in the current study included enzyme-free gastric and intestinal fluids to determine lipid release alone. Also, the model used in all the experiments did not include simulation of the large intestine, since the study was designed to determine the bioaccessibility of lipids at the site of their digestion/absorption, and most of these processes occur in the small intestine, specifically the duodenum.

4.3 Materials and methods

4.3.1 Gastric digestion

For each type of almond, raw and roasted, two different sets of samples were loaded into the DGM: four individual samples of 28 g each (pooled samples, PS) and duplicates of combined samples obtained from the fifteen volunteers (combined samples, CS). The boluses obtained from each volunteer following the mastication of the four almonds were too small to be individually loaded onto the DGM, hence the requirement of combining them. Four volunteers (2 males, 2 females) taking part in the mastication study were requested to masticate and expectorate a sample of each type of almond (raw and roasted), which represents a usual almond portion size (28 g) when consumed as a snack, in order to investigate potential inter-subject variation. The volunteers masticated the almonds as they will normally do, which means that the number of almonds per mouthful differed between subjects. The masticated samples were then loaded into the DGM followed by an *in vitro* static intestinal model in order to simulate both gastric and intestinal digestion as described in details in the *Materials and methods* section (*Chapter 2, Section 2.4.3*). The amounts of enzymes and acid secretions added during gastric digestion were as described in Table 4.1.

Table 4.1 Volume (in mL) of acid and enzyme solutions added during the gastric digestion of raw and roasted masticated almonds, for PS (volunteers 1 to 4) and CS (combined sample 1 and 2).

Sample	Acid solution (mL)		Enzyme solution (mL)	
	Raw	**Roasted**	**Raw**	**Roasted**
Volunteer 1	15.0	20.0	22.4	22.0
Volunteer 2	21.0	16.0	17.3	25.0
Volunteer 3	18.8	21.0	14.9	15.0
Volunteer 4	15.0	18.0	21.4	22.0
Mean	**17.5**	**18.8**	**19.0**	**21.0**
Combined sample 1	45.0	52.0	51.0	50.0
Combined sample 2	30.0	42.0	54.0	57.0
Mean	**37.5**	**47.0**	**52.5**	**53.5**

Six PS and eleven CS samples were recovered at different time points of the 1 h gastric digestion then aliquoted for duodenal digestion (7 g), CW (~2 g) and lipid loss (remaining) analyses, and microscopy.

4.3.2 Duodenal digestion

A pooled sample (42 g) obtained from an aliquot (7 g) of each gastric sample was transferred to a plastic tube for duodenal digestion. For the 28 g samples, 8.4 mL of simulated bile solution and 23.5 mL of pancreatic enzyme solution were added, and for the combined samples 16.8 and 47 mL of bile and enzyme solutions, respectively, were used. The duodenal digestion was performed at 37°C for 2 h.

4.3.3 Analyses

Particle sizing (laser diffraction), crude lipid analysis (Soxlet automatic Soxtec 2050), and CW analysis were performed on samples collected after mastication, and after simulated gastric and duodenal digestions. The details of the methods used are described in *Chapter 2*.

4.3.4 Microscopy

Samples collected after mastication and *in vitro* digestion were prepared for LM as detailed in *Chapter 2*.

For practical reasons the masticated samples were stored at -80°C before being sent to the IFR which led to lipid coalescence (*Section 4.4.4.1*). The mastication and digestion procedures were therefore repeated at the IFR using an alternative untested approach developed by Dr Mary Parker. This method consisted in first separating the cells in the raw, roasted and digested

almond tissue using CDTA (as described in *Section 2.2.1.2*), then examining these cells by bright field or fluorescence microscopy to view directly their individual lipid content. To assess the feasibility of this novel approach, a preliminary experiment was carried out using well-defined 2 mm^3 blocks of raw, roasted almonds as well as raw almonds that underwent gastric and duodenal digestions. The samples were prepared using sharp razor blades to minimise tissue damage. For bright field microscopy, the softened blocks were then gently pressed with a spatula in a drop of CDTA on a microscope slide to separate the cells. For fluorescence microscopy, blocks were pressed in a drop of 0.01% (w/v) Nile blue. Separated cells were examined and imaged using an Olympus BX60 microscope (Olympus, Japan), with ProgRes® Capture Pro 2.1 software (Jenoptik, Germany). To localise lipids stained with Nile blue, the NB filter cube (U-MNB, exciter filter BP470-490; barrier filter BA515) of the microscopy was used.

The results of this feasibility study (Figure 4.12) showed that in CDTA-separated almond cells, lipid either as OBs, coalesced droplets, or partially-digested material, is readily identifiable by light microscopy, without the need for embedding or the use of hazardous chemicals such as osmium tetroxide. Therefore, microscopy analysis of some of the 1-2 mm particles of masticated raw and roasted, and digested raw almond tissues was undertaken using the same method.

4.3.5 Statistical analysis

The data were analysed using SPSS version 17.0. For all tests, the significance level was set at $P < 0.05$ (2 tailed). All data are expressed as mean ± SEM. Analysis of variance (ANOVA) was used to test for differences in CW composition and lipid release after gastric and gastric plus duodenal digestion. If a significant difference ($P < 0.05$) was found, post-hoc analysis using Tukey Honestly Significant Difference (HSD) was used to examine each pairwise difference. Two sample *t*-tests (2-tailed) were used to examine differences between raw and roasted almonds.

4.4 Results

4.4.1 Particle sizing

Figure 4.6 shows the average PSD of raw (A and C) and roasted (B and C) almonds following mastication and simulated digestions. PSD of the samples post mastication and post gastric digestion were multimodal and broad, especially for the roasted almonds. The individual expectorated almonds had to be combined to obtain a sample large enough to be loaded into the DGM. The particles composing PS and CS had similar sizes, which suggested that in the present experiment the bite size did not have an impact on the PSD. Some of the data are therefore presented as the average of PS and CS. Also for reason of clarity, the d(0.5) were used to compare the size of almond particles composing the boluses and digesta.

The results of the sizing analysis of the digested samples were found to be similar to those obtained for the masticated boluses. Thus, digested roasted almond samples were composed of particles of smaller size than raw almond; for gastric digestion, the d(0.5) were 468 and 332 µm for raw and roasted almonds, respectively; for gastric plus duodenal digestion, the d(0.5) were 640 and 576 µm for raw and roasted almonds, respectively. No significant difference was found in the overall distribution between masticated and DGM samples (d(0.5) were 506 and 346 µm for raw and roasted almonds, respectively). The digesta recovered at the end of the gastric digestion were composed of a large proportion of particles with a size superior to 500 µm (47% for raw almond and 36% for roasted almond). It was demonstrated in *Chapter 3* that particles of this size and above have a low lipid bioaccessibility (≤ 21%, see *Appendix B*). Therefore, negligible changes in the particle size of almond particles occur during gastric digestion. Duodenal digestion appeared to have a more significant effect. The almond digesta from the duodenal phase was composed of a greater proportion of particles with a large size (61 and 56% with a size > 500 µm for raw and roasted, respectively); however this unexpected PSD may be due to the coalescence of small particles together to generate

large aggregates (*data not shown*). Indeed, the duodenal measurements on size were quite difficult to interpret because the samples formed a viscous and fibrous cluster of particles. Another possible explanation could be that small particles are more disrupted and digested into fine particles not measurable by the laser diffraction (< 0.2 µm).

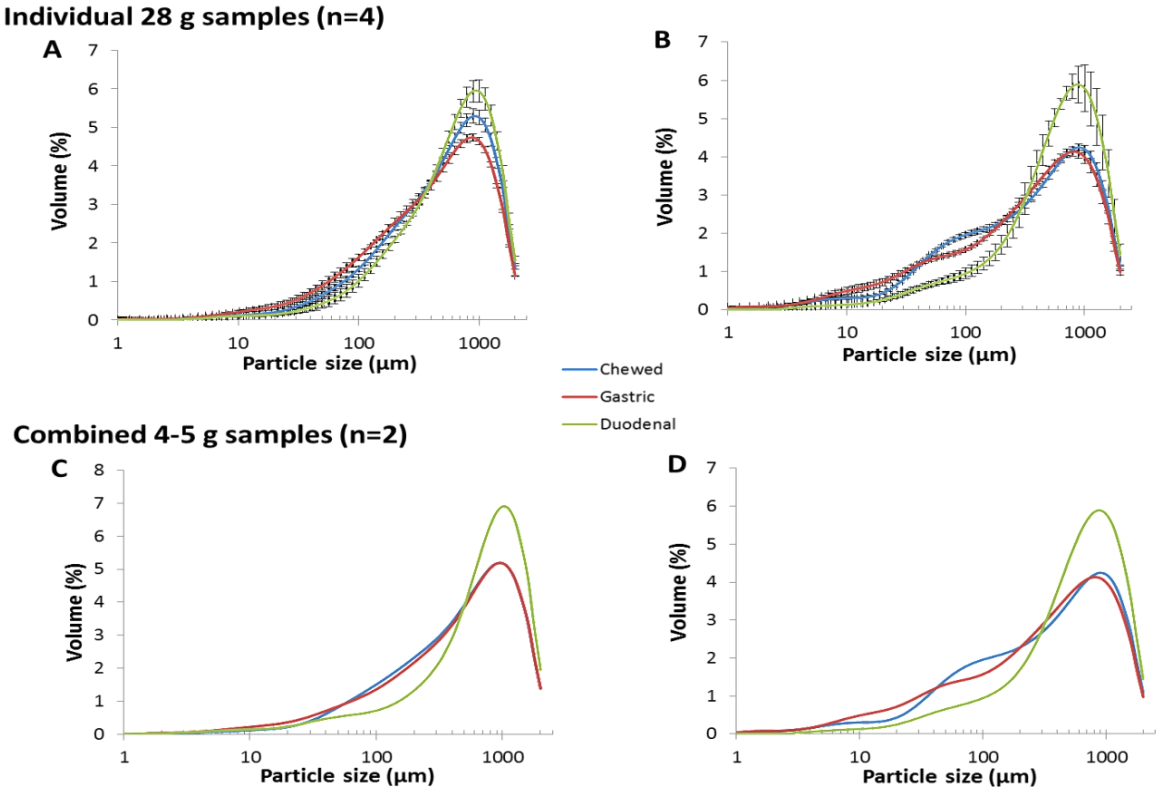

Figure 4.6 Particle size distribution of raw (A and C) and roasted (B and D) almonds recovered after mastication, gastric and duodenal digestions. Values are means (± SEM for A and B only). Significant differences found between raw and roasted were calculated by Student's paired t-test (P < 0.001).

4.4.2 Lipid losses

The lipid release expressed as a percentage of the original amount present in the sample for raw and roasted almonds, following mastication, simulated gastric and gastric plus duodenal digestion is shown in Figure 4.7 A. Between 7.9 and 11.1% of the original lipid has been released as a result of mastication (*Chapter 3*), with no significant differences between the two forms of almonds. A substantial increase in lipid release was observed during the duodenal phase (32.2 ± 1.15 and 32.7 ±

2.23% for raw and roasted almonds, respectively) over that detected in the gastric environment (16.4 ± 0.83 and 17.3 ± 1.00% for raw and roasted almonds, respectively). In a control set of experiments performed without addition of enzymes, no increase in lipid release was detected in the duodenal compartment (*data not shown*). These findings differ from the previous investigation performed by our group using almond cubes and finely ground almonds, where the gastric and duodenal digestions produced only a slight increase in lipid release (Figure 4.7 B) (Mandalari *et al.*, 2008a).

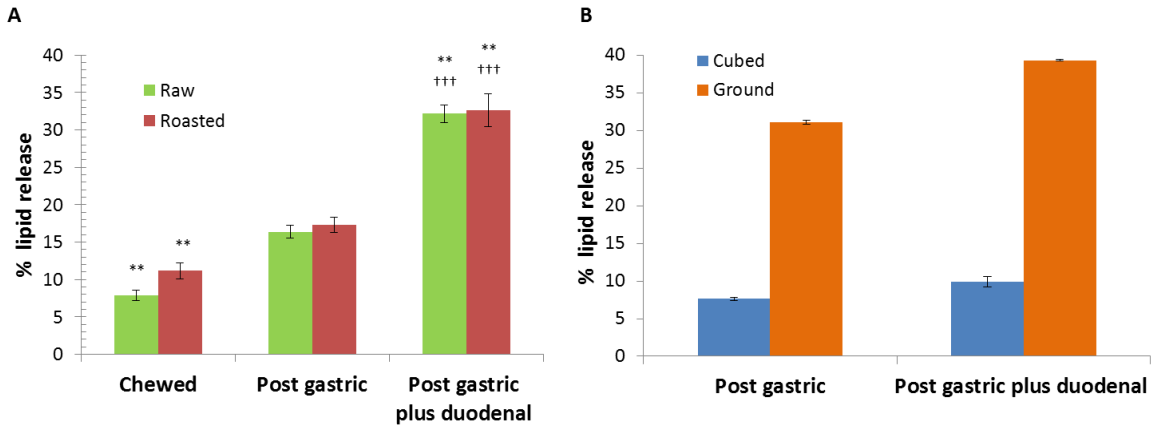

*Figure 4.7 Cumulative percentage of lipid release at the different stages of digestion from this study (A) and from previous work (Mandalari et al., 2008a) (B), (n=4, means ± SEM). Significant differences after the gastric and gastric–duodenal digestion phases were calculated by ANOVA (P < 0.05). ** Mean values were significantly different from those for the post-gastric condition (P < 0.05). ††† Mean values were significantly different from those for the chewed condition (P < 0.05).*

4.4.3 Cell wall analysis

4.4.3.1 Gas liquid chromatography method

The sugar compositions of almond CW at the different stages of digestion are presented in Figure 4.8. As expected, the sugar residues found in digested almonds were identical to the native and masticated samples. ANOVA analysis showed no differences in the CW sugar composition between raw and roasted almonds after gastric and gastric plus duodenal digestion. However, a significant

increase in galacturonic acid as well as a small loss of arabinose after duodenal digestion of raw almonds were observed.

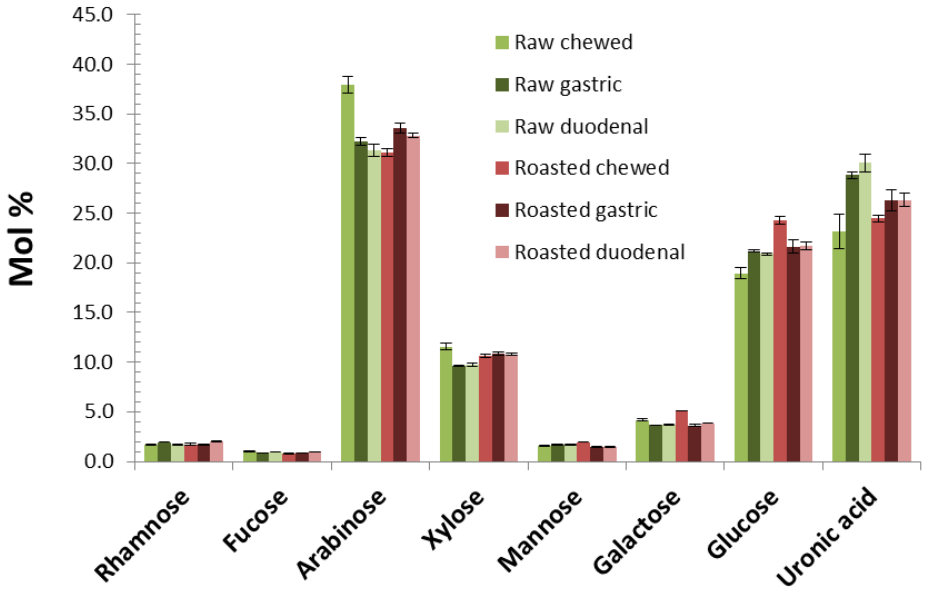

Figure 4.8 Monosaccharide composition (mol%) of raw and roasted almond at the different stages of digestion. Values are means ± SEM (triplicates).

4.4.3.2 Method using antibodies

The results obtained from the Willats's analysis (see *Chapter 2*, *Section 2.3.4.2*) for whole raw and roasted almonds is presented (Figure 4.9). This method provided additional details regarding the structure and organisation of the sugar residues within the CW. The results are similar to those produced by GLC analysis, in that the antibody data indicated that almond CW are mostly made of pectin and xyloglucans, with little xylan (and presumably cellulose) present, which suggests a CW composition reflecting **type I CW** (Carpita and Gibeaut, 1993). According to this model, xyloglucans are the predominant polysaccharides interlocking the cellulose microfibrils, which is in agreement with the data in Figure 4.9. On the other hand, arabinoxylan, the most abundant polysaccharides present in a type II CW (i.e. in cereals such as wheat), was generally absent in the almond samples. AGPs were also found in the almond samples. The greater proportion of pectins (i.e. HG and

arabinan) observed in raw and roasted almonds compared with other compounds could be attributable to the almond skin since pectic polysaccharides occurred to a lesser extent in blanched almonds.

Due to the nature of the technique (i.e. difference in detection limits and spot morphologies between arrays) (Pedersen *et al.*, 2012), it is not possible to compare the values between Figures 4.9 and 4.10. However, the oligosaccharides can be identified without quantification. Therefore, native and digested raw almond appeared to have the same composition: pectins (i.e. HG and arabinan), xyloglucan and AGP. Therefore, no significant changes occurred in the composition of the CWs after digestion, suggesting that the CWs remained largely intact, providing some further evidence of the importance of the link between CW structure and lipid bioaccessibility.

Extraction	Sample	HG with a low DE (mAb JIM5)	HG with a high DE (mAb JIM7)	HG non-blockwise, partially methylesterified (mAb LM7)	HG Partially methylesterified (mAb LM18)	HG Partially methylesterified (mAb LM19)	HG Partially methylesterified (mAb LM20)	Xylogalacturonan (mAb LM8)	Arabinan (mAb LM13)	(1→5)-α-L-arabinan (mAb LM6)	Feruloylated arabinan (mAb LM12)	(1→4)-β-D-galactan (mAb LM5)	Feruloylated (1→4)-β-D-galactan (mAb LM9)	Xyloglucan (mAb LM15)	(1→4)-β-D-xylan (mAb LM10)	(1→4)-β-D-xylan/arabinoxylan (mAb LM11)	Terminal xylose (mAb LM25)	Mannan/galactomannan (mAb LM22)	Extensin (mAb JIM19)	Extensin (mAb JIM20)	Extensin (mAb LM3)	AGP (mAb JIM8)	AGP (mAb JIM13)	AGP (mAb LM2)
CDTA	Raw almond	27	36	0	42	43	0	19	21	10	0	0	3	2	0	0	0	0	0	7	6	19	38	0
	Roasted almond	33	59	0	37	44	30	27	35	19	0	0	3	0	0	0	0	0	0	2	0	10	32	0
	Blanched almond	15	10	0	30	30	0	2	0	4	0	0	0	9	0	0	0	0	0	2	6	12	31	0
	Almond skin	70	95	0	71	75	75	64	52	28	0	0	0	0	0	0	0	0	0	13	8	11	26	5
NaOH	Raw almond	9	0	0	11	45	0	6	5	22	0	0	0	95	0	7	29	0	0	10	7	0	34	0
	Roasted almond	10	0	0	12	47	0	11	9	22	0	0	0	91	0	7	32	0	0	10	8	0	36	0
	Blanched almond	9	0	0	11	46	0	0	0	21	0	0	0	99	0	7	29	0	0	2	2	0	33	0
	Almond skin	0	0	0	0	12	0	20	13	9	0	0	0	54	2	11	4	0	0	19	10	0	23	0

Pectins **Hemicelluloses** **Proteins**

0 10 20 30 40 50 60 70 80 90 100
Relative mean signal

Figure 4.9 Heat map of the distribution of CW polysaccharides in raw, roasted and blanched almond as well as almond skin. HG: homogalacturonan, DE: degree of methyl-esterification, mAb: monoclonal antibodies, AGP: arabinogalactan protein.

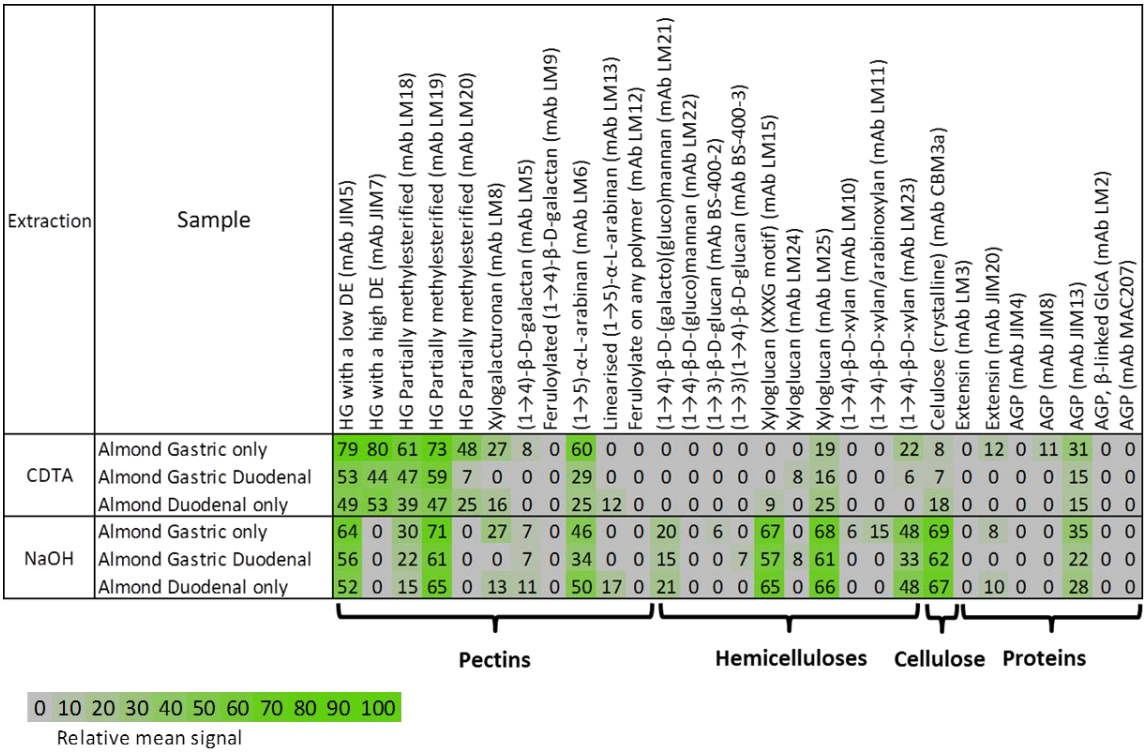

Figure 4.10 Heat map of the distribution of CW polysaccharides in digested raw almond. HG: homogalacturonan, DE: degree of methyl-esterification, mAb: monoclonal antibodies, AGP: arabinogalactan protein.

4.4.4 Microstructural analysis

4.4.4.1 Microscopy of large particles

Micrographs of masticated and digested raw and roasted almond particles are presented in Figure 4.11. As previously observed (*Chapter 3*), only the outer layers of the particles have their cells fractured and their intracellular contents 'released' and thus more available to the digestive fluids in the gut. The cells underneath these layers appear to be relatively intact and retain their nutrients. No marked disruption in the structure of the particles recovered after mastication and gastric digestion was detected, which is supported by the PSD data. The microscopy images and the measured lipid release data are also in good agreement, showing that most of lipid digestion occurred in the

duodenum. The micrographs also show that some of the lipid contained in the seemingly intact cells was lost.

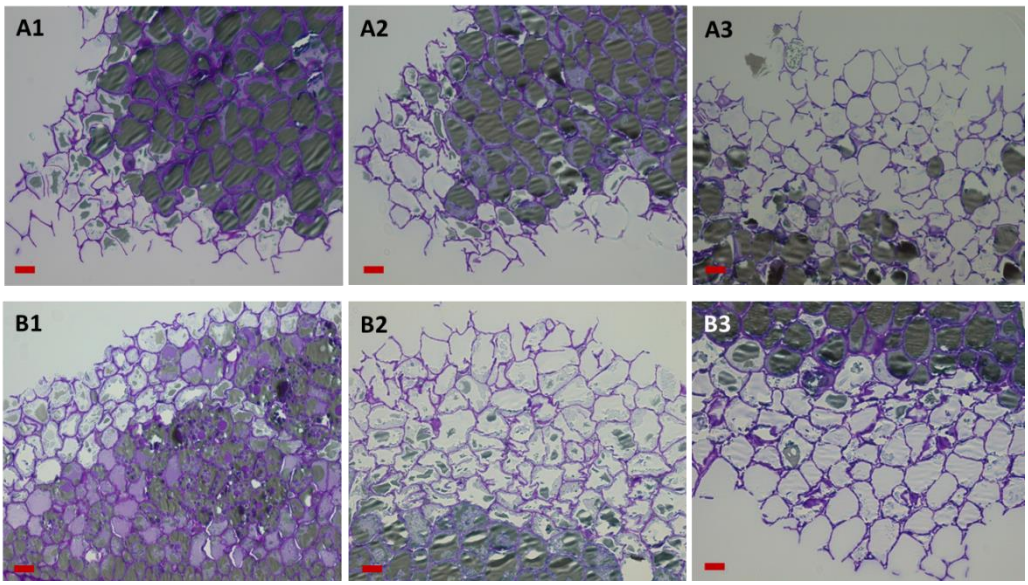

Figure 4.11 Micrographs of raw (A) and roasted (B) almond particles collected after mastication (A1 and B1), gastric (A2 and B2) and duodenal (A3 and B3) digestions (performed by Mary Parker at the IFR). Lipids appear as grey and cell walls as purple. Scale bars: 20 µm.

4.4.4.2 Microscopy of separated cells

Figure 4.12 shows raw (NA) and roasted (RA) almond as well as digested raw almond (i.e. gastric and duodenal, NA G+D) cells separated using the CDTA method (*Section 2.2.1.2)*. In all the NA cells, lipids were evenly distributed as observed by Nile blue fluorescent staining (a1) and bright field (Figure 4.12 a2), and are located in OBs (Figure 4.12 a3). In roasted tissue, lipids were unevenly distributed in all cells as seen in Figures 4.12 b1 and b2, having coalesced into larger droplets (Figure 4.12 b3, arrows). In digested raw tissue (NA G+D), lipid distribution varied between cells, those from the centre of the particle contained OBs (Figure 4.12 c1 and c2), and those from the outer layers contained large lipid droplets (Figure 4.12 c2, arrows) which showed irregular shapes (Figure 4.12 c3, arrows).

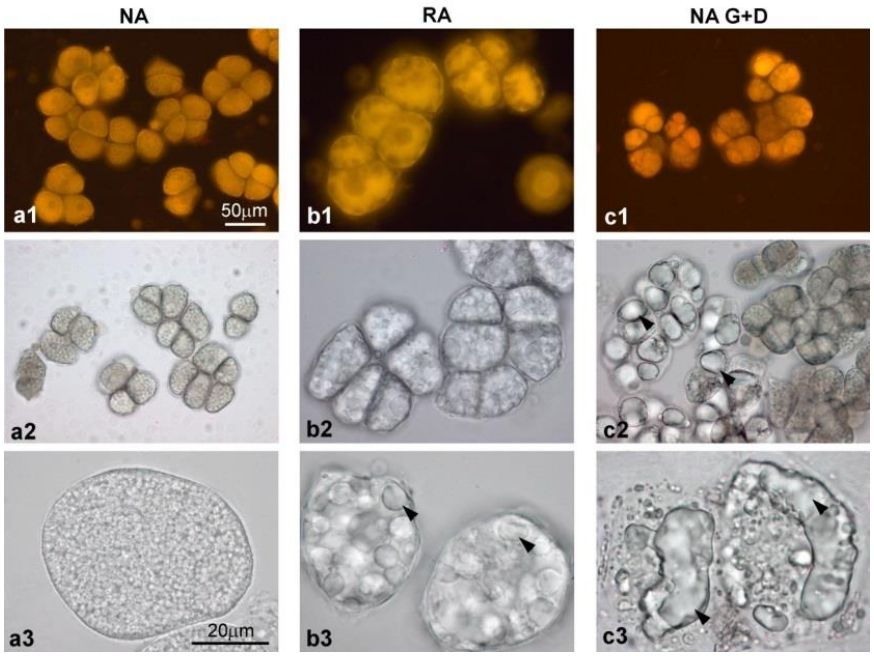

Figure 4.12 Feasibility study for imaging lipid in cells of sharp-cut almond tissue blocks softened in CDTA. Scale bars: a1, b1, c1, a2, b2 and c2 = 50 µm; a3, b3 and c3 = 20 µm. NA, raw almond; RA, roasted almond; G, gastric phase; D, duodenal phase.

The same experiments were repeated using masticated samples before submitting them to *in vitro* gastric (G) and duodenal (D) digestions (Figure 4.13). Lipids in raw almond cells (Figure 4.13 a1) remained predominantly as OBs but some cells were damaged by the mastication process and contained very little lipid (arrow). In NA cells following gastric digestion (Figure 4.13 a2), some lipid coalescence occurred and there were empty cells (arrow). In NA G+D (Figure 4.13 a3) there were cells with OBs, cells with large lipid aggregates, and empty cells (arrow). Those empty cells were most likely from the surface of the particles as showed in Figure 4.11. Roasting caused most lipids to coalesce (Figure 4.13 b1), and tissue became brittle resulting in cell damage (arrow). Cells of RA G were full of coalesced lipid (Figure 4.13 b2), or empty. Cells of RA G+D (Figure 4.13 b3) contained irregular masses typical of lipid digestion or empty cells (arrow).

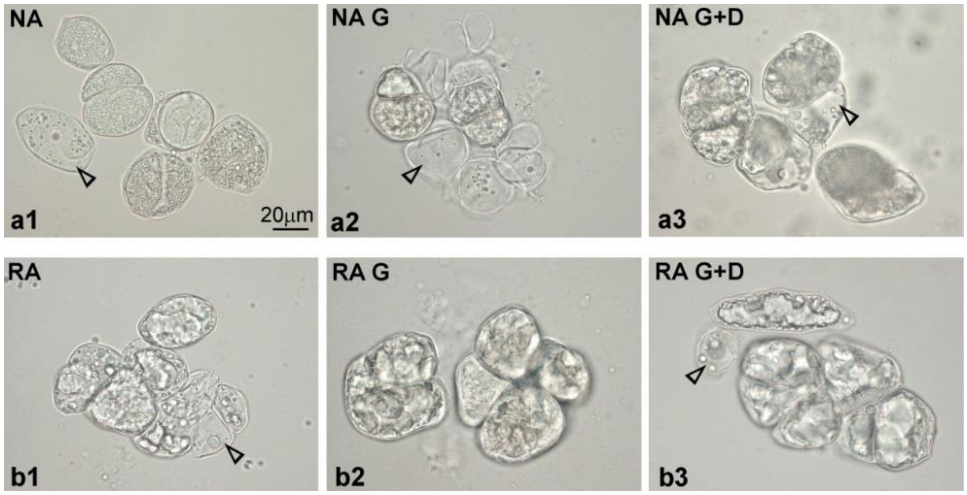

Figure 4.13 Bright field images of chewed raw (NA), roasted (RA) and digested almond cells separated by CDTA. Scale bar: a1, b1, a2, b2, a3 and b3 = 20 μm. G: gastric phase; D: duodenal phase.

The microscopy of separated cells is an interesting method to study the structure of the cells and their content at the different stages of digestion. The images should however be interpreted with care as the preparation itself could have altered the samples (e.g. CW damage and crushing of the cell). Moreover, this method would be difficult to apply to large particles (> 1.0 mm) as the cells become more resistant to separation as the size of the particle increases. Used conjointly with a more traditional approach (i.e. fixation and resin embedment), this novel method provided useful qualitative information about the transformation occurring to the almond tissue during digestion. The former method also confirmed the location of the cells within the almond particle, either at the edges or the core of the particle.

4.5 Discussion

The present work demonstrated that a significant proportion of lipid remained undigested after the *in vitro* gastric (~83%) and duodenal (~68%) phases; the majority of the lipids contained in the

almonds was encapsulated by intact CW and was therefore unavailable for hydrolysis by lipase. This is consistent with previous studies showing that a high proportion of the lipid in almonds is not digested in the upper GIT (Mandalari *et al.*, 2008a). Some of the undigested lipid is available for microbial fermentation as previously reported (Ellis *et al.*, 2004; Mandalari *et al.*, 2008b). Both raw and roasted almonds have a hard texture that resists the shear forces created by peristalsis in the gastric and duodenal phases as demonstrated by the large particles remaining after the digestion. It is currently assumed that particles in the stomach need to reach a size inferior to 1-2 mm before being emptied into the duodenum (McClements and Li, 2010). Furthermore, meals with high fat content have a longer gastric residence time (Mackie *et al.*, 2012). Lipids present in the stomach are not emptied at the same rate as other compounds of solid and liquid food as they float on the top of the gastric content (Meyer *et al.*, 1986). These two characteristics, the presence of large particles and high lipid content, should promote lipid digestibility/availability as shown with allergens (Mackie *et al.*, 2012), since almond would spend more time in the gastric compartment. However, if the particles are too difficult to break down ('indigestible'), they may eventually flow from the stomach when the emptying of the digestible solid is completed and the fasting motility pattern is resumed (Kelly, 1980).

Between the oral and the gastric compartment, an important amount of lipid was lost from the particles despite the absence of major structural changes (i.e. size). When almonds are masticated, the cells on the surface of the generated particles fracture, and even though intracellular lipid content is 'released' it remains on the surface (Figure 3.10). This phenomenon is probably caused by the hydrophobicity of the lipids that prevent them from solubilising in the liquid (saliva) present in the oral cavity. Also, the released intracellular proteins may have created a network into which lipids are entrapped. In the stomach, some of the lipids would be removed from the surface of the particles as a result of emulsification by gastric contractions and activity of digestive agents, in particular gastric lipase. The lower pH and presence of pepsin would have disturbed the protein

structure/conformation and thereby the network they formed at the surface of the particles, which would have led to the release of some of the entrapped lipids (Maldonado-Valderrama *et al.*, 2010).

The size reduction occurring during mastication facilitates the digestibility of the nutrients enclosed within a food matrix. In almond seeds, the CWs are a robust structure, probably impermeable to the agents involved in lipid digestion (i.e. lipase and BS, see *Chapter 7*), so the particles need to have a relatively small size for the lipid to be released and digested (see *Chapter 3*). The mode of disintegration of different solid foods including raw almond has been examined and it was reported that the initial food texture and the changes occurring during mastication and gastric digestion varied greatly among different foods (Kong and Singh, 2009b). The authors found that, in the stomach, erosion, defined by them as the degradation of the food surface due to the contact/impact with the solid material contained in the gastric fluid, was the main mechanism responsible for the disintegration of nuts. Furthermore, compared with other foods (i.e. carrot and ham), almonds absorb the highest amount of water (from 3.3% to 30.7%) when performing a static soaking test and show a significant reduction in hardness in a stomach model. Kong and Singh have also suggested that almonds disintegrate in a delayed-sigmoidal profile due to water absorption and softening (Kong and Singh, 2009a). Therefore, after a prolonged residence time in the aqueous environment of the stomach and the duodenum, the texture of the almond would be modified as well as its disintegration mode. Combined with the erosion mechanism this could explain the large increase in lipid release observed in the intestinal compartment. The rise in lipid loss from the almond tissue may have also been caused by the diffusion of lipases and BS into the tissues along internal fractures, followed by the diffusion of the lipolytic products (mixed micelles). Indeed, it would be expected that the crushing action of mastication would cause deep fractures into the tissue thereby creating fissures that facilitates the diffusion of digestive agents. Finally, the swelling of the CW may have occurred, as previously reported by our group (Mandalari *et al.*, 2008a), which potentially could increase their porosity and lead to the digestion of the contents of the intact cells. However, contrary to the work of Kong and Singh, the roasting process did not lead to significant differences either in

particle disintegration or lipid loss (Kong and Singh, 2009a). It has also been recently reported in pigs, that no differences in physical properties between raw and roasted almonds, i.e. particle size, texture and rheological flow behaviour were seen following gastric digestion (Bornhorst *et al.*, 2013). The difference in roasting conditions applied to the almonds may explain the disagreement with the work from Kong and Singh.

Despite an increase in the amount of lipids that were released into the duodenal compartment, this was only about a third of the total content of the almond. As the digestion progressed, alterations in the integrity of the OBs appeared (Figures 4.12 and 4.13), but most of the intact cells retained their content (Figure 4.11). Hypothetically, the almond tissue reaching the colon would therefore contain an important proportion of nutrients and DF. These undigested materials could undergo bacterial degradation but presumably not to its full extent (Ellis *et al.*, 2004; Mandalari *et al.*, 2008b).

The different trends observed between the results from this study and some previous work by our group (Mandalari *et al.*, 2008a) could be explained by the use of DGM in this study, where the digestion products were removed during the time course of the experiment in order to prevent product inhibition. Also, the absence of mastication may have affected the digestion process; saliva might facilitate the subsequent digestion steps notably by lubricating and softening the ingested food. Therefore, the difference in the methodology used between the two studies (static vs dynamic models) makes comparison difficult. However, the static model study previously reported by Mandalari and colleagues demonstrated that the degree of processing had a major impact on lipid digestibility, as finely ground almonds (200 µm) had a greater lipid release than 2 mm almond cubes (Figure 4.7 B) (Mandalari *et al.*, 2008a). This difference in lipid release was also predicted from the

theoretical model (*Chapter 3*), based on the large differences in the number of fractured cells between flour and cubes (Grassby *et al.*, 2014).

In the DGM, lipid bioaccessibility from almond tissue relies on several digestion parameters, in particular mechanical forces, stomach emptying rate, and removal of lipolytic products, which is built into the model system, hence the suitability of the DGM in that context. Currently, there are no models that accurately reproduce all the complex processes occurring during *in vivo* digestion (Guerra *et al.*, 2012), and therefore a combination of *in vitro* models and human studies is the most appropriate approach. It is very difficult to replicate the mechanical disruption occurring during the oral processing of almonds, principally due to the wide range of sizes composing almond boluses. However, the physical characteristics of the almond boluses were shown to be consistent over time, with acceptable intra- and inter-subject variation (see *Chapter 3*); therefore, almond mastication by human volunteers was the most convenient and accurate method in this particular project even though performed on different days. The use of the DGM conjointly with the Ileostomy study (*Chapter 6*) gives an excellent appraisal of changes in almond microstructure and the extent of lipid digestion in the different compartments of the GIT.

CHAPTER 5

EFFECT OF THE STRUCTURE OF ALMOND MATERIALS ON LIPID DIGESTIBILITY

5.1 Introduction

As described in *Chapter 1*, almonds are predominantly made of lipids (around 50-55%, of which 60 to 80% oleic acid, O; 15 to 20% linoleic acid, L; and 5% palmitic acid, P), which are assembled into OBs in the form of TAG (Dourado *et al.*, 2004; Ellis *et al.*, 2004; Yada *et al.*, 2011). Thus, the typical TAG species found in almond oil have the following fatty acid compositions: OLO, OLL, OOO, POO, and LLL (Holcapek *et al.*, 2003; Jakab *et al.*, 2002). The OBs have a diameter ranging approximately from 1 to 5 µm and are surrounded by a single layer of phospholipids in which proteins, mainly oleosins, are embedded (Beisson *et al.*, 2001b; Ellis *et al.*, 2004; Huang, 1994). Oleosins ensure the stability of the amphiphile layer.

Since the TAGs cannot freely transfer across the enterocyte barrier because of their size and polarity, they must be degraded and presented in a form that permits their absorption (Figure 5.1). The human body is actually very efficient at digesting and absorbing TAG - around 95 to 98% efficiency (Mu and Hoy, 2004). The lipids present in milk are naturally organised in the form of emulsions (Fave *et al.*, 2004). For most other foods, they require to be liberated from the food matrix during mastication and by mechanical and chemical digestion in the GIT and then converted into lipid droplets. The lipid digestion includes emulsification via mixing and action of amphiphile molecules, hydrolysis and micelle formation, and finally uptake by the enterocytes. The hydrolysis of TAG is performed in the stomach as well as in the small intestine predominantly via the activity of two enzymes, HGL and HPL (Bauer *et al.*, 2005). The hydrolysis of other lipid molecules such as cholesterol esters, phospholipids and vitamins is occurring in the duodenum via the activity of two enzymes, cholesterol esterase, also called carboxyl ester hydrolase (CEH), and phospholipase A_2 (Carey *et al.*, 1983). Since the pH required for its activity is broad (3 to 6), HGL can act in the stomach as well as the intestine whereas HPL acts specifically in the duodenum as it is irreversibly denatured at pH 4 and lower (Miled *et al.*, 2000). HGL activity accounts for 5 to 40% of the lipid hydrolysis to which is added ~7.5% that can occurr in the duodenum, as opposed to 40 to 70% of lipid hydrolysis

by HPL (Armand, 2007). Other lipases are also involved in the degradation of lipids and more details of this are presented in *Chapter 7*.

The solubilisation of the lipolytic products is an important step in the absorption of lipid by the enterocytes. First, they have to be removed from the droplet interface in order to prevent inhibition of the lipase(s).

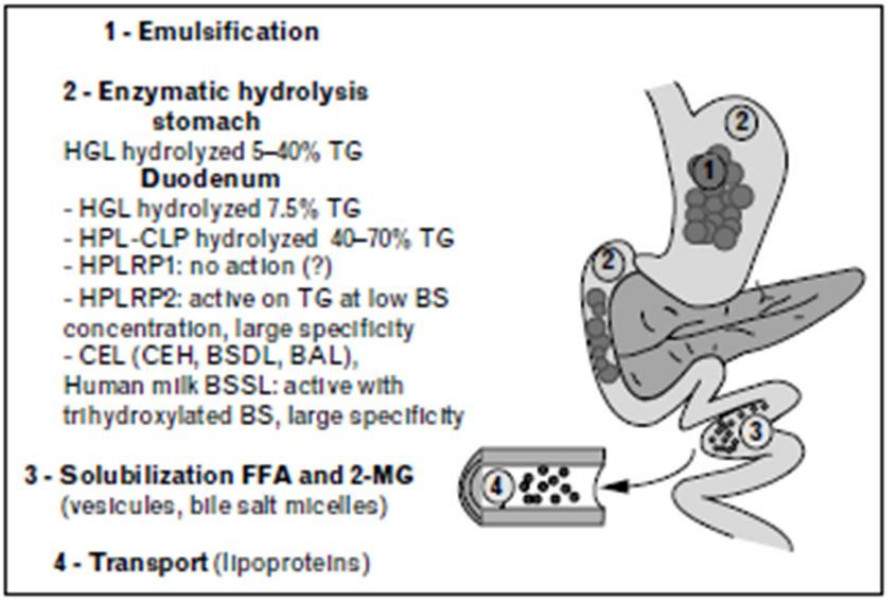

Figure 5.1 Enzymic and physiological steps involved in TAG digestion (Armand, 2007).

Abbreviations: BAL, bile-salt activated lipase; BS, bile salts; BSDL, bile-salt dependent lipase; BSSL, bile-salt stimulated lipase; CEL, carboxyl ester lipase; CEH, cholesterol ester hydrolase; CLP, colipase; FFA, free fatty acids; HGL, human gastric lipase; HPL, human pancreatic lipase; HPLRP1 or 2, human pancreatic protein-related 1 or 2; 2-MG, 2 monoglycerides; TG, triglycerides.

5.2 Aims

Chapters 3 and *4* demonstrated that almond particles of different sizes were generated following mastication and that a large proportion of the lipids contained in those particles remained encapsulated (undigested) after gastrointestinal digestion. It was hypothesised that the more complex the structure level the lower the amount of FFAs produced from TAG hydrolysis. Indeed,

lipids present on the fractured surface of the almond particles would be much more susceptible to hydrolysis, whereas the encapsulated lipid content of the intact cells is considerably less susceptible to digestion, unless digestive agents such as lipase and BS gain access to the intracellular lipid.

The purpose of the present study was to determine the effect of pancreatic lipase on the rate and extent of lipid digestion (expressed as the amount of FFA released) in raw and roasted almond materials, which have been manipulated so that they exhibit marked differences in lipid bioaccessibility. These materials include ground and chewed particles of almond and almond cells that have been separated in the laboratory (see *Section 2.2.1.2*). In addition, raw and roasted almond oil emulsions were included as reference samples with a high lipid bioaccessibility (100%). To address this main objective, two methods were employed to measure the FFAs release, the pH-stat method and GLC analysis. Microscopy methods were also used to study the structural changes of the separated lipid-rich cells pre- and post-digestion.

5.3 Materials and methods

5.3.1 Method

The preparation and protocols used are given in detail in *Chapter 2*. Briefly, duodenal digestion using the pH-stat was performed on ground almond particles of different sizes (1000 to 2000, 500 to 1000, 250 to 500, and < 250 μm), masticated whole almonds (obtained as described in *Chapter 3*), separated cells and emulsions of triolein, tributyrin and almond oils. For each material, both raw and roasted almonds were used. The simulated digestion mixture contained lipid material dissolved in β-Lg solution (amount of material used adjusted to obtain 300 mg of lipid), 12.5 mM BS solution, 150 mM NaCl solution and 10 mM $CaCl_2$ solution. Test runs were then performed by incubating (1h at 37°C, pH 7) the mixture with 2.4 mg/mL of pancreatic lipase. As a control, the pH fluctuation of the

assay mixture alone was determined by running the titration without any lipase; the volume obtained was then deducted from the volume data produced from the subsequent test lipid samples. Since the conditions were identical for each assay, the difference in lipolysis extent and rate would indicate that there was a difference in lipid accessibility between these materials.

Conjointly, lipids were extracted at different time points (0, 1, 2, 5, 10, 15, 20, 30, 45 and 60 min) and analysed by GLC as described in *Section 2.3.1.2.2*. The fatty acids were identified and quantified by comparing their relative retention time with those of standards. The concentration of FFA release was determined using the C15 IS and expressed in micromolar (μM) terms.

Lipid released for each particle size ranges was predicted using the mathematical model presented in *Chapter 3*.

5.3.2 Statistical analysis

The data were analysed using SPSS version 17.0. For all tests, the significance level was set at $P < 0.05$ (2 tailed). Percentages of FFA release, fatty acids concentrations and reaction rates were assessed by repeated-measures ANOVA with time and materials (i.e. emulsion, cells and particles) as 'within-sample' factors. Differences between raw and roasted samples as well as between the milled (four size ranges from < 250 to 2000 μm) and chewed samples were analysed by Student's paired *t*-test.

5.4 Results

5.4.1 Particle size of emulsions

The mean droplet size of the emulsions was similar for raw and roasted almond oils, 3.2 ± 0.04 ($d_{3,2}$ = 1.1 ± 0.02 µm) and 3.4 ± 0.27 µm ($d_{3,2}$ = 1.1 ± 0.02 µm), respectively (Figure 5.2). Tributyrin emulsions were composed of droplets of slightly greater mean size (3.9 ± 0.23 µm; $d_{3,2}$ = 3.1 ± 0.11 µm) than the almond oils, but for triolein emulsion the mean droplet size (2.9 ± 0.07 µm; $d_{3,2}$ = 2.0 ± 0.03 µm) was slightly lower than the almond oils, but significantly lower than the tributyrin droplets. However, the size differences were statistically significant ($P < 0.05$) only between triolein and each of the other oils.

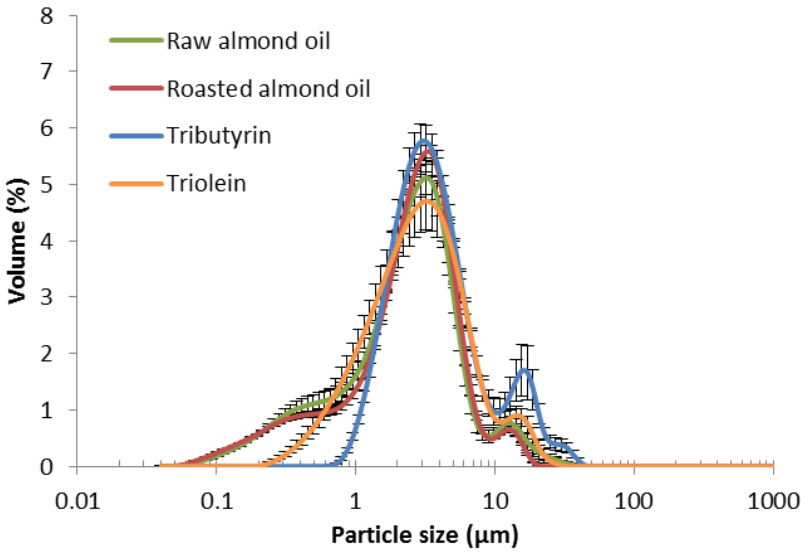

Figure 5.2 Particle size distributions of raw and roasted almond oils, tributyrin, and triolein emulsions (n=3, means ± SEM).

5.4.2 Release of FFA measured with the pH-stat

Figure 5.3 presents the FFA release from a 1 h reaction. The maximum amount of FFAs produced during the 60 min duodenal digestion of almond emulsion is used as a reference sample (100% FFA

release after 60 min) when comparing the lipolysis profiles of the different almond particles and cells. For both raw and roasted almonds, lipid digestion was significantly more limited for separated cells (~31% for both raw and roasted almond cells) compared with the reference emulsion. Lipid digestion was also markedly restricted for the raw and roasted almond particles (from 44 to 64% and 39 to 60% for raw and roasted almond particles, respectively). Furthermore, an inverse relationship between particle size and FFA release was found, for instance for raw almond, 44.2 ±.5.3% of FFA were released from particles with a size between 1000 and 2000 μm compared with 64.0 ± 1.6% for particles with a size < 250 μm.

A measurable amount of FFAs was produced from the digestion of almond cells which is probably due to the cell preparation containing a small proportion of ruptured cells (see Figures 5.5 A and 7.2) and thus bioaccessible lipid. Indeed, it is extremely difficult to obtain a preparation that is completely devoid of free lipids and cell fragments. The released lipid in the fractured cells of the preparation would have been susceptible to digestion (hence the ~20% of FFA release observed). Microscopy observations of the cell preparations revealed that a greater proportion of the pre-digested cells within the roasted almonds preparation were found to be damaged compared with the raw almond cells (Figures 5.5 A and E).

Furthermore for all materials studied here, the reaction rate plateaued after about 20 min of reaction indicating that no further digestion had occurred, possibly the lipase had neither access to the encapsulated lipids nor to the lipids that may have diffused out of the cell. This levelling out (reaching a plateau) could be attributed to a loss of enzyme activity, and/or product inhibition in the case of digestion of the almond oil emulsions, but this explanation cannot be used for the almond particles or cells, since a much lower amount of FFAs was produced from these materials.

Values for the extent of digestion, which were calculated as the amount of FFAs produced relative to the total amount of TAG in the sample over 60 min and expressed as a percentage FFA, and for the

initial reaction rates (µmol/min), are presented in Table 5.1. Repeated-measures ANOVA showed that there were significant differences ($P < 0.005$) in % FFA production and the initial reaction rates between tributyrin and the other emulsions and oils. The initial rates of reaction as well as the quantity of FFA produced were significantly greater for emulsions ($P < 0.05$) compare with unemulsified raw and roasted almond oils. The initial reaction rates were also statistically different ($P < 0.001$) between the different almond materials (Table 5.2), but the values were found to be similar between raw and roasted.

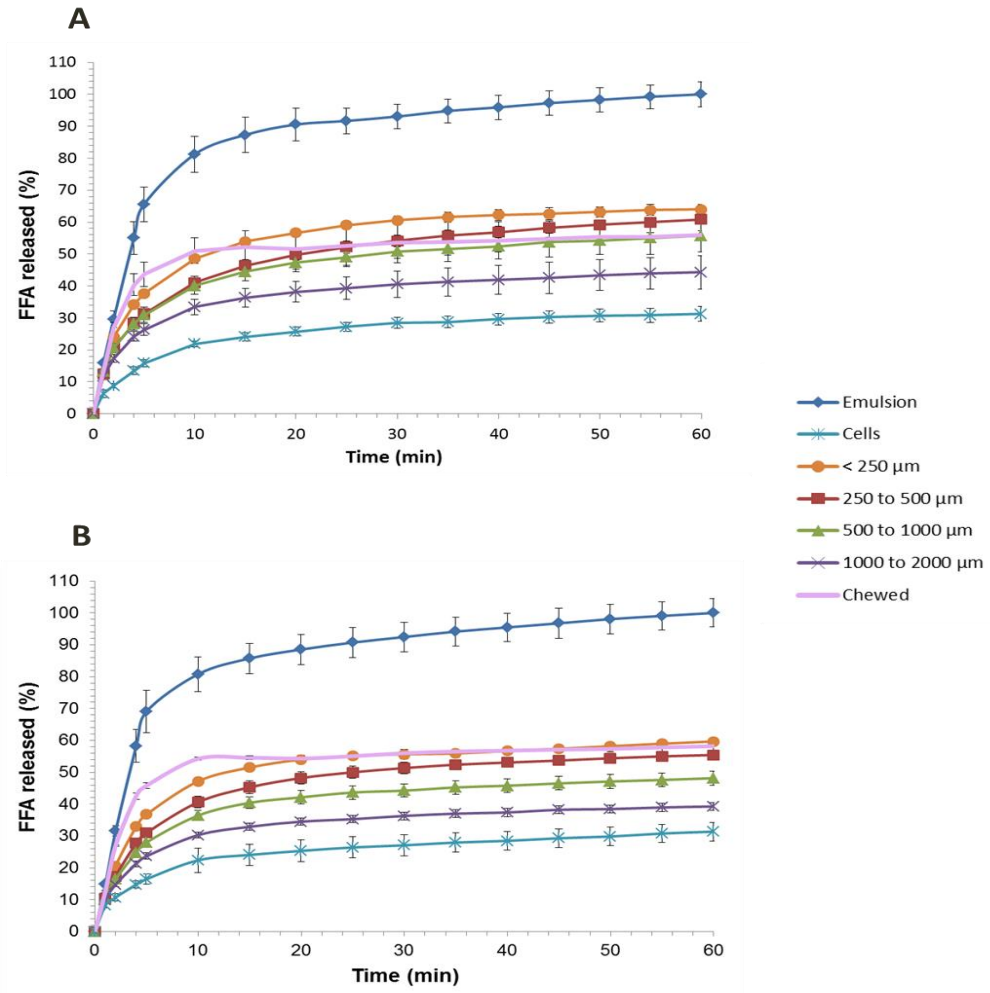

Figure 5.3 Percentage of FFA released versus lipolysis time over 60 min of raw (A) or roasted (B) almond materials prepared with different degrees of lipid bioaccessibility: almond particles, chewed almonds and separated almond cells. Values are presented as means ± SEM (n = 3). Significant differences, calculated by repeated-measures ANOVA (P < 0.005), were found between all materials, apart from the masticated almonds.

Table 5.1 Percentage of FFA released (% of total fatty acids) after 60 min and initial reaction rate (µmol/min) for lipolysis of emulsions and unemulsified oils with pancreatin. Values are presented as means ± SEM (n = 3).

	Particle size (d_{43} in µm)	**FFA (%) at 60 min**	**Initial reaction rate (µmol /min)**
Tributyrin emulsion	3.9 ± 0.2	99.1 ± 2.1	401.0 ± 21.5
Triolein emulsion	2.9 ± 0.1[1,2]	70.9 ± 2.7[1,2]	78.1 ± 3.1[1,2]
Raw almond emulsion	3.2 ± 0.0[1,2]	67.8 ± 2.7[1,2]	71.3 ± 6.3[1,2]
Roasted almond emulsion	3.4 ± 0.3[1,2]	70.4 ± 3.1[1,2]	78.1 ± 4.4[1,2]
Raw almond oil	ND	19.3 ± 0.9[1]	31.8 ± 2.1[1]
Roasted almond oil	ND	20.2 ± 0.6[1]	32.1 ± 4.2[1]

[1]Statistically significant differences compared with tributyrin emulsion ($P < 0.05$). [2]Statistically significant differences compared with almond oil, both raw and roasted ($P < 0.05$). ND: not determined.

Table 5.2 Initial reaction rate (µmol/min) for lipolysis of milled (size from < 250 to 2000 µm) and chewed raw and roasted almonds. Lipolysis rate values are presented as means ± SEM (n = 3).

	Particle size	**Predicted lipid released (%)***	**Initial reaction rate (µmol/min)**
Raw almonds	1000 to 2000 µm	8.5	41.3 ± 3.7[1]
	500 to 1000 µm	16.0	49.7 ± 3.6[1]
	250 to 500 µm	30.0	50.6 ± 2.7
	< 250 µm	39.0	58.6 ± 1.6
	Cells	0.0	18.0 ± 1.7[1]
	Chewed	8.5	64.0 ± 3.5
Roasted almonds	1000 to 2000 µm	8.5	34.1 ± 1.5[1]
	500 to 1000 µm	16.0	39.1 ± 3.1[1]
	250 to 500 µm	30.0	41.7 ± 3.0[1]
	< 250 µm	39.0	51.3 ± 2.0[1]
	Cells	0.0	24.8 ± 3.1[1]
	Chewed	11.3	64.6 ± 0.1

[1]Significant difference between milled particles and chewed samples ($P < 0.05$). *Calculated using the mathematical model (se *Chapter 3*).

5.4.3 Release of FFA measured with GLC

The amount of lipolytic products (μmol) generated from the duodenal digestion of raw and roasted almond emulsions, chewed almonds and almond cells, as measured by pH-stat and GLC, are presented in Figure 5.4. The lipolysis profiles clearly show a difference in FFA release between materials with the lowest values observed for cells. In all cases, most of the lipolysis took place in the first 10 min of digestion. Identical trends were observed for both raw and roasted samples. The FFA release data obtained from both the pH-stat and GLC methods followed more or less the same trend although the FFA curves for GLC analysis of chewed almonds and almond cells were slightly lower. In a recent study by Helbig and coworkers using an emulsion only, GLC analysis was found to give FFA values 2-3 times higher than values obtained by pH-stat (Helbig *et al.*, 2012). The methodology used by Helbig and colleagues was however different to that employed by our group, in particular the GLC method. The discrepancy between the hydrolysis curves for pH-stat and the GLC curves observed in the current experiments for the chewed almonds and separated cells is likely to be attributed to the limitation associated with the extraction procedure for the GLC preparation. Indeed, it is possible that some of the hydrolysed lipid products were lost during the solid phase extraction and the preparation of the samples for GLC analysis.

5.4.4 Microstructural analysis of separated cells before and after digestion

Figure 5.5 clearly show that most of the intracellular lipids remained intact after digestion as encapsulated by the CW. However, oil droplets appear coalesced inside the roasted almond cells (Figure 5.5 F) suggesting that some transformation occurred (i.e. BS and/or lipase penetration).

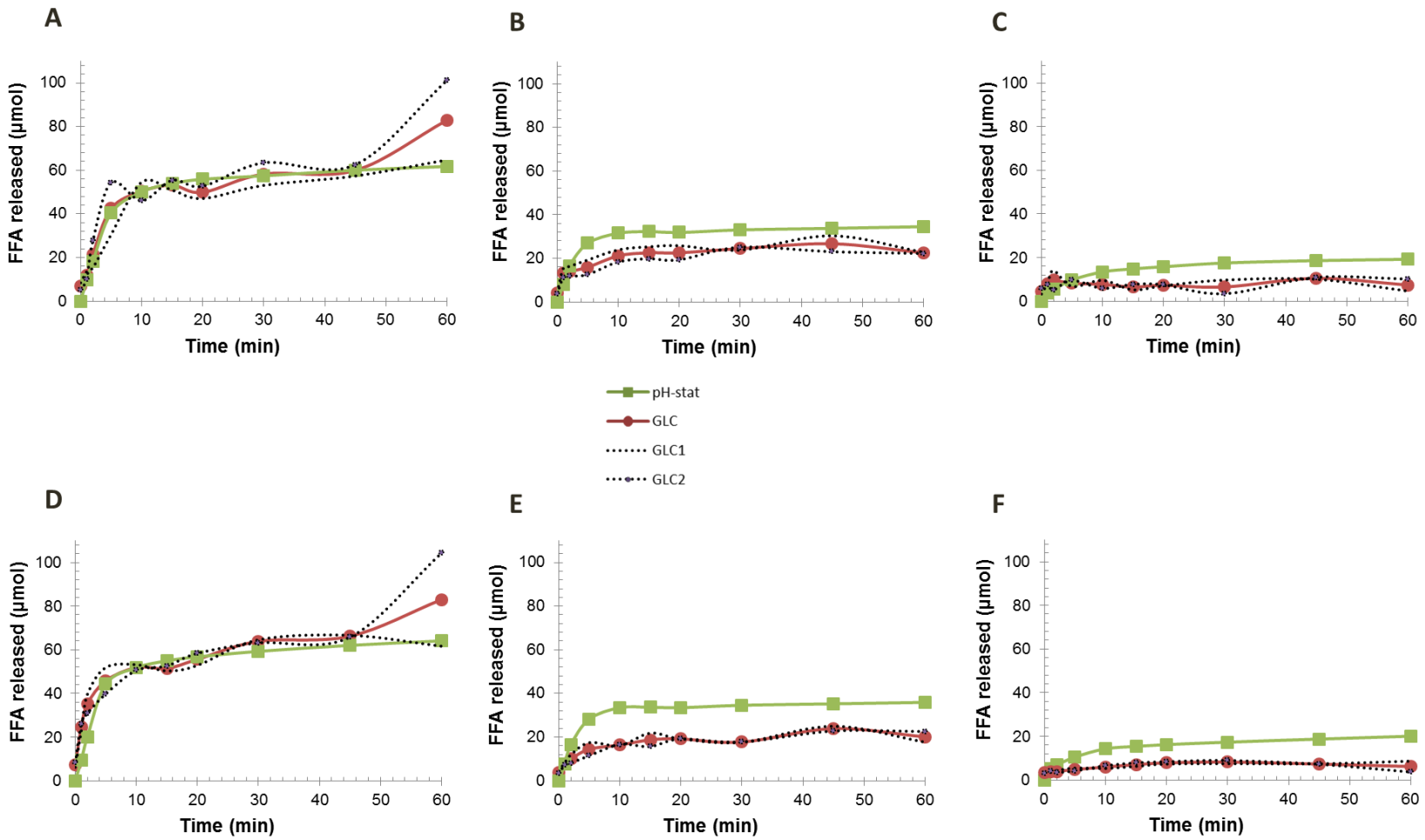

Figure 5.4 FFA released (µmol) over a 60 min time period during duodenal digestion using the pH-stat method (green) and GLC analysis (red, average values of duplicates GLC1 and GLC2) for raw (A-C) and roasted (D-F) almond; almond emulsions (A and D), chewed almonds (B and E) and separated almonds cells (C and F). Significant differences found between materials were calculated by repeated-measures ANOVA ($P < 0.005$).

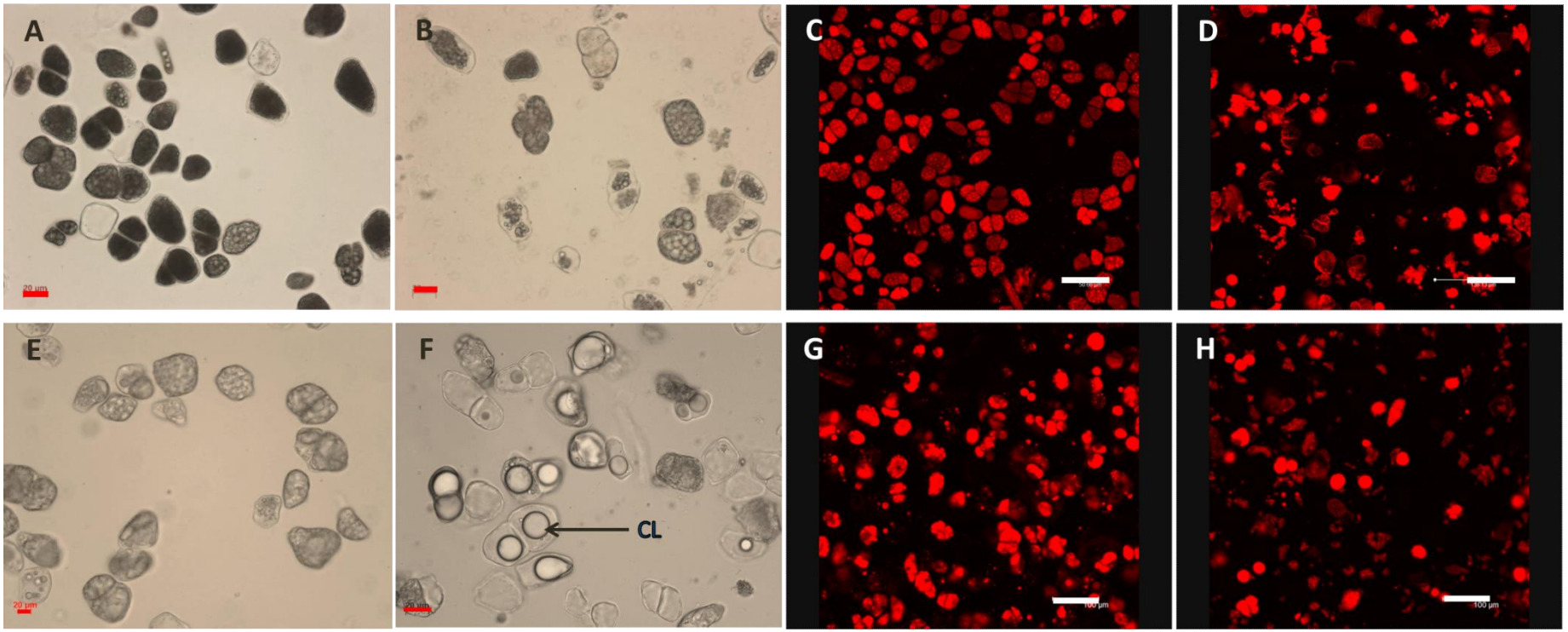

Figure 5.5 Representative images of separated, raw (A-D) and roasted (E-H) almond cells before (A, C, E and G) and after (B, D, F and H) digestion as examined by optical (A, B, E and F) or confocal (C, D, G and H) microscopy. CL: Coalesced lipids. Lipid in C, D, G and H are stained with Nile red. Scale bars: A, B, E and F = 20 µm; C, D, G and H = 100 µm.

5.5 Discussion

Pancreatic lipase catalyses the hydrolysis of TAG into FFAs and MAGs; a reaction that can be monitored by maintaining a constant pH by automated addition of NaOH, which neutralises the newly formed FFAs. The volume of NaOH thus added corresponds to the amount of FFA released. This study focused on duodenal digestion as the majority of lipid hydrolysis takes place in the duodenum as discussed in *Chapter 1*. Between 67 to 70% of the initial almond oil present in the reaction vessel was digested, which is in accordance with physiological values especially since gastric digestion was omitted (Bauer *et al.*, 2005).

As previously reported, the rate and extent of lipid digestion were strongly influenced by the structure and composition of the lipid-water interface (Li *et al.*, 2011c), and significantly increased with the decrease in emulsion droplet sizes because of the larger surface area (Armand *et al.*, 1992). The lipid composition of the emulsion is another key feature that influences lipolysis (Zhu *et al.*, 2013). Indeed, the long chain lipids (i.e. oleic and linoleic fatty acids) generated from the hydrolysis of triolein and almond oils are relatively water insoluble and therefore not easily removed from the interface. Hence the smaller amount of FFA released compared with those generated from tributyrin lipolysis are probably explained by product inhibition at the lipid-water interface. However, it is important to be cautious when interpreting the outcomes of digestibility experiments where oils with different fatty acids mixture have been used. With the pH-stat, the digestion of identical molar amount of different fatty acids could lead to great variability in the quantity of NaOH added (Zhu *et al.*, 2013). Compared with the values of fatty acids in pure molecular solution, pKas have been reported to be 1.5 to 2.0 pH units higher than the pKas of the same species in a fatty acid mixture. In the current study, this issue was taken into consideration since, apart from tributyrin, the fatty acid composition of each material studied was similar, the variability being in the proportion of cells

ruptured. Furthermore, the consistency between the GLC (total FFA release calculations based on individual fatty acids) and pH-stat data for almond oil emulsions confirms that the latter method gave an accurate measure of the level of lipolysis.

Thus, in the static model used in this study, the products of digestion were not removed as the digestion proceeded and so they accumulated at the interface. This is likely to have the effect of inhibiting the lipase before the lipolytic products are incorporated into micelles by BS, as recently reported (Golding and Wooster, 2010), leading to incomplete lipolysis. The generated MAGs are indeed strong interfacial active molecules; if they are not removed by BS, they inhibit lipase activity by 'monopolising' the surface of the oil droplet (Reis *et al.*, 2009). On the other hand, the lipase almost completely hydrolysed tributyrin since butyric acid is easily solubilised, which leads to an attenuation of product inhibition phenomenon (Borgström, 1967).

Since triolein and almond oils showed an equivalent degree of lipolysis, it seems that the presence of linoleic acid in almond oils did not influence the course of the reaction and this was observed in spite of the slight difference in droplet sizes between the two emulsions. This result is consistent with a previous *in vitro* digestion study showing that no preferential selection in the type of fatty acids hydrolysed occurs during lipolysis (Mandalari *et al.*, 2008a). No statistically significant differences were found in either the reaction rate or lipid released between raw and roasted almond oils emulsions which was expected given that their fatty acids composition were similar. This also indicated that the roasting process had no effect on the oil behaviour (i.e. droplet size and phases structure) during emulsification. Also, these results are not unexpected given that the characterisation of the almond oil showed that the roasting process had no effect on droplet size (i.e. surface area to volume ratio).

As lipase is only active at the interface, it was expected to observe a lag time during which the enzyme adsorbs onto the emulsion surface (Beisson *et al.*, 2001a). The 'interfacial quality', governed notably by the interfacial molecular organisation, including the presence of lipolytic products, and the interfacial conformations of lipids, is highly relevant to the kinetics of the lipase (Verger and de Haas, 1976). In the present work, BS and calcium ions were added in the reaction system together with the substrate, prior to the addition of lipase, and any other surface-active molecules should have been removed, thus facilitating the immediate adsorption of the enzyme at the interface. As discussed in *Chapter 1*, BS are unusual surfactants that play a crucial role in lipid digestion and absorption (Maldonado-Valderrama *et al.*, 2011). The interfacial proteins network (e.g. β-Lg) is displaced by BS (Maldonado-Valderrama *et al.*, 2008), and the interface thus covered by BS is known to promote colipase, and subsequently lipase, adsorption. BS are also required to remove the lipolytic products that accumulate onto the interface and prevent lipase inhibition. Given that different BS exhibit different behaviour at the interface (promoting either colipase/lipase anchoring to the interface or displacement of lipolytic products) (Parker *et al.*, 2014), it is therefore preferable to use a mixture of BS such as, for instance, NaTC and NaGDC.

It would have been anticipated that the lipid droplets, formed from the release of lipid from ground and chewed almond, had interfaces of different composition than the emulsion droplets, which could have affected the lipolysis rate. These interfaces may have been composed of β-Lg, storage proteins initially present in the almond tissue, and phospholipids and oleosins that covered the surface of the OBs. However, when the interface is exposed to BS solution with a concentration > 5 mM, as it is the case in these experiments, the BS would have displaced β-Lg. The interface is thus likely to have been dominated by the BS and not the proteins and phospholipids (Maldonado-Valderrama *et al.*, 2008).

The higher concentration of FFAs generated from smaller particles compared with the largest particles is attributed to the greater number of ruptured cells, and therefore increased lipids bioaccessibility as previously shown (Ellis *et al.*, 2004; Grassby *et al.*, 2014). As predicted, the extent and rate of lipolysis was the highest for the particles with the smallest size (≤ 250 μm) which correspond to the sample with the largest proportion of ruptured cells, with lipid content more accessible to the lipase. Despite the significant amount of large particles contained in the chewed almond boluses (35-40% of particles > 500 μm) (*Chapter 3*), the initial lipolysis rate was more rapid than the milled almond samples of similar average particle size (Table 5.2). However, this result is less surprising when the broad size distribution of particles of chewed almonds is taken into consideration, as reported in *Chapter 3*. Thus, although mm sized particles were present in chewed samples, they also contained relatively small sized particles ~50% of which had sizes ≤ 125 μm for both raw and roasted almonds. Such small particles contain a greater proportion of bioaccessible (available) lipid relative to larger particles with lower surface: volume ratios and thus less lipid release. On this basis, we would have expected to observe a similar high initial rate of lipolysis for almond flour (i.e. < 250 μm), but both raw and roasted types had significantly lower lipolysis rates than the chewed samples. This suggests that there may be additional factors, other than particle size, that explain the relatively high rates of lipolysis of masticated almonds.

For instance, the method of trituration applied to almonds is likely to affect the physical characteristics of almond particles. Thus, the chewing of almond seeds crushes and compresses the particles resulting in cell damage (rupture) on and beneath the fractured surfaces, compared with a laboratory blending process employing sharp blades that seem to generate less damaged particles with smoother cut surfaces (*data not shown*).

No significant differences in the amount of FFAs produced (Figure 5.3) and reaction rate (Table 5.2) were observed between raw and roasted particles, indicating that thermal processing had negligible

effects on digestion kinetics. Figure 5.5 clearly shows that much of the intracellular lipids still remained encapsulated inside the almond cells after digestion and changes in cell morphology seemed minimal, except for extensive lipid coalescence in roasted samples, which is consistent with data seen in *Chapter 4*. However, some microstructural studies have shown that the roasting of almonds also alters the shape of almond parenchyma cells, ruptures some of the CWs, produces uneven distribution and coalescence of the OBs, and causes some aggregation of the protein bodies (Pascual-Albero *et al.*, 1998; Varela *et al.*, 2008b). It is possible, therefore, that roasting may have increased the porosity of the CW, thereby allowing greater access of digestive fluid, but did not facilitate significant intracellular lipolysis because of the presence of coalesced lipids (i.e. oil droplets with lower surface area). Large lipid aggregates can be seen inside the roasted almond cells after digestion (Figure 5 B) suggesting that some transformation had occurred (e.g. by BS and/or lipase penetration). These two mechanisms, i.e. increase in CW porosity and lipid coalescence, may explain the slight increase (not significant) in lipid loss (*Chapter 4*) and digestibility obtained for the roasted compared with the raw almond samples.

GLC analysis was used in the present study in order to validate the use of the pH-stat with almond materials (particles and cells). This objective was achieved given that the two methods followed the same trend particularly at the beginning of the lipolysis where most of the lipids are digested. Furthermore, a good overall reproducibility, as showed by the dash lines, was obtained between GLC measurements which confirmed the validity of the results. We have to bear in mind that chewed almond and separated cells are difficult materials to study.

The titrimetric method such as the pH-stat has been described as a rapid and convenient tool to study lipolysis generally occurring in the duodenal compartments and on synthetic lipids (e.g. tributyrin and triolein) and olive oil (Beisson *et al.*, 2000; Hasan *et al.*, 2009; McClements and Li, 2010). The pH-stat method has been widely used (Armand *et al.*, 1992; Beisson *et al.*, 2001a; Gallier

and Singh, 2012; Helbig *et al.*, 2012; Li *et al.*, 2011c; Wickham *et al.*, 1998; Zhu *et al.*, 2013) and the investigations have not been restricted just to the pancreatic lipase, since the activity of gastric lipase has also been studied (Capolino *et al.*, 2011; Carriere *et al.*, 2000). The current study was performed to compare the digestibility of lipids contained in almond materials with various degree of complexity using a model simulating the duodenal conditions under well-controlled conditions. For this purpose, the pH-stat was the simplest, cheapest and most convenient technique that permitted continuous measurements of lipolysis.

Many different types of DF, which are largely present in plant foods as CWs, are known to inhibit the rate and extent of digestion and absorption of nutrients, including lipids (Grassby *et al.*, 2013; Gunness and Gidley, 2010; Lairon *et al.*, 2007a; McClements *et al.*, 2009). However, the mechanisms by which fibre achieves this varies depending on its characteristics, including molecular and supramolecular structure and physical form within the GIT. First, some types of fibre are water soluble and have the capacity to raise the viscosity of digesta (Dikeman and Fahey, 2006), which can interfere with the functional properties of BS that play a key role in lipid digestion. Thus for example, soluble fibre is thought to have an impact on BS recycling plus mixing and transport of mixed micelles (Gunness *et al.*, 2012). Second, soluble fibre may interact or perhaps 'bind' to the BS thereby affecting the emulsification process and removal of lipolytic products (Cuesta-Alonso and Gilliland, 2003; Kritchevsky and Story, 1974). Third, soluble forms of fibre may also interact with (a) the intestinal mucus layer, thus creating a barrier to absorption of lipolytic products and BS (Gunness and Gidley, 2010), and (b) lipase and the lipase-colipase complex, leading to inhibition of lipolysis (Schneeman and Gallaher, 1985). Recent work done by Alan Mackie and his group (the IFR) on the diffusion of lipid released from a meal containing salmon and barley, revealed that β-glucan released from the barley clogged the mucus and limited the diffusion of the lipid (*data unpublished*). *Figure 5.6* shows fluorescence (lipid concentration) increasing as it builds up in the mucus with only a small

fraction of the smallest micelles diffusing through the mucus layer to be absorbed by the enterocytes.

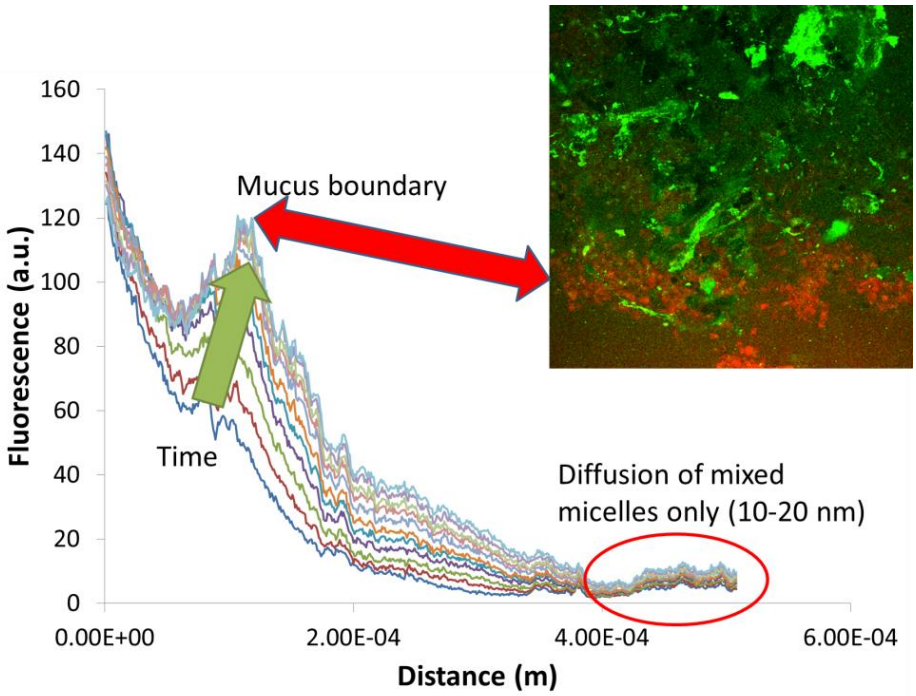

Figure 5.6 Change in lipid concentration with time (unpublished data provided by Alan Mackie). The lipid concentration is directly related to the fluorescence intensity, so it is possible to follow the flow of lipids into the mucus by time lapse confocal microscopy. In the image on the right corner, the intestinal mucus layer is shown in green and the lipids in red.

An additional mechanism, which is highlighted by the results presented in the current chapter, is the role that DF plays as structurally intact CWs in acting as a physical barrier to lipase diffusion into the lipid-rich almond cells. Our results provide compelling evidence for an encapsulation mechanism in hindering lipid digestion of almonds. The importance of CW integrity is illustrated in Figure 5.5, showing separated lipid-rich cells where the extracellular environment is devoid of lipids. Therefore physical processes such as mastication and mechanical processing (milling) increases the number of ruptured cells and, has a direct effect on the amount of lipid and other nutrients released from the food matrix and potentially available for digestion, confirming previous findings by our group (Ellis *et*

al., 2004; Grassby *et al.*, 2014; Mandalari *et al.*, 2008a). Our new findings do highlight the importance of the structural integrity of the CW at the fractured surface of almond particles.

An early study performed on peanuts indicated that the structure of the food altered the quantity of fat absorbed (Levine and Silvis, 1980), and these findings have recently been confirmed (Traoret *et al.*, 2007). Mandalari *et al.* reported that finely ground almonds were more digestible than 2 mm almond cubes (Mandalari *et al.*, 2008a). The different chemical and physical processes occurring during digestion appear to be unable to disturb the resilient CW matrix of hard, brittle plant foods such as peanuts and almonds. Since the lipids provide most of the energy obtained from almonds, a significant discrepancy would be expected to arise between their estimated calorie content found on a food label and the actual energy available from digestion and absorption. Indeed, it has been recently revealed that the commonly used Atwater factors markedly overestimated the available energy found in both pistachios (Baer *et al.*, 2012) and almonds (Novotny *et al.*, 2012) compared with the experimental measurements of metabolisable energy.

Thermal processing of the food prior to ingestion also modifies nutrient bioaccessibility, although in our study roasting did not appear to affect this or the rate and extent of lipolysis. However, blanched almonds have been demonstrated to possess a slightly higher level of lipid digestion compared to raw almonds (Mandalari *et al.*, 2008a). The heat treatment needed to obtain the blanched material denatures the proteins and thus may have reduced the potential interactions occurring between them and the lipids, and/or altered the almond cellular structure resulting in an increase in lipid accessibility.

These results showed that depending on the physical state of the almond materials, modified by mastication and mechanical processing, the accessibility of lipase to the lipid substrate, and the

amount of FFAs produced from the hydrolysis of TAG varied significantly. The concentration of FFA release was greater for smaller particles compared with larger particles due to the greater proportion of ruptured cells, and therefore the amount of released (free) lipid available for digestion. The marked differences in lipid digestion between almond emulsion and lipid-rich almond particles, including separated cells, confirm the role of PCW as a physical barrier against nutrient release and digestion. Despite their small size (~30 to 35 µm), almond cells had less FFA release than almond particles supporting the idea that lipid bioaccessibility relies not only on the available surface area but more importantly on the extent of damaged cells. No significant differences were observed between raw and roasted almond samples. Roasting may have an effect on plant CW integrity, but the coalescence of lipids may diminish further digestion from occurring.

CHAPTER 6

IN VIVO AND *IN VITRO* DIGESTION OF ALMOND MEALS OF DIFFERENT BIOACCESSIBILITY

6.1 Introduction

Using a simple *in vitro* model, the results reported in *Chapter 5* show that the bioaccessibility (release) of lipid and its subsequent digestion varied according to the size of the almond particle. These digestibility experiments provided detailed information about the behaviour of a wide range of almond materials in well-controlled conditions. However, digestion occurring in a human digestive tract is much more complex and it is helpful to validate *in vitro* model data by performing human digestibility studies. Therefore this chapter describes a human intervention study undertaken in ileostomy subjects to investigate lipid digestibility in almond meals with different lipid bioaccessibility values. The ileostomy study was performed at the same time as the gut model (DGM and SDM) experiments using the same almond meals.

Digestion has been investigated in humans and animals with a ileostomy since the early 1940s using dogs (Werch and Ivy, 1941) and then in the 1980s using human volunteers (Berghouse *et al.*, 1984; Englyst and Cummings, 1985; Sandberg *et al.*, 1981; Sandberg *et al.*, 1986; Sandstrom *et al.*, 1986). Ileostomies are performed on individuals suffering from diseases of the colon and rectum such as inflammatory bowel disease (i.e. ulcerative colitis or Crohn's disease) or colorectal cancer. This surgical procedure consists in bringing out the end of the ileum through an opening made in the abdominal wall (stoma), often following the removal of the colon as presented in Figure 6.1 (Melville and Baker, 2011). The digested food passes out of the body through the stoma and is collected in a pouch.

The majority of nutrient absorption takes place in the upper-GIT, so studying the amount of lipid and starch digestion at the terminal ileum is of particular interest. As recovery of material from this part of the gut is not easily achieved, the ileostomy model, particularly in long standing stable patients, is recognised as the best option, and enables researchers to examine the digesta in the relevant region without resorting to invasive procedures (Andersson, 1992; Cummings and Macfarlane, 1991).

Furthermore, it is more relevant to investigate effluent rather than faeces as microorganisms present in the colon further degrade the food and thereby overestimates nutrient release. Other advantages of the ileostomy model are the shorter intestinal transit time that permits the collection of effluent subsequent to the digestion of food consumed during the day (Englyst and Cummings, 1986; Sandberg *et al.*, 1981) and the consistency in ileal output within individuals (Andersson, 1992). Finally, it is easier to collect excretions from ileostomy subjects than individuals with intact colon given that handling of effluent is a routine matter for those subjects and ileal fluid is collected into pouches.

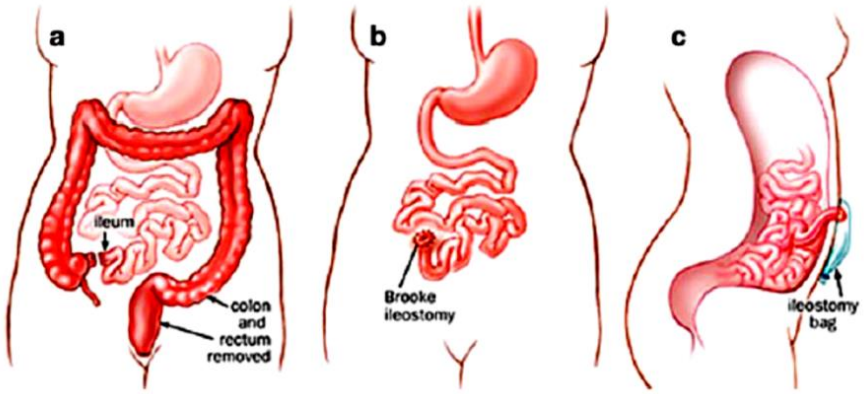

Figure 6.1 Schematic representation of the proctocolectomy (a), the Brooke (or standard) ileostomy following the operation (b), and view side with the pouch (c) (M'Koma et al., 2007).

In the UK, normal bowel habit has been estimated to be on average about 106 g of faeces per day, with subjects passing between 40 and 208 g/day (Cummings *et al.*, 1992). Mouth to anus transit time corresponds approximately to 55 h for men and 72 h for women. Individuals with established ileostomy will pass on average 500 to 1000 mL of effluent per day depending on type and quantity of food/liquid consumed (Hill, 1976; Kock *et al.*, 1977). The pouch is required to be changed or emptied every few hours (5 to 8 times a day). The greater volume of ileal fluid compared with faeces can be explained by the fact that most of the water is absorbed in the colon, hence the deficit in total body

water and sodium observed in ileostomy subjects (Clarke *et al.*, 1967; Hill *et al.*, 1975; Kennedy *et al.*, 1983). Despite the major changes occurring to the morphology of GIT following an ileostomy, the digestive process remains similar to the one of an individual with a whole GIT (Hill, 1976). The patient's body adapts in order to increase the absorptive capacity of the small intestine thus reducing fluid flow and electrolyte losses (Kennedy *et al.*, 1983; Wright *et al.*, 1969). Therefore, ileostomy subjects, in particular those who suffer from ulcerative colitis, are likely to have healthy, normal-functioning upper GIT (Andersson *et al.*, 1999).

Compared to normal ileal content, the effluent flora is quantitatively, the bacterial count in effluent is 100 times higher than the ileal flora but 20 times lower than the faecal flora (Andersson, 1992); and also qualitatively (Finegold *et al.*, 1970; Ruseler-van-embden *et al.*, 1991) different. The flora of the effluent is variable between subjects but stable within individuals. Nevertheless, high inter-subject variability is also observed in the microbial flora of individuals with a whole GIT probably due to genetic variations, lifestyle and dietary habits (Eckburg *et al.*, 2005). These bacteria have various functions including protection against certain pathogens and also metabolic activities (i.e. fermentation of non-digestible nutrients, production of vitamin K, folate and short chain fatty acids, and ion absorption) (O'Hara and Shanahan, 2006).

If collected regularly and frozen rapidly after collection, the effluent undergo minimal microbial degradation including the DF components (Andersson, 1992); however, great care is needed to ensure this and some degradation is invevitable. Similar enzyme activity have been reported between subjects with and without an ileostomy (Hill, 1976). Transit time through the stomach and small intestine appeared consistent among those two categories of individuals. Also, the ileostomy does not seem to have an impact on the ileal break (Soper *et al.*, 1990).

6.2 Aim and objectives

Nutrients bioaccessibility can be manipulated by altering the proportion of CW encapsulated nutrients (i.e. particle size) in test meals. It was hypothesised that a greater amount of lipid would be recovered (i.e. 'undigested/unavailable') in ileal effluent after consumption of a lower nutrient bioaccessibility meal. Also, meals designed to have a lower nutrient availability (lipid and starch) would elicit an attenuation in the postprandial rise in blood lipid and glucose concentrations than meals designed to have higher nutrient availability.

The main aim of the study described in this chapter was to investigate the effect of meals with contrasting degree of encapsulation (i.e. proportion of intact CW) on nutrient release using both *in vitro* (gut models: DGM and SDM) and *in vivo* (ileostomy model) methods. The main objectives of this investigation, referred to here as the Biogut study, were to:

(a) Quantify the loss of lipid from almond tissue due to lipid release and recovered at different stages of gastrointestinal digestion (*in vitro* and *in vivo*);

(b) Examine the changes in the physical state/microstructure of the almond materials before and after digestion; and

(c) Compare the changes in lipid release and digestion (*in vitro* and *in vivo*) with the postprandial blood lipid, glucose and gut hormone responses observed *in vivo*.

6.3 Materials and methods

The Biogut study was designed and conducted in collaboration with another PhD student, Cathrina Edwards, who was responsible for a separate arm of the study investigating starch digestion (Study 2). The methods and results presented below focus on the lipid digestion arm of the study (Study 1).

Because of difficulties encountered by some of the volunteers (obstruction of the stoma), Study 1 had to be interrupted prematurely. Consequently, to support this study's outcomes, the meals were also tested using the DGM/SDM. The almond muffins were masticated by a volunteer and the expectorated bolus loaded onto the DGM.

6.3.1 Test meals

The almond muffins were specifically designed to vary in nutrient bioaccessibility, which consisted predominantly of lipid (48 g from almond). The test meals consisted of 220 g muffin made of either almond flour (**AF**, particles size ~187 µm) or almond particles (**AP**, particles size between 1700 to 2000 µm), given with 80 g of custard (Bird's Instant Custard; Premier Ambient Products, Lincolnshire, UK). Both muffins contained 48 g of lipid, 25 g of protein, 79 g of available carbohydrate (starch and sugars) and 10 g of DF, and the total energy content was 742 kcal (3161 kJ). Details on the preparation and composition of the muffins can be found in *Appendix D.*

In this project the term flour was used to describe almonds that were ground to a powder consistency as opposed to particles that could be visible to the naked eye. The test meals containing almonds were prepared to maximise differences in lipid bioaccessibility, so that the almond flour and large particles are characterised as high and low bioaccessibility samples, respectively (see *Section 2.2.1.1* for details about the preparation of the almond particles and flour). Volunteers were requested to swallow the meal with little mastication, which was rendered possible by the soft matrix of the muffin, in order to limit further particle size reduction and to study exclusively the effect of gastric and duodenal digestion. Data from previous studies performed by our group (Berry *et al.*, 2008; Mandalari *et al.*, 2008a), showed that 1700 to 2000 µm was the maximum particle size possible to ensure minimal mastication without loss in palatability whilst allowing for minimal lipid release during digestion. Using the mathematical model, lipid bioaccessibility of 1700 to 2000 µm

particles was estimated to be about 6%, compared with 49% for the flour (see *Appendix B*). Unfortunately, due to the limitation in the size range covered by the Malvern 2000® laser diffraction particle sizer (0.2 to 2000 µm), the large particles used in AP could not be precisely measured due to the risk of obstructing the machine.

6.3.2 In vitro digestion of almond muffins

6.3.2.1 Mastication of the almond muffins

Sections 6.3.1.2 to 6.3.1.4 were adapted from a protocol developed in collaboration with Dr Mandalari at the IFR. A volunteer was recruited by the Human Nutrition Unit at the IFR and asked to masticate half a muffin until ready to swallow. Each muffin was cut vertically into half while still frozen and one half defrosted at 4°C the day before the study day. The remaining half was kept frozen until needed. The same volunteer was used throughout the study. The protocol was reviewed and given a favourable opinion by the Research Ethics Committee of the North London National Research Ethics Service (reference no. 10/H0717/096) and the Research and Development office at Guy's and St Thomas Hospitals NHS Foundation Trust (reference no. RJ111/N032).

6.3.2.2 In vitro gastric digestion

The solutions were prepared as detailed in *Chapter 2*. In brief, 180 g of masticated muffin and 20 mL of priming acid were loaded in the model that ran for about 1 h; 7 samples (~35 g each) collected at 9 min intervals. During the course of the gastric digestion, 39 mL of enzyme solution and 13 mL of acid solution were added. Each gastric sample was weighed, its pH recorded and adjusted to 7.0 with 1 M NaOH to inhibit gastric enzyme activity, and weighed again. Each gastric sample had 8 g removed for pooled sample for further digestion, and 10 g for lipid analysis.

6.3.2.3 In vitro duodenal digestion

A pooled sample (42 g), obtained from combining aliquots (8 g) of each gastric sample was transferred to a Sterilin plastic tube for duodenal digestion. The remainder of the gastric pool were retained for lipid analysis. To the pooled sample, simulated bile solution (10.42 mL) and pancreatic enzyme solution (29.18 mL) were added and the mixture incubated at 37°C under shaking conditions (170 rpm) for 8 h. Aliquots (10 g at 1 to 6 h, 15 g at 7 and 8 h) were taken every hour and replaced with fresh bile (1.2 mL) and pancreatic enzymes (3.5 mL). Each sample was stored on ice until the run was complete and then frozen at -20 °C.

6.3.2.4 Samples analysis

Masticated, pooled gastric and pooled duodenal samples were analysed for lipid loss using an automated Soxhlet as described in *Chapter 2 Section 2.3.1.2.1*.

For microscopy, the originals (undigested) and digested samples were prepared according to the methods described in *Chapter 2*. Briefly, for the digested samples, aliquots were collected and placed in vials containing the fixative. The samples containing only small particles were placed directly on a microscopy slide and Nile red used to identify lipids. The large almond particles recovered were prepared as previously explained in *Chapter 2 Section 2.3.3.1*.

6.3.2.5 Statistical analysis

The data were analysed using SPSS version 17.0. For all tests, the significance level was set at $P < 0.05$ (2 tailed). All data are expressed as mean ± SEM. Repeated-measures ANOVA was used to test for differences in lipid release after mastication, gastric and duodenal digestion with muffin type as

'within-sample' factor. Differences in lipid release between AF and AP were analysed by Student's paired *t*-test.

6.3.3 In vivo study

6.3.3.1 Subjects and location

Nine adults (7 females, 2 males) who had previously undergone proctocolectomy for ulcerative colitis, Crohn's disease (pure colonic form), or colorectal cancer with normal stoma function (i.e. able to digest and excrete food without any difficulty), were included in the study. The number of subjects required for this study was estimated with a power calculation based on the difference in TAG Incremental areas under the curve (iAUC) between macroparticles and almond oil and defatted almond flour from another study from our group (Berry *et al.*, 2008). This power calculation (performed using G-Power© 3.1.2 software) predicted that 8 subjects would give 80% power to detect a difference between means values of 267 for TAG IAUC at a significance level (alpha) of 0.05 (two-tailed).

Volunteers were identified via the Ileostomy Association, Inside Out, Stomawise, and the events organised by these associations. The subjects willing to take part were sent the participant information sheet (approved by South East Coast Kent Ethical Committee, *see Appendix E*) and asked to complete two screening questionnaires about their general health and dietary habits. Volunteers who were likely to be eligible were invited to attend a screening visit which involved anthropometric measurements, blood analysis, and a medical examination to assess eligibility (*Appendix F: 'Volunteers screening and visit procedures'*). Volunteers were excluded if they were allergic to almonds or related products, gluten and any other added ingredients in the recipe of the test meals; had previously suffered obstruction of the stoma, had a body mass index < 20 kg/m^2 or > 35 kg/m^2; had a diagnosed mouth, throat or GIT problem (other than ileostomy) that might affect normal

ingestion and digestion of food; had total plasma cholesterol > 7.8 mmol/L, plasma TAG > 3 mmol/L, and plasma glucose > 7 mmol/L; had liver function and blood cell counts not within prescribed limits or had diabetes. Once checked for eligibility, volunteers attended up to four study visits at the Clinical Research Facility (CRF) of St Thomas' Hospital, Westminster Bridge Road, London SE1 7EH.

6.3.3.2 Study design

Two single-blind (researcher-blind), randomized, cross-over design studies were undertaken to test lipid- (Study 1) or starch- (Study 2) rich meals varying in nutrient availability. Volunteers were randomly allocated to interventions (AF or AP) using an electronic randomisation program (http://www.randomizer.org/form.htm). Investigators were blinded to the analysis of the samples using a code; the intervention (AF or AP) assigned by a researcher independent to the study. The test meal was prepared and presented to the volunteer by an un-blinded investigator.

Potential volunteers then attended a screening session at the CRF. This session comprised a brief medical examination (blood pressure, waist and hip circumferences, weight and height) and fasting blood collection. Volunteers were excluded at this stage if fasting blood results were found to be outside the normal ranges. Following screening, volunteers were asked to attend the CRF on 2 to 4 separate occasions with a gap of at least one week between visits as outlined in Figure 6.2 and *Appendix F*.

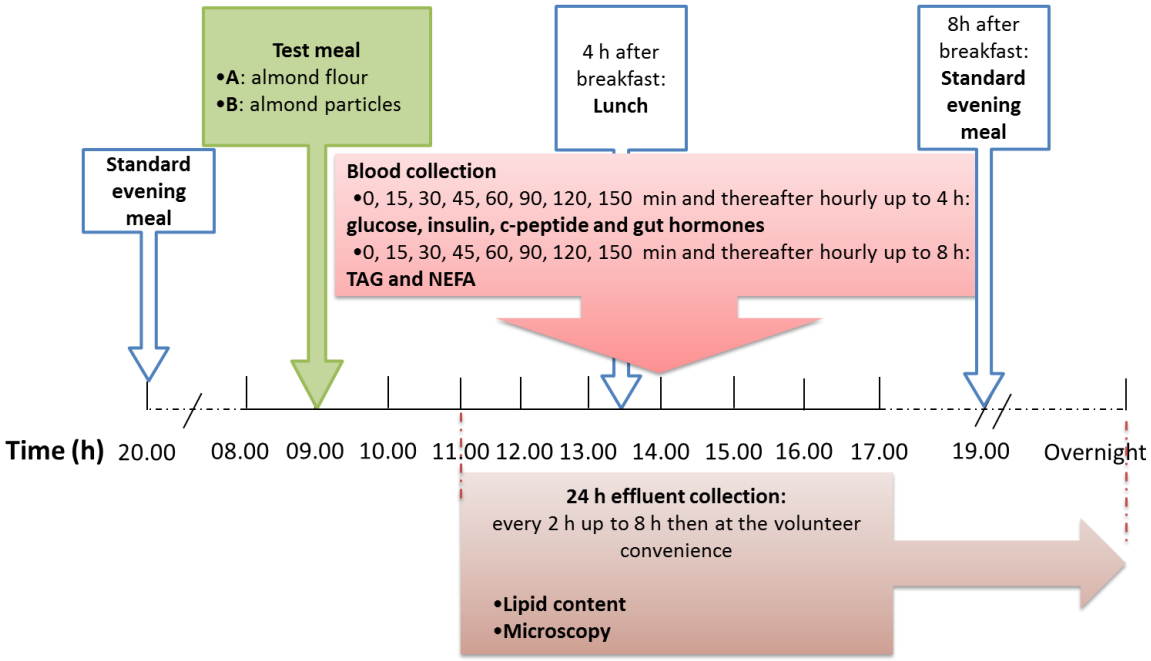

Figure 6.2 Outline of study protocol

The study was reviewed and given a favourable opinion by the Research Ethics Committee of South East Coast, Kent (reference no. 12/LO/1016) and the Research and Development office at Guy's and St Thomas Hospital (reference no. RJ112/N237). The study was also approved by the International Standard Randomised Control Trial (number: ISRCTN40517475). All the volunteers provided written informed consent. All samples were handled, transported and disposed of in accordance with the Human Tissue Act 2004. Each participant was assigned an identification number at screening. Confidential information was kept in a secure locker and on a password protected encrypted hard drive, and was only accessible to designated researchers working on the trial (in accordance with the Data Protection Act 1988). The use of the CRF was authorised by an independent Scientific Advisory Board prior to the commencement of the study.

6.3.3.3 Test meals

During the visits, volunteers were given for breakfast a muffin containing either almond flour or almond macroparticles (see *Section 6.3.1)*; most of the ingested lipid coming from the almond (see *Appendix G*). The lunch meal provided little amount of lipid (0.7 g) and fibre (2.7 g). It was assumed that the lipids present in all the food consumed by the volunteers on each visit, apart from the muffin test meals, were more readily available and absorbed in the duodenum, and thus absent from the collected effluents. Moreover, the low-fat yoghurt given for lunch showed to have no effect on the postprandial lipaemic response (Berry *et al.*, 2008).

6.3.3.4 Collection and handling of blood samples

The postprandial blood response corresponds to a variation in the concentrations of circulating dietary compounds and hormones (e.g. TAG, glucose or insulin) following ingestion of a meal. The measurement of these indicators over time provides information about the rate and extent of nutrient absorption (e.g. lipid) and associated physiological response (e.g. gastric emptying and satiety). Insulin regulates blood glucose concentration by increasing glucose uptake by fat and muscle cells in hyperglycaemic state (Saltiel and Kahn, 2001). It also promotes the synthesis and storage of lipids and proteins. C-peptide and insulin concentrations conjointly measured gave an accurate estimate of insulin metabolism (Polonsky and Rubenstein, 1984). Insulin and C-peptide are co-secreted in equimolar concentrations and vary with physiological circumstances (i.e. fasting or after food intake). But contrary to insulin, C-peptide has a constant metabolic clearance rate and lacks hepatic extraction. Therefore, C-peptide peripheral blood measurements correlate with the portal vein absorption. Given that carbohydrate digestion has an impact on lipid metabolism (Lairon *et al.*, 2007a), measurements of glucose, insulin and C-peptide were necessary.

A cannula (Venflon PRO 22GA, Becton-Dickinson Oxford, UK) was inserted into the antecubital vein of the forearm; blood samples were collected into a syringe and dispensed into the appropriate vacutainers (*Appendix H*).

The blood collected during the screening session was directly delivered to the GSTS pathology laboratory of St Thomas' Hospital and analysed for baseline glucose, lipid profile, liver function tests and full blood counts. Blood samples collected during each visit were analysed for glucose, TAG and NEFA using ILab 650 auto-analyser (Instrumentation Laboratories, see *Appendix H* for more details). The analysis for insulin and C-peptide were also performed at the GSTS pathology laboratory of St Thomas' Hospital. The vacutainers intended for insulin and C-peptide analyses were delivered to the GSTS lab immediately after venesection. The analysis of gut hormones PYY, CCK, GLP-1 and GIP were performed at King's College Hospital in Denmark Hill.

6.3.3.5 Samples analysis

6.3.3.5.1 Blood samples analysis

The details of the methodology for the analysis of glucose, TAG and NEFA with ILab 650 auto-analyser and gut hormones performed at Denmark Hill can be found in *Appendix H*. Briefly, glucose (glucose oxidase ILTest™ kit), TAG (triglycerides ILTest™ kit) and NEFA (Randox NEFA kit) concentrations were measured using colorimetric assays. Insulin, C-peptide and gut hormones (GIP, GLP-1, CCK, and PYY) were analysed by GSTS pathology using chemiluminescence or immunoassays.

The iAUC, over 360 min for TAG and over 240 min for glucose, insulin and C-peptide, were calculated using the macro available in SigmaPlot 12.0.

6.3.3.5.2 Effluent samples

Nutrient losses

About 50 g of sample was placed in a pre-weighed aluminium dish, which was then stored at -40 °C. The sample was freeze-dried to estimate moisture content and total fatty acids was obtained by lipid extraction of the dried effluent samples with a Soxhlet extraction using hexane as solvent (method details in *Chapter 2*).

The overnight samples, once arrived at KCL, were left to defrost at room temperature and then processed in a similar manner than the samples collected during the visits.

Mean transit time

Mean transit time was calculated from the lipid content of ileal effluent using an Equation 6.1 adapted from (Englyst and Cummings, 1985):

$$MTT = \frac{\sum_0^N (Lipid\ in\ sample \times t)}{Total\ lipid\ recovered} \qquad \text{(Eq. 6.1)}$$

where *MTT* is the mean transit time in hours, the amount of lipid in sample and total lipid are in g and t is the time in hours.

Microscopy

An aliquot of the effluent was collected at each time point and prepared for microscopy as described in *Section 6.3.2.5*.

6.4 Results

6.4.1 In vitro gastrointestinal digestion

6.4.1.1 Lipid loss

Table 6.1 shows the percentage of lipid release in the different compartments of the GIT, with a total of 97.1% for AF and 57.6% for AP after duodenal digestion. As expected, the amount of lipids that becomes available increased throughout the digestion process with a significant difference between AF and AP ($P < 0.005$). Repeated-measures ANOVA also showed that the differences in lipid released observed between the different compartments of the GIT were significant ($P < 0.001$).

Table 6.1 Cumulative percentage of lipid released and deduced total undigested lipids from the almond particles (AF and AP) at the different stages of in vitro digestion. Values are presented mean ± SEM (n=3).

	AF	**AP**
Lipid released in the mouth (%)	4.4 ± 0.4	1.9 ± 0.2
Lipid released in the stomach (%)	41.6 ± 1.6	5.8 ± 0.1
Lipid released in the duodenum (%)	97.1 ± 1.7	57.6 ± 1.1
Undigested lipids (%)	**2.9 ± 1.7**	**42.4 ± 1.1**

6.4.1.2 Microstructural analysis

6.4.1.2.1 Muffin containing almond flour

The images of recovered almond flour particles are showed in Figures 6.3. As previously observed, negligible changes in the particles microstructure were observed between samples at baseline (before ingestion) and mastication or gastric digestion. Empty cells and cell debris were more abundant in the later stage of digestion, intestinal phase (Figure 6.3 D).

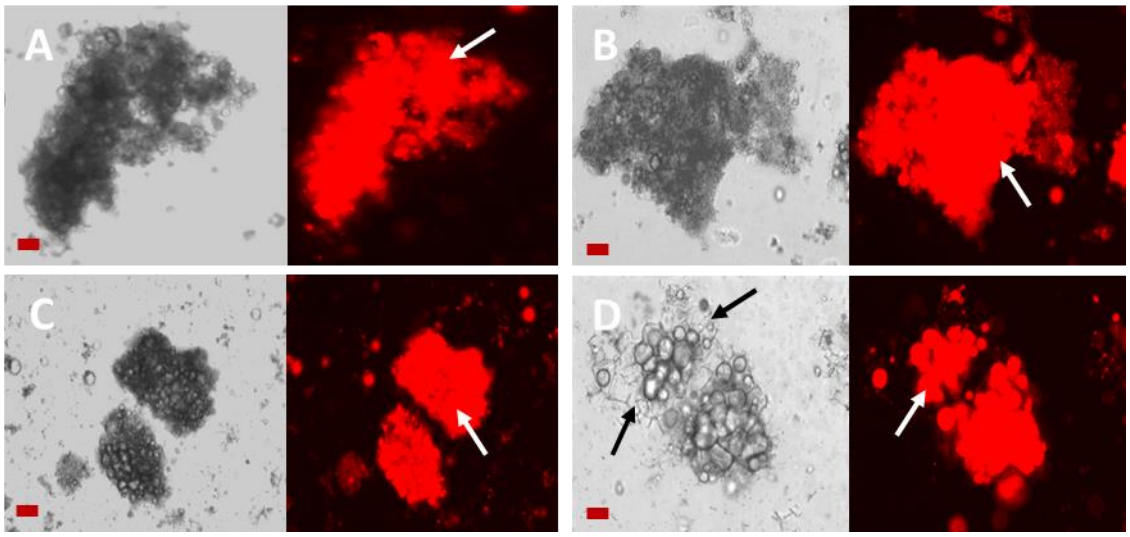

Figure 6.3 LM sections of raw almond particles from AF recovered at different stages of digestion: baseline (A), chewed (B), post-gastric (C), and post-duodenal (D). Lipids are stained in red with Nile red. The coalesced lipids and empty cells are indicated by the white and black arrows, respectively. Scale bars = 20 µm.

6.4.1.2.2 Muffin containing large almond particles

Large particles were recovered after simulated gastric and duodenal digestions (Figure 6.4). The lipids remained enclosed inside the almond tissue, although it appears that some of the CW fractured during the preparation of the muffins (Figure 6.5 A1 and A2). The cells within the almond tissue appeared to be tightly packed together and the lipids coalesced.

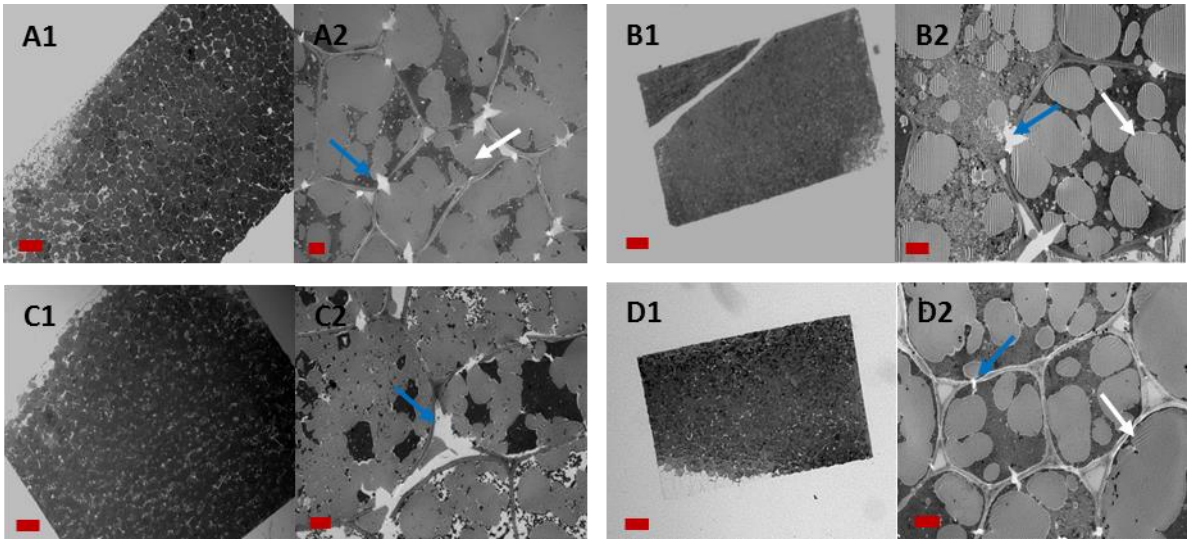

Figure 6.4 LM (1) and TEM (2) sections of raw almond particles from AP recovered in ileal effluents at different stages of digestion: baseline (A), chewed (B), post-gastric (C), and post-duodenal (D). The coalesced lipids and the fractured cells are indicated by the white and blue arrows, respectively. Scale bars: B1 and D1 = 100 µm; A1 and C1 = 50 µm; A2, B2, C2 and D2 = 5 µm.

6.4.2 In vivo study

6.4.2.1 Volunteer and effluent samples characteristics

Only one female volunteer completed the lipid study, because some volunteers had complications (i.e. obstruction of the stoma) following the ingestion of the muffin with large almond particles and consequently it was decided to interrupt this arm of the study (Figure 6.5). This volunteer had an ileostomy operation more than 2 years before the start of the study due to ulcerative colitis. Her usual dietary intake was within the UK reference ranges for women for most nutrients apart from protein intake that was double that in the normal range (Table 6.2). Fat intake was also high especially for saturated fat. Blood pressure, BMI, fasted plasma glucose, TAG and cholesterol concentrations were all within normal range, and the subject was of good health. Study 2 revealed that data from this volunteer (i.e. starch recovery and blood profiles following ingestion of the wheat meal) were within one standard deviation of the population mean so for example for smooth

particles wheat porridge, the starch recovery weight was 3.63 g compared with the mean value of the group (n = 9) of 3.00 ± 1.1 g (Edwards, 2014).

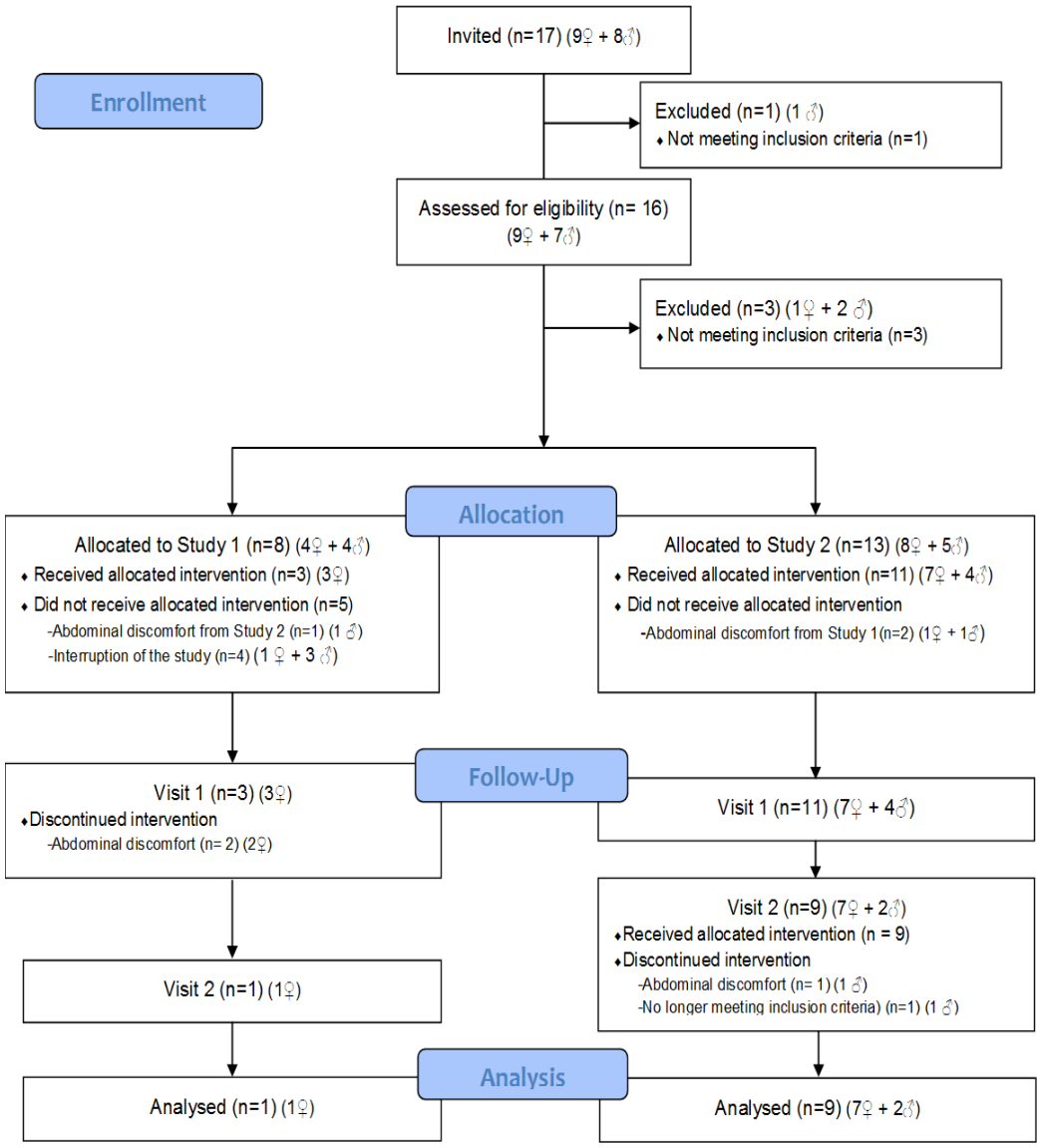

Figure 6.5 CONSORT diagram of subject flow throughout the study. One subject completed Study 1, and a total of 9 subjects completed Study 2.

Table 6.2 Baseline dietary intake of the volunteers included in the study (means ± SEM).

	Values (n=9)[1,2]	Study 1 volunteer's values
Dietary intake at baseline		
Energy (kJ/d, (kcal/d))	8012 ± 1088 (1938 ± 255)	7842 (2081)
Protein (g/d)	96.3 ± 17.9	93.8
Carbohydrate (g/d)	191.1 ± 26.8	175.4
Fat (g/d)	78.5 ± 10.9	100.4
Dietary fibre (g/d)	19.4 ± 3.6	19.7
Physical characteristics		
Age (years)	48.2 ± 6.0	52
BMI (kg/m^2)	24.0 ± 1.3	19.6
Waist (cm)	83.3 ± 4.0	72.2
Hip (cm)	100.7 ± 2.3	93.2
Waist/hip	0.8 ± 0.03	0.8
Systolic / diastolic BP (mmHg)	110.3 ± 5.4 / 70.3 ± 3.1	89 / 66
Pulse (beats/min)	69.1 ± 4.1	81
Biochemistry		
Plasma glucose (mmol/L)	5.1 ± 0.23	4.8
Plasma TAG (mmol/L)	1.0 ± 0.15	0.76
Plasma total cholesterol (mmol/L)	4.9 ± 0.32	4.9

[1]Values are presented mean ± SEM. [2]Dietary intake as analysed by NetWisp 3.0 (Tinuviel© software).

The characteristics of the effluents collected from 0 to 10 h and the corresponding MTT are outlined in Figure 6.6 A; the last time points were excluded since the collected samples contained the remainder of the evening meal, consumed 8 h after the test meal. The amount of dry matter excreted by the volunteer was higher for AP (47.4%) than for AF (42.2%), in contrast to the values obtained for moisture content, which were 88.8 and 91.2 % for AP and AF, respectively. This implies that AF was digested to a greater extent than AP which is confirmed by the total lipid content in the effluent (for the 10 h period: 1.7 and 20.9 g for AF and AP, respectively). The transit time values, calculated over 10 h following the test meals ingestion, indicated that AP took longer to be digested than AF. Over the 24 h period, a total of 52.3 and 85.0 g of dry matter was excreted following AF and AP consumption, respectively (Figure 6.6 B). For most time points, more effluent matter was

recovered for AP than for AF. An important amount of large particles (AP only) were recovered even after long residence time (*data not shown*), although it is worth noting that some of the effluent originated from the meal consumed for the evening meal.

A

	AF	AP
Total weight (g)	465.8	423.9
Average moisture content (%)	91.2	88.8
Total dry matter (g)	42.2	47.4
Total lipid (g)	1.7	20.9
MTT (h)	5.5	6.7

B

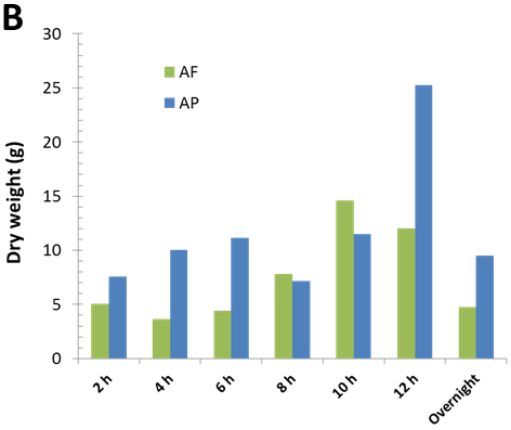

Figure 6.6 Characteristics of ileal effluents and mean transit time (A) from 0 to 10 h of digestion, and dry weight of matter recovered over 24 h (B) for AF and AP.

6.4.2.2 Lipid loss

The concentration of undigested lipids in recovered effluent at each postprandial time point, calculated as a percentage of the dry weight of the effluent samples, is presented on Figure 6.7. A marked difference in the percentage of undigested lipids could be observed between the two interventions with a maximum of 12.4% at 2 h for AF and 53% at 10 h for AP. The percentage of recovered lipids was much greater for AP compared to AF, and this at each time point with a maximum difference of ~51% at 10 h. Apart for this peak at 2 h, the digestion of lipid contained in the almond flour appeared to be constant overtime. The total amount of undigested lipids for the whole 24 h period, calculated from the original ingested almonds, was 6.2% for the almond flour and 58.7% for the 2000 µm almond particles.

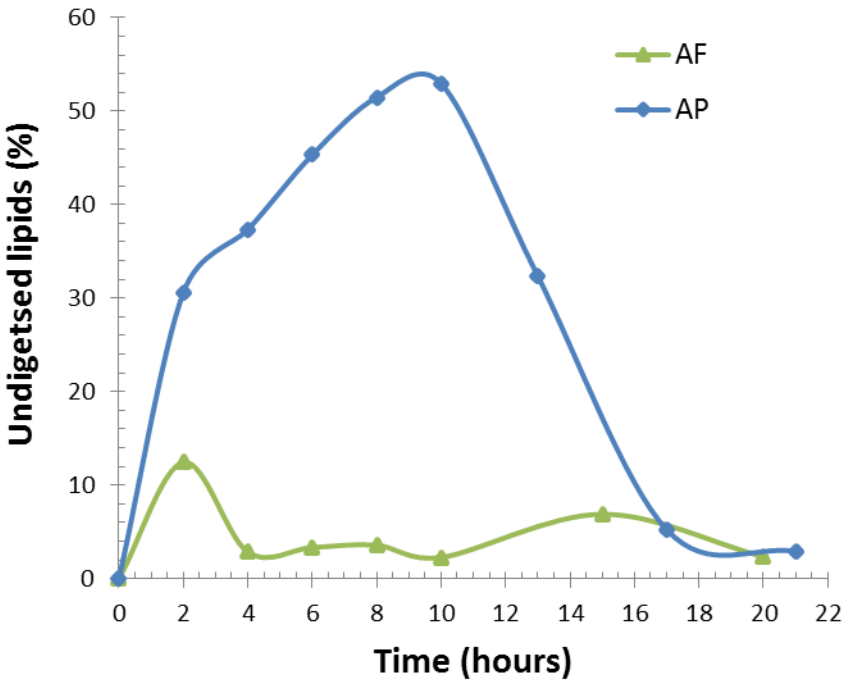

Figure 6.7 Concentration of lipid in the effluent samples recovered at each postprandial time point from the terminal ileum of the ileostomy volunteer (n=1) for AF (green) and AP (blue). Values are calculated as a percentage of the dry weight of the effluent samples. Much of the lipid found in the effluent remained enclosed in the particles of almond tissue (see Section 6.4.2.3).

6.4.2.3 Microstructural analysis

For both interventions particles of almond could be easily seen and identified in the effluent samples.

6.4.2.3.1 Muffin containing almond flour

Figure 6.8 (A-F) illustrates typical almond particles removed from effluent that had been collected at the terminal ileum at different time points following the ingestion of AF. On examination of these particles, it is clearly noticeable that a large proportion of lipids were still present within the recovered particles, even though many were of relatively small size (i.e. Figure 6.8 shows particles of

~300 µm, but particles with sizes as small as ~75 µm were also observed, *data not shown*). The structure of the particles is also visible implying that little alteration occurred to these particles throughout the digestion, although some of the content appeared to have been digested especially at the surface (6.8 B, C and D).

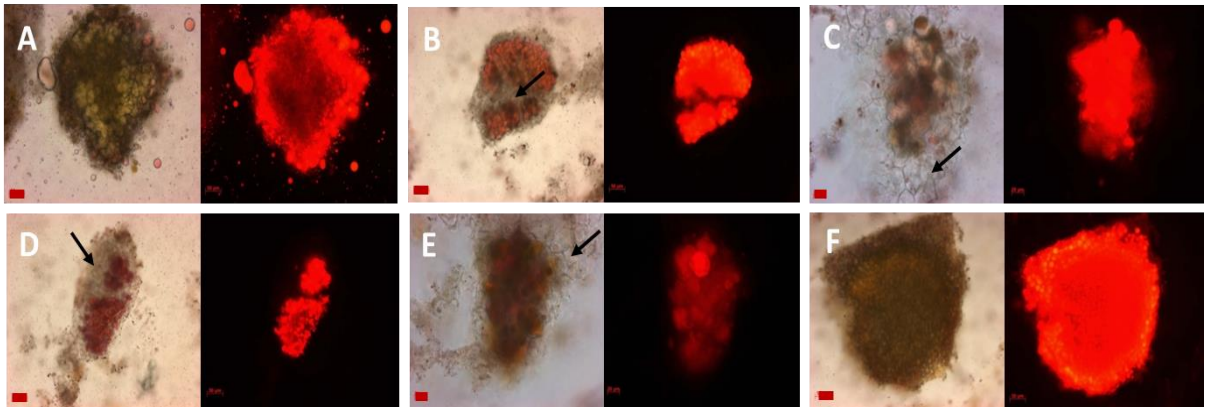

Figure 6.8 LM sections of raw almond particles from AF recovered in ileal effluents at different time points: 2 h (A), 4 h (B), 6 h (C), 8 h (D), 10 h (E) and overnight (F). Lipids are stained in red with Nile red. The empty cells are indicated by the black arrows. Scale bars: A, B, D and F = 50 µm; C and E = 20 µm.

6.4.2.3.2 Muffin containing large almond particles

A large proportion of undigested lipids remained inside the macroparticles recovered at the terminal ileum (Figure 6.9 A-G). These observations correlate with the lipid measurements presented in Figure 6.7. There was a progressive loss of lipid from the surface towards the core of the large particles. This lipid loss was never complete, but this became more noticeable at the later stages of digestion (> 10 h). Only the cells on the first (surface) layer were depleted of their lipid content after 2 and 4 h of digestion (Figure 6.9 A1 and B1) compared with cells in 3-4 surface or near surface layers at 10 and 12 h (Figure 6.9 E1 and F1). Moreover, as previously reported (Mandalari *et al.*, 2008a), the almond CWs seemed to show evidence of swelling, in particular at the latest stages of digestion (Figures 6.9 F2 and G2).

At each stage of digestion, CW degradation and lipid coalescence of the almond tissue could be discerned. Despite these alterations, that may have occurred during the muffin preparation (i.e. cooking and freezing; Figure 6.4 A), lipid digestibility was limited. Similarly to the *in vitro* data, the tissue firmness, tight cell-cell adhesion and absence of cell separation may have prevented leaking of the lipid to the extracellular environment and diffusion of digestive agents (i.e. lipase). The extent of digestion and the resulting degradation of the almond particles looked similar *in vivo* and *in vitro* for identical residence time (i.e. 8 h).

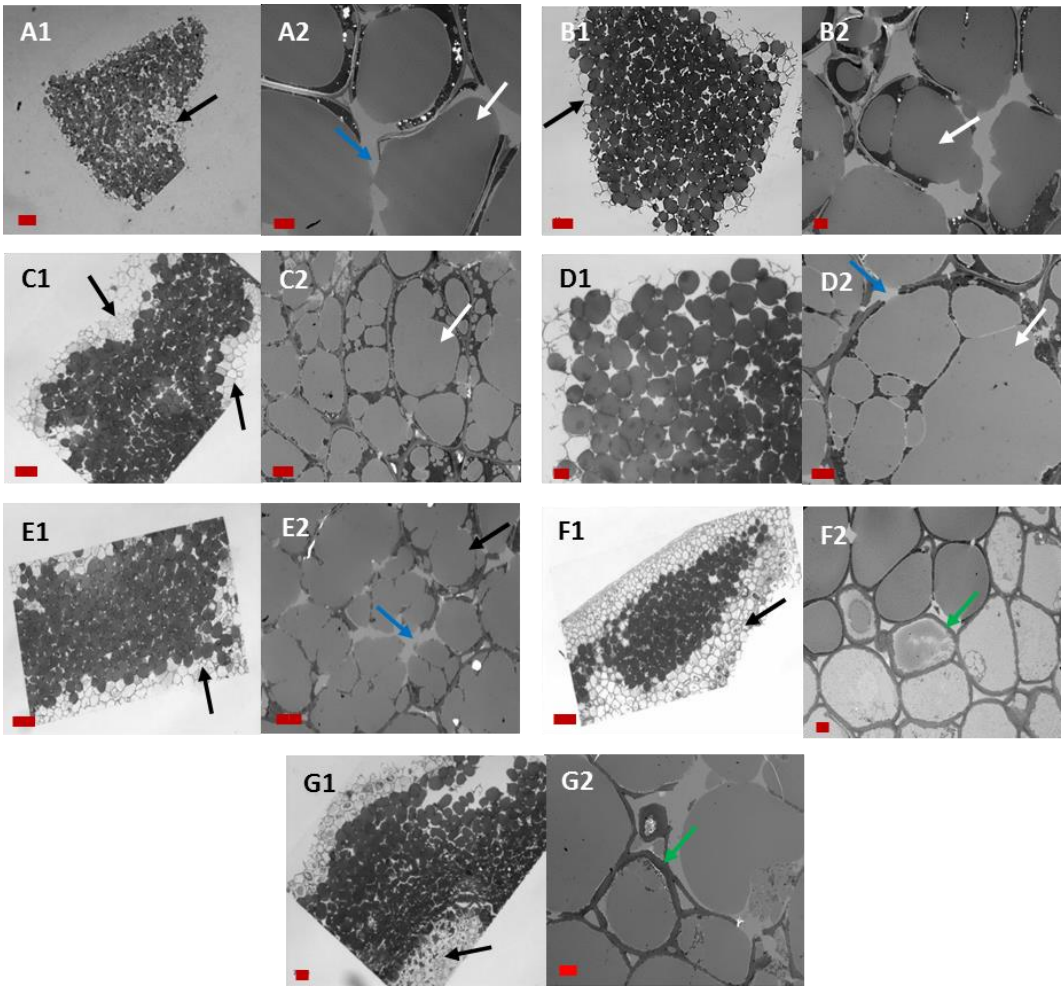

Figure 6.9 LM (1) and TEM (2) sections of raw almond particles from AP recovered in ileal effluents at 2 h (A), 4 h (B), 6 h (C), 8 h (D), 10 h (E), 12 h (F) and 21 h (G) of digestion. The coalesced lipids, empty cells, fractured cells and swollen CW are indicated by the white, black, blue and green arrows, respectively. Scale bars: A1 = 100 µm; B1, C1, E1 and F1 = 50 µm; G1 and D1 = 20 µm; A2, B2, C2, D2, F2 and G2 = 5 µm.

6.4.2.4 Postprandial responses

6.4.2.4.1 Plasma lipids, glucose, insulin and C-peptide concentrations

The changes from fasting in postprandial TAG and NEFA concentrations after the two test meals are presented in Figure 6.10 with the TAG iAUC in the inset. Overall, AF elicited a greater rise in TAG blood levels than AP, the iAUC was ~28% lower for the latter. TAG concentrations reached peak values at 2 h 30 for AF (difference of 0.63 mmol/L from fasting) and 4 h for AP (difference of 0.42 mmol/L from fasting). Plasma concentrations of NEFA following the ingestion of AF and AP were lower than during fasting, and this for the entire duration of the intervention day. NEFA concentrations were higher after AF up to about 3 h where the trend reversed.

The postprandial glucose, insulin and C-peptide responses showed a different pattern to those seen for plasma TAG and NEFA (Figure 6.11). All three curves followed the same trend and showed a sharp peak at 30 min for AP (i.e. 7.8 mmol/L, 491 pmol/L and 2648 pmol/L at 30 min for plasma glucose, insulin and C-peptide concentrations, respectively) and a much lower peak rise at 3 h for AF (i.e. 6.9 mmol/L, 239 pmol/L and 2076 pmol/L at 30 min for plasma glucose, insulin and C-peptide concentrations, respectively). Another interesting observation is the difference in shape profiles between AF and AP; the steady rise in glucose concentrations for AF indicates that the starch present in the muffin is being slowly digested; the insulin, C-peptide profiles being consistent with the glucose data.

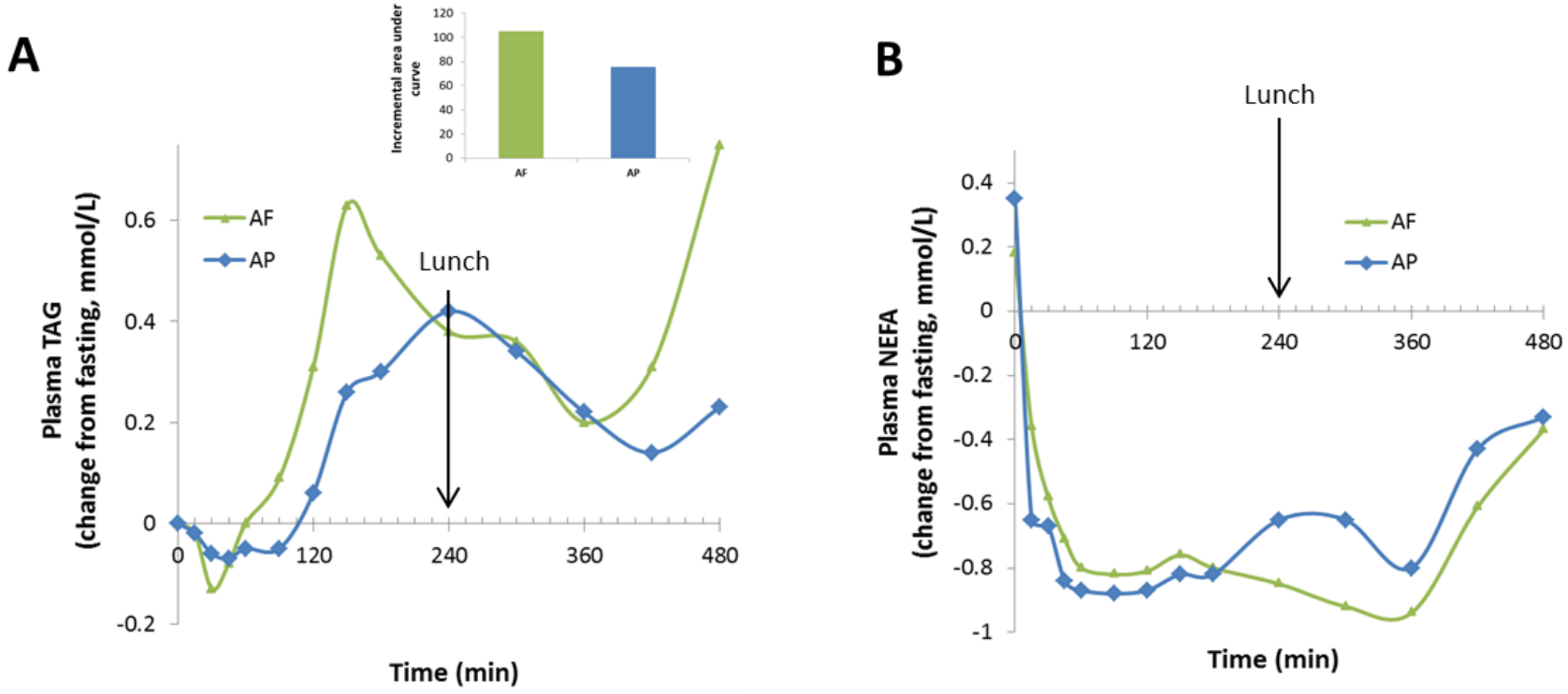

Figure 6.10 Changes from fasting in plasma TAG (A) and NEFA (B) concentrations in an ileostomy volunteer (n=1) after the test meals containing 48 g of lipids from AF (green) or AP (blue). Inset: Incremental area under the curve. The raw data can be found in Appendix I.

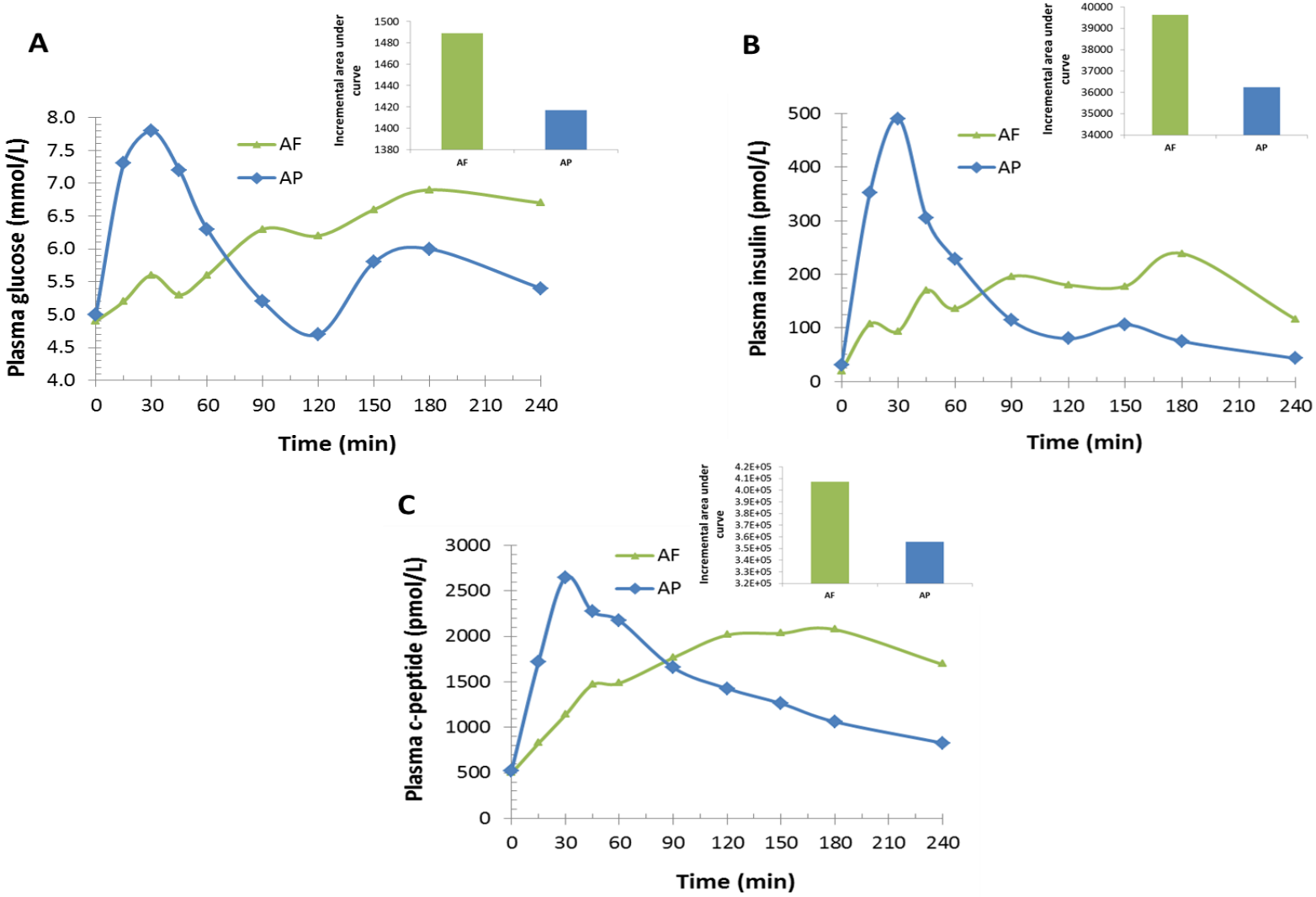

Figure 6.11 Plasma glucose (A), insulin (B) and C-peptide (C) concentrations in an ileostomy volunteer (n=1) after consumption of AF (green) or AP (blue).

6.4.2.4.2 Gut hormones concentrations

Postprandial plasma GIP, GLP-1, CCK and PYY concentrations in responses to the two test meals are shown in Figure 6.12. The muffin with the larger almond particles elicited sharp and early elevation in GIP, GLP-1 and PYY concentrations (329 ng/L at 30 min for GIP; 67 pmol at 15 min for GLP-1; and 154 ng/L at 15 min for PYY). While GLP-1 levels remained relatively constant overtime following the ingestion of AF, GIP and PYY increase to ~520 ng/L at 90 min and ~200 ng/L at 30 min, respectively. CCK concentrations showed constant fluctuation over 3 h, especially for AP, but seemed to flatten off in the last hour.

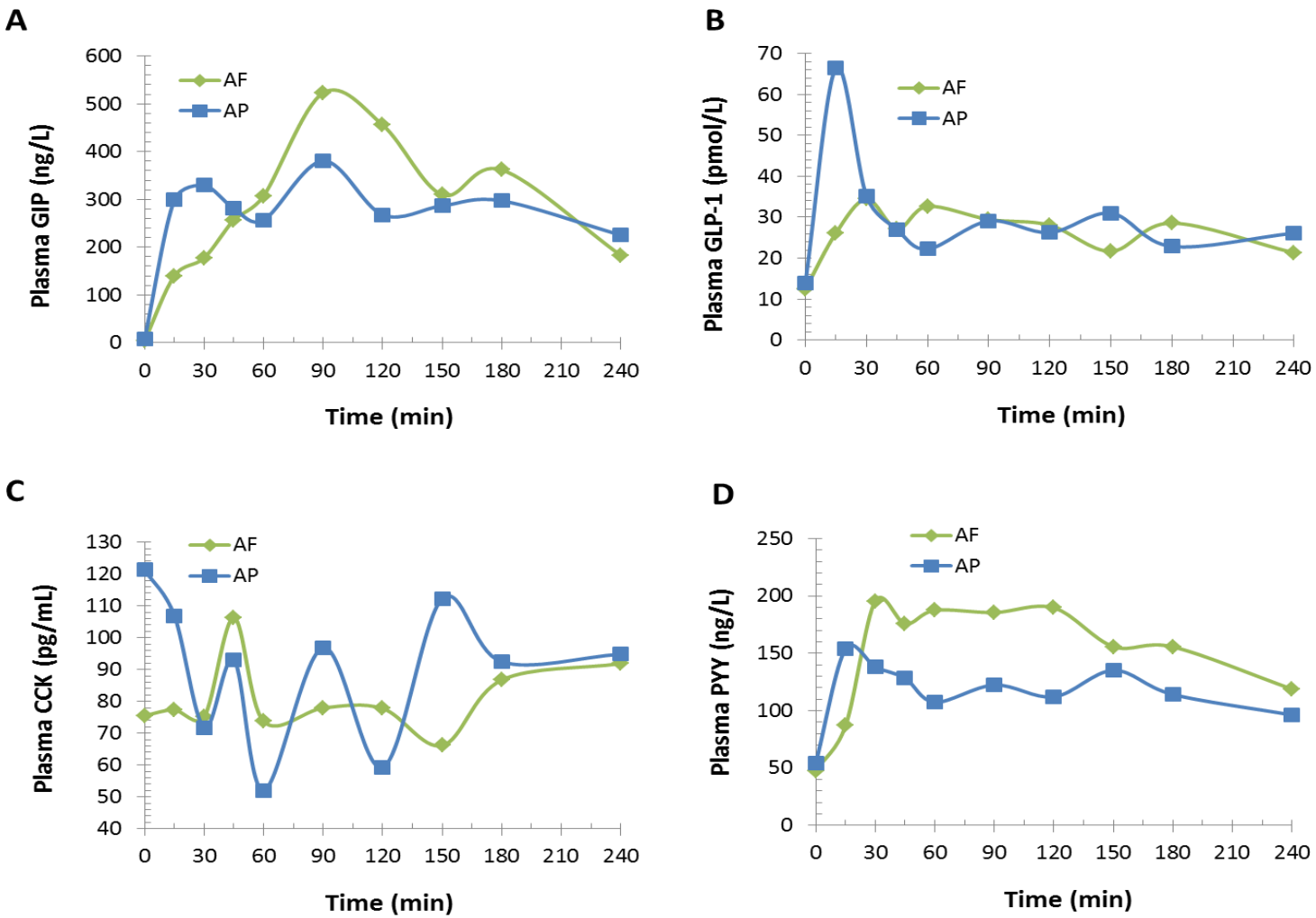

Figure 6.12 Plasma GIP (A), GLP-1 (B), CCK (C)and PYY (D) concentrations in an ileostomy volunteer (n=1) after the test muffin meals containing 48 g of lipids from AF (green) or AP (blue).

6.5 Discussion

This chapter describes the results of an ileostomy study in which digested lipid (i.e. lipid excreted) and the subsequent blood responses were measured following the consumption of two test muffin meals that were identical in composition, but contained almonds that differed in their physical structure (i.e. particle size and consequently lipid bioaccessibility). The importance of food structure and the role of CW in influencing the lipid availability has been previously identified by our group (Ellis *et al.*, 2004; Mandalari *et al.*, 2008a). The current study was designed to improve our understanding of the mechanisms of lipid bioaccessibility and digestion of almonds in the upper GIT, and how this is linked to postprandial lipaemia. The use of microstructural analysis of digested almonds in combination with measuring the extent of lipid digestion and plasma TAG concentrations in ileostomy patients is a novel approach. Unfortunately the almond meals, in particular AP, was not well-tolerated by the volunteers and only one of them was able to complete the study; hence the requirement of performing an additional *in vitro* digestibility study.

The structure of lipid or starch rich foods and its impact on blood responses have been investigated in many previous studies using human volunteers with a complete GIT (Holm and Bjorck, 1992; Kristensen *et al.*, 2010; McKiernan *et al.*, 2010). However, many of these studies lacked detailed physicochemical characterisation of the ingested food (i.e. structure of the food matrix, type and quantity of DF, and particle size) and also of the food materials reaching the terminal ileum, prior to fermentation by gut microflora. Lia *et al.* investigated the effect of DF from oat and wheat (DF content was 16.3 and 6.4 g for oat and wheat meal, respectively) on lipaemia in ileostomy volunteers (Lia *et al.*, 1997). In contrast to the study design presented in this chapter, the lipids were not included in the food matrix but added separately to the test meal. They found that plasma TAG concentrations and fat excretion increased to a greater extent after the oat meal. A more recent

study investigated the effect of a food matrix on the release of omega-3 long chain PUFA in ileostomy volunteers (Sanguansri *et al.*, 2013). In their study, the authors use fairly readily available lipids (fish oil microencapsulated inside a starch mixture) and the food matrix differed greatly (i.e. orange juice, yoghurt and cereal bar), therefore there was no major modification *per se* in the degree of nutrient encapsulation. However, this study showed that food matrix played a role in delivering omega-3 long chain PUFA, cereal bar (i.e. the most complex food matrix) eliciting the highest lipid recovery.

Comparison between ileostomy subjects and individuals with their normal intact GIT indicated similarities in many aspects of the digestion process between these two groups (Andersson, 1992), including lipid absorption (Tornqvist *et al.*, 1986). However, subjects who underwent proctocolectomy were reported to have elevated blood concentration in most hormones including insulin (M'Koma *et al.*, 2007).

The changes in lipid digestibility between AF and AP obtained with the DGM/SDM and the ileostomy volunteer were consistent; the percent decrease in undigested lipid between the two meals being 94 and 89% for *in vitro* and *in vivo*, respectively. As anticipated, the proportion of lipid release was greater for the muffins containing almond particles than raw and roasted whole almonds digested using the DGM (~68% for both almond types, see *Chapter 4*). The data therefore confirmed that the amount of nutrient released from the almond tissue depends on its physical state when it reaches the stomach and emphasised the importance of mastication and the pre-ingestion transformations.

It is plausible that the small particles, due to the nature of the almonds and their physical properties (e.g. strong cell-cell adhesion), may have fractured in a different manner to the large ones during grinding in a similar way to the phenomenon observed during mastication (*Chapter 3, Figure 3.7*). However, physical disruption of the CW during the meal preparation was not sufficient to obtain a

complete lipid digestion especially if the particles were large. The overall almond tissue integrity (i.e. cells still tightly packed together) appeared to be conserved despite the mechanical damages; this behaviour along with the lipid coalescence may have limited the penetration of the digestive agents (e.g. lipase and BS) and thereby hindered lipid digestion. Indeed, as demonstrated in *Chapter 5*, the digestion of lipid with a large droplet size is not kinetically favourable.

As hypothesised, the low-lipid-bioaccessibility meal (almond particles) resulted in an attenuated lipaemic response, albeit in one subject, compared with the high-lipid-bioaccessibility (almond flour) meal. These results correlate with a similar study done on males and females where the authors reported a delayed peak in TAG concentration (~1.3 mmol/L at 5 h) for the test meal containing almond seeds compared with the almond oil test meal (~1.3 mmol/L at 3 h) (Burton-Freeman *et al.*, 2004). Our group also showed that in men, muffins containing either almond oil and flour (AO) or large particles of almond (WA) elicited peak TAG concentrations at 5 h with values of 2.31 and 1.5 mmol/L for AO and WA, respectively (Berry *et al.*, 2008). The greater fluctuations in TAG concentrations obtained in the Berry *et al*'s study could have been due to the difference in lipid bioaccessibility between almond oil compared with the almond flour used in the current study. Indeed, the lipid in the almond oil was more bioaccessible (and digestible) than in the almond flour, since the former was first extracted from the particles before being incorporated into the muffin along with the residual fat-free almond tissue, which included the CWs (DF). The discrepancy between these two studies could also be attributed to the ileostomy operation that may have had a greater impact than predicted on the almond digestion, and to possible differences in microbial flora. However, caution is needed when making interpretations of the current human study due to the lack of statistical power with only one subject completing the protocol.

Since the gut hormones are secreted in response to the presence of both lipid and glucose in the duodenum (Wu *et al.*, 2013), it is difficult to assess the contribution each of these nutrients make to the fluctuations in the hormone concentrations. However, analysed conjointly with lipid loss as well as lipid and glucose blood profiles it is reasonable to suggest that the initial rise in blood glucose is caused by the hydrolysis of the starch contained in the muffin. It is highly likely that the muffin matrix (i.e. starch-rich part) was disrupted in the stomach very early on and then transited to the duodenum, whereas the almond particles remained in the gastric compartment for a prolonged period of time. For both meals, GIP response had two peaks occurring later for AF possibly matching the entering of nutrients in the duodenum and, by extrapolation, gastric emptying. Also, the early GIP response to AP reflects the rise in glucose concentrations observed in Figure 6.11. The presence of 'free' lipids in the small intestine following the consumption of AF, as opposed to the encapsulated lipids within the particles of AP, may have reduced the postprandial glucose and increased the GIP response as previously observed (Collier *et al.*, 1984). However, the mechanism(s) involved are likely to be complex and perhaps even multifactorial, e.g. a reduced gastric emptying rate and thus slower delivery to the duodenum, and possibly interaction with starch (Derycke *et al.*, 2005).

PYY secretions were overall more important for AF than AP implying than more lipid was released from the digestion of this test meal. PYY is secreted in the more distal sections of the GIT and it is thought to inhibit gastrointestinal motility in the presence of lipid in the ileum (i.e. 'ileal break') (Wu *et al.*, 2013). The rapid increase following the consumption of the test meals is likely to have been caused by the presence of readily available nutrients (lipid or starch). Given that CCK is secreted when lipids and lipolytic products reach the duodenum, it is plausible that the curves reflect the release of lipid from the almond particles. However, CCK is involved in other physiological processes (e.g. satiety and gastric emptying) which make the interpretation of these data challenging. The postprandial CCK responses obtained in the current study differed from Burton-Freeman data

(Burton-Freeman *et al.*, 2004). They found that for women, in contrast to the low-lipid-bioaccessibility meal (max ~8.5 pmol/L), the muffin containing the almond oil produced a distinct increase in the CCK response with a peak value at 2 h of ~14.5 pmol/L.

The increased lipid losses obtained following the consumption of AP compared with AF coincided with observations of almonds after different degrees of mastication (Cassady *et al.*, 2009). Cassady observed that a higher number of chews resulted in a greater proportion of small particles and thereby faecal energy losses. During prolonged mastication, greater sensations of satiety were also obtained subsequent to the high initial postingestive GLP-1 response. In the present work, the opposite was seen where plasma GLP-1 concentrations were higher for AP than AF. The presence of other nutrients in the muffins (i.e. starch from the maize and wheat flours) could most probably explain this observation. Furthermore, the highly dynamic nature of the postprandial phase make the interpretation of the data challenging especially since only one volunteer completed the intervention. However, an interesting observation is that after AP, larger increases in insulin and GIP concentrations were measured, compared with the responses to the AF. Similarly, a greater reduction in NEFA was measured after AF compared with AP. These response patterns are usually observed following the consumption of a meal rich in carbohydrate (Frayn, 2010). Indeed, the two gut hormones suppress the production of FFA from TAG hydrolysis which is manifested by a reduction in plasma NEFA and thereby promotes the utilisation of the absorbed glucose (Saltiel and Kahn, 2001).

The present study provides further evidence that by decreasing the size of almond particles lipid release is enhanced. We also showed that, before entering the colon, large almond particles still contained a significant quantity of lipids even after long residence time. Finally, these results support the hypothesis that different degrees of lipids encapsulation elicit different blood lipid, glucose and gut hormone responses.

CHAPTER 7

PERMEABILITY OF ALMOND CELL WALLS TO DIGESTIVE ENZYMES

7.1 Introduction

Previous studies have provided evidence that the physical encapsulation of intracellular nutrients (i.e. lipid or starch) by intact CW restricts the access of digestive enzymes and the release of nutrients (Ellis *et al.*, 2004; Mandalari *et al.*, 2008a). Modifications in the morphology of the CW seem to occur after prolonged retention time (i.e. 12 h of digestion) in the GIT. However, there is currently no evidence on whether or not lipases, colipase and the other digestive agents such as BS could penetrate the CW at the initiation of digestion or at its later stages.

7.1.1 Lipases

Several lipolytic enzymes, are involved in the degradation of dietary lipids (see Figure 5.1): gastric and colipase-dependent pancreatic lipases that are well known for the digestion of TAG, pancreatic lipase-related proteins (PLRP) and pancreatic carboxyl ester hydrolase (CEH), which display various lipolytic activities, and pancreatic phospholipase A2 (sPLA2) that has an activity against phospholipids. Three human pancreatic lipases have been identified: (1) 'classical' pancreatic lipase, (2) pancreatic lipase-related protein 1 (PLRP1), and (3) pancreatic lipase-related protein 2 (PLRP2) (Thirstrup *et al.*, 1994). Human PLRP1 (HPLRP1) and PLRP2 (HPLRP2) share 68 and 65% similarity in their amino acid sequence, respectively, predominantly located in the lid, with the 'classical' PL (Giller *et al.*, 1992). Despite its high occurrence in various species (De Caro *et al.*, 1998), including very high levels in dogs and cats, no significant lipolytic activity has been detected for PLRP1 regardless of the species (Crenon *et al.*, 1998; Roussel *et al.*, 1998). From the 3D structure of dog PLRP1 and site-directed mutagenesis, it has been shown that PLRP1 activity is impaired by two amino acid substitutions relative to classical PL and steric hindrance in the vicinity of the catalytic triad, these amino acid substitutions being specific of PLRP1 whatever the species (Roussel *et al.*, 1998). So far the function of PLRP1 is still unknown, although its interaction with colipase has been

shown. PLRP2s are enzymically-active proteins and their kinetic properties differ from those of classical PL, with some differences among species (Hjorth *et al.*, 1993; Thirstrup *et al.*, 1994). Human PLRP2 activity on medium/long chain TAG is mainly inhibited in the presence of bile salts and poorly restored by colipase; it is not interfacially activate and possesses a phospholipase A1 activity and a galactolipase activity *in vitro* (De Caro *et al.*, 1998; Eydoux *et al.*, 2007; Sias *et al.*, 2004). Based on these *in vitro* properties, the authors presumed that dietary TAGs were not its physiological substrate. HPLRP2 has been found to lack interfacial activity as well as to act preferentially on more soluble substrates (monoacylglycerols, phospholipids and galactolipids) than the 'classical' pancreatic lipase. The 3D structures of classical human PL and human PLRP2 also differ in their lid domain, a structural element that controls the access to the active site and the overall amphiphilicity of the enzyme (Eydoux *et al.*, 2008). In addition to its phospholipase A1 activity, PLRP2 is also active on MAG (Eydoux *et al.*, 2007; Eydoux *et al.*, 2008), vitamin A esters (Reboul *et al.*, 2006) and non-natural esters like PEG esters found in pharmaceutical formulations (Fernandez *et al.*, 2007) or CITREM (citric acid esters of MAG) found in infant formula (Amara *et al.*, 2014). Finally, PLRP2 is secreted by the pancreas but it is also found in various others tissues depending on the species, i.e. T lymphocytes in the mice (Lowe *et al.*, 1998), monocytes in humans (Record *et al.*, 2011) and seminal plasma in the goat (Sias *et al.*, 2005), suggesting a role in immune mechanisms. sPLA2 is synthesised from the pancreatic acinar cells and catalyses the hydrolysis of the ester bond located in the sn-2 position of the phospholipid (Burke and Dennis, 2009).

CEH, also called bile salt-stimulated lipase (found in human milk) or bile-salt dependent lipase, has for substrates cholesterol esters, MAGs, and vitamin A and E esters (Hui and Howles, 2002; Lombardo, 2001). The latter is produced by the acinar cells of the pancreas and the lactating mammary glands (Nilsson *et al.*, 1990).

Controversy currently exists regarding the presence of lingual lipase in the human mouth as demonstrated by its recent occurrence in the literature (Kulkarni and Mattes, 2014; Stewart *et al.*, 2010). The enzyme has been demonstrated to be present and active in rat tongue but the evidence is equivocal in humans (Bernback *et al.*, 1990; DeNigris *et al.*, 1988; Hamosh, 1984; Moreau *et al.*, 1988b; Moreau *et al.*, 1988a). The rat lingual lipase has identical gene structure and physiological function to gastric lipase, albeit secreted in the oral cavity (DeNigris *et al.*, 1988; Lohse *et al.*, 1997), and they belong to the same family of preduodenal lipases. Preduodenal lipases have been identified in various species from the tongue to the pylorus (Moreau *et al.*, 1988b; Moreau *et al.*, 1988a; Moreau *et al.*, 1989), and this has been possible in humans through organ donors (Moreau *et al.*, 1988a). In each of the species tested, the preduodenal lipase activity was found to be mainly associated with a single tissue, which was located either in the lingual (rat and mouse), pharyngeal (calf, lamb and sheep) or gastric region (humans, cat, rabbit, dog, monkey, horse, pig and guinea pig). Concerning the secretion of lipase in the upper GIT, an extremely high level of lipase activity (> 100 µmoles of FFA released per min per mL) was measured in human gastric juice (Ville *et al.*, 2002), whereas no such levels of activity have been measured so far in human saliva (Kulkarni and Mattes, 2014; Stewart *et al.*, 2010). In line with this, human preduodenal lipase has been purified only from gastric juice (Tiruppathi and Balasubramanian, 1982). Human gastric lipase was detected in the chief cells of the gastric mucosa, using antibodies raised against the lipase purified from gastric juice (Moreau *et al.*, 1989). No data of this kind are available for human lingual lipase. As far as human preduodenal lipase gene expression is concerned, the mRNA was detected only in the gastric mucosa (Bodmer *et al.*, 1987) while the homologous mRNA of rat lingual lipase is found in the tongue (Docherty *et al.*, 1985). Consequently, the debate on the existence of a lingual lipase in humans is not supported by strong experimental data in contrast with the accumulation of evidence obtained for gastric lipase.

7.1.2 Almond cells

Figure 7.1 illustrates the structure of the almond cells within the tissue. The almond cells have an average diameter of about 35 µm (between 20 and 50 µm) and are surrounded by a CW (about 0.1 µm thickness). The cells are tightly bound together within the cotyledon matrix, and when in solution (e.g. separated) they have a globular conical shape (Figure 7.2). Separated cells in almonds do not exist naturally but they are a valuable tool for investigating the mechanisms behind lipid digestion in almond tissue.

CWs are made of complex heterogeneous networks of cellulose, hemicelluloses and pectic substances (see *Chapter 1*). The combination of cellulose microfibrils, cross-linking glycan and pectin network provides strength and rigidity to the CW. Indeed, in type I CW such as in almond cells, the cellulose-xyloglucan framework is embedded within the pectin matrix, which regulates the porosity of the CW (Carpita and Gibeaut, 1993). It is therefore likely that the access to the substrate (lipids) by lipases will be hindered by the CW when the latter is still intact. It can be anticipated that the rate and extent of lipid digestion will be reduced in intact cells compared with readily available lipid (i.e. OBs or emulsion).

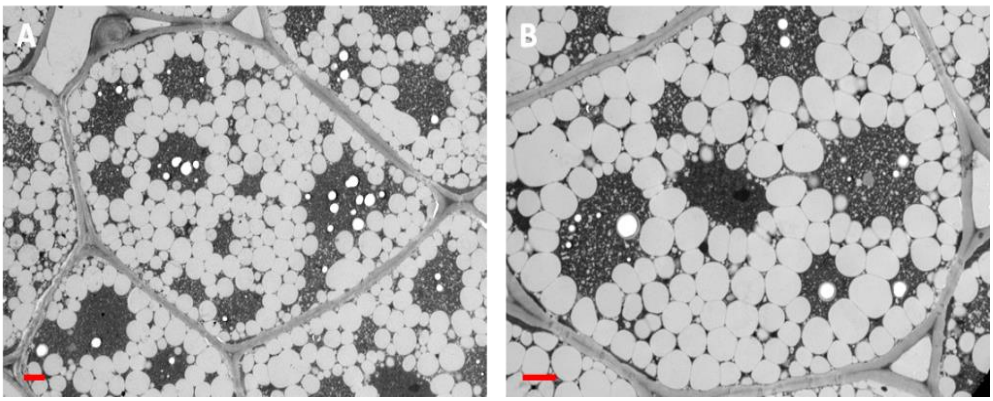

Figure 7.1 TEM images of almond seed showing oil bodies (white inclusions), scale bars = 2 µm.

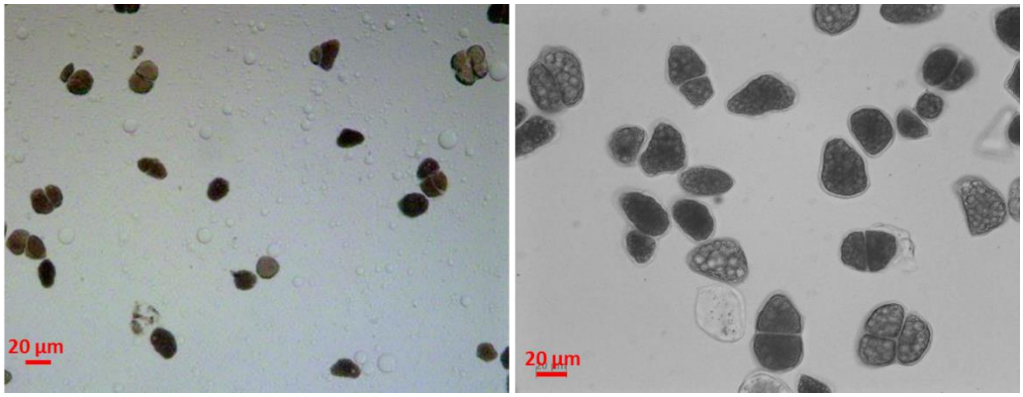

Figure 7.2 LM images of separated almond cells.

7.1.3 Oil bodies

Almond, similarly to other plant seeds, stores its lipids as TAG in OBs until they are eventually mobilised upon seed germination (Figure 7.1). The TAGs constitute about 94 to 98% of OBs total dry weight (Beisson *et al.*, 2001b; Huang, 1994). OBs are small, spherical organelles enclosed in a monolayer of phospholipids into which unique proteins, mainly oleosins, are embedded (Figure 7.3). Oleosins represent between 1 to 4% of the mass of OBs; caleosins and steroleosins are also proteins specific to OBs, the latter being an enzyme (Purkrtova *et al.*, 2008). Oleosins are proteins of low MW (15 to 26 kDa) with high isoelectric point that are predicted to contain three structural domains: (i) an amphipathic N-terminal domain (6 to 68 residues), (ii) a central hydrophobic domain (72 residues), and (iii) an amphipathic C-terminal domain that may adopt an α-helical structure (28 to 1000 residues) (Hsieh and Huang, 2004; Huang, 1994). The first domain varies significantly between species and it is located at the surface of the oil body (Figure 7.4 B). Due to its unusual and extremely high content of hydrophobic amino acid residues, the central domain might be positioned within the TAG matrix whereas the last domain might interact with the phospholipid layer. Oleosins maintain the integrity of the OBs by forming a stable amphipathic layer (prevent steric hindrance and electronegative repulsion) with the phospholipids and thereby prevent coalescence and

aggregation of the OBs during desiccation. They also act as a recognition signal for lipase during germination and may contain a lipase binding site (Huang, 1992).

Because of the presence of phospholipids on the surface of the OBs, the rate of the lipolysis by digestive lipases is expected to be reduced compared to that of TAG emulsions (Beisson *et al.*, 2001a). Phospholipids are fundamental for the stability of OBs, which is likely to make it more difficult for the pancreatic lipase to have access to its substrate (TAG), as observed with lecithin-stabilized emulsions (Gargouri *et al.*, 1986a).

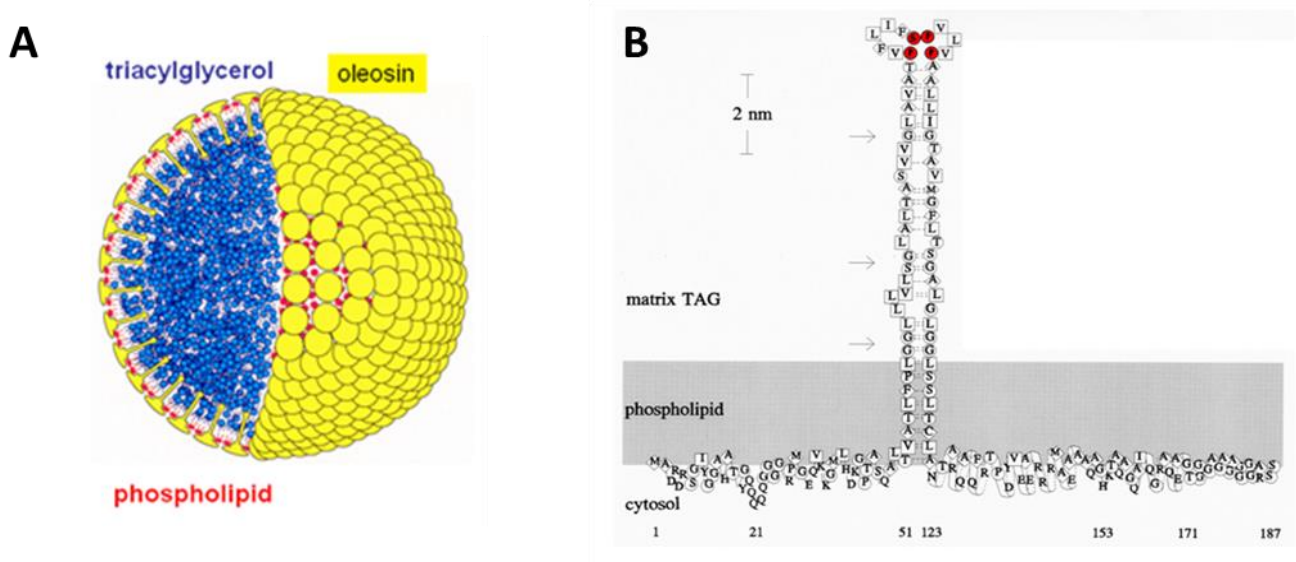

Figure 7.3 Model of an oil body (A) and the structure of oleosin (B) from maize (Huang, 1994).

There is a huge gap in knowledge regarding the diffusion of digestive enzymes, including lipases, across CW. The specific mode of action of the enzyme, especially the difference in water solubility between the lipase and its substrate, and the change in the lipase conformation occurring during lipolysis, makes lipase activity difficult to study. The approach that was used in this work permitted various problems to be overcome by directly (lipase localisation) and indirectly (kinetic studies) determine if digestive enzymes could penetrate the CW or not.

7.2 Aims

This part of the project was performed in collaboration with Dr David Gray from the University of Nottingham (OBs preparation and characterisation), Prof Frédéric Carrière from EIPL in Marseille (kinetic work using various lipases), and Drs Alan Mackie and Balazs Bajka from the IFR (localisation of lipase within almond substrate).

The exact mechanism of TAG hydrolysis by lipases, in almond tissue, is far from being fully understood. Hypothetically, the complete digestion of nutrients held within **intact cells** relies on the following three steps: diffusion of the enzymes into the plant cells, hydrolysis of substrate inside cells and diffusion of hydrolysed products out of cells so they can be absorbed in the enterocytes.

The main objective of this particular piece of work was to provide further evidence on whether or not the limited lipid digestion observed in almond cells was due to the CW and/or to the structure of the OBs themselves. We investigated the potential diffusion of various digestive lipases through almond CWs and determined the rate and extent of lipid digestion. To address these questions, the following methodology was implemented:

(a) The main lipolytic enzymes found in the GIT were tested (gastric lipase, pancreatic lipase and colipase, pancreatic lipase-related protein 2), alone or in combination to simulate *in vitro* gastric and intestinal phases of digestion;

(b) Kinetic studies to measure the release of lipolysis products from almond cells, as well as from purified almond OBs used as controls. Lipids were extracted after 1 h of incubation and analysed by TLC and GLC analysis. The kinetics of almond cell and OB (crude and washed) lipolysis was also investigated using the pH-stat technique. By comparing the extent of hydrolysis between encapsulated (almond cells) and accessible lipid bodies (OBs), it was possible to obtain a better insight of the role of CWs in nutrient digestion; and

(c) Microstructural analysis using confocal microscopy was performed to localise the pancreatic lipase within the almond matrices (cells and OBs) and verify the integrity of the OBs.

A detailed characterisation of the OBs was performed in order to highlight any component that could have a major impact on lipase activity. For instance, the lipolysis rate was expected to be reduced when TAGs are within these organelles due to the presence of proteins and phospholipids on their surface (Beisson *et al.*, 2001a). It was therefore anticipated that the greatest lipolysis rate would be obtained on OBs with the following mixture of enzymes: protease from pancreatic extract (degradation of proteins – oleosins), phospholipase (degradation of the monolayer of phospholipids) and lipase (degradation of TAGs).

7.3 Materials and methods

7.3.1 Samples preparation and characterisation

Cells and OBs from raw and roasted almonds were prepared as described in detail in *Chapter 2*. The crude OBs then obtained were washed, either using 9 M urea or 0.1 M $NaHCO_3$, in order to remove cell debris and proteins. To assess the affinity of the protein to the lipid phase of the OBs, total protein was measured in both crude and washed preparations. Mild treatment such as 0.1 M $NaHCO_3$, removed the extrinsic proteins (storage proteins) from the surface of the OBs while preserving their secondary structures, whereas a strong chaotropic agent (i.e. 9 M urea) denatured the proteins by destabilizing internal, non-covalent bonds (Huang, 1996).

7.3.1.1 Compositional analysis of OBs

OBs were analysed for moisture, total lipid as well as fatty acid and phospholipids composition; the details of these methods are found in *Chapter 2* (*Section 2.3.1*). Protein content and composition were determined by the BCA method and SDS-page (see *Section 2.3.1.3*).

7.3.1.2 Particle size distribution and ζ-potential measurements

OB suspensions were formulated by dispersing the preparation into water (10% oil, w/w). The average size of the OBs was measured using a Beckman Coulter LS13320® and their zeta potential (ζ-potential) with a Beckman Coulter Delsa™Nano C (Beckman Coulter Ltd, High Wycombe, UK).

Zeta-potential is the measure, in mV, of the electrical charge at the interface of the particle (Beckman Coulter, High Wycombe, UK). More precisely, the ζ-potential is the electrical potential that exists at the hydrodynamic plane of shear (slipping plane) (Figure 7.4). As a result, it gives an indication of the degree of repulsion between particles in a colloidal suspension or the dispersion stability. The higher the ζ-potential the more stable the dispersion: particles with high ζ-potential will repel each other (± 30 mV), whereas those with low ζ-potential will attract each other which can lead to aggregation or flocculation.

The sample was placed into the flow cell using syringes, and then a laser beam illuminated the cell. The electrophoretic mobility of the particles was measured using Laser Doppler Anemometry (LDA). Any charged particle moved toward an electrode of opposite surface charge. The light, scattered by the particles, is shifted from the incident light (laser) at a frequency that is proportional to the velocity of the particles movement. The ζ-potential is then obtained using the Smoluchowski equation (Sze *et al.*, 2003):

$$\zeta = \frac{\eta \nu}{\varepsilon_0 \varepsilon_d} \qquad \text{(Eq. 7.1)}$$

where η is the dispersant viscosity, v the particle velocity, ε_0 dielectric constant *in vacuo* and ε_d dielectric constant of the dispersant.

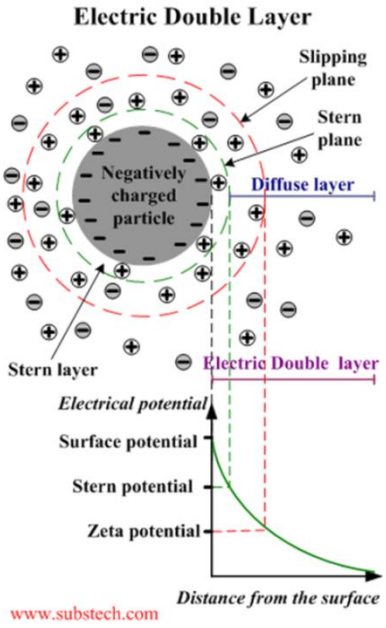

Figure 7.4 Illustration of the electrical double layer of a negatively charged particle. The ζ-potential is the electrical potential at the slipping plane.

The measurements were performed at 25°C with a dispersant (water) refractive index of 1.330, viscosity of 0.891 mPa·s, and relative dielectric constant of 79.0. The electrode spacing was 50.0 mm. The ζ-potential was calculated by the instrument Software based on the Smoluchowski equation (Eq. 7.1). Each measurement was reported as the mean of three readings.

7.3.2 Lipolysis of almond lipids

The enzymes used for the experiments were provided by Prof Carrière, and were as follows (assay conditions described in *Section 2.4.2.1*):

-**RGE**: lipase SA of 77 U/mg of powder on tributyrin at pH 5.5, corresponding to 62 % w/w of lipase per milligram of powder,

-**PPE**: lipase SA of about 464 U/mg of powder on tributyrin at pH 8, corresponding to 5.8 % w/w of lipase per milligram of powder,

-**PPL**: purified enzyme with lipase SA of about 1000 U/mg of protein on tributyrin at pH 8,

-**GPLRP2** acts on galactolipids, monoglycerides, and phospholipids (phospholipase A1 activity). SA of about 1700 U/mg of protein on tributyrin and 500 U/mg of protein on egg lecithin.

7.3.2.1 Analysis by chromatography of in vitro gastrointestinal digestions

Almond materials were added into Eppendorf tubes for a weight equivalent to 50 mg of lipids, which corresponded to about 120 mg of cell preparation and 50 mg of OBs. Each reaction system had a volume of 1 mL and was left incubating for 1 h at 37°C. The buffer consisted of either 10 mM MES (i.e. gastric phase) or Tris (duodenal and gastric and duodenal phases) containing 150 mM of NaCl. BS were omitted in these experiments and permitted to highlight the inhibition effect of the lipolytic products. The reactions were performed using RGE (1 mg/mL) and PPE (20 mg/mL), alone and in combination, as well as PPL (1 mg/mL) with colipase (added at a 2 to 1 excess molar ratio). GPLRP2 (2.3 mg/mL, on OBs only) was also used in conditions identical to the duodenal phase. After incubation, the lipids were extracted then separated and quantified by either GLC or TLC as outlined in *Section 2.3.1.2*.

7.3.2.2 Assays of lipase activity with the pH-stat technique

The extent and rate of lipolysis (method in *Chapter 5*) and the SA of the lipases on almond materials were measured using the pH-stat technique. The reaction system for SA measurements is outlined in

Table 7.1. Back titrations were performed for assaying the activity of gastric lipase (RGE) at acidic pH. NaTDC was used in these experiments instead of the mixture of NaTC and NaGDC used in *Chapters 4 and 6* as these BS tend to precipitate at acidic pH.

Table 7.1 Experimental conditions for lipase assays with the different enzymes.

	RGE	**PPE**	**PPL + colipase**
Enzyme concentration (mg/mL)	10	20	1 + 1
Enzyme volume used for the assay (µL)	10	10	10 + 50
Assay solution composition		Tris 1 mM	Tris 1 mM
	NaCl 150 mM	NaCl 150 mM	NaCl 150 mM
	BSA 0.1 g/L	$CaCl_2$ 5 mM	$CaCl_2$ 5 mM
	NaTDC 2 mM	NaTDC 4 mM	NaTDC 4 mM
Assay solution volume (mL)	15	15	15
Substrate/lipids (mg)	100	100	100
pH	5.5	8	8

7.3.3 Penetration of pancreatic lipase inside the cellular compartment

7.3.3.1 Preliminary work using FITC labelled dextran

Raw and roasted separated almond cells were incubated with fluorescein isothiocyanate (FITC, Sigma, No FD-20 and No FD-40) labelled dextran of MW 20 and 40 kDa (radius of gyration, R_g ~34 and ~50 Å, respectively) (Andrieux *et al.*, 2002). The diffusion of the molecules was observed with an optical Zeiss Axioskop 2 mot plus microscope using the Zeiss Filter Set 10 (excitation around 450-490 nm and emission around 515 to 585 nm).

7.3.3.2 Pancreatic lipase diffusion

This work was done in collaboration with the IFR (Drs Alan Mackie and Balazs Bajka). Pancreatic lipase was separated and purified from porcine extract (type II from sigma, # L3126) using

concanavalin A-sepharose (sigma, #C9017). The enzyme was purified/desalted using a Centripure P25 desalting column (Generon, # GEN-CP-0108-25). This step permitted the dispersing solution to be changed from Tris buffer to phosphate buffered saline (PBS buffer). The purified lipase was then labelled with Alexa Fluor 488 nm (Life Technologies™, # A10235) as described by the manufacturer.

The labelling molecules of Alexa Fluor 488 are low MW (~855 Da) carboxylic acids containing TFP (tetrafluorophenyl) esters moieties. They bind to primary amide ($R'NH_2$) in proteins to produce conjugates with excitation/emission of 495/515 nm. Because of its low MW, the increase in the size of the labelled enzyme compared with the lipase alone is negligible.

SA of the labelled lipase was performed by Neil Rigby from the IFR according to the protocol in *Section 2.4.2.1* and was found to be 289 U/mg, which means that the enzyme retained about 25% of its activity after labelling. The protein concentration of the lipase was 0.76 mg/mL (determined using the BCA assay). Finally, the bound and eluted protein fraction was examined by SDS-PAGE on a 10% BisTris gel run in MES buffer under reducing conditions (Figure 7.5).

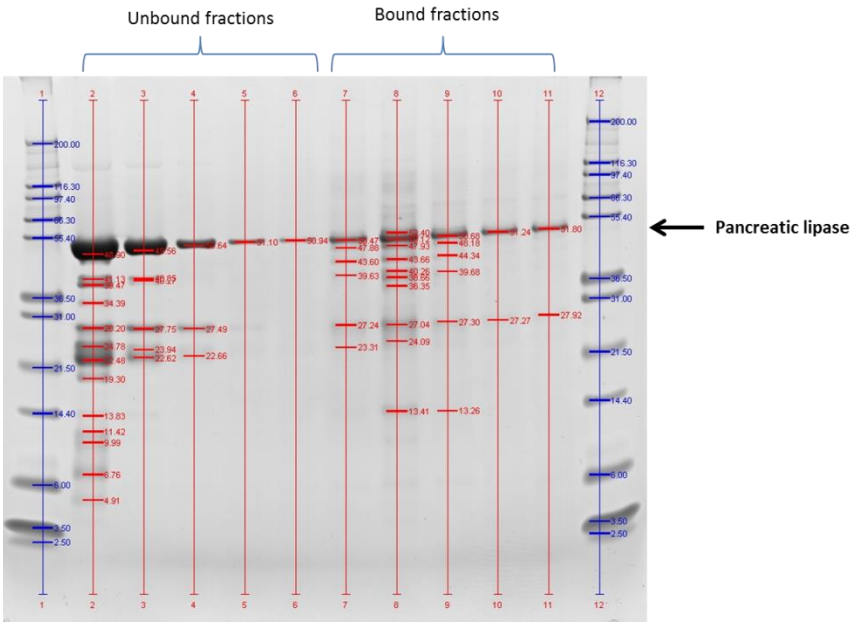

Figure 7.5 Protein composition of unlabelled (unbound fractions) and labelled (bound fractions) lipase type II (SDS-page provided by Neil Rigby from Alan Mackie's group at the IFR).

The reaction environment contained 25 µL of diluted (1/10 in BS solution) cell or OB preparation, 1 µL of Nile red solution (saturated in polyethylene glycol), 1 µL of calcofluor white (2% w/v in deionised water), 25 µL of labelled lipase (0.76 mg/mL) and 4 µL of colipase (1 mg/mL). Aliquots were taken at different time points (0, 30, 60 and 120 min, and ~20 h of digestion) and visualised using a confocal microscope.

7.4 Results

7.4.1 Characterisation of the OBs

7.4.1.1 Particle size distribution and ζ-potential measurements

The PSDs of almond OBs are shown in Figure 7.6. The average diameter of the OBs was significantly different ($P < 0.005$) between raw and roasted almonds: 2.6 ± 0.09 ($d_{3,2}$ = 2.0 ± 0.07 µm) and 3.8 ± 0.11 ($d_{3,2}$ = 2.4 ± 0.08 µm) µm, respectively. This is in agreement with the data from other groups (Beisson *et al.*, 2001a; Gallier *et al.*, 2012) as well as the microscopy images that illustrated OBs with sizes between 0.5 and 5 µm (Figure 7.1). OBs washed with urea had an average size of 7.6 ± 0.45 µm ($d_{3,2}$ = 3.6 ± 0.07 µm) and the ones washed with $NaHCO_3$ 6.0 ± 0.28 µm ($d_{3,2}$ = 3.0 ± 0.35 µm). The significant increase ($P < 0.001$) in particle size for these two OB preparations compared to the crude OBs is likely to have been caused by loss in OB integrity (i.e. dispersion and coalescence) following the washing process.

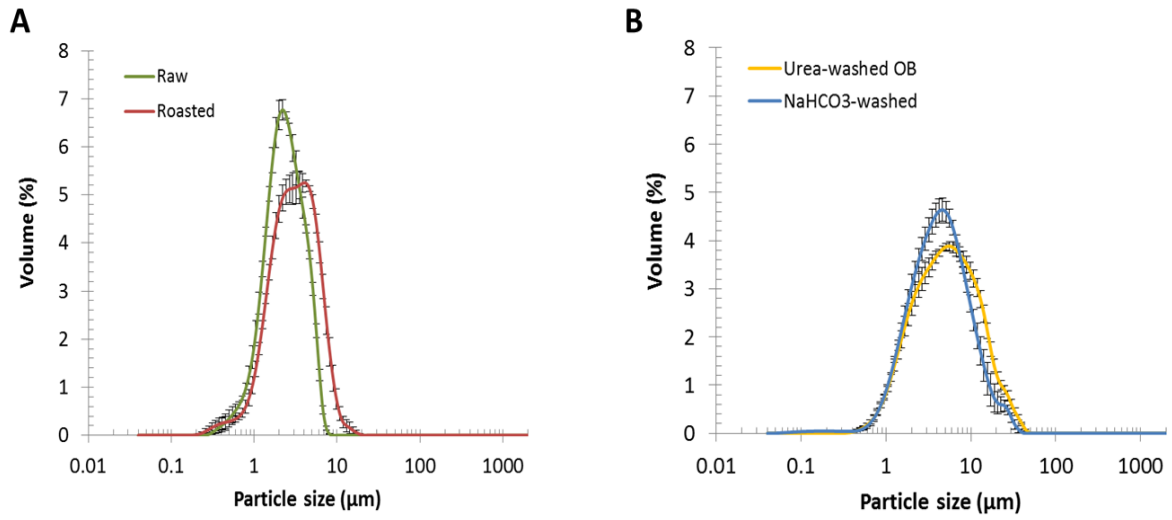

Figure 7.6 Particle size distribution of raw and roasted almond OBs (A) and raw almond OBs washed with urea or sodium bicarbonate (B) (n=3, means ± SEM).

The ζ-potential of raw, roasted, urea-washed and $NaHCO_3$-washed almond OBs were -33.7 ± 1.54, -27.7 ± 1.32, -31.7 ± 1.04 and -34.5 ± 2.61 mV, respectively. The crude OB values are in agreement with previous work (Bonsegna *et al.*, 2011; Gallier *et al.*, 2012). The structure of the OB interface (anionic phospholipids and protein molecules) is responsible for the negative surface charges obtained which prevent coalescence of the OBs. The ζ-potential values confirmed that raw almond OBs, similarly to OBs found in other seeds, are stable even in isolated preparations. On the other hand, roasted and washed almond OBs tend to aggregate and coalesce as demonstrated notably by the variability in their particle size. The roasting process presumably disturbed the proteins embedded in the phospholipid layer thus compromising the OBs stability.

7.4.1.2 Lipid composition

Crude lipid analyses indicated that OBs contained between 85 and 94% of lipid depending on the preparation, but the differences observed were not statistically significant (Table 7.2). A non-

negligible fraction of the total weight could not be identified (contamination by cell debris such as polysaccharides form the CW) as previously noticed (Makkhun, 2012). This unidentified mass could also have contained some of the degradation products formed from the OBs by the seed, between harvest and pasteurisation, to generate energy as sugars, amino acids (mainly asparagine, aspartate, glutamine and glutamate) and carbon chains required for embryonic growth (more details in *Sections 7.4.2.1 and 7.4.2.2*) (Barros *et al.*, 2010).

Table 7.2 Total lipid and protein content of crude and washed OBs.

OB type	Total lipid (% dry wt basis)[1]	Protein (% dry wt basis)[1]	Unidentified mass (% dry wt basis)[1]
Crude raw almond	89.3 ± 2.00	5.8 ± 0.70	4.9
Crude roasted almond	85.1 ± 1.54	5.3 ± 1.39	9.7
Raw almond urea-washed	90.5 ± 2.06	0.6 ± 0.09	8.9
Raw almond $NaHC0_3$-washed	94.4 ± 3.60	1.5 ± 0.29	4.1

[1]Values are presented as means ± SEM (n=3). Wt: weight.

The membrane of OBs contained principally phosphatidylcholine (PC, 50-60%), phosphatidylserine (20-30%), phosphatidylethanolamine (PE), phosphatidylinositol (PI), and phosphatidic acid (PA) (David *et al.*, 2013). The phospholipids previously found in almond OBs are PC (60%), PI (25%), PE (12%), and PA (3%) (Beisson *et al.*, 2001a). These four phospholipids were similarly identified only in the raw almond OBs (Figure 7.7). Roasted almond OBs appear to be lacking some of the phospholipids species, including PA. In a similar way to the embedded proteins (see *Section 7.4.1.3*), phospholipid composition appeared to have been affected by the roasting process. The presence of PA could be due to the enzymic degradation of phospholipids by phospholipases D occurring prior to almond pasteurisation (Gallier *et al.*, 2012) similar to TAGs degradation (*Section 7.4.2.1*). The roasting process might have inactivated the phospholipase D and thus protected phospholipids from degradation. The deleterious effect of endogeneous phospholipase D on phospholipid composition is

a well-known phenomenon occurring in the course of oil seed production and refining (Kovari, 2004).

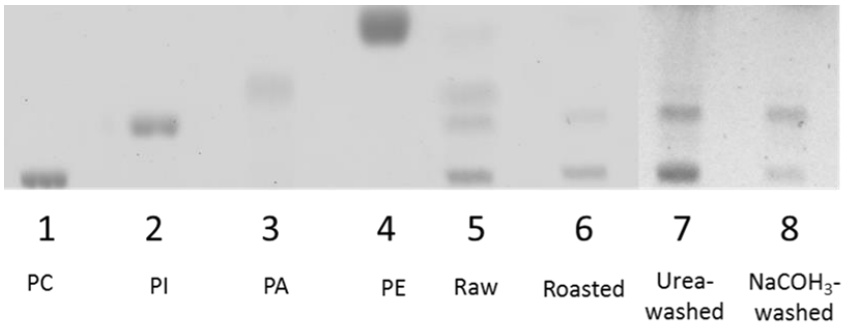

Figure 7.7 TLC analysis of phospholipids from raw and roasted almond OBs.

7.4.1.3 Protein composition

As expected, the protein content of raw almond OBs decreased significantly ($P < 0.05$) between the crude and washed preparations (Table 7.3). The proteins were a mixture of intrinsic proteins (i.e oleosins) and proteins originating from the degradation of the protein bodies during milling of the almonds. Other authors have also reported that OB preparations can be contaminated extensively by storage proteins due to electrostatic interactions (Jolivet *et al.*, 2004). Washing however removed most of these extrinsic proteins (Figure 7.8).

The proteins present in the crude OBs had MW of 15, 23, 35, 38 and 40 kDa. The gel patterns were very similar to the ones obtained in other studies (Beisson *et al.*, 2001b; Gallier *et al.*, 2012). The proteins with the largest MW are identified as amandine which is the major storage protein found in almond (Sathe *et al.*, 2002). Amandin (62 to 66 kDa) consists of two polypeptides, a basic β-chain of MW ranging from 20 to 22 kDa and an acidic α-chain of MW between 40 and 42 kDa. The treatment of the samples with β-mercaptoethanol cleaved the disulphide bonds found in amandine and destroyed the oligomeric form of the protein. The proteins with a MW of 15 kDa are likely to be

oleosins, only one isoform of the molecule could be distinctly seen. It could also be plausible that some of the proteins were degraded by endogenous proteases prior to the almond pasteurisation in the same way as what we observed with lipids (*Sections 7.4.1.2 and 7.4.2.1*).

Proteins with similar MW (so presumably they are likely to be identical) were found in raw and roasted almonds, but, as expected, most of the storage proteins were removed by the washing (Figure 7.8). It is possible that the OBs were in fact hybrid oil droplets stabilised by extrinsic proteins which may explain the larger OBs obtained after washing (Makkhun, 2012).

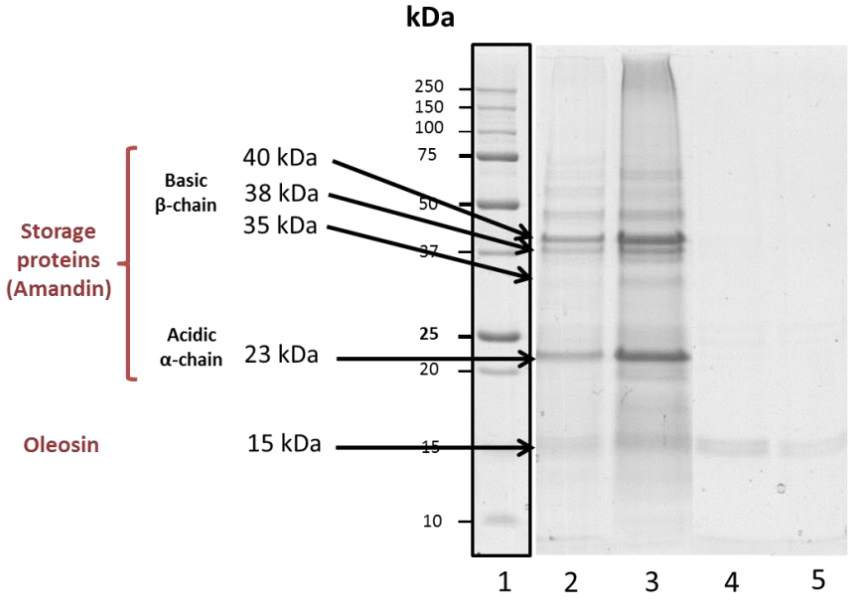

Figure 7.8 Protein composition of oil bodies. Lane 1 M_w marker, lane 2 crude raw almond, lane 3 crude roasted almond, lane 4 urea-washed raw almond, and lane 5 $NaHCO_3$-washed raw almond.

7.4.2 Lipolysis of almond lipids

7.4.2.1 Identification of endogenous lipase activity

Analysis of neutral lipids was performed by TLC of blanched (native almonds placed in boiling water for 15 min) versus native almonds after incubation in Tris buffer (*composition described in Table 7.2*). The TLC plate revealed the presence of lipolysis products (1,3- and 1,2-DAG, MAG and FFA) as well as

TAG in absence of any gastric and pancreatic lipases (Figure 7.9) for both blanched and unblanched almonds. These results indicated that between the harvest and the pasteurisation of the almonds, endogenous lipase digested part of the TAG. This phenomenon has previously been detected (Beisson *et al.*, 2001a). TLC analysis of phospholipids (Figure 7.7) also suggests the presence of endogeneous phospholipase D as identified in another work (Gallier *et al.*, 2012).

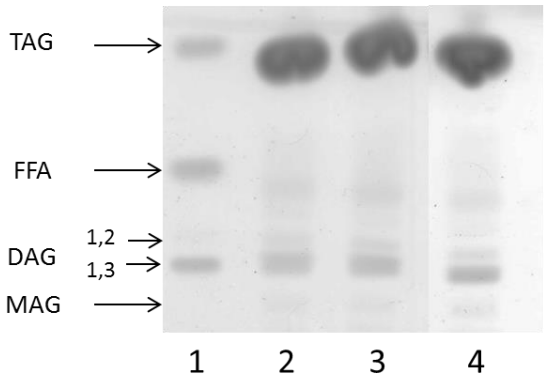

Figure 7.9 TLC analysis of neutral lipids present in blanched and native raw almond milk. Lane 1, neutral lipid standards; lane 2, blanched almonds; lanes 3 and 4, native almonds at 0 and 60 min.

7.4.2.2 Analysis by chromatography of in vitro gastrointestinal digestions

Figure 7.10 illustrates the extent of digestion for almond OBs and cells by gastric and pancreatic lipases. The TLC-densitometry method permitted the identification and quantification of both TAG and lipolytic products (Table 7.3). 1,3-DAG should not have been visible in these samples since pancreatic and gastric lipases preferentially hydrolyse ester bonds located at *sn*-1 and *sn*-3 positions. Pancreatic lipase has a strict regioselectivity for these positions (Constantin *et al.*, 1960). Gastric lipase can potentially cleave the ester bond at sn-2 position (Carriere *et al.*, 1991) but this is never observed before other esters bonds are cleaved (Rodriguez *et al.*, 2008). Therefore, in compliance with the results from Figure 7.9, this implies TAG hydrolysis catalysed by almond seed's endogenous lipase(s) is non-regiospecific (Barros *et al.*, 2010) or that some isomerisation of 1,2-DAG in 1,3-DAG may have occurred after enzymic lipolysis.

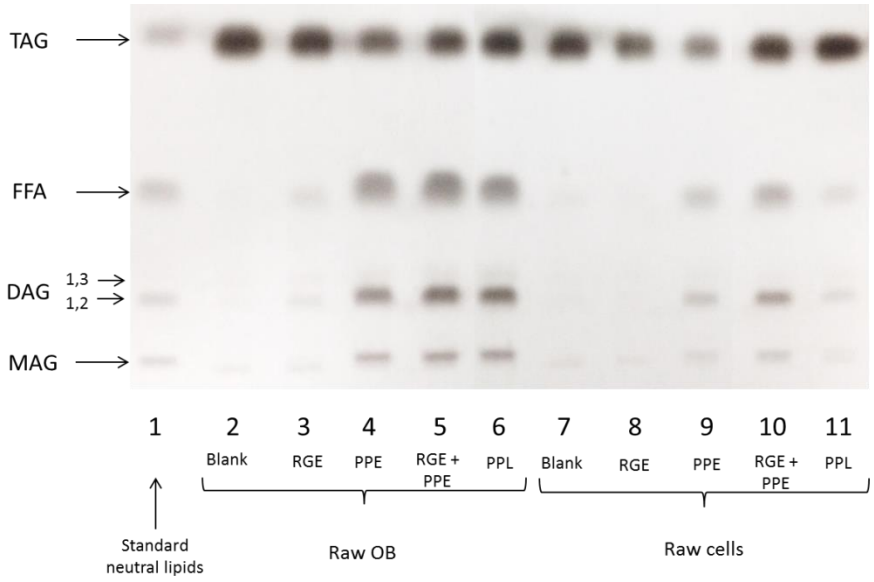

Figure 7.10 TLC analysis of digested raw almond oil bodies and cells with various enzymes.

Table 7.3 Quantitative data of the TLC plate obtained by densitometry following 1 h incubation of the raw almond samples, OBs and cells (mean of duplicates).

		TAG (µmol)	DAG (µmol)	MAG (µmol)	FFA (µmol)	Hydrolysis % (FFA vs total acyl chains)
OBs	*Blank*	14.06	0.31	0.41	1.23	**2.8%**
	RGE	13.03	0.63	0.86	3.38	**7.6%**
	PPE	7.16	2.28	6.42	12.38	**27.6%**
	PPL	8.17	2.00	4.77	11.98	**26.5%**
Cells	*Blank*	7.14	0.21	0.3	1.04	**4.5%**
	RGE	5.92	0.21	0.67	1.17	**5.8%**
	PPE	4.9	0.59	0.91	3.84	**18.6%**
	PPL	5.24	0.66	0.74	3.08	**14.8%**

The lipid digestion appeared more limited for separated cells than OBs and this regardless of the enzyme preparation used, i.e. average of ~34% decrease in FFA release for cells relative to the OBs. The samples incubated with RGE and PPE were digested to a greater extent than PPE alone. Also, lipolysis occurred in a more significant manner in presence of PPE than pancreatic lipase (PPL) alone. Given that the extract contains a mixture of different enzymes (i.e. PPL, CEH, proteases and phospholipase A2, see *Figure 2.10*), most probably, degradation of oleosins and phospholipids on

the surface of OBs occurred, which permitted better access of the PPL to its substrate (TAG). Phospholipase activities were indeed clearly seen for both GPLRP2 and PPE as illustrated by the loss in intensity of the phospholipid bands, especially for the washed OBs, in the TLC plates in Figure 7.11. A synergistic action of lipolytic enzymes may have also increased the overall lipolysis rate.

As mentioned above, PA were absent only in the roasted almond OBs, suggesting that the roasting process may have degraded the phospholipase D probably still active in raw almonds. Due to the higher concentration of sample used, other species of phospholipids could be discerned which could correspond to phosphatidylglycerol, cardiolipin and/or N-acylphosphatidylethanolamine (Gallier *et al.*, 2012).

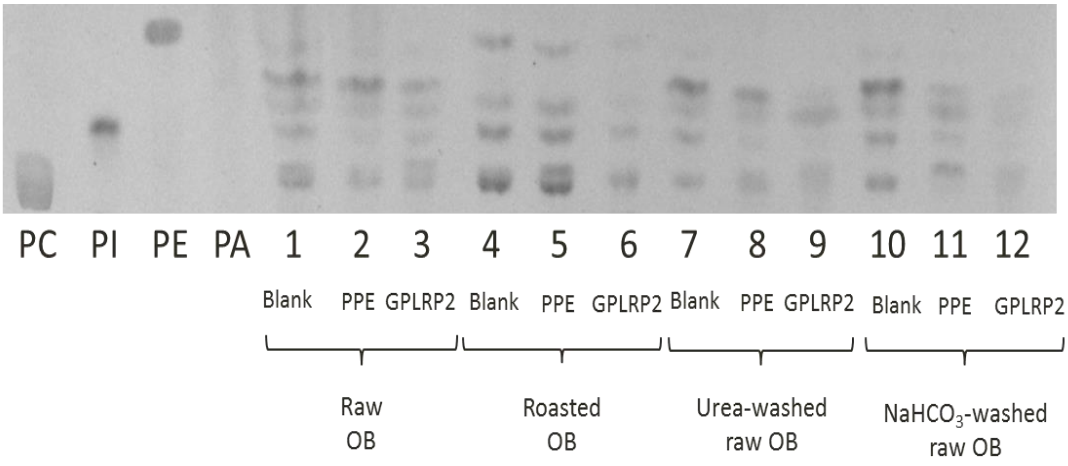

Figure 7.11 TLC analysis of phospholipids of raw almond OB, crude and digested with either PPE or GPLRP2.

The average level of lipolysis, analysed by GLC, was also greater for OBs and cells (27.4% and 12.8% for OBs and cells, respectively) when PPE was included in the reaction system (Figure 7.12). The washed OBs showed the greatest extent of digestion in particular when PPE and GPLRP2 were combined despite the product inhibition that occurred due to the absence of BS.

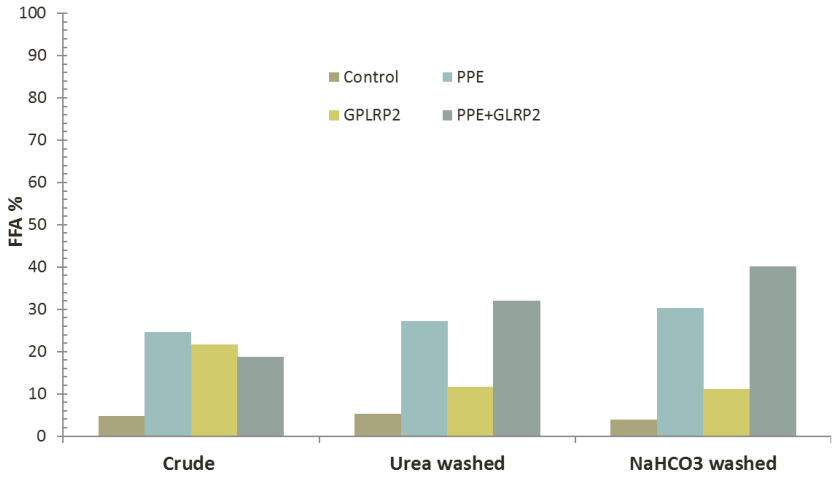

Figure 7.12 Percentage of residual FFA of almond OBs (crude, urea and $NaHCO_3$) determined by GLC analysis after 1 h duodenal digestion by PPE and GPLRP2, alone or in combination (mean of duplicates).

7.4.2.3 Assays of lipase activity with the pH-stat technique

The extent and rate of lipolysis in almond OBs and cells were measured with the pH-stat technique (Table 7.4). The amount of FFA released following 1 h of digestion as well as the initial reaction rate were similar between the different OB types. Lipolysis by HPL has been reported to be reduced with crude OBs when compared to almond oil emulsion (Beisson *et al.*, 2001b); however the protease and phospholipase contained in the PPE used in this investigation would have promoted TAG hydrolysis. The presence of the proteins on the surface of the OBs did not lead to alteration in lipid digestibility maybe because of the slight variability in lipase content between experiments which concealed any potential variations. Indeed, a large proportion of the PPE was insoluble and settled out; this was reflected by a slight fluctuation in lipase activity.

On the other hand, a marked decrease ($P < 0.05$) in FFA release (~67%) was recorded during cell digestion when compared with the FFA formed during the digestion of OBs.

Table 7.4 Percentage of FFA released (% of total fatty acids) and initial reaction rate (µmol/min) for lipolysis of almond OBs and cells with pancreatin.

		FFA (%) at 1h[1]	Initial reaction rate (µmol FFA/min)[1]
OBs	*Raw*	68.8 ± 2.64	71.3 ± 2.04
	Roasted	57.5 ± 6.15	66.0 ± 1.19
	$NaHCO_3$-washed	70.6 ± 7.58	61.9 ± 6.46
	Urea-washed	66.3 ± 1.79	61.3 ± 1.02
Cells	*Raw*	21.2 ± 1.59	36.5 ± 5.21
	Roasted	22.1 ± 2.04	42.5 ± 3.35

[1]Values are presented as means ± SEM (n=3).

For each enzyme the SA decreased as the complexity of the substrate increased: tributyrin > OBs > cells (Table 7.5). The same trend was observed for both raw and roasted almonds. The activity of the gastric lipase was not detected with almond cells.

Table 7.5 Specific activity of lipases on different materials in U/mg (mean of duplicates).

		Tributyrin	Raw OBs	Raw cells	Roasted OBs	Roasted cells
RGE	*mg of powder*	76.5	0.79	ND	1.05	ND
PPE	*mg of powder*	464	65	2.8	51	2.5
	mg of protein	8000	1121	48.5	873	43.1
PPL + colipase	*mg of powder*	10000	1388	113	1550	94

ND: not determined.

7.4.3 Penetration of pancreatic lipase inside the cellular compartment

7.4.3.1 Preliminary work using FITC labelled dextran

Figure 7.13 shows the diffusion of 20 kDa dextran (Rg ~34 Å) inside the cells for both raw and roasted almond but this did not occur when using 40 kDa dextran (Rg ~50 Å). It is therefore presumed, that lipases should not be able to penetrate the CW of the almond cells (MW ~50 kDa), however, MW

alone is not sufficient to characterise the size of a biopolymer. Indeed, other information such as shape, charge (pH environment) and behaviour in solution are necessary. Therefore further experiments were carried out using fluorescently labelled pancreatic lipase.

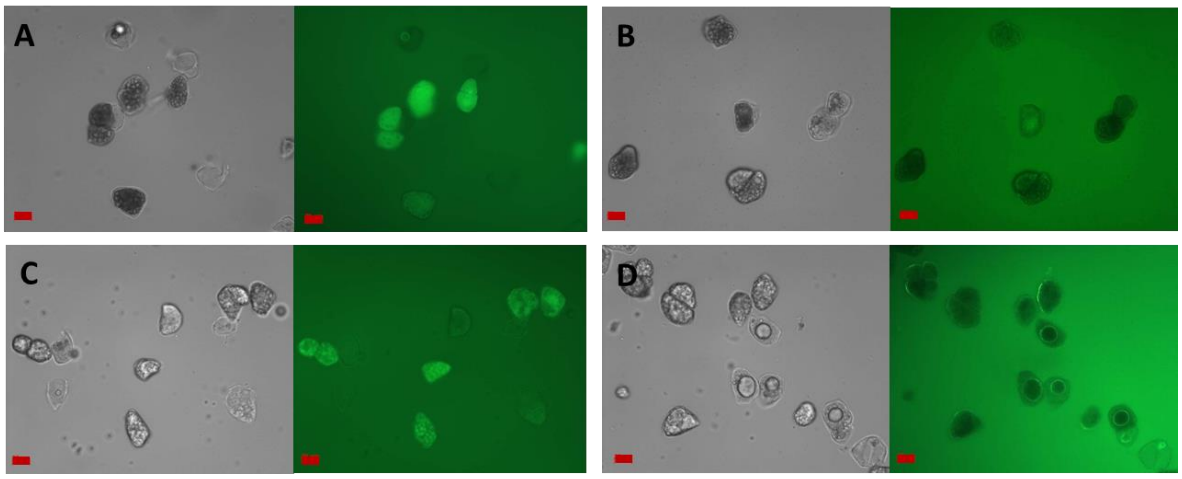

Figure 7.13 Micrographs of FITC-dextran permeation into separated raw (A and B) and roasted (C and D) almond cells. FITC-dextran molecular weights were 20 (A and C) or 40 (B and D) kDa. Grey (left): bright field, green (right): FITC-dextran under filtered light. Scale bars = 20 µm.

7.4.3.2 Pancreatic lipase diffusion

In Figure 7.14, clusters of labelled lipase were visible in the vicinity of the oil droplets. A reduction in the size of OBs confirmed that lipolysis took place. However, the incubation of almond cells, similar to the observations made in *Chapter 6*, revealed that their lipid content was still intact even after extended incubation time (Figure 7.15). One interesting observation is the uneven distribution of the labelled lipases between the intra- and extracellular environments, so that the bulk of green areas appeared in some, probably damaged, cells (Figure 7.16). The OBs inside these cells have lost their integrity which most likely occurred during the preparation of the separated cells. Unfortunately, it is virtually impossible to obtain a preparation devoid of any broken or fragmented cells; however the majority of the cells were intact as shown in Figure 7.15 H.

It is possible that the lipase binds preferentially to lipolytic products generated from the droplets and forms other types of aggregates after being released from the droplet. The apparent absence of lipase on free lipids could be due to the fact that only a small fraction of the lipase adsorbed to the interface as seen with various systems (e.g. monolayers)(Benarouche *et al.*, 2013).

BS are strong surfactants and could induce changes in the partitioning of the lipase between the aqueous phase and the interface (i.e. competition for the interface) (Delorme *et al.*, 2011). Lipase could also move from bulk phase to the interface and back with rapid adsorption-desorption from the interface (Haiker *et al.*, 2004).

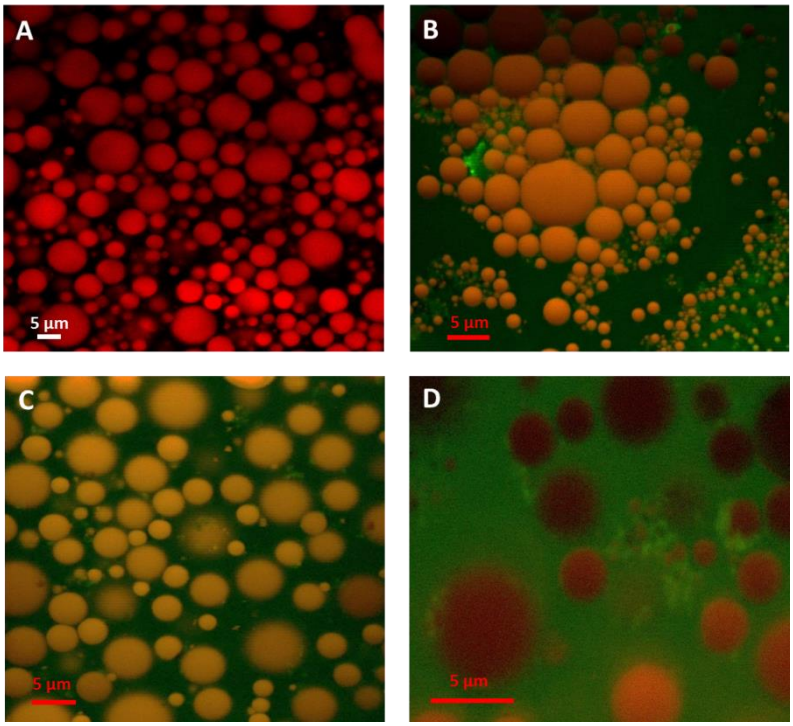

Figure 7.14 CLSM images of crude raw almond OBs stained with Nile red (A) and in presence of labelled pancreatic lipase (green) after 30 min incubation (B, C and D). Scale bars: A-D = 5 µm.

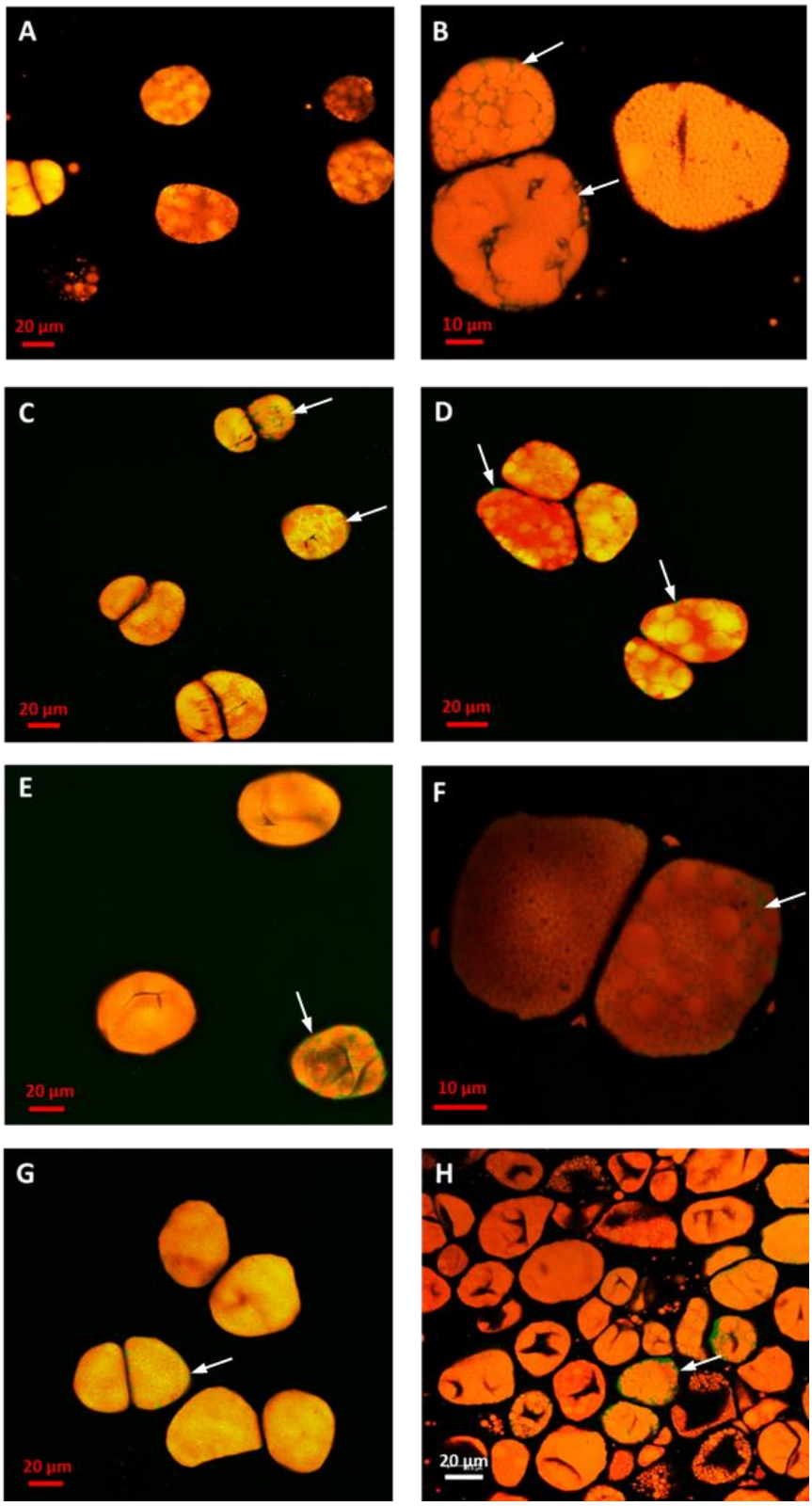

Figure 7.15 CLSM images of raw almond cells stained with Nile red (B) and in presence of labelled pancreatic lipase at baseline (A), 0 min (B), 30 min (C), 1 h (D) 1 h 30 (E), 2 h (F), 3 h (G) and 20 h (H) of incubation. The areas coloured in green, where the lipase diffused inside the cell, are indicated by the white arrows. Scale bars: A, C, D, E, G and H = 20 µm; B and F = 10 µm.

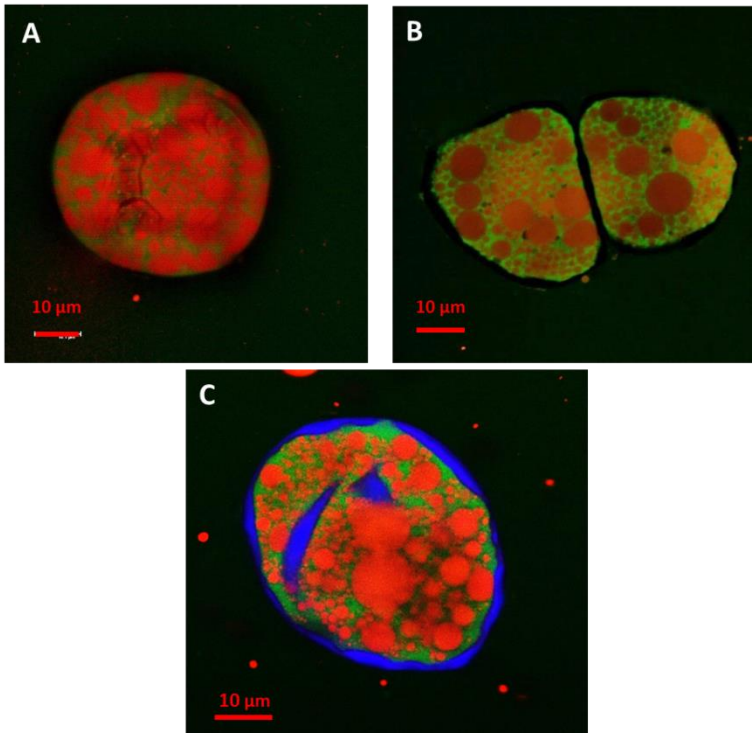

Figure 7.16 CLSM images of raw almond cells after 1 h incubation showing the diffusion of lipase through the CW. Lipids are stained in red and labelled lipase appears in green. In image C, the CW was stained in blue with calcofluor white. Scale bars: A, B and C = 10 µm.

7.5 Discussion

Lipids contained within a food are released at different stages of the digestion process to form lipid droplets. However, for plant foods such as seeds and nuts, the majority of their content remains within the food matrix for a long period of time and are still present in the lower part of the GIT. As mentioned in *Chapter 5*, DF are able to inhibit lipid digestion in different ways either by binding to BS, interfering with the emulsification process, increasing the viscosity of intestinal content, and/or by interacting with lipase or lipase substrates (Gunness and Gidley, 2010; Lairon *et al.*, 2007a). On the other hand, intact plant CW appear to limit lipid digestibility by encapsulating the lipids and thus preventing digestive enzymes including lipase(s) having direct access to their substrate. In another study done by our group on 2 mm almond cubes (Mandalari *et al.*, 2008a), it was revealed that after

12 h of *in vivo* digestion the lipid content of undisturbed cells located 3 to 5 layers underneath the layer of fractured cells appeared to be leaching. Two hypotheses can arise from this observation:

-the **lipids** may have diffused out of the cells through the different layers to reach the extracellular environment where they were then hydrolysed by lipase

-or the **lipase** may have diffused through the different cell layers and CWs to degrade the TAGs inside the cell, the lipolytic products then diffusing out to the extracellular environment.

The almond CW is a complex matrix that reduces the accessibility of the lipase to the intracellular TAG and thus impairs hydrolysis as shown by the lessened lipid digestibility in cells compared with OBs and this occurs regardless of the mixture of enzymes or the measurement method used. If the TAG hydrolysis takes place in the intracellular compartment, the enzyme has to be able to penetrate the cell via 'pores' or following endocytosis. The size range of CW pores of different plants has been estimated to be between 35 to 52 Å (Carpita *et al.*, 1979). The polysaccharide network, and the cross-links between them affect the digestibility of the food, but also at a microscopic level the size of the pore (Fleischer *et al.*, 1999). Gastric and pancreatic lipases (50 kDa) have a R_g of about 16.7 and 19.0 Å, respectively (Peters *et al.*, 1996; Selvan *et al.*, 2010). This is below the pore size that could enable free diffusion of the lipase through the CW. Since FITC labelled dextran of 20 kDa (R_g of 34 Å) permeated through the CW, presumably lipases can also penetrate the cell. Moreover, an investigation made on alginate beads revealed that lipase could penetrate the beads and hydrolyse the lipids they contained (Li *et al.*, 2011b). However, the pore diameter of alginate beads has been estimated to be between 30 and 450 nm, much larger than lipases (Chan and Neufeld, 2009). Diffusion experiments revealed that dextran with a R_g of 34 Å penetrated the almond CW whereas dextran of 50 Å did not, so based on this R_g rather than MW, lipases could presumably freely diffuse inside the almond cell. Nevertheless, as explained in *Chapter 1*, pancreatic lipase on its own is not sufficient for the hydrolysis to occur; colipase, BS and other agents (i.e. calcium) are also needed.

The R_g of the lipase-colipase complex has been estimated at 26 Å (Pignol *et al.*, 2000). The relative mobility of the colipase molecule within the lipase-colipase complex implies that the size of the latter may vary according to the intra- and intercellular composition, in particular the presence of BS (Breg *et al.*, 1995). Another group stated that when the lid adopted a different conformation, some residues were shifted over a distance of 30 Å (Verger *et al.*, 1995). However, these variations may occur once the enzyme penetrates the cell, when in contact with the substrate (open conformation), and it clearly relies on the location where the complex forms (it is likely to be formed at the interface rather than in solution). In the presence of BS, it has been shown that the lid can open in solution (Belle *et al.*, 2007). In contrast to the structure of gastric lipase, which has a globular shape, pancreatic lipase possesses two structural domains and an elongated form. The lipase-colipase complex has a maximum longitudinal section of 90 Å for a transverse section of 42 Å, which suggests that the cell penetration of the HPL as a procolipase-lipase complex is unlikely (Miled *et al.*, 2000).

At interfaces, pancreatic lipase activity is high either in emulsions, monolayers or OBs (Beisson *et al.*, 2001a; Verger, 1984). Consequently, once inside the cell, the enzyme should theoretically be able to efficiently hydrolyse the TAGs contained in the OBs. Lipolysis of OBs is facilitated by their small size that provides a large surface area per unit TAG (~2700 cm^2/mL for crude OBs). The phospholipids present in OB membranes are likely to slow down the lipolysis by PL. However, it was formerly shown that the addition of phospholipase (i.e. GPLRP2) did not enhance the TAG hydrolysis by pancreatic lipase (Beisson *et al.*, 2001a). The absence of proteases in that particular experiment may provide an explanation for these results since proteases are also involved in the break down in OBs. Indeed, phospholipid hydrolysis occurred only when the oleosin were removed (Tzen and Huang, 1992) which is consistent with the results illustrated in Figure 7.11. Beisson *et al.* also showed that oleosins were partially protected from protease digestion due to the central hydrophobic domain they contain (Beisson *et al.*, 2001b). Other work performed on almond milk showed digestion of the

proteins (i.e. amandin and oleosin) by the action of pepsin and subsequently trypsin and chymotrypsin which affected the microstructure of the OBs and permitted their lipolysis (Gallier and Singh, 2012).

The absence of BS in some of the experiments highlighted the importance of the lipolytic product inhibition phenomenon (about 28% of lipolysis for raw almond, crude OBs without BS versus 69% in their presence). This also indicated that these surface active molecules interacted with the lipids and proteins present in the OB membrane. The cells on the other hand had similar degree of lipolysis in both cases (19 and 22% of FFA release with and without BS, respectively) which implies that they are not a good substrate for the pancreatic lipase. Before reaching the encapsulated lipids, the enzyme would have had to cross different barriers (i.e. CW, possibly plasma membrane and the OBs monolayer) and interact with components of a different nature (e.g. polysaccharides, phospholipids and proteins). The activity quantified is likely to be a 'background measurement' of cell preparation showing the diversity and complexity of this material, including the fragmented and damaged cells in which the lipid substrate is available to the lipase and also intact cells which are protected from lipolysis by the CWs. The high initial reaction rates but low amount of FFAs released relative to the OBs also point toward the conclusion that some of the lipids in the preparation were freely available, and thus rapidly hydrolysed, whereas the encapsulated substrate remain undigested.

Digestibility experiments performed on washed OBs did not indicate any impact of the extraneous proteins on the surface of the OBs. It is however possible that the washing procedure compromised the integrity of the OBs by changing the structure of their membrane as showed by the increase in the size of these OBs. This decrease in their relative surface area reduced their digestibility. The

current work also confirmed the evidence presented in *Chapter* 6 that the roasting process did not have a bearing on either the extent or the rate of lipolysis either for OBs or cells.

Localisation of pancreatic lipase within the almond matrices (i.e. cells and OBs) provided further explanations on the mechanisms governing lipolysis in almonds. The loss of structural integrity of the OBs within the cells, caused by the preparation of the material, led to lipid coalescence; these coalesced lipids could not pass through the CW and remained inside the cell as formerly observed (*Chapters 4 and 6*). Lipase on the other hand appeared to be reaching the intracellular compartment but only when disruption occurred to the CW and subsequently the OBs. Presumably, the permeability of the CW increased due to the treatment used to separate the cells. A video (*data not shown*), performed for 3 h, on the digestion of almond cells by pancreatic lipase, including both 'damaged' and intact cells (identified by the integrity of the OBs within the cells), displayed no visual modification in the overall cell structure (i.e. lipid droplets or CW) apart from the diffusion of lipases in the damaged cells. Nevertheless, most of the lipids were still enclosed inside these cells, albeit some of the lipase appeared to diffuse through the CWs. Therefore, if the same mechanisms take place *in vivo*, the lipid content of this material would remain unavailable when reaching the colon. The potential presence of lipolytic products within the damaged cells, generated from endogenous lipases prior to pasteurisation, may explain the accumulation of lipase inside certain cells and the predominant green colour observed. Indeed, similar to the increase in lipid digestibility occurring following the gastric phase, this 'pre-digestion' (i.e. formation of mixed micelles and oil droplets of small surface area) may have facilitated the activity of the pancreatic lipase and promoted their migration inside these cells.

The results from this chapter provide clear evidence that the CW of almond cells acts as a physical barrier to lipid digestibility. Even though lipase(s) and other digestive agents could diffuse through the CW, and lipolysis occurred, the majority of the lipids remained enclosed within the cells and this even after 20 h of incubation. This study has revealed also that OBs are highly digestible substrates and lipolysis does appear to be affected by their structure compared with almond emulsions. Finally, the roasting process may have altered the CW and its porosity, but this had little or no effect on the rate and extent of lipid hydrolysis, probably because of the resulting coalesced lipids.

CHAPTER 8

GENERAL DISCUSSION AND CONCLUSION

The main objective of the project described in this thesis was to investigate the role of cell walls (CWs) in regulating the bioaccessibility of lipid from almond seeds, a lipid-rich plant food. The structural changes and extent of digestion of raw and roasted almond seeds were studied using a multidisciplinary approach involving a novel combination of *in vivo*, *in vitro* and *in silico* methods.

This project was a continuation of previous work performed by our group (Berry *et al.*, 2008; Ellis *et al.*, 2004; Mandalari *et al.*, 2008a). The release of lipid from almonds was formerly investigated using faecal excretion studies in which structural analysis of digested material revealed that a significant proportion of lipid remained undigested mainly due to the entrapment of lipid by intact CW (Ellis *et al.*, 2004). It was also demonstrated that the consumption of muffins made with macroparticles of almonds (low lipid bioaccessibility) produced a much lower rise in postprandial lipaemia, compared with a muffin meal containing almond flour (high lipid bioaccessibility) (Berry *et al.*, 2008). Almond consumption and the resulting physiological responses such as the effects on satiety and gut hormone stimulation (e.g. GLP-1 and PYY) have also been previously investigated by others (Cassady *et al.*, 2009; Frecka *et al.*, 2008).

While evidence existed on the health benefits associated with the inclusion of almonds in the diet (Cohen and Johnston, 2011; Jenkins *et al.*, 2006; Joice *et al.*, 2008; Li *et al.*, 2011a; Sabate and Ang, 2009; Tan and Mattes, 2013), the mechanisms that explain the physiological effects and the long term benefits are not well understood, in particular, the behaviour of almond CWs in each compartment of the GIT (i.e. mouth, stomach and intestine). Obtaining information about the changes occurring to the structure of the almond tissue as the digestion process progresses and the mechanisms of lipid release were considered to be of crucial importance (Ellis *et al.*, 2004). One specific aspect of interest of this project was to identify the site, rate and extent of lipid release and digestion. Finally, the effect of processing, notably roasting, on lipid bioaccessibility was examined.

Overall, the results of the *in vitro* and *in vivo* studies reported in this thesis confirmed that almonds consumed whole and processed were not fully digested, and the lipids were released slowly during

the digestion process. This behaviour is strongly linked to the resistance of almond tissue to chemical and physical breakdown in the mouth, stomach and small intestine. A significant proportion of undigested almond tissue, with intracellular lipid encapsulated by CWs, was recovered at the terminal ileum of an ileostomy volunteer (i.e. beyond the site of lipid absorption). Thus, CWs appear to play a key role as a physical barrier against lipid release and digestion even though other mechanisms (e.g. lipid coalescence) also hinder lipid digestibility once the CWs are ruptured.

8.1 Mastication and digestion of whole almond seeds

Mastication of raw or roasted almonds produced boluses made of particles with a wide range of sizes (< 20 to > 3350 µm), leading to an average size of approximately 500 µm. The different sized particles generated during chewing had different properties/characteristics, with the large particles showing only damage to fractured surfaces characterised by CW rupture, whereas the smaller particles displayed much deeper fractures in all areas of the tissue (see Figure 3.7). The damage to these smaller particles may have occurred as a result of receiving a larger number of deformations during mastication. We then demonstrated in *Chapters 4 and 6* that the overall structure of almond tissue during gastric digestion was relatively unaffected, especially for large particles. However, at the cellular level some CW swelling was observed close to the surfaces of the tissue after prolonged residence time as previously observed in other digestion studies (Mandalari *et al.*, 2008a; Tydeman *et al.*, 2010).

Lipid release following mastication was estimated using the mathematical model developed by our group (Grassby *et al.*, 2014). The mastication study detailed in *Chapter 3* showed that a high proportion of almond cells within particles remain undisturbed after oral processing with only ~8 and 11% of lipid released from ruptured cells on the fractured surfaces of masticated raw and

roasted almonds, respectively. The values obtained experimentally were reassuringly close to the predicted values from the theoretical model. After gastric and duodenal digestions, almond digestion was still incomplete with ~68% of lipid remaining encapsulated, which was consistent with the particles size and structure (i.e. PSD and images of almond microstructure). However, the amounts of lipid release as well as the disruption of the almond tissue were found to be more noticeable during intestinal digestion than in the gastric phase. The surface active proteins contained in saliva, its viscosity and pH generated a 'network' around the surface of the almond particles making the boluses cohesive and, at the same time, lipid appeared to strongly adhere to the particle surface (see Figure 3.10), thus becoming less available to digestive enzymes in the stomach (Carpenter, 2013). Under gastric conditions, some of the adsorbed proteins may have been removed and solubilised into the aqueous phase; however, the addition of BS in the duodenal compartment is likely to have promoted the disruption of this network to a greater extent thus 'liberating' the lipids from the particles surface (Maldonado-Valderrama *et al.*, 2010). Further degradation of the almond tissue could be anticipated in the colon since our early study showed that about 10% of lipids from a diet rich in almond seeds were excreted in the faeces (Ellis *et al.*, 2004). Microbial fermentation of the nutrients enclosed within the almond cells and CW most probably explain the lower amount of lipid recovered (Ellis *et al.*, 2004; Mandalari *et al.*, 2008b).

Particles of smaller size had more fractured cells and thereby greater lipid losses than large particles. Cells within the almond tissue rupture rather than separate, the proportion of ruptured cells relying on the number of fractured surfaces created by mechanical processing and/or mastication. Cells of plant food may either rupture or separate depending on the strength of their cell-cell adhesion, which is largely structure of the the pectic polysaccharides and the calcium crosslinking between these polymers in the middle lamella. The composition and overall structure of the CW, specific to the plant studied, has consequences on its behaviour in the GIT and the nutrients bioaccessibility,

depending also on processing conditions. For instance, wheat cells appear to be similar to almonds by rupturing when mechanically disrupted (e.g. miling or mastication), whereas chickpeas cells are known to separate when they have been hydrothermally processed, but will rupture during milling (Edwards, 2014). When the cells fracture, their contents empty in the GIT and thereby evoke a physiological response (i.e. hormone secretions linked to effects such as adjustment of gastric emptying and gastrointestinal contractions). On the other hand, when the cells are intact (separated) and encapsulate the nutrients they contained, they transit towards the colon without being further digested as observed in white beans (Noah *et al.*, 1998).

Mastication is a crucial step in the digestion process and it impacts on energy intake and gut hormones secretion (Cassady *et al.*, 2009). The work from Mattes and his group demonstrated that prolonged mastication of almond elicited higher feeling of satiety which was reflected by a rise in GLP-1 concentrations. Nutrients released from the almond tissues in the oral cavity and the subsequent GIT parts trigger neuronal and humoral signals that have an impact on the digestion (i.e. gastric emptying, contractions and ileal brake) (Feltrin *et al.*, 2004; Maljaars *et al.*, 2008). However, if the nutrients are still enclosed within the food matrix it is highly probable that the digesta transit throughout the GIT without specific nutrients being 'detected'. Some of the content of intact cells may nevertheless get digested after prolonged residence time due to swelling of the CW that rendered them permeable to digestive enzymes (Figures 4.11 and 6.9). Under identical mechanisms, and assuming that other microorganisms present are unable to digest the CW, the microbial lipases may have only limited access to their substrate. It is for these reasons and despite the common belief that TAGs are absent in stool of healthy individuals (Carey and Hernell, 1992), that the digestion of lipids contained in almond ingested whole is not total and lipids were recovered in effluent (*Chapter 6*) as well as faecal (Ellis *et al.*, 2004) samples.

More particles of small sizes were produced after mastication of roasted than raw almonds however mastication parameters (i.e. duration and number of chews) showed little variation between these two almond forms. This suggests that the differences in particle size distribution were due to the nature of the almond (i.e. raw vs roasted) rather than the way subjects masticated them. Roasted almonds fractured differently when submitted to a mechanical force (e.g. mastication) because of the changes that occurred during the roasted process (i.e. dehydration of the tissues). The amount of lipid release in the oral cavity was more important for roasted almonds but this difference was less clear in the subsequent GIT compartments. The loss in the OB integrity and the resulting lipid coalescence in the roasted almonds is a plausible explanation to the consistency in lipid digestibility between raw and roasted almonds.

The results from these *in vivo* and *in vitro* studies revealed that the majority of the almond tissue disruptions and the subsequent lipid digestion took place during the duodenal phase. Therefore, there was a requirement to investigate the behaviour of various almond materials (particles with different sizes as well as 'free' lipids) at this stage of digestion.

8.2 Lipid digestibility of different almond materials

Characterisation of the native almonds used during this project, before addition of lipase into the reaction environment, indicated the presence of lipolytic products, FFAs and PA, due to the degradation of TAGs and phospholipids, respectively, either prior to pasteurisation or during storage (see *Chapter 7*). This would have led to a slight overestimation of the amount of FFAs generated and thereby extent of lipolysis. Interestingly, the roasting process seemed to have prevented this phenomenon as shown by the absence of phosphatidic acid. It is thus conceivable that the lipolyses occurred after pasteurisation.

The nature and physical characteristics of the particles within the bolus (i.e. size and degree of disruption) are of crucial importance since they have a direct impact on the functions of the stomach, in particular on the mixing of the food and its delivery to the small intestine as explained above. The duodenal digestibility experiments presented in *Chapter 5* revealed that separated almond cells had the lowest digestibility, and that there was an inverse relationship between particle size of almonds and the rate and extent of their digestion.

One of the original objectives of this project was the examination of the potential diffusion of lipase through CWs using initially FITC-dextrans and then labelled lipase. This approach permitted us to have a closer examination of the potential for lipid digestion occurring within intact cells. To our knowledge, the exact value of the pore radius of almond CW, corresponding to the pore size expressed as Stoke's radius of a molecule that is sufficient to restrict its free diffusion through the CW (Carpita *et al.*, 1979), is lacking. Dextrans of 34 Å penetrated the CW so pancreatic lipase (19 Å) should have done this, which was not the case. This contradiction highlights the complexity of the diffusion phenomenon, possibly the spatial arrangement and charge of the enzyme may have prevented its permeation when CWs were intact. Furthermore, not all ruptured cells contained labelled lipase suggesting that other mechanisms may hinder lipase diffusion. Microscopy of digested almond particles indicated that lipase succeeded in penetrating the intracellular environment in the latest stages of digestion. Alterations in the structure (not the composition since it was consistent throughout digestion, *Chapter 4*) of the CW such as swelling, may have rendered the almond cells permeable to the lipase(s) and other enzymes.

The *in vitro* data from *Chapter 5* are in accordance with the results from the human study (*Chapter 6*) where 6 and 59% of lipids remained undigested in almond flour (AF) and large particles (AP), respectively. Based on the particle size of the almond contained in each muffin, it was predicted from the mathematical model (*Appendix B*) that about 49% of the lipids contained in AF and 6% in AP were released and therefore potentially available for digestion from the almond tissue at the

early stage of digestion (i.e. oral phase). Presumably a further 45 and 36% of lipids were released from AF and AP, respectively, between the gastric phase and the excretion at the terminal ileum. Particles within the muffins therefore resulted in an important recovery of lipids, if whole almond were ingested we could have expected an even higher recovery rate as indicated by the results from *Chapter 5*. Unfortunately the results were only from one volunteer since the subsequent feeding of whole almond to other ileostomy volunteers had to be terminated because of the risks of stoma obstruction. This by itself demonstrated the difficulty of digesting almond. Nevertheless, the results from the participant that tolerated the meal provide valuable evidence that *in vitro* observations were compatible with the data obtained *in vivo*.

Beside the macrostructure of the material reaching the stomach and intestine, the microstructure of the lipid within it is also of importance. It is likely that the processing of the almonds within the muffins, grinding, cooking and then freezing, enhanced the lipid bioaccessibility compared with whole almonds because it generated fractures in the CW (Figure 6.4 A). The size of the droplets release during mastication and digestion is likely to differ between almonds depending on the processing they underwent. We showed in *Chapters 5 and 7* that the amounts of lipid digested between raw and roasted almond were similar. It was however expected to find a greater lipid digestibility in the roasted form, in particular for the chewed samples, since their mastication led to a larger number of particles with smaller sizes (i.e. increased lipid bioaccessibility) compared with the raw chewed almonds. Roasting affects the CWs and OBs integrity of the almond (Perren and Escher, 2013). The disruption of the OBs and the resulting lipid coalescence made them less favourable to lipase hydrolysis because of the increase in their surface area. Mastication and processing (i.e. roasting, cooking and grinding) of the almonds is likely to have resulted in the release of lipid droplets with different properties/characteristics (e.g. size, surface active molecules present

on the interface). Finally, it is also possible that the roasting process led to the formation of compounds, such as phenolic compounds, that could have inhibited the lipase (Yang *et al.*, 2014).

Vors *et al.* developed an interesting concept of 'slow vs fast' lipids, stating that postprandial lipaemia could be modulated by the physical structure of the lipid droplets (i.e. emulsified and unemulsified) contained in a food/meal (Vors *et al.*, 2013). Emulsified lipid induced higher intestinal absorption and thereby postprandial response. We can postulate that the coalesced lipids within the almond tissue may have attenuated the postprandial response observed in *Chapter 6* compared with lipid that would have been present as OBs. *Chapters 5* and *7* validated that idea as unemulsified almond oil had a lower rate and extent of lipolysis compared with emulsions and OBs.

Intact CWs therefore play an important role in limiting lipid bioaccessibility and lipolysis as they physically encapsulate the intracellular lipid. We revealed that the size of the lipid droplets and the 'quality' of the interface (e.g. type of proteins and other molecules adsorbed) had a significant impact on these processes, as formerly established (Verger and de Haas, 1976), but more importantly the overall structure of the food matrix (i.e. 'compaction' of the cells together within the tissue) plays a key role in inhibiting lipolysis.

8.3 Modelling of the digestion process with almond as plant food

In this project, gastric and intestinal digestions were simulated using a wide range of techniques and approaches, from the simplest (i.e. pH-stat) to the most realistic model (i.e. ileostomy 'model'). *In vitro* models may not entirely mimic the complex phenomena taking place during human digestion (e.g. hormonal response) but they do have the advantages of being more rapid, less expensive, less

labour intensive, and having no ethical restriction (Guerra *et al.*, 2012). A wide range of food and pharmaceutical products can therefore be easily investigated with those models. The mechanical and chemical processes can be reproduced but the complex postprandial responses and feedback mechanisms are more problematic, and supposedly large disparities exist between individuals.

The DGM has proved to be the optimal method to simulate the mechanical and biochemical processes occurring in the stomach. Combined with a static duodenal phase (SDM), it permitted the examination of the extent of lipid digestibility in native and processed almonds; the results obtained with the almond muffins were in good agreement with the data from our ileostomy volunteer. Regardless of its high sophistication and the complex software associated with it, the model is still missing some important parameters present in humans such as for instance the microflora. However, introducing a microflora 'model' is extremely challenging given the variability in bacterial species populating the human digestive system (Eckburg *et al.*, 2005).

The pH-stat method permits a comparison, under well-controlled conditions, of a wider range of almond materials than the DGM/SDM and allows continuously monitoring of lipolysis without the requirement of further analysis. Combined with other *in vitro* techniques (i.e. chromatography and microscopy analyses), it gave detailed information about the different mechanisms taking place during almond digestion. However, caution must be taken when interpreting the data generated as the device does not provide absolute values and product inhibitions may underestimate the amount of FFAs produced. Future experiments should include a back titration step to ensure that the total amount of the FFAs produced is ionised and neutralised with NaOH, especially if studying TAGs made of long chain fatty acids (i.e. pKa of FFA > pH of digestion).

Human studies remain the gold-standard but difficulties still exist in collecting digesta samples in a non-invasive manner between the oral and colonic phases. Ileostomy volunteers could overcome part of the issue as analysis of the materials excreted at the terminal ileum could be performed but this model is not a good option to investigate almond digestibility. Indeed, high risk of obstruction persisted despite the attention taken before and during the trial, especially the meticulous selection of volunteers. Furthermore, information was lacking regarding the state of the digested almond, in terms of structure and lipid content, in the proximal GIT sites (e.g. stomach and duodenum).

8.4 Health benefits and relevance to the industry

It is of interest to encourage consumption of foods which evoke a desirable blood lipid or glucose response. Evidence from various sources indicates that high and prolonged blood lipid and glucose levels following a meal are associated with increased risk of coronary heart disease and other life-style related health implications (Jenkins *et al.*, 2002b; O'Keefe *et al.*, 2008; Patsch *et al.*, 1992). However, further work was needed in order to understand the factors that affect the blood lipid response. The programme of research work reported in this thesis has brought additional knowledge about the mechanisms by which plant tissue disassemble during mastication and digestion. The beneficial health effects of almonds therefore rely not only on their nutritional composition, they are a good source of unsaturated fatty acids (i.e. MUFA and PUFA), vitamin E, and polyphenol (Yada *et al.*, 2011), but also their structure when ingested. The physical form of almonds that are consumed leads to variability in lipid digestibility (*Chapters 5 and 7*) and consequently evokes different lipid profile and gut hormones release (*Chapter 6*).

Energy values of raw almond calculated using Atwater factors overestimated their actual energy content (Novotny *et al.*, 2012). These findings together with the results obtained during this project

raise questions about the validity of the information found on food labels that are based on food composition data and Atwater correction factors. Indeed, almond meals with different degree of lipid bioaccessibility led to different rates and extents of lipolysis (and different postprandial responses); hence the importance of considering the structure of the food when estimating its nutritional value. The concept of bioaccessibility and bioavailability in plant food is well recognised for micronutrients such as carotenoids, polyphenol and lycopene (Parada and Aguilera, 2007) but this should be applied to macronutrients especially within complex food matrix such as vegetables, nuts, seeds and cereals.

With regards to the industrial impact, the current work provided further information on the functional properties of processed almond. By gaining a better understanding of nutrient availability and how it is affected by food structure it may be possible to develop healthier processed food products with benefits to consumer health. During processing (i.e. roasting and grinding), the structure of the food matrix is altered resulting in a modification of the proportion of nutrients encapsulated by CWs. Therefore, by applying different processing treatments to the almond seeds, it could become possible to control or sustain the release of lipids and other nutrients they contain. Consumption of whole almonds and other nuts could lead to appetite control, weight management and prevention of diet-related diseases such as CVD and type II diabetes. Alternatively, nutrient uptake could be increased as needed by althletes and undernourished populations (i.e. premature babies, the elderly and patients with chronic diseases such as HIV and cancer) by including processed almonds, e.g. marzipan and finely ground almonds, in their diet.

8.5 Final comments and further prospective

Following the work on particle sizing we recommend using for ground, masticated or digested tree nuts and other hard food a laser diffraction technique combined with mechanical sieving if the size range is not totally covered by the laser instrument. However, since both particle sizing methods employed wet samples, it has to be ensured that the material studied does not absorb water. One should bear in mind also that a direct comparison of the two techniques is not easy to achieve as they give particles sizes in two different units (i.e. volume vs weight). Analysis of the shapes of the particles according to their size was performed by Sympatec, in Germany, using dynamic image analysis (QICPIC; *data not shown*) which showed that the shape of particles changed with size. However, obtaining a shape factor that allowed the two types of data to coincide was difficult as particle shape has to be constant over the size ranges (Wang *et al.*, 2006). The process was also compromised by the multimodal pattern of the PSDs. Using the latest particle sizer from Malvern (Malvern Mastersizer 3000®) could overcome these issues as the instrument has the capacity to measure particles, wet and dry, with sizes ranging from 0.01 to 3500 µm.

Further work could include the investigation of the integrity of almond cells and particles within the colon. Submitting the digested almonds to the colonic phase could provide information about their behaviour and structure in this compartment. As we showed that a significant proportion of almond particles remained after intestinal digestion, studying the impact of microbiota activity on that material would be of interest, in particular the degree of degradation of almond materials with different characteristics (i.e. size, shape, separated cells vs freely available lipids). For instance, particles that have damaged CW when ingested, as observed in almonds contained in the muffins, may eventually lead to a total digestibility of the lipid they contain. Grinding, cooking and freezing are treatments that are likely to be employed by the industry to generate this type of product (i.e.

muffins containing nuts), so it may be of commercial interest to gain knowledge on nutrients digestibility in the colonic phase.

It could also be worthwhile to investigate the potential existence of a plasma membrane underneath the CW. In the current project, we assumed that the two elements were combined but it is possible that the plasma membrane is absent in almonds. Having intact CW and plasma membrane may compromise even further the digestibility of the lipid contained in intact cells. The mechanisms monitoring the diffusion of lipase through CW are likely to be different from those governing the crossing of the plasma membrane. In the colonic phase, polysaccharides from the CW as well as phospholipids and other molecules composing the plasma membrane ought to be metabolised by bacteria. However, studying the structure and spatial organisation of the CW is a challenging task so is the isolation of the potential plasma membrane from the CW and intracellular compounds, including other lipid bilayers.

8.6 Conclusions

The work described in this thesis provides further evidence that CWs act as a physical barrier that limit and sometimes prevent lipid bioaccessibility and digestibility. I revealed that the transformations performed on the almond tissue, either during the meal preparation or the mastication itself, have a crucial impact on its structure and properties in the GIT and therefore on its lipid digestibility. Lipase and other digestive agents may be able to diffuse through the CW but this is more likely to happen when its integrity has been compromised or there has been an increase in CW porosity. These findings showed the complexity of the mechanisms involved in the digestion of nutrients contained in almonds and provide some explanations on the beneficial effects associated with their consumption.

REFERENCES

Agrawal, K. R., Lucas, P. W., Prinz, J. F. and Bruce, I. C. (1997). Mechanical properties of foods responsible for resisting food breakdown in the human mouth. *Archives of Oral Biology,* 42**:** 1-9.

Al-Ali, F., Heath, M. R. and Wright, P. S. (1999). Simplified method of estimating masticatory performance. *Journal of Oral Rehabilitation,* 26**:** 678-683.

Alasalvar, C. and Shahidi, F. (2009). *Tree Nuts: Composition, Phytochemicals, and Health Effects,* Boca Raton: CRC Press.

Allen, T. (1997). *Particle Size Measurement: Powder Sampling and Particle Size Measurement,* London: Chapman & Hall.

Almond Board of California (2013). *Global Usage* [Online]. Available: www.almonds.com/consumers/about-almonds/global-almond-usage [Accessed 02/09/2013].

Amara, S., Patin, A., Giuffrida, F., Wooster, T. J., Thakkar, S. K., Benarouche, A., Poncin, I., Robert, S., Point, V., Molinari, S., Gaussier, H., Diomande, S., Destaillats, F., Cruz-Hernandez, C. and Carriere, F. (2014). *In vitro* digestion of citric acid esters of mono- and diglycerides (CITREM) and CITREM-containing infant formula/emulsions. *Food & Function,* 5**:** 1409-1421.

Anderson, J. W., Baird, P., Davis, R. H., Jr., Ferreri, S., Knudtson, M., Koraym, A., Waters, V. and Williams, C. L. (2009). Health benefits of dietary fiber. *Nutrition Reviews,* 67**:** 188-205.

Andersson, H. (1992). The ileostomy model for the study of carbohydrate digestion and carbohydrate effects on sterol excretion in man. *European Journal of Clinical Nutrition,* 46 Suppl 2**:** 69S-76S.

Andersson, H. B., Ellegard, L. H. and Bosaeus, I. G. (1999). Nondigestibility characteristics of inulin and oligofructose in humans. *Journal of Nutrition,* 129**:** 1428S-1430S.

Andrieux, K., Lesieur, P., Lesieur, S., Ollivon, M. and Grabielle-Madelmont, C. (2002). Characterization of fluorescein isothiocyanate-dextrans used in vesicle permeability studies. *Analytical Chemistry,* 74**:** 5217-5226.

Armand, M. (2007). Lipases and lipolysis in the human digestive tract: where do we stand? *Current Opinion in Clinical Nutrition and Metabolic Care,* 10**:** 156-164.

Armand, M., Pasquier, B., Andre, M., Borel, P., Senft, M., Peyrot, J., Salducci, J., Portugal, H., Jaussan, V. and Lairon, D. (1999). Digestion and absorption of 2 fat emulsions with different droplet sizes in the human digestive tract. *American Journal of Clinical Nutrition,* 70**:** 1096-1106.

Armand, M., Borel, P., Pasquier, B., Dubois, C., Senft, M., Andre, M., Peyrot, J., Salducci, J. and Lairon, D. (1996). Physicochemical characteristics of emulsions during fat digestion in human stomach and duodenum. *American Journal of Physiology - Gastrointestinal and Liver Physiology,* 34**:** G172-G183.

Armand, M., Borel, P., Dubois, C., Senft, M., Peyrot, J., Salducci, J., Lafont, H. and Lairon, D. (1994). Characterization of emulsions and lipolysis of dietary lipids in the human stomach. *American Journal of Physiology,* 266**:** G372-G381.

Armand, M., Borel, P., Ythier, P., Dutot, G., Melin, C., Senft, M., Lafont, H. and Lairon, D. (1992). Effects of droplet size, triacylglycerol composition, and calcium on the hydrolysis of complex emulsions by pancreatic lipase: an in *vitro* study. *Journal of Nutritional Biochemistry,* 3**:** 333-341.

Armstrong, W. P. (2009). *Fruits Called Nuts* [Online]. Available: http://waynesword.palomar.edu/ecoph8.htm [Accessed 14/06/2011].

Arterburn, L. M., Hall, E. B. and Oken, H. (2006). Distribution, interconversion, and dose response of n-3 fatty acids in humans. *American Journal of Clinical Nutrition,* 83**:** 1467S-1476S.

Baer, D. J., Gebauer, S. K. and Novotny, J. A. (2012). Measured energy value of pistachios in the human diet. *British Journal of Nutrition,* 107**:** 120-125.

Bao, Y., Han, J., Hu, F. B., Giovannucci, E. L., Stampfer, M. J., Willett, W. C. and Fuchs, C. S. (2013). Association of nut consumption with total and cause-specific mortality. *New England Journal of Medicine,* 369**:** 2001-2011.

Baron-Epel, O., Gharyal, P. K. and Schindler, M. (1988). Pectins as mediators of wall porosity in soybean cells. *Planta,* 175**:** 389-395.

Barros, M., Fleuri, L. F. and Macedo, G. A. (2010). Seed lipases: sources, applications and properties - a review. *Brazilian Journal of Chemical Engineering,* 27**:** 15-29.

Bauer, E., Jakob, S. and Mosenthin, R. (2005). Principles of physiology of lipid digestion. *Asian - Australasian Journal of Animal Sciences,* 18**:** 282-295.

Beardshall, K., Morarji, Y., Bloom, S. R., Frost, G., Domin, J. and Calam, J. (1989). Saturation of fat and cholecystokinin release: implications for pancreatic carcinogenesis. *Lancet,* 334**:** 1008-1010.

Beguin, P. and Aubert, J.-P. (1994). The biological degradation of cellulose. *FEMS Microbiology Reviews,* 13**:** 25-58.

Beisson, F., Ferte, N., Bruley, S., Voultoury, R., Verger, R. and Arondel, V. (2001a). Oil-bodies as substrates for lipolytic enzymes. *Biochimica et Biophysica Acta - Molecular and Cell Biology of Lipids,* 1531**:** 47-58.

Beisson, F., Ferte, N., Voultoury, R. and Arondel, V. (2001b). Large scale purification of an almond oleosin using an organic solvent procedure. *Plant Physiology and Biochemistry,* 39**:** 623-630.

Beisson, F., Tiss, A., Riviere, C. and Verger, R. (2000). Methods for lipase detection and assay: a critical review. *European Journal of Lipid Science and Technology,* 102**:** 133-153.

Belle, V., Fournel, A., Woudstra, M., Ranaldi, S., Prieri, F., Thome, V., Currault, J., Verger, R., Guigliarelli, B. and Carriere, F. (2007). Probing the opening of the pancreatic lipase lid using site-directed spin labeling and EPR spectroscopy. *Biochemistry,* 46**:** 2205-2214.

Benarouche, A., Point, V., Parsiegla, G., Carriere, F. and Cavalier, J. F. (2013). New insights into the pH-dependent interfacial adsorption of dog gastric lipase using the monolayer technique. *Colloids and Surfaces B: Biointerfaces,* 111C**:** 306-312.

Benzonana, G. (1968). [On role of Ca^{2+} during hydrolysis of insoluble triglycerides by pancreatic lipase in presence of bile salts]. *Biochimica et Biophysica Acta,* 151**:** 137-146.

Benzonana, G. and Desnuelle, P. (1965). [Kinetic study of the action of pancreatic lipase on emulsified triglycerides. Enzymology assay in heterogeneous medium]. *Biochimica et Biophysica Acta,* 105**:** 121-136.

Berghouse, L., Hori, S., Hill, M., Hudson, M., Lennard-Jones, J. E. and Rogers, E. (1984). Comparison between the bacterial and oligosaccharide content of ileostomy effluent in subjects taking diets rich in refined or unrefined carbohydrate. *Gut,* 25**:** 1071-1077.

Bernback, S., Blackberg, L. and Hernell, O. (1990). The complete digestion of human milk triacylglycerol *in vitro* requires gastric lipase, pancreatic colipase-dependent lipase, and bile salt-stimulated lipase. *Journal of Clinical Investigation,* 85**:** 1221-1226.

Berry, S. E., Tydeman, E. A., Lewis, H. B., Phalora, R., Rosborough, J., Picout, D. R. and Ellis, P. R. (2008). Manipulation of lipid bioaccessibility of almond seeds influences postprandial lipemia in healthy human subjects. *American Journal of Clinical Nutrition,* 88**:** 922-929.

Bilecen, D., Scheffler, K., Seifritz, E., Bongartz, G. and Steinbrich, W. (2000). Hydro-MRI for the visualization of gastric wall motility using RARE magnetic resonance imaging sequences. *Abdominal Imaging,* 25**:** 30-34.

Blahovec, J. (2007). Role of water content in food and product texture. *International Agrophysics,* 21**:** 209-215.

Blakeney, A. B., Harris, P. J., Henry, R. J. and Stone, B. A. (1983). A simple and rapid preparation of alditol acetates for monosaccharide analysis. *Carbohydrate Research,* 113**:** 291-299.

Blumenkrantz, N. and Asboe-Hansen, G. (1973). New method for quantitative determination of uronic acids. *Analytical Biochemistry,* 54**:** 484-489.

Boden, G. (1997). Role of fatty acids in the pathogenesis of insulin resistance and NIDDM. *Diabetes,* 46**:** 3-10.

Bodmer, M. W., Angal, S., Yarranton, G. T., Harris, T. J. R., Lyons, A., King, D. J., Pieroni, G., Riviere, C., Verger, R. and Lowe, P. A. (1987). Molecular cloning of a human gastric lipase and expression of the enzyme in yeast. *Biochimica et Biophysica Acta - Gene Structure and Expression,* 909**:** 237-244.

Bolling, B. W., Dolnikowski, G., Blumberg, J. B. and Chen, C. Y. O. (2010). Polyphenol content and antioxidant activity of California almonds depend on cultivar and harvest year. *Food Chemistry,* 122**:** 819-825.

Bonsegna, S., Bettini, S., Pagano, R., Zacheo, A., Vergaro, V., Giovinazzo, G., Caminati, G., Leporatti, S., Valli, L. and Santino, A. (2011). Plant oil bodies: novel carriers to deliver lipophilic molecules. *Applied Biochemistry and Biotechnology,* 163**:** 792-802.

Borel, P., Armand, M., Ythier, P., Dutot, G., Melin, C., Senft, M., Lafont, H. and Lairon, D. (1994). Hydrolysis of emulsions with different triglycerides and droplet sizes by gastric lipase *in vitro*. Effect on pancreatic lipase activity. *Journal of Nutritional Biochemistry,* 5**:** 124-133.

Borgström, B., Wieloch, T. and Erlanson-Albertsson, C. (1979). Evidence for a pancreatic pro-colipase and its activation by trypsin. *FEBS Letters,* 108**:** 407-410.

Borgström, B. (1977). The action of bile salts and other detergents on pancreatic lipase and the interaction with colipase. *Biochimica et Biophysica Acta,* 488**:** 381-391.

Borgström, B. (1967). Partition of lipids between emulsified oil and micellar phases of glyceride-bile salt dispersions. *Journal of Lipid Research,* 8**:** 598-608.

Bornhorst, G. M., Roman, M. J., Dreschler, K. C. and Singh, R. P. (2013). Physical property changes in raw and roasted almonds during gastric digestion *in vivo* and *in vitro*. *Food Biophysics,* 9**:** 39-48.

Boron, W. F. and Boulpaep, E. L. (2009). *Medical Physiology: a Cellular and Molecular Approach,* Philadelphia: Elsevier.

Borovicka, J., Schwizer, W., Mettraux, C., Kreiss, C., Remy, B., Asal, K., Jansen, J. B., Douchet, I., Verger, R. and Fried, M. (1997). Regulation of gastric and pancreatic lipase secretion by CCK and cholinergic mechanisms in humans. *American Journal of Physiology,* 273**:** G374-G380.

Borriello, S. (1986). Microbial flora of the gastrointestinal tract. *In:* Hill, M. J. (ed.) *Microbial Metabolisms in the Digestive Tract*, Boca Raton: CRC Press.

Bourre, J. M. (2006). Effects of nutrients (in food) on the structure and function of the nervous system: update on dietary requirements for brain. Part 2: macronutrients. *Journal of Nutrition Health and Aging,* 10**:** 386-399.

Bray, G. A., Paeratakul, S. and Popkin, B. M. (2004). Dietary fat and obesity: a review of animal, clinical and epidemiological studies. *Physiology & Behavior,* 83**:** 549-555.

Breg, J. N., Sarda, L., Cozzone, P. J., Rugani, N., Boelens, R. and Kaptein, R. (1995). Solution structure of porcine pancreatic procolipase as determined from 1H homonuclear two-dimensional and three-dimensional NMR. *European Journal of Biochemistry,* 227**:** 663-672.

Brett, C. and Waldron, K. (1996). *Physiology and Biochemistry of Plant Cell Walls,* Cambridge: Chapman & Hall.

Brittain, H. G. (2001). Particle size distribution, part I: representations of particle shape, size, and distribution. *Pharmaceutical Technology,* 25**:** 38-45.

Brockman, H. (2002). Colipase-induced reorganization of interfaces as a regulator of lipolysis. *Colloids and Surfaces B: Biointerfaces,* 26**:** 102-111.

Brockman, H. L. (1984). General features of lipolysis: reaction scheme, interfacial structure and experimental approaches. *In:* Borgstrom, B. and Brockman, H. L. (eds.) *Lipases*, Amsterdam: Elsevier Science.

Brownlee, I. A. (2011). The physiological roles of dietary fibre. *Food Hydrocolloids,* 25**:** 238-250.

Brownlee, I. A., Forster, D. J., Wilcox, M. D., Dettmar, P. W., Seal, C. J. and Pearson, J. P. (2010). Physiological parameters governing the action of pancreatic lipase. *Nutrition Research Reviews,* 23**:** 146-154.

Buchanan, B., W., G. and R., J. (2002). *Biochemistry and Molecular Biology of Plants,* Rockville: Wiley-Blackwell.

Burdge, G. C. and Wootton, S. A. (2002). Conversion of alpha-linolenic acid to eicosapentaenoic, docosapentaenoic and docosahexaenoic acids in young women. *British Journal of Nutrition,* 88**:** 411-420.

Burke, J. E. and Dennis, E. A. (2009). Phospholipase A2 structure/function, mechanism, and signaling. *Journal of Lipid Research,* 50**:** S237-S242.

Burton, R. A., Gidley, M. J. and Fincher, G. B. (2010). Heterogeneity in the chemistry, structure and function of plant cell walls. *Nature Chemical Biology,* 6**:** 724-732.

Burton-Freeman, B., Davis, P. A. and Schneeman, B. O. (2004). Interaction of fat availability and sex on postprandial satiety and cholecystokinin after mixed-food meals. *American Journal of Clinical Nutrition,* 80**:** 1207-1214.

Buschang, P. H., Throckmorton, G. S., Travers, K. H. and Johnson, G. (1997). The effects of bolus size and chewing rate on masticatory performance with artificial test foods. *Journal of Oral Rehabilitation,* 24**:** 522-526.

Butterworth, P. J., Warren, F. J., Grassby, T., Patel, H. and Ellis, P. R. (2012). Analysis of starch amylolysis using plots for first-order kinetics. *Carbohydrate Polymers,* 87**:** 2189-2197.

Caffall, K. H. and Mohnen, D. (2009). The structure, function, and biosynthesis of plant cell wall pectic polysaccharides. *Carbohydrate Research,* 344**:** 1879-1900.

Calder, P. C. (2010). Omega-3 fatty acids and inflammatory processes. *Nutrients,* 2**:** 355-374.

Canaan, S., Roussel, L., Verger, R. and Cambillau, C. (1999). Gastric lipase: crystal structure and activity. *Biochimica et Biophysica Acta - Molecular and Cell Biology of Lipids,* 1441**:** 197-204.

Capolino, P., Guerin, C., Paume, J., Giallo, J., Ballester, J.-M., Cavalier, J.-F. and Carriere, F. (2011). *In vitro* gastrointestinal lipolysis: replacement of human digestive lipases by a combination of rabbit gastric and porcine pancreatic extracts. *Food Digestion,* 2**:** 43-51.

Cara, L., Dubois, C., Borel, P., Armand, M., Senft, M., Portugal, H., Pauli, A. M., Bernard, P. M. and Lairon, D. (1992). Effects of oat bran, rice bran, wheat fiber, and wheat germ on postprandial lipemia in healthy adults. *American Journal of Clinical Nutrition,* 55**:** 81-88.

Carey, M. C. and Hernell, O. (1992). Digestion and absorption of fat. *Seminars in Gastrointestinal Disease,* 3**:** 189-208.

Carey, M. C., Small, D. M. and Bliss, C. M. (1983). Lipid digestion and absorption. *Annual Review of Physiology,* 45**:** 651-677.

Carpenter, G. H. (2013). The secretion, components, and properties of saliva. *Annual Review of Food Science and Technology,* 4**:** 267-276.

Carpita, N. C. and Gibeaut, D. M. (1993). Structural models of primary-cell walls in flowering plants - consistency of molecular-structure with the physical-properties of the walls during growth. *Plant Journal,* 3**:** 1-30.

Carpita, N. C., Sabularse, D., Montezinos, D. and Delmer, D. P. (1979). Determination of the pore size of cell walls of living plant cells. *Science,* 205**:** 1144-1147.

Carriere, F., Renou, C., Lopez, V., De Caro, J., Ferrato, F., Lengsfeld, H., De Caro, A., Laugier, R. and Verger, R. (2000). The specific activities of human digestive lipases measured from the *in vivo* and *in vitro* lipolysis of test meals. *Gastroenterology,* 119**:** 949-960.

Carriere, F., Barrowman, J. A., Verger, R. and Laugier, R. (1993). Secretion and contribution to lipolysis of gastric and pancreatic lipases during a test meal in humans. *Gastroenterology,* 105**:** 876-888.

Carriere, F., Moreau, H., Raphel, V., Laugier, R., Benicourt, C., Junien, J.-L. and Verger, R. (1991). Purification and biochemical characterization of dog gastric lipase. *European Journal of Biochemistry,* 202**:** 75-83.

Cassady, B. A., Hollis, J. H., Fulford, A. D., Considine, R. V. and Mattes, R. D. (2009). Mastication of almonds: effects of lipid bioaccessibility, appetite, and hormone response. *American Journal of Clinical Nutrition,* 89**:** 794-800.

Champ, M., Langkilde, A. M., Brouns, F., Kettlitz, B. and Bail-Collet, Y. L. (2003). Advances in dietary fibre characterisation. 2. Consumption, chemistry, physiology and measurement of resistant starch; implications for health and food labelling. *Nutrition Research Reviews,* 16**:** 143-161.

Chan, A. W. and Neufeld, R. J. (2009). Modeling the controllable pH-responsive swelling and pore size of networked alginate based biomaterials. *Biomaterials,* 30**:** 6119-6129.

Chapus, C., Sari, H., Semeriva, M. and Desnuelle, P. (1975). Role of colipase in the interfacial adsorption of pancreatic lipase at hydrophilic interfaces. *FEBS Letters,* 58**:** 155-158.

Chaudhri, O., Small, C. and Bloom, S. (2006). Gastrointestinal hormones regulating appetite. *Philosophical Transactions of the Royal Society of London,* 361**:** 1187-1209.

Cheirsilp, B., Jeamjounkhaw, P. and H-Kittikun, A. (2009). Optimizing an alginate immobilized lipase for monoacylglycerol production by the glycerolysis reaction. *Journal of Molecular Catalysis B: Enzymatic,* 59**:** 206-211.

Choe, S. Y., Neudeck, B. L., Welage, L. S., Amidon, G. E., Barnett, J. L. and Amidon, G. L. (2001). Novel method to assess gastric emptying in humans: the Pellet Gastric Emptying Test. *European Journal of Pharmaceutical Sciences,* 14**:** 347-353.

Chow, C. K. (2000). *Fatty Acids in Foods and their Health Implication,* New York: CRC Press.

Clarke, A. M., Chirnside, A., Hill, G. L., Pope, G. and Stewart, M. K. (1967). Chronic dehydration and sodium depletion in patients with established ileostomies. *Lancet,* 2**:** 740-743.

Cohen, A. E. and Johnston, C. S. (2011). Almond ingestion at mealtime reduces postprandial glycemia and chronic ingestion reduces hemoglobin A1c in individuals with well-controlled type 2 diabetes mellitus. *Metabolism,* 60**:** 1312-1317.

Collier, G., McLean, A. and O'Dea, K. (1984). Effect of co-ingestion of fat on the metabolic responses to slowly and rapidly absorbed carbohydrates. *Diabetologia,* 26**:** 50-54.

Constantin, M. J., Pasero, L. and Desnuelle, P. (1960). Quelques remarques complémentaires sur l'hydrolyse des triglycerides par la lipase pancréatique. *Biochimica et Biophysica Acta,* 43**:** 103-109.

Crawley, J. N. and Corwin, R. L. (1994). Biological actions of cholecystokinin. *Peptides,* 15**:** 731-755.

Crenon, I., Foglizzo, E., Kerfelec, B., Verine, A., Pignol, D., Hermoso, J., Bonicel, J. and Chapus, C. (1998). Pancreatic lipase-related protein type I: a specialized lipase or an inactive enzyme. *Protein Engineering,* 11**:** 135-142.

Cuesta-Alonso, E. P. and Gilliland, S. E. (2003). Binding of bile salts by soluble fibers and its effect on deconjugation of glycocholate by *Lactobacillus acidophilus* and *Lactobacillus casei*. *Journal of Food Science,* 68**:** 2086-2089.

Cummings, D. E. and Overduin, J. (2007). Gastrointestinal regulation of food intake. *Journal of Clinical Investigation,* 117**:** 13-23.

Cummings, J. H., Bingham, S. A., Heaton, K. W. and Eastwood, M. A. (1992). Fecal weight, colon cancer risk, and dietary intake of nonstarch polysaccharides (dietary fiber). *Gastroenterology,* 103**:** 1783-1789.

Cummings, J. H. and Macfarlane, G. T. (1991). The control and consequences of bacterial fermentation in the human colon. *Journal of Applied Bacteriology,* 70**:** 443-459.

Cummings, J. H. (1981). Short chain fatty acids in the human colon. *Gut,* 22**:** 763-779.

Cygler, M. and Schrag, J. D. (1997). Structure as basis for understanding interfacial properties of lipases. *Methods in Enzymology,* 284**:** 3-27.

Dalgleish, D. G. (1997). Adsorption of protein and the stability of emulsions. *Trends in Food Science & Technology,* 8**:** 1-6.

Davenport, H. W. (1982). *Physiology of the Digestive Tract: an Introductory Text,* Chicago: Year Book Medical Publishers.

David, A., Yadav, S. and Bhatla, S. C. (2013). Plant oil bodies and oleosins: structure, functions and biotechnological applications. *In:* Rehm, B. H. A. (ed.) *Bionanotechnology: Biological Self-Assembly and its Applications*, Norfolk: Caister Academic Press.

De Boever, P., Deplancke, B. and Verstraete, W. (2000). Fermentation by gut microbiota cultured in a simulator of the human intestinal microbial ecosystem is improved by supplementing a soygerm powder. *Journal of Nutrition,* 130**:** 2599-2606.

De Caro, J., Carriere, F., Barboni, P., Giller, T., Verger, R. and De Caro, A. (1998). Pancreatic lipase-related protein 1 (PLRP1) is present in the pancreatic juice of several species. *Biochimica et Biophysica Acta,* 1387**:** 331-341.

De Schepper, H. U., Cremonini, F., Chitkara, D. and Camilleri, M. (2004). Assessment of gastric accommodation: overview and evaluation of current methods. *Neurogastroenterology and Motility,* 16**:** 275-285.

Degrace-Passilly, P. and Besnard, P. (2012). CD36 and taste of fat. *Current Opinion in Clinical Nutrition and Metabolic Care,* 15**:** 107-111.

Delorme, V., Dhouib, R., Canaan, S., Fotiadu, F., Carriere, F. and Cavalier, J.-F. (2011). Effects of surfactants on lipase structure, activity, and inhibition. *Pharmaceutical Research,* 28**:** 1831-1842.

DeNigris, S. J., Hamosh, M., Kasbekar, D. K., Lee, T. C. and Hamosh, P. (1988). Lingual and gastric lipases: species differences in the origin of prepancreatic digestive lipases and in the localization of gastric lipase. *Biochimica et Biophysica Acta,* 959**:** 38-45.

Derycke, V., Vandeputte, G. E., Vermeylen, R., De Man, W., Goderis, B., Koch, M. H. J. and Delcour, J. A. (2005). Starch gelatinization and amylose–lipid interactions during rice parboiling investigated by temperature resolved wide angle X-ray scattering and differential scanning calorimetry. *Journal of Cereal Science,* 42**:** 334-343.

Dikeman, C. L. and Fahey, G. C. (2006). Viscosity as related to dietary fiber: a review. *Critical Reviews in Food Science and Nutrition,* 46**:** 649-663.

Docherty, A. J., Bodmer, M. W., Angal, S., Verger, R., Riviere, C., Lowe, P. A., Lyons, A., Emtage, J. S. and Harris, T. J. (1985). Molecular cloning and nucleotide sequence of rat lingual lipase cDNA. *Nucleic Acids Research,* 13**:** 1891-1903.

Dourado, F., Barros, A., Mota, M., Coimbra, M. A. and Gama, F. M. (2004). Anatomy and cell wall polysaccharides of almond (*Prunus dulcis D. A. Webb*) seeds. *Journal of Agricultural and Food Chemistry,* 52**:** 1364-1370.

Drago, S. R., Panouille, M., Saint-Eve, A., Neyraud, E., Feron, G. and Souchon, I. (2011). Relationships between saliva and food bolus properties from model dairy products. *Food Hydrocolloids,* 25**:** 659-677.

Dubois, C., Beaumier, G., Juhel, C., Armand, M., Portugal, H., Pauli, A. M., Borel, P., Latge, C. and Lairon, D. (1998). Effects of graded amounts (0-50 g) of dietary fat on postprandial lipemia and lipoproteins in normolipidemic adults. *American Journal of Clinical Nutrition,* 67**:** 31-38.

Eckburg, P. B., Bik, E. M., Bernstein, C. N., Purdom, E., Dethlefsen, L., Sargent, M., Gill, S. R., Nelson, K. E. and Relman, D. A. (2005). Diversity of the human intestinal microbial flora. *Science,* 308**:** 1635-1638.

Edwards, C. H. (2014). *The Role of Plant Cell Walls in Influencing Starch Bioaccessibility,* Thesis: King's College London.

Egloff, M. P., Marguet, F., Buono, G., Verger, R., Cambillau, C. and van Tilbeurgh, H. (1995). The 2.46 A resolution structure of the pancreatic lipase-colipase complex inhibited by a C11 alkyl phosphonate. *Biochemistry,* 34**:** 2751-2762.

Ehwald, R., Woehlecke, H. and Titel, C. (1992). Cell-wall microcapsules with different porosity from suspension cultured *Chenopodium album*. *Phytochemistry,* 31**:** 3033-3038.

Ellis, P. R., Kendall, C. W., Ren, Y., Parker, C., Pacy, J. F., Waldron, K. W. and Jenkins, D. J. (2004). Role of cell walls in the bioaccessibility of lipids in almond seeds. *American Journal of Clinical Nutrition,* 80**:** 604-613.

Embleton, J. K. and Pouton, C. W. (1997). Structure and function of gastro-intestinal lipases. *Advanced Drug Delivery Reviews,* 25**:** 15-32.

Englyst, H. N., Kingman, S. M. and Cummings, J. H. (1992). Classification and measurement of nutritionally important starch fractions. *European Journal of Clinical Nutrition,* 46 Suppl 2**:** S33-S50.

Englyst, H. N. and Cummings, J. H. (1986). Digestion of the carbohydrates of banana (*Musa paradisiaca sapientum*) in the human small intestine. *American Journal of Clinical Nutrition,* 44**:** 42-50.

Englyst, H. N. and Cummings, J. H. (1985). Digestion of the polysaccharides of some cereal foods in the human small intestine. *American Journal of Clinical Nutrition,* 42**:** 778-787.

Esau, K. (1977). *Anatomy of Seed Plants,* New York: John Wiley & Sons.

Eydoux, C., Spinelli, S., Davis, T. L., Walker, J. R., Seitova, A., Dhe-Paganon, S., De Caro, A., Cambillau, C. and Carriere, F. (2008). Structure of human pancreatic lipase-related protein 2 with the lid in an open conformation. *Biochemistry,* 47**:** 9553-9564.

Eydoux, C., De Caro, J., Ferrato, F., Boullanger, P., Lafont, D., Laugier, R., Carriere, F. and De Caro, A. (2007). Further biochemical characterization of human pancreatic lipase-related protein 2 expressed in yeast cells. *Journal of Lipid Research,* 48**:** 1539-1549.

FAOSTAT (2009). *Statistics Division, Food and Agriculture Organisation of the World* [Online]. Available: http://faostat3.fao.org/faostat-gateway/go/to/download/FB/FB/E [Accessed 03/06/2013].

Fave, G., Peyrot, J., Hamosh, M. and Armand, M. (2007). Digestion des lipides alimentaires : intérêt de la lipase gastrique humaine ? *Cahiers de Nutrition et de Dietetique,* 42**:** 183-190.

Fave, G., Coste, T. C. and Armand, M. (2004). Physicochemical properties of lipids: new strategies to manage fatty acid bioavailability. *Cellular and Molecular Biology* 50**:** 815-831.

Feltrin, K. L., Little, T. J., Meyer, J. H., Horowitz, M., Smout, A. J., Wishart, J., Pilichiewicz, A. N., Rades, T., Chapman, I. M. and Feinle-Bisset, C. (2004). Effects of intraduodenal fatty acids on appetite, antropyloroduodenal motility, and plasma CCK and GLP-1 in humans vary with their chain length. *American Journal of Physiology - Regulatory, Integrative and Comparative Physiology,* 287**:** R524-R533.

Femenia, A., Garcia-Marin, M., Simal, S., Rossello, C. and Blasco, M. (2001). Effects of supercritical carbon dioxide (SC-CO_2) oil extraction on the cell wall composition of almond fruits. *Journal of Agricultural and Food Chemistry,* 49**:** 5828-5834.

Fernandez, S., Jannin, V., Rodier, J. D., Ritter, N., Mahler, B. and Carriere, F. (2007). Comparative study on digestive lipase activities on the self emulsifying excipient Labrasol, medium chain glycerides and PEG esters. *Biochimica et Biophysica Acta,* 1771**:** 633-640.

Fernandez-Garcia, E., Carvajal-Lerida, I. and Perez-Galvez, A. (2009). *In vitro* bioaccessibility assessment as a prediction tool of nutritional efficiency. *Nutrition Research,* 29**:** 751-760.

Finegold, S. M., Sutter, V. L., Boyle, J. D. and Shimada, K. (1970). The normal flora of ileostomy and transverse colostomy effluents. *Journal of Infectious Diseases,* 122**:** 376-381.

Fleischer, A., O'Neill, M. A. and Ehwald, R. (1999). The pore size of non-graminaceous plant cell walls is rapidly decreased by borate ester cross-linking of the pectic polysaccharide rhamnogalacturonan II. *Plant Physiology,* 121**:** 829-838.

Flynn, C. S., Foster, K. D., Bronlund, J. E., Lentle, R. G., Jones, J. R. and Morgenstern, M. P. (2011). Identification of multiple compartments present during the mastication of solid food. *Archives of Oral Biology,* 56**:** 345-352.

Folch, J., Lees, M. and Sloane Stanley, G. H. (1957). A simple method for the isolation and purification of total lipides from animal tissues. *Journal of Biological Chemistry,* 226**:** 497-509.

Food and Agriculture Organization of the United Nations (2009). *FAOSTAT* [Online]. Available: www.faostat.fao.org [Accessed 15/04/2013].

Food Standards Agency (2013). *FSA Nutrient and Food Based Guidelines for UK Institutions* [Online]. Available: http://multimedia.food.gov.uk/multimedia/pdfs/nutguideuk.pdf [Accessed 15/09/2013].

Frayn, K. N. (2010). *Metabolic Regulation: a Human Perspective,* Oxford: Wiley-Blackwell.

Frecka, J. M., Hollis, J. H. and Mattes, R. D. (2008). Effects of appetite, BMI, food form and flavor on mastication: almonds as a test food. *European Journal of Clinical Nutrition,* 62**:** 1231-1238.

French, S. J. (1999). The effects of specific nutrients on the regulation of feeding behaviour in human subjects. *Proceedings of the Nutrition Society,* 58**:** 533-539.

Fromer, M. and Merolla, M. (2012). *Pancreatic Triacylglycerol Lipase* [Online]. Available: http://maptest.rutgers.edu/drupal/?q=node/50 [Accessed 02/11/2012].

Fry, S. C. (1986). Cross-linking of matrix polymers in the growing cell walls of angiosperms. *Annual Review of Plant Biology,* 37**:** 165-186.

Gallier, S. and Singh, H. (2012). Behavior of almond oil bodies during *in vitro* gastric and intestinal digestion. *Food & Function,* 3**:** 547-555.

Gallier, S., Gordon, K. C. and Singh, H. (2012). Chemical and structural characterisation of almond oil bodies and bovine milk fat globules. *Food Chemistry,* 132**:** 1996-2006.

Gargouri, Y., Pieroni, G., Riviere, C., Lowe, P. A., Sauniere, J. F., Sarda, L. and Verger, R. (1986a). Importance of human gastric lipase for intestinal lipolysis: an *in vitro* study. *Biochimica et Biophysica Acta,* 879**:** 419-423.

Gargouri, Y., Pieroni, G., Lowe, P. A., Sarda, L. and Verger, R. (1986b). Human gastric lipase. The effect of amphiphiles. *European Journal of Biochemistry,* 156**:** 305-310.

Gargouri, Y., Julien, R., Bois, A. G., Verger, R. and Sarda, L. (1983). Studies on the detergent inhibition of pancreatic lipase activity. *Journal of Lipid Research,* 24**:** 1336-1342.

Gemen, R., de Vries, J. F. and Slavin, J. L. (2011). Relationship between molecular structure of cereal dietary fiber and health effects: focus on glucose/insulin response and gut health. *Nutrition Reviews,* 69**:** 22-33.

Giller, T., Buchwald, P., Blum-Kaelin, D. and Hunziker, W. (1992). Two novel human pancreatic lipase related proteins, hPLRP1 and hPLRP2. Differences in colipase dependence and in lipase activity. *Journal of Biological Chemistry,* 267**:** 16509-16516.

Golding, M. and Wooster, T. J. (2010). The influence of emulsion structure and stability on lipid digestion. *Current Opinion in Colloid and Interface Science,* 15**:** 90-101.

Goni, I., Garcia-Alonso, A. and Saura-Calixto, F. (1997). A starch hydrolysis procedure to estimate glycemic index. *Nutrition Research,* 17**:** 427-437.

Grassby, T., Picout, D. R., Mandalari, G., Faulks, R. M., Kendall, C. W. C., Rich, G. T., Wickham, M. S. J., Lapsley, K. and Ellis, P. R. (2014). Modelling of nutrient bioaccessibility in almond seeds based on the fracture properties of their cell walls. *Food and Function,* 5**:** 3096-3106.

Grassby, T., Edwards, C. H., Grundy, M. and Ellis, P. R. (2013). Functional components and mechanisms of action of 'dietary fibre' in the upper gastrointestinal tract: implications for health. *Stability of Complex Carbohydrate Structures: Biofuels, Foods, Vaccines and Shipwrecks*, Cambridge: The Royal Society of Chemistry.

Grundy, S. M. and Denke, M. A. (1990). Dietary influences on serum lipids and lipoproteins. *Journal of Lipid Research,* 31**:** 1149-1172.

Guerra, A., Etienne-Mesmin, L., Livrelli, V., Denis, S., Blanquet-Diot, S. and Alric, M. (2012). Relevance and challenges in modeling human gastric and small intestinal digestion. *Trends in Biotechnology,* 30**:** 591-600.

Gunness, P., Flanagan, B. M., Shelat, K., Gilbert, R. G. and Gidley, M. J. (2012). Kinetic analysis of bile salt passage across a dialysis membrane in the presence of cereal soluble dietary fibre polymers. *Food Chemistry,* 134**:** 2007-2013.

Gunness, P. and Gidley, M. J. (2010). Mechanisms underlying the cholesterol-lowering properties of soluble dietary fibre polysaccharides. *Food and Function,* 1**:** 149-155.

Gurr, M. I., Harwood, J. L. and Frayn, K. N. (2002). *Lipid Biochemistry: an Introduction,* Oxford: Wiley-Blackwell.

Guyton, A. C. and Hall, J. E. (2010). *Textbook of Medical Physiology,* Philadelphia: Saunders.

Haag, M. (2003). Essential fatty acids and the brain. *Canadian Journal of Psychiatry,* 48**:** 195-203.

Haiker, H., Lengsfeld, H., Hadváry, P. and Carrière, F. (2004). Rapid exchange of pancreatic lipase between triacylglycerol droplets. *Biochimica et Biophysica Acta - Molecular and Cell Biology of Lipids,* 1682**:** 72-79.

Hamosh, M. (1984). Lingual lipase. *In:* Borgström, B. and Brockman, H. L. (eds.) *Lipases*, Amsterdam: Elsevier Science.

Hamosh, M. and Scow, R. O. (1973). Lingual lipase and its role in digestion of dietary lipid. *Journal of Clinical Investigation,* 52**:** 88-95.

Harnack, K., Andersen, G. and Somoza, V. (2009). Quantitation of alpha-linolenic acid elongation to eicosapentaenoic and docosahexaenoic acid as affected by the ratio of n6/n3 fatty acids. *Nutrition & Metabolism,* 6**:** 8.

Harris, P. J. and Smith, B. G. (2006). Plant cell walls and cell-wall polysaccharides: structures, properties and uses in food products. *International Journal of Food Science and Technology,* 41**:** 129-143.

Hasan, F., Shah, A. A. and Hameed, A. (2009). Methods for detection and characterization of lipases: a comprehensive review. *Biotechnology Advances,* 27**:** 782-798.

Heath, M. R. (2002). The oral management of food: the bases of oral success and for understanding the sensations that drive us to eat. *Food Quality and Preference,* 13**:** 453-461.

Heddle, R., Collins, P. J., Dent, J., Horowitz, M., Read, N. W., Chatterton, B. and Houghton, L. A. (1989). Motor mechanisms associated with slowing of the gastric emptying of a solid meal by an intraduodenal lipid infusion. *Journal of Gastroenterology and Hepatology,* 4**:** 437-447.

Helbig, A., Silletti, E., Timmerman, E., Hamer, R. J. and Gruppen, H. (2012). *In vitro* study of intestinal lipolysis using pH-stat and gas chromatography. *Food Hydrocolloids,* 28**:** 10-19.

Henderson, L., Gregory, J., Irving, K. and Swan, G. (2003). *The National Diet and Nutrition Survey: adults aged 19 to 64 years. Volume 2: Energy, protein, carbohydrate, fat and alcohol intake,* London.

Hernell, O., Staggers, J. E. and Carey, M. C. (1990). Physical-chemical behavior of dietary and biliary lipids during intestinal digestion and absorption. 2. Phase analysis and aggregation states of luminal lipids during duodenal fat digestion in healthy adult human beings. *Biochemistry,* 29**:** 2041-2056.

Hiiemae, K. (2004). Mechanisms of food reduction, transport and deglutition: how the texture of food affects feeding behavior. *Journal of Texture Studies,* 35**:** 171-200.

Hiiemae, K., Heath, M. R., Heath, G., Kazazoglu, E., Murray, J., Sapper, D. and Hamblett, K. (1996). Natural bites, food consistency and feeding behaviour in man. *Archives of Oral Biology,* 41**:** 175-189.

Hildebrand, P., Petrig, C., Burckhardt, B., Ketterer, S., Lengsfeld, H., Fleury, A., Hadváry, P. and Beglinger, C. (1998). Hydrolysis of dietary fat by pancreatic lipase stimulates cholecystokinin release. *Gastroenterology,* 114**:** 123-129.

Hill, G. L. (1976). Normal ileostomy physiology. *In:* Hill, G. L. (ed.) *Ileostomy: Surgery, Physiology and Management*, New York: Grune & Stratton.

Hill, G. L., Goligher, J. C., Smith, A. H. and Mair, W. S. (1975). Long term changes in total body water, total exchangable sodium and total body potassium before and after ileostomy. *British Journal of Surgery,* 62**:** 524-527.

Hjorth, A., Carriere, F., Cudrey, C., Woldike, H., Boel, E., Lawson, D. M., Ferrato, F., Cambillau, C., Dodson, G. G., Thim, L. and Verger, R. (1993). A structural domain (the lid) found in pancreatic lipases is absent in the guinea pig (phospho)lipase. *Biochemistry,* 32**:** 4702-4707.

Hoad, C., Rayment, P., Risse, V., Cox, E., Ciampi, E., Pregent, S., Marciani, L., Butler, M., Spiller, R. and Gowland, P. (2011). Encapsulation of lipid by alginate beads reduces bio-accessibility: an *in vivo* ^{13}C breath test and MRI study. *Food Hydrocolloids,* 25**:** 1190-1200.

Hoebler, C., Devaux, M. F., Karinthi, A., Belleville, C. and Barry, J. L. (2000). Particle size of solid food after human mastication and *in vitro* simulation of oral breakdown. *International Journal of Food Sciences and Nutrition,* 51**:** 353-366.

Holcapek, M., Jandera, P., Zderadicka, P. and Hruba, L. (2003). Characterization of triacylglycerol and diacylglycerol composition of plant oils using high-performance liquid chromatography-atmospheric pressure chemical ionization mass spectrometry. *Journal of Chromatography A,* 1010**:** 195-215.

Holm, J. and Bjorck, I. (1992). Bioavailability of starch in various wheat-based bread products: evaluation of metabolic responses in healthy subjects and rate and extent of *in vitro* starch digestion. *American Journal of Clinical Nutrition,* 55**:** 420-429.

Horowitz, M., Dent, J., Fraser, R., Sun, W. and Hebbard, G. (1994). Role and integration of mechanisms controlling gastric emptying. *Digestive Diseases and Sciences,* 39**:** S7-S13.

Hsieh, K. and Huang, A. H. (2004). Endoplasmic reticulum, oleosins, and oils in seeds and tapetum cells. *Plant Physiology,* 136**:** 3427-3434.

Hu, F. B. and Stampfer, M. J. (1999). Nut consumption and risk of coronary heart disease: a review of epidemiologic evidence. *Current Atherosclerosis Reports,* 1**:** 204-209.

Huang, A. H. C. (1996). Oleosins and oil bodies in seeds and other organs. *Plant Physiology,* 110**:** 1055-1061.

Huang, A. H. C. (1994). Structure of plant seed oil bodies. *Current Opinion in Structural Biology,* 4**:** 493-498.

Huang, A. H. C. (1992). Oil bodies and oleosins in seeds. *Annual Review of Plant Biology,* 43**:** 177-200.

Hui, D. Y. and Howles, P. N. (2002). Carboxyl ester lipase: structure-function relationship and physiological role in lipoprotein metabolism and atherosclerosis. *Journal of Lipid Research,* 43**:** 2017-2030.

Humphrey, S. P. and Williamson, R. T. (2001). A review of saliva: normal composition, flow, and function. *Journal of Prosthetic Dentistry,* 85**:** 162-169.

Hur, S. J., Decker, E. A. and McClements, D. J. (2009). Influence of initial emulsifier type on microstructural changes occurring in emulsified lipids during *in vitro* digestion. *Food Chemistry,* 114**:** 253-262.

Hvizdos, K. M. and Markham, A. (1999). Orlistat - A review of its use in the management of obesity. *Drugs,* 58**:** 743-760.

Iqbal, J. and Hussain, M. M. (2009). Intestinal lipid absorption. *American Journal of Physiology - Endocrinology and Metabolism,* 296**:** E1183-E1194.

Jakab, A., Heberger, K. and Forgacs, E. (2002). Comparative analysis of different plant oils by high-performance liquid chromatography-atmospheric pressure chemical ionization mass spectrometry. *Journal of Chromatography A,* 976**:** 255-263.

Jalabert-Malbos, M. L., Mishellany-Dutour, A., Woda, A. and Peyron, M. A. (2007). Particle size distribution in the food bolus after mastication of natural foods. *Food Quality and Preference,* 18**:** 803-812.

Jandacek, R. J., Whiteside, J. A., Holcombe, B. N., Volpenhein, R. A. and Taulbee, J. D. (1987). The rapid hydrolysis and efficient absorption of triglycerides with octanoic acid in the 1 and 3 positions and long-chain fatty acid in the 2 position. *American Journal of Clinical Nutrition,* 45**:** 940-945.

Jarvis, M. C. (1982). The proportion of calcium-bound pectin in plant cell walls. *Planta,* 154**:** 344-346.

Jenkins, D. J. A., Kendall, C. W. C., Josse, A. R., Salvatore, S., Brighenti, F., Augustin, L. S. A., Ellis, P. R., Vidgen, E. and Rao, A. V. (2006). Almonds decrease postprandial glycemia, insulinemia, and oxidative damage in healthy individuals. *Journal of Nutrition,* 136**:** 2987-2992.

Jenkins, D. J. A., Kendall, C. W. C., Marchie, A., Parker, T. L., Connelly, P. W., Qian, W., Haight, J. S., Faulkner, D., Vidgen, E., Lapsley, K. G. and Spiller, G. A. (2002a). Dose response of almonds on coronary heart disease risk factors: Blood lipids, oxidized low-density lipoproteins, lipoprotein(a), homocysteine, and pulmonary nitric oxide - A randomized, controlled, crossover trial. *Circulation,* 106**:** 1327-1332.

Jenkins, D. J. A., Kendall, C. W. C., Augustin, L. S. A., Franceschi, S., Hamidi, M., Marchie, A., Jenkins, A. L. and Axelsen, M. (2002b). Glycemic index: overview of implications in health and disease. *American Journal of Clinical Nutrition,* 76**:** S266-S273.

Jiffry, M. T. M. (1981). Analysis of particles produced at the end of mastication in subjects with normal dentition. *Journal of Oral Rehabilitation,* 8**:** 113-119.

Johnson, L. R. (1991). *Gastrointestinal Physiology,* St. Louis: Mosby-Year Book.

Joice, C., Lapsley, K. and Blumberg, J. B. (2008). Almonds as a value added ingredient - Benefits of a nutrient rich, high fibre nut. *Agro Food Industry Hi-Tech,* 19**:** 16-18.

Jolivet, P., Roux, E., d'Andrea, S., Davanture, M., Negroni, L., Zivy, M. and Chardot, T. (2004). Protein composition of oil bodies in *Arabidopsis thaliana* ecotype WS. *Plant Physiology and Biochemistry,* 42**:** 501-509.

Jurado, E., Camacho, F., Luzon, G., Fernandez-Serrano, M. and Garcia-Roman, M. (2006). Kinetic model for the enzymatic hydrolysis of tributyrin in O/W emulsions. *Chemical Engineering Science,* 61**:** 5010-5020.

Kanicky, J. R. and Shah, D. O. (2002). Effect of degree, type, and position of unsaturation on the pKa of long-chain fatty acids. *Journal of Colloid and Interface Science,* 256**:** 201-207.

Keller, J. and Layer, P. (2005). Human pancreatic exocrine response to nutrients in health and disease. *Gut,* 54 Suppl 6**:** vi1-vi28.

Kelly, K. A. (1980). Gastric emptying of liquids and solids: roles of proximal and distal stomach. *American Journal of Physiology,* 239**:** G71-G76.

Kendall, C. W. C., Esfahani, A. and Jenkins, D. J. A. (2010). The link between dietary fibre and human health. *Food Hydrocolloids,* 24**:** 42-48.

Kennedy, H. J., Al-Dujaili, E. A., Edwards, C. R. and Truelove, S. C. (1983). Water and electrolyte balance in subjects with a permanent ileostomy. *Gut,* 24**:** 702-705.

Kimura, M., Shizuki, M., Miyoshi, K., Sakai, T., Hidaka, H., Takamura, H. and Matoba, T. (1994). Relationship between the molecular-structures and emulsification properties of edible oils. *Bioscience, Biotechnology, and Biochemistry,* 58**:** 1258-1261.

Klein, P. D. (2001). ^{13}C breath tests: visions and realities. *Journal of Nutrition,* 131**:** S1637-S1642.

Knockaert, G., Lemmens, L., Van Buggenhout, S., Hendrickx, M. and Van Loey, A. (2012). Changes in β-carotene bioaccessibility and concentration during processing of carrot puree. *Food Chemistry,* 133**:** 60-67.

Kock, N. G., Darle, N., Hulten, L., Kewenter, J., Myrvold, H. and Philipson, B. (1977). Ileostomy. *Current Problems in Surgery,* 14**:** 1-52.

Kohyama, K., Sasaki, T. and Hayakawa, F. (2008). Characterization of food physical properties by the mastication parameters measured by electromyography of the jaw-closing muscles and mandibular kinematics in young adults. *Bioscience, Biotechnology, and Biochemistry,* 72**:** 1690-1695.

Kong, F. and Singh, R. P. (2010). A human gastric simulator (HGS) to study food digestion in human stomach. *Journal of Food Science,* 75**:** E627-E635.

Kong, F. and Singh, R. P. (2009a). Digestion of raw and roasted almonds in simulated gastric environment. *Food Biophysics,* 4**:** 365-377.

Kong, F. and Singh, R. P. (2009b). Modes of disintegration of solid foods in simulated gastric environment. *Food Biophysics,* 4**:** 180-190.

Kong, F. and Singh, R. P. (2008). Disintegration of solid foods in human stomach. *Journal of Food Science,* 73**:** R67-R80.

Kovari, K. (2004). Recent developments, new trends in seed crushing and oil refining. *Oilseeds & fats Crops and Lipids,* 11**:** 381–387.

Kris-Etherton, P. M., Krummel, D., Russell, M. E., Dreon, D., Mackey, S., Borchers, J. and Wood, P. D. (1988). The effect of diet on plasma lipids, lipoproteins, and coronary heart disease. *Journal of the American Dietetic Association,* 88**:** 1373-1400.

Kristensen, M., Jensen, M. G., Riboldi, G., Petronio, M., Bugel, S., Toubro, S., Tetens, I. and Astrup, A. (2010). Wholegrain vs. refined wheat bread and pasta. Effect on postprandial glycemia, appetite, and subsequent ad libitum energy intake in young healthy adults. *Appetite,* 54**:** 163-169.

Kritchevsky, D. and Story, J. A. (1974). Binding of bile salts *in vitro* by nonnutritive fiber. *Journal of Nutrition,* 104**:** 458-462.

Krul, C., Luiten-Schuite, A., Baandagger, R., Verhagen, H., Mohn, G., Feron, V. and Havenaar, R. (2000). Application of a dynamic *in vitro* gastrointestinal tract model to study the availability of food mutagens, using heterocyclic aromatic amines as model compounds. *Food and Chemical Toxicology,* 38**:** 783-792.

Kshirsagar, H. H., Fajer, P., Sharma, G. M., Roux, K. H. and Sathe, S. K. (2011). Biochemical and spectroscopic characterization of almond and cashew nut seed 11S legumins, amandin and anacardein. *Journal of Agricultural and Food Chemistry,* 59**:** 386-393.

Kulkarni, B. V. and Mattes, R. D. (2014). Lingual lipase activity in the orosensory detection of fat in humans. *American Journal of Physiology - Regulatory, Integrative and Comparative Physiology,* 306**:** R879-R885.

Kwiatek, M. A., Steingoetter, A., Pal, A., Menne, D., Brasseur, J. G., Hebbard, G. S., Boesiger, P., Thumshirn, M., Fried, M. and Schwizer, W. (2006). Quantification of distal antral contractile motility in healthy human stomach with magnetic resonance imaging. *Journal of Magnetic Resonance Imaging,* 24**:** 1101-1109.

Lairon, D. (2009). Digestion and absorption of lipids. *Designing Functional Foods: Measuring and Controlling Food Structure Breakdown and Nutrient Absorption*, Cambridge, UK: Woodhead Publishing.

Lairon, D., Play, B. and Jourdheuil-Rahmani, D. (2007a). Digestible and indigestible carbohydrates: interactions with postprandial lipid metabolism. *Journal of Nutrition,* 18**:** 217-227.

Lairon, D., Lopez-Miranda, J. and Williams, C. (2007b). Methodology for studying postprandial lipid metabolism. *European Journal of Clinical Nutrition,* 61**:** 1145-1161.

Lassauzay, C., Peyron, M. A., Albuisson, E., Dransfield, E. and Woda, A. (2000). Variability of the masticatory process during chewing of elastic model foods. *European Journal of Oral Sciences,* 108**:** 484-492.

Lauer, O. (1966). *Grain Size Measurements on Commercial Powders - A Guide for Experts,* Ausberg: Alpine.

Lauritzen, L., Hansen, H. S., Jorgensen, M. H. and Michaelsen, K. F. (2001). The essentiality of long chain n-3 fatty acids in relation to development and function of the brain and retina. *Progress in Lipid Research,* 40**:** 1-94.

Lavialle, M. and Laye, S. (2010). Polyunsaturated fatty acids (omega 3, omega 6) and brain functions. *Innovations Agronomiques,* 10**:** 25-42.

Lemmens, L., Van Buggenhout, S., Van Loey, A. M. and Hendrickx, M. E. (2010). Particle size reduction leading to cell wall rupture is more important for the beta-carotene bioaccessibility of raw compared to thermally processed carrots. *Journal of Agricultural and Food Chemistry,* 58**:** 12769-12776.

Lengsfeld, H., Beaumier-Gallon, G., Chahinian, H., De Caro, A., Verger, R., Laugier, R. and Carriere, F. (2004). Physiology of gastrointestinal lipolysis and therapeutical use of lipases and digestive lipase inhibitors. *In:* Müller, G. and Petry, S. (eds.) *Lipases and Phospholipases in Drug Development*, Weinheim: Wiley-VCH.

Lentle, R. G. and Janssen, P. W. M. (2008). Physical characteristics of digesta and their influence on flow and mixing in the mammalian intestine: a review. *Journal of Comparative Physiology B,* 178**:** 673-690.

Levine, A. S. and Silvis, S. E. (1980). Absorption of whole peanuts, peanut oil, and peanut butter. *New England Journal of Medicine,* 303**:** 917-918.

Levine, M. J. (1993). Salivary macromolecules - a structure/function synopsis. *Annals of the New York Academy of Sciences,* 694**:** 11-16.

Li, S.-C., Liu, Y.-H., Liu, J.-F., Chang, W.-H., Chen, C.-M. and Chen, O. C. Y. (2011a). Almond consumption improved glycemic control and lipid profiles in patients with type 2 diabetes mellitus. *Metabolism,* 60**:** 474-479.

Li, Y., Hu, M., Du, Y. M., Xiao, H. and McClements, D. J. (2011b). Control of lipase digestibility of emulsified lipids by encapsulation within calcium alginate beads. *Food Hydrocolloids,* 25**:** 122-130.

Li, Y., Hu, M. and McClements, D. J. (2011c). Factors affecting lipase digestibility of emulsified lipids using an *in vitro* digestion model: proposal for a standardised pH-stat method. *Food Chemistry,* 126**:** 498-505.

Li, Y. and McClements, D. J. (2010). New mathematical model for interpreting pH-stat digestion profiles: impact of lipid droplet characteristics on *in vitro* digestibility. *Journal of Agricultural and Food Chemistry,* 58**:** 8085-8092.

Lia, A., Andersson, H., Mekki, N., Juhel, C., Senft, M. and Lairon, D. (1997). Postprandial lipemia in relation to sterol and fat excretion in ileostomy subjects given oat-bran and wheat test meals. *American Journal of Clinical Nutrition,* 66**:** 357-365.

Lohse, P., Chahrokh-Zadeh, S. and Seidel, D. (1997). The acid lipase gene family: three enzymes, one highly conserved gene structure. *Journal of Lipid Research,* 38**:** 880-891.

Lombardo, D. (2001). Bile salt-dependent lipase: its pathophysiological implications. *Biochimica et Biophysica Acta,* 1533**:** 1-28.

Lovejoy, J. C., Most, M. M., Lefevre, M., Greenway, F. L. and Rood, J. C. (2002). Effect of diets enriched in almonds on insulin action and serum lipids in adults with normal glucose tolerance or type 2 diabetes. *American Journal of Clinical Nutrition,* 76**:** 1000-1006.

Lowe, M. E. (2002). The triglyceride lipases of the pancreas. *Journal of Lipid Research,* 43**:** 2007-2016.

Lowe, M. E. (1999). Assays for pancreatic triglyceride lipase and colipase. *Methods in Molecular Biology,* 109**:** 59-70.

Lowe, M. E., Kaplan, M. H., Jackson-Grusby, L., D'Agostino, D. and Grusby, M. J. (1998). Decreased neonatal dietary fat absorption and T cell cytotoxicity in pancreatic lipase-related protein 2-deficient mice. *Journal of Biological Chemistry,* 273**:** 31215-31221.

Lowe, M. E. (1997). Structure and function of pancreatic lipase and colipase. *Annual Review of Nutrition,* 17**:** 141-158.

Lucas, P. W. and Luke, D. A. (1986). Is food particle size a criterion for the initiation of swallowing? *Journal of Oral Rehabilitation,* 13**:** 127-136.

Lucca, P. A. and Tepper, B. J. (1994). Fat replacers and the functionality of fat in foods. *Trends in Food Science & Technology,* 5**:** 12-19.

M'Koma, A. E., Wise, P. E., Muldoon, R. L., Schwartz, D. A., Washington, M. K. and Herline, A. J. (2007). Evolution of the restorative proctocolectomy and its effects on gastrointestinal hormones. *International Journal of Colorectal Disease,* 22**:** 1143-1163.

Mackie, A., Knulst, A., Le, T.-M., Bures, P., Salt, L., Mills, C. E. N., Malcolm, P., Andreou, A. and Ballmer-Weber, B. K. (2012). High fat food increases gastric residence and thus thresholds for objective symptoms in allergic patients. *Molecular Nutrition & Food Research,* 56**:** 1708-1714.

Madenci, D. and Egelhaaf, S. U. (2010). Self-assembly in aqueous bile salt solutions. *Current Opinion in Colloid & Interface Science,* 15**:** 109-115.

Makkhun, S. (2012). *Gastrointestinal Digestion of Sunflower Seed Oil Bodies,* Thesis: University of Nottingham.

Maldonado-Valderrama, J., Wilde, P., Macierzanka, A. and Mackie, A. (2011). The role of bile salts in digestion. *Advances in Colloid and Interface Science,* 165**:** 36-46.

Maldonado-Valderrama, J., Miller, R., Fainerman, V. B., Wilde, P. J. and Morris, V. J. (2010). Effect of gastric conditions on beta-lactoglobulin interfacial networks: influence of the oil phase on protein structure. *Langmuir,* 26**:** 15901-15908.

Maldonado-Valderrama, J., Woodward, N. C., Gunning, A. P., Ridout, M. J., Husband, F. A., Mackie, A. R., Morris, V. J. and Wilde, P. J. (2008). Interfacial characterization of β-lactoglobulin networks: displacement by bile salts. *Langmuir,* 24**:** 6759-6767.

Maljaars, P. W. J., Peters, H. P. F., Mela, D. J. and Masclee, A. A. M. (2008). Ileal brake: a sensible food target for appetite control. A review. *Physiology & Behavior,* 95**:** 271-281.

Malone, M. E., Appelqvist, I. A. M. and Norton, I. T. (2003). Oral behaviour of food hydrocolloids and emulsions. Part 1. Lubrication and deposition considerations. *Food Hydrocolloids,* 17**:** 763-773.

Malvern (2011a). *Basic Principles of Particle Size Analysis* [Online]. Available: www.malvern.com/en/support/resource-center/application-notes/AN020710BasicPrinciplesPSA.aspx [Accessed 16/03/2011].

Malvern (2011b). *Mastersizer 2000* [Online]. Available: http://www.malvern.com/en/products/product-range/mastersizer-range/mastersizer-2000/ [Accessed 03/02/2011].

Mandalari, G., Grundy, M. M.-L., Grassby, T., Parker, M. L., Cross, K. L., Chessa, S., Bisignano, C., Barreca, D., Bellocco, E., Lagana, G., Butterworth, P. J., Faulks, R. M., Wilde, P. J., Ellis, P. R.

and Waldron, K. W. (2014). The effects of processing and mastication on almond lipid bioaccessibility using novel methods of in vitro digestion modelling and micro-structural analysis. *British Journal of Nutrition,* 112**:** 1521-1529.

Mandalari, G., Bisignano, C., Filocamo, A., Chessa, S., Saro, M., Torre, G., Faulks, R. and Dugo, P. (2013). Bioaccessibility of pistachio polyphenols, carotenoids and tocopherols in the upper gastrointestinal tract. *Nutrition,* 29**:** 338-344.

Mandalari, G., Tomaino, A., Arcoraci, T., Martorana, M., Lo Turco, V., Cacciola, F., Rich, G. T., Bisignano, C., Saija, A., Dugo, P., Cross, K. L., Parker, M. L., Waldron, K. W. and Wickham, M. S. J. (2010a). Characterization of polyphenols, lipids and dietary fibre from almond skins (*Amygdalus communis L.*). *Journal of Food Composition and Analysis,* 23**:** 166-174.

Mandalari, G., Tomaino, A., Rich, G. T., Lo Curto, R., Arcoraci, T., Martorana, M., Bisignano, C., Saija, A., Parker, M. L., Waldron, K. W. and Wickham, M. S. J. (2010b). Polyphenol and nutrient release from skin of almonds during simulated human digestion. *Food Chemistry,* 122**:** 1083-1088.

Mandalari, G., Faulks, R. M., Rich, G. T., Lo Turco, V., Picout, D. R., Lo Curto, R. B., Bisignano, G., Dugo, P., Dugo, G., Waldron, K. W., Ellis, P. R. and Wickham, M. S. J. (2008a). Release of protein, lipid and vitamin E from almonds seeds during digestion. *Journal of Agricultural and Food Chemistry,* 56**:** 3406-3416.

Mandalari, G., Nueno-Palop, C., Bisignano, G., Wickham, M. S. and Narbad, A. (2008b). Potential prebiotic properties of almond (*Amygdalus communis L.*) seeds. *Applied and Environmental Microbiology,* 74**:** 4264-4270.

Mann, J. I. and Cummings, J. H. (2009). Possible implications for health of the different definitions of dietary fibre. *Nutrition Metabolism and Cardiovascular Diseases,* 19**:** 226-229.

Marangoni, A. G. (1994). Enzyme kinetics of lipolysis revisited: the role of lipase interfacial binding. *Biochemical and Biophysical Research Communications,* 200**:** 1321-1328.

Marciani, L., Gowland, P. A., Spiller, R. C., Manoj, P., Moore, R. J., Young, P. and Fillery-Travis, A. J. (2001). Effect of meal viscosity and nutrients on satiety, intragastric dilution, and emptying assessed by MRI. *American Journal of Physiology - Gastrointestinal and Liver Physiology,* 280**:** G1227-G1233.

Marciani, L., Gowland, P. A., Spiller, R. C., Manoj, P., Moore, R. J., Young, P., Al-Sahab, S., Bush, D., Wright, J. and Fillery-Travis, A. J. (2000). Gastric response to increased meal viscosity assessed by echo-planar magnetic resonance imaging in humans. *Journal of Nutrition,* 130**:** 122-127.

Mathews, C. K., van Holde, K. E. and Ahern, K. G. (2000). *Biochemistry,* London: Addison-Wesley.

Mattes, R. D. and Dreher, M. L. (2010). Nuts and healthy body weight maintenance mechanisms. *Asia Pacific Journal of Clinical Nutrition,* 19**:** 137-141.

Mattes, R. D. (2005). Fat taste and lipid metabolism in humans. *Physiology & Behavior,* 86**:** 691-697.

Mattes, R. D. (2002). Oral fat exposure increases the first phase triacylglycerol concentration due to release of stored lipid in humans. *Journal of Nutrition,* 132**:** 3656-3662.

McCann, M. C., Wells, B. and Roberts, K. (1992). Complexity in the spatial localization and length distribution of plant cell-wall matrix polysaccharides. *Journal of Microscopy,* 166**:** 123-136.

McCann, M. C., Wells, B. and Roberts, K. (1990). Direct visualization of cross-links in the primary plant cell wall. *Journal of Cell Science,* 96**:** 323-334.

McClements, D. J. and Li, Y. (2010). Review of *in vitro* digestion models for rapid screening of emulsion-based systems. *Food and Function,* 1**:** 32-59.

McClements, D. J., Decker, E. A. and Park, Y. (2009). Controlling lipid bioavailability through physicochemical and structural approaches. *Critical Reviews in Food Science and Nutrition,* 49**:** 48-67.

McDougall, G. J., Morrison, I. M., Stewart, D. and Hillman, J. R. (1996). Plant cell walls as dietary fibre: range, structure, processing and function. *Journal of the Science of Food and Agriculture,* 70**:** 133-150.

McIntosh, C. H. S., Widenmaier, S. and Kim, S. J. (2009). Glucose-dependent insulinotropic polypeptide (gastric inhibitory polypeptide; GIP). *In:* Gerald, L. (ed.) *Vitamins & Hormones*: Academic Press.

McKiernan, F., Lokko, P., Kuevi, A., Sales, R. L., Costa, N. M., Bressan, J., Alfenas, R. C. and Mattes, R. D. (2010). Effects of peanut processing on body weight and fasting plasma lipids. *British Journal of Nutrition,* 104**:** 418-426.

Mead, J. F., Alfin-Slater, R. B., Howton, D. R. and Popjak, G. (1986). *Lipids: Chemistry, Biochemistry and Nutrition,* New York: Plenum Press.

Melville, D. and Baker, C. (2011). Ileostomies and colostomies. *Surgery,* 29**:** 39-43.

Meyer, B. M., Werth, B. A., Beglinger, C., Hildebrand, P., Jansen, J. B. M. J., Zach, D., Rovati, L. C. and Stadler, G. A. (1989). Role of cholecystokinin in regulation of gastrointestinal motor functions. *Lancet,* 2**:** 12-15.

Meyer, J. H. and Doty, J. E. (1988). GI transit and absorption of solid food - multiple effects of guar. *American Journal of Clinical Nutrition,* 48**:** 267-273.

Meyer, J. H., Gu, Y., Elashoff, J., Reedy, T., Dressman, J. and Amidon, G. (1986). Effects of viscosity and fluid outflow on postcibal gastric-emptying of solids. *American Journal of Physiology,* 250**:** G161-G164.

Michalski, M. C., Genot, C., Gayet, C., Lopez, C., Fine, F., Joffre, F., Vendeuvre, J. L., Bouvier, J., Chardigny, J. M. and Raynal-Ljutovac, K. (2013). Multiscale structures of lipids in foods as parameters affecting fatty acid bioavailability and lipid metabolism. *Progress in Lipid Research,* 52**:** 354-373.

Milbury, P. E., Chen, C. Y., Dolnikowski, G. G. and Blumberg, J. B. (2006). Determination of flavonoids and phenolics and their distribution in almonds. *Journal of Agricultural and Food Chemistry,* 54**:** 5027-5033.

Miled, N., Canaan, S., Dupuis, L., Roussel, A., Riviere, M., Carriere, F., de Caro, A., Cambillau, C. and Verger, R. (2000). Digestive lipases: from three-dimensional structure to physiology. *Biochimie,* 82**:** 973-986.

Mishellany, A., Woda, A., Labas, R. and Peyron, M.-A. (2006). The challenge of mastication: preparing a bolus suitable for deglutition. *Dysphagia,* 21**:** 87-94.

Mondello, L., Zappia, G., Bonaccorsi, I., Dugo, G. and McNair, H. M. (2000). Fast GC for the analysis of natural matrices. Preliminary note: the determination of fatty acid methyl esters in natural fats. *Journal of Microcolumn Separations,* 12**:** 41-47.

Moreau, H., Bernadac, A., Gargouri, Y., Benkouka, F., Laugier, R. and Verger, R. (1989). Immunocytolocalization of human gastric lipase in chief cells of the fundic mucosa. *Histochemistry,* 91**:** 419-423.

Moreau, H., Laugier, R., Gargouri, Y., Ferrato, F. and Verger, R. (1988a). Human preduodenal lipase is entirely of gastric fundic origin. *Gastroenterology,* 95**:** 1221-1226.

Moreau, H., Gargouri, Y., Lecat, D., Junien, J. L. and Verger, R. (1988b). Screening of preduodenal lipases in several mammals. *Biochimica et Biophysica Acta,* 959**:** 247-252.

Mowlana, F., Heath, M., Van Der Bilt, A. and Van Der Glas, H. (1994). Assessment of chewing efficiency: a comparison of particle size distribution determined using optical scanning and sieving of almonds. *Journal of Oral Rehabilitation,* 21**:** 545-551.

Mu, H. and Hoy, C. E. (2004). The digestion of dietary triacylglycerols. *Progress in Lipid Research,* 43**:** 105-133.

Mun, S., Decker, E. A., Park, Y., Weiss, J. and McClements, D. J. (2006). Influence of interfacial composition on *in vitro* digestibility of emulsified lipids: potential mechanism for chitosan's ability to inhibit fat digestion. *Food Biophysics,* 1**:** 21-29.

N'Goma, J.-C. B., Amara, S., Dridi, K., Jannin, V. and Carriere, F. (2012). Understanding the lipid-digestion processes in the GI tract before designing lipid-based drug-delivery systems. *Therapeutic Delivery,* 3**:** 105-124.

Nilsson, J., Blackberg, L., Carlsson, P., Enerback, S., Hernell, O. and Bjursell, G. (1990). cDNA cloning of human-milk bile-salt-stimulated lipase and evidence for its identity to pancreatic carboxylic ester hydrolase. *European Journal of Biochemistry,* 192**:** 543-550.

Noah, L., Guillon, F., Bouchet, B., Buleon, A., Molis, C., Gratas, M. and Champ, M. (1998). Digestion of carbohydrate from white beans (*Phaseolus vulgaris L.*) in healthy humans. *Journal of Nutrition,* 128**:** 977-985.

Novotny, J. A., Gebauer, S. K. and Baer, D. J. (2012). Discrepancy between the Atwater factor predicted and empirically measured energy values of almonds in human diets. *American Journal of Clinical Nutrition,* 96**:** 296-301.

O'Hara, A. M. and Shanahan, F. (2006). The gut flora as a forgotten organ. *EMBO Reports,* 7**:** 688-693.

O'Keefe, J. H., Gheewala, N. M. and O'Keefe, J. O. (2008). Dietary strategies for improving post-prandial glucose, lipids, inflammation, and cardiovascular health. *Journal of the American College of Cardiology,* 51**:** 249-255.

Olthoff, L. W., van der Bilt, A., Bosman, F. and Kleizen, H. H. (1984). Distribution of particle sizes in food comminuted by human mastication. *Archives of Oral Biology,* 29**:** 899-903.

Ooi, T. C., Robinson, L., Graham, T., Kolovou, G. D., Mikhailidis, D. P. and Lairon, D. (2011). Proposing a "lipemic index" as a nutritional and research tool. *Current Vascular Pharmacology,* 9**:** 313-317.

Osborne, T. B. and Campbell, G. F. (1896). Conglutin and vitellin. *Journal of the American Chemical Society,* 18**:** 609-623.

Ow, R. K., Carlsson, G. E. and Karlsson, S. (1998). Relationship of masticatory mandibular movements to masticatory performance of dentate adults: a method study. *Journal of Oral Rehabilitation,* 25**:** 821-829.

Owen, R. W. (1986). Metabolism of bile acids. *In:* Hill, M. J. (ed.) *Microbial Metabolisms in the Digestive Tract*, Boca Raton: CRC Press.

Pal, A., Brasseur, J. G. and Abrahamsson, B. (2007). A stomach road or "Magenstrasse" for gastric emptying. *Journal of Biomechanics,* 40**:** 1202-1210.

Panaiotov, I. and Verger, R. (2000). Enzymatic reactions at interfaces: Interfacial and temporal organization of enzymatic lipolysis. *In:* Baszkin, A. and Norde, W. (eds.) *Physical chemistry of biological interfaces*, New York: CRC Press.

Panaiotov, I., Ivanova, M. and Verger, R. (1997). Interfacial and temporal organization of enzymatic lipolysis. *Current Opinion in Colloid & Interface Science,* 2**:** 517-525.

Parada, J. and Aguilera, J. (2007). Food microstructure affects the bioavailability of several nutrients. *Journal of Food Science,* 72**:** R21-R32.

Parker, C. C., Parker, M. L., Smith, A. C. and Waldron, K. W. (2003). Thermal stability of texture in chinese water chestnut may be dependent on 8,8'-diferulic acid (aryltetralyn form). *Journal of Agricultural and Food Chemistry,* 51**:** 2034-2039.

Parker, M. L. and Waldron, K. W. (1995). Texture of chinese water chestnut: involvement of cell wall phenolics. *Journal of the Science of Food and Agriculture,* 68**:** 337-346.

Parker, R., Rigby, N. M., Ridout, M. J., Gunning, A. P. and Wilde, P. J. (2014). The adsorption-desorption behaviour and structure function relationships of bile salts. *Soft Matter,* 10**:** 6457-6466.

Pascual-Albero, M. J., Perez-Munuera, I. and Lluch, M. A. (1998). Cotyledon structure of raw, soaked and roasted almond (*Prunus amygdalus L.*). *Food Science and Technology International,* 4**:** 189-197.

Patsch, J. R., Miesenböck, G., Hopferwieser, T., Mühlberger, V., Knapp, E., Dunn, J. K., Gotto, A. M. and Patsch, W. (1992). Relation of triglyceride metabolism and coronary artery disease. Studies in the postprandial state. *Arteriosclerosis, Thrombosis, and Vascular Biology,* 12**:** 1336-1345.

Pedersen, H. L., Fangel, J. U., McCleary, B., Ruzanski, C., Rydahl, M. G., Ralet, M. C., Farkas, V., von Schantz, L., Marcus, S. E., Andersen, M. C., Field, R., Ohlin, M., Knox, J. P., Clausen, M. H. and Willats, W. G. (2012). Versatile high resolution oligosaccharide microarrays for plant glycobiology and cell wall research. *Journal of Biological Chemistry,* 287**:** 39429-39438.

Pera, P., Bucca, C., Borro, P., Bernocco, C., De Lillo, A. and Carossa, S. (2002). Influence of mastication on gastric emptying. *Journal of Dental Research,* 81**:** 179-181.

Perren, R. and Escher, F. E. (2013). Impact of roasting on nut quality. *In:* Harris, L. J. (ed.) *Improving the Safety and Quality of Nuts* Cambridge: Woodhead Publishing

Peters, G. H., van Aalten, D. M., Edholm, O., Toxvaerd, S. and Bywater, R. (1996). Dynamics of proteins in different solvent systems: analysis of essential motion in lipases. *Biophysical Journal,* 71**:** 2245-2255.

Peyron, M. A., Mishellany, A. and Woda, A. (2004). Particle size distribution of food boluses after mastication of six natural foods. *Journal of Dental Research,* 83**:** 578-582.

Pignol, D., Ayvazian, L., Kerfelec, B., Timmins, P., Crenon, I., Hermoso, J., Fontecilla-Camps, J. C. and Chapus, C. (2000). Critical role of micelles in pancreatic lipase activation revealed by small angle neutron scattering. *Journal of Biological Chemistry,* 275**:** 4220-4224.

Pinsirodom, P. and Parkin, K. L. (2001). Lipase assays. *Current Protocols in Food Analytical Chemistry*: John Wiley & Sons.

Pitino, L., Randazzo, C. L., Mandalari, G., Lo Curto, A., Faulks, R. M., Le Marc, Y., Bisignano, C., Caggia, C. and Wickham, M. S. J. (2010). Survival of Lactobacillus rhamnosus strains in the upper gastrointestinal tract. *Food Microbiology,* 27**:** 1121-1127.

Polonsky, K. S. and Rubenstein, A. H. (1984). C-peptide as a measure of the secretion and hepatic extraction of insulin. Pitfalls and limitations. *Diabetes,* 33**:** 486-494.

Prinz, J. F. and Lucas, P. W. (1997). An optimization model for mastication and swallowing in mammals. *Proceedings of the Royal Society B: Biological Sciences,* 264**:** 1715-1721.

Prinz, J. F. and Lucas, P. W. (1995). Swallow thresholds in human mastication. *Archives of Oral Biology,* 40**:** 401-403.

Proschel, P. and Hofmann, M. (1988). Frontal chewing patterns of the incisor point and their dependence on resistance of food and type of occlusion. *Journal of Prosthetic Dentistry,* 59**:** 617-624.

Purkrtova, Z., Jolivet, P., Miquel, M. and Chardot, T. (2008). Structure and function of seed lipid body-associated proteins. *Comptes Rendus Biologies,* 331**:** 746-754.

Ranawana, V., Monro, J. A., Mishra, S. and Henry, C. J. (2010). Degree of particle size breakdown during mastication may be a possible cause of interindividual glycemic variability. *Nutrition Research,* 30**:** 246-254.

Reboul, E., Berton, A., Moussa, M., Kreuzer, C., Crenon, I. and Borel, P. (2006). Pancreatic lipase and pancreatic lipase-related protein 2, but not pancreatic lipase-related protein 1, hydrolyze retinyl palmitate in physiological conditions. *Biochimica et Biophysica Acta,* 1761**:** 4-10.

Record, M., Amara, S., Subra, C., Jiang, G., Prestwich, G. D., Ferrato, F. and Carriere, F. (2011). Bis (monoacylglycero) phosphate interfacial properties and lipolysis by pancreatic lipase-related protein 2, an enzyme present in THP-1 human monocytes. *Biochimica et Biophysica Acta,* 1811**:** 419-430.

Redard, C. L., Davis, P. A. and Schneeman, B. O. (1990). Dietary fiber and gender: effect on postprandial lipemia. *American Journal of Clinical Nutrition,* 52**:** 837-845.

Reis, P., Holmberg, K., Watzke, H., Leser, M. E. and Miller, R. (2009). Lipases at interfaces: a review. *Advances in Colloid and Interface Science,* 147-148**:** 237-250.

Roda, A., Hofmann, A. F. and Mysels, K. J. (1983). The influence of bile salt structure on self-association in aqueous solutions. *Journal of Biological Chemistry,* 258**:** 6362-6370.

Rodriguez, J. A., Mendoza, L. D., Pezzotti, F., Vanthuyne, N., Leclaire, J., Verger, R., Buono, G., Carriere, F. and Fotiadu, F. (2008). Novel chromatographic resolution of chiral diacylglycerols and analysis of the stereoselective hydrolysis of triacylglycerols by lipases. *Analytical Biochemistry,* 375**:** 196-208.

Rondeau-Mouro, C., Defer, D., Leboeuf, E. and Lahaye, M. (2008). Assessment of cell wall porosity in *Arabidopsis thaliana* by NMR spectroscopy. *International Journal of Biological Macromolecules,* 42**:** 83-92.

Roussel, A., de Caro, J., Bezzine, S., Gastinel, L., de Caro, A., Carriere, F., Leydier, S., Verger, R. and Cambillau, C. (1998). Reactivation of the totally inactive pancreatic lipase RP1 by structure-predicted point mutations. *Proteins Structure Function and Genetics,* 32**:** 523-531.

Ruiz, J., Antequera, T., Andres, A. I., Petron, M. J. and Muriel, E. (2004). Improvement of a solid phase extraction method for analysis of lipid fractions in muscle foods. *Analytica Chimica Acta,* 520**:** 201-205.

Ruseler-van-embden, J. G. H., Kool, J., Van Lieshout, L. M. C. and Hazenberg, M. P. (1991). Enzymic activity in ileostomy effluent with reference to the characteristic flora. *Microbial Ecology in Health and Disease,* 4**:** 215-222.

Sabate, J. and Ang, Y. (2009). Nuts and health outcomes: new epidemiologic evidence. *American Journal of Clinical Nutrition,* 89**:** 1643S-1648S.

Salles, C., Tarrega, A., Mielle, P., Maratray, J., Gorria, P., Liaboeuf, J. and Liodenot, J. J. (2007). Development of a chewing simulator for food breakdown and the analysis of *in vitro* flavor compound release in a mouth environment. *Journal of Food Engineering,* 82**:** 189-198.

Saltiel, A. R. and Kahn, C. R. (2001). Insulin signalling and the regulation of glucose and lipid metabolism. *Nature,* 414**:** 799-806.

Samra, R. A. (2010). Fats and Satiety. *In:* Montmayeur, J. P. and Le Coutre, J. (eds.) *Fat Detection: Taste, Texture, and Post Ingestive Effects*, Boca Raton: CRC Press.

Sandberg, A. S., Andersson, H., Kivisto, B. and Sandstrom, B. (1986). Extrusion cooking of a high-fibre cereal product. 1. Effects on digestibility and absorption of protein, fat, starch, dietary fibre and phytate in the small intestine. *British Journal of Nutrition,* 55**:** 245-254.

Sandberg, A. S., Andersson, H., Hallgren, B., Hasselblad, K., Isaksson, B. and Hulten, L. (1981). Experimental model for *in vivo* determination of dietary fibre and its effect on the absorption of nutrients in the small intestine. *British Journal of Nutrition,* 45**:** 283-294.

Sanders, T. A. B. (2003). Dietary fat and postprandial lipids. *Current Atherosclerosis Reports,* 5**:** 445-451.

Sandstrom, B., Andersson, H., Kivisto, B. and Sandberg, A. S. (1986). Apparent small intestinal absorption of nitrogen and minerals from soy and meat-protein-based diets. A study on human ileostomy subjects. *Journal of Nutrition,* 116**:** 2209-2218.

Sanguansri, L., Shen, Z., Weerakkody, R., Barnes, M., Lockett, T. and Augustin, M. A. (2013). Omega-3 fatty acids in ileal effluent after consuming different foods containing microencapsulated fish oil powder - an ileostomy study. *Food & Function,* 4**:** 74-82.

Sarda, L. and Desnuelle, P. (1958). Action de la lipase pancreatique sur les esters en emulsion. *Biochimica et Biophysica Acta,* 30**:** 513-521.

Sathe, S. K., Wolf, W. J., Roux, K. H., Teuber, S. S., Venkatachalam, M. and Sze-Tao, K. W. C. (2002). Biochemical characterization of amandin, the major storage protein in almond (*Prunus dulcis L.*). *Journal of Agricultural and Food Chemistry,* 50**:** 4333-4341.

Scheller, H. V. and Ulvskov, P. (2010). Hemicelluloses. *Annual Review of Plant Biology,* 61**:** 263-289.

Schneeman, B. O. and Gallaher, D. (1985). Effects of dietary fiber on digestive enzyme activity and bile acids in the small intestine. *Experimental Biology and Medicine,* 180**:** 409-414.

Schneider, G. and Senger, B. (2001). Coffee beans as a natural test food for the evaluation of the masticatory efficiency. *Journal of Oral Rehabilitation,* 28**:** 342-348.

Schulze, K. (2006). Imaging and modelling of digestion in the stomach and the duodenum. *Neurogastroenterology and Motility,* 18**:** 172-183.

Schwizer, W., Steingoetter, A. and Fox, M. (2006). Magnetic resonance imaging for the assessment of gastrointestinal function. *Scandinavian Journal of Gastroenterology,* 41**:** 1245-1260.

Selvan, A., Seniya, C., Chandrasekaran, S. N., Siddharth, N., Anishetty, S. and Pennathur, G. (2010). Molecular dynamics simulations of human and dog gastric lipases: Insights into domain movements. *FEBS Letters,* 584**:** 4599-4605.

Selvendran, R. R. (1984). The plant cell wall as a source of dietary fiber : chemistry and structure. *American Journal of Clinical Nutrition,* 39**:** 320-337.

Sherman, P. (1968). *Emulsion Science,* London: Academic Press.

Shimoyama, Y., Kusano, M., Kawamura, O., Zai, H., Kuribayashi, S., Higuchi, T., Nagoshi, A., Maeda, M. and Mori, M. (2007). High-viscosity liquid meal accelerates gastric emptying. *Neurogastroenterology and Motility,* 19**:** 879-886.

Showalter, A. M. (2001). Arabinogalactan-proteins: structure, expression and function. *Cellular and Molecular Life Sciences,* 58**:** 1399-1417.

Shulman, G. I. (2000). Cellular mechanisms of insulin resistance. *Journal of Clinical Investigation,* 106**:** 171-176.

Sias, B., Ferrato, F., Pellicer-Rubio, M. T., Forgerit, Y., Guillouet, P., Leboeuf, B. and Carriere, F. (2005). Cloning and seasonal secretion of the pancreatic lipase-related protein 2 present in goat seminal plasma. *Biochimica et Biophysica Acta,* 1686**:** 169-180.

Sias, B., Ferrato, F., Grandval, P., Lafont, D., Boullanger, P., De Caro, A., Leboeuf, B., Verger, R. and Carriere, F. (2004). Human pancreatic lipase-related protein 2 is a galactolipase. *Biochemistry,* 43**:** 10138-10148.

Silletti, E., Vingerhoeds, M. H., Norde, W. and Van Aken, G. A. (2007). The role of electrostatics in saliva-induced emulsion flocculation. *Food Hydrocolloids,* 21**:** 596-606.

Simonovic, B. R. and Momirovic, M. (1997). Determination of critical micelle concentration of bile acid salts by micro-calorimetric titration. *Mikrochim Acta,* 127**:** 101-104.

Simopoulos, A. P. (2002). Omega-3 fatty acids in inflammation and autoimmune diseases. *Journal of the American College of Nutrition,* 21**:** 495-505.

Singh, H., Ye, A. Q. and Horne, D. (2009). Structuring food emulsions in the gastrointestinal tract to modify lipid digestion. *Progress in Lipid Research,* 48**:** 92-100.

Small, D. M. (1991). The effects of glyceride structure on absorption and metabolism. *Annual Review of Nutrition,* 11**:** 413-434.

Smith, M. E. and Morton, D. G. (2001). *The Digestive System: Basic Science and Clinical Conditions,* London: Churchill Livingstone.

Smith, P. K., Krohn, R. I., Hermanson, G. T., Mallia, A. K., Gartner, F. H., Provenzano, M. D., Fujimoto, E. K., Goeke, N. M., Olson, B. J. and Klenk, D. C. (1985). Measurement of protein using bicinchoninic acid. *Analytical Biochemistry,* 150**:** 76-85.

Somerville, C., Bauer, S., Brininstool, G., Facette, M., Hamann, T., Milne, J., Osborne, E., Paredez, A., Persson, S., Raab, T., Vorwerk, S. and Youngs, H. (2004). Toward a systems approach to understanding plant-cell walls. *Science,* 306**:** 2206-2211.

Soper, N. J., Chapman, N. J., Kelly, K. A., Brown, M. L., Phillips, S. F. and Go, V. L. (1990). The 'ileal brake' after ileal pouch-anal anastomosis. *Gastroenterology,* 98**:** 111-116.

Spiller, G. A., Miller, A., Olivera, K., Reynolds, J., Miller, B., Morse, S. J., Dewell, A. and Farquhar, J. W. (2003). Effects of plant-based diets high in raw or roasted almonds, or roasted almond butter on serum lipoproteins in humans. *Journal of the American College of Nutrition,* 22**:** 195-200.

Stewart, J. E., Feinle-Bisset, C., Golding, M., Delahunty, C., Clifton, P. M. and Keast, R. S. (2010). Oral sensitivity to fatty acids, food consumption and BMI in human subjects. *British Journal of Nutrition,* 104**:** 145-152.

Stinco, C. M., Fernández-Vázquez, R., Escudero-Gilete, M. L., Heredia, F. J., Meléndez-Martínez, A. J. and Vicario, I. M. (2012). Effect of orange juice's processing on the color, particle size, and bioaccessibility of carotenoids. *Journal of Agricultural and Food Chemistry,* 60**:** 1447-1455.

Stone, N. J. (1990). Diet, lipids, and coronary heart disease. *Endocrinology and Metabolism Clinics of North America,* 19**:** 321-344.

Sze, A., Erickson, D., Ren, L. Q. and Li, D. Q. (2003). Zeta-potential measurement using the Smoluchowski equation and the slope of the current-time relationship in electroosmotic flow. *Journal of Colloid and Interface Science,* 261**:** 402-410.

Tan, S. Y. and Mattes, R. D. (2013). Appetitive, dietary and health effects of almonds consumed with meals or as snacks: a randomized, controlled trial. *European Journal of Clinical Nutrition,* 67**:** 1205-1214.

Temple, N. J. (1994). Diet, blood lipids and coronary heart disease - current controversies. *South African Medical Journal,* Suppl**:** 30-31.

Thakur, B. R., Singh, R. K. and Handa, A. K. (1997). Chemistry and uses of pectin - a review. *Critical Reviews in Food Science and Nutrition,* 37**:** 47-73.

Thirstrup, K., Verger, R. and Carriere, F. (1994). Evidence for a pancreatic lipase subfamily with new kinetic properties. *Biochemistry,* 33**:** 2748-2756.

Thompson (1986). Metabolism of neutral steroids. *In:* Hill, M. J. (ed.) *Microbial Metabolisms in the Digestive Tract*, Boca Raton: CRC Press.

Tiruppathi, C. and Balasubramanian, K. A. (1982). Purification and properties of an acid lipase from human gastric juice. *Biochimica et Biophysica Acta,* 712**:** 692-697.

Tornqvist, H., Rissanen, A. and Andersson, H. (1986). Balance studies in patients with intestinal resection: how long is enough? *British Journal of Nutrition,* 56**:** 11-16.

Tougas, G., Anvari, M., Dent, J., Somers, S., Richards, D. and Stevenson, G. W. (1992). Relation of pyloric motility to pyloric opening and closure in healthy subjects. *Gut,* 33**:** 466-471.

Traoret, C. J., Lokko, P., Cruz, A. C. R. F., Oliveira, C. G., Costa, N. M. B., Bressan, J., Alfenas, R. C. G. and Mattes, R. D. (2007). Peanut digestion and energy balance. *International Journal of Obesity,* 32**:** 322-328.

Tydeman, E. A., Parker, M. L., Faulks, R. M., Cross, K. L., Fillery-Travis, A., Gidley, M. J., Rich, G. T. and Waldron, K. W. (2010). Effect of carrot (*Daucus carota*) microstructure on carotene bioaccessibility in the upper gastrointestinal tract. 2. *In vivo* digestions. *Journal of Agricultural and Food Chemistry,* 58**:** 9855-9860.

Tzen, J. T. C., Cao, Y. Z., Laurent, P., Ratnayake, C. and Huang, A. H. C. (1993). Lipids, proteins, and structure of seed oil bodies from diverse species. *Plant Physiology,* 101**:** 267-276.

Tzen, J. T. C. and Huang, A. H. (1992). Surface structure and properties of plant seed oil bodies. *Journal of Cell Biology,* 117**:** 327-335.

United States Department of Agriculture, A. R. S. (2010). USDA National Nutrient Database for Standard Reference. Nutrient Data Laboratory Home Page.

Van Citters, G. W. and Lin, H. C. (2006). Ileal brake: neuropeptidergic control of intestinal transit. *Current Gastroenterology Reports,* 8**:** 367-373.

Van Citters, G. W. and Lin, H. C. (1999). The ileal brake: A fifteen-year progress report. *Current Gastroenterology Reports,* 1**:** 404-409.

van der Bilt, A., Engelen, L., Pereira, L. J., van der Glas, H. W. and Abbink, J. H. (2006). Oral physiology and mastication. *Physiology & Behavior,* 89**:** 22-27.

van der Bilt, A., Abbink, J. H., Mowlana, F. and Heath, M. R. (1993). A comparison between data analysis methods concerning particle size distributions obtained by mastication in man. *Archives of Oral Biology,* 38**:** 163-167.

van Tilbeurgh, H., Bezzine, S., Cambillau, C., Verger, R. and Carriere, F. (1999). Colipase: structure and interaction with pancreatic lipase. *Biochimica et Biophysica Acta - Molecular and Cell Biology of Lipids,* 1441**:** 173-184.

van Tilbeurgh, H., Sarda, L., Verger, R. and Cambillau, C. (1992). Structure of the pancreatic lipase-procolipase complex. *Nature,* 359**:** 159-162.

Vardakou, M., Mercuri, A., Barker, S. A., Craig, D. Q., Faulks, R. M. and Wickham, M. S. (2011). Achieving antral grinding forces in biorelevant *in vitro* models: comparing the USP Dissolution Apparatus II and the Dynamic Gastric Model with human *in vivo* data. *AAPS PharmSciTech,* 12**:** 620-626.

Varela, P., Salvador, A. and Fisman, S. (2008a). On the assessment of fracture in brittle foods: the case of roasted almonds. *Food Research International,* 41**:** 544-551.

Varela, P., Aguilera, J. M. and Fiszman, S. (2008b). Quantification of fracture properties and microstructural features of roasted *Marcona* almonds by image analysis. *LWT- Food Science and Technology,* 41**:** 10-17.

Varela, P., Chen, J., Fiszman, S. and Povey, M. J. W. (2006). Crispness assessment of roasted almonds by an integrated approach to texture description: texture, acoustics, sensory and structure. *Journal of Chemometrics,* 20**:** 311-320.

Vaughan, J. G. (1970). *The Structure and Utilization of Oil Seeds,* London: Chapman & Hall

Venema, K., Havenaar, R. and Minekus, M. (2009). Improving *in vitro* simulation of the stomach and intestines. *In:* Mcclements, D. J. and Decker, E. A. (eds.) *Designing Functional Foods: Measuring and Controlling Food Structure Breakdown and Nutrient Absorption*, Cambridge, UK: Woodhead Publishing.

Verger, R. (1997). 'Interfacial activation' of lipases: facts and artifacts. *Trends in Biotechnology,* 15**:** 32-38.

Verger, R., Ferrato, F., Carriere, F., Cudrey, C., Rugani, N., Gargouri, Y., Hjorth, A., Woldike, H., Boel, E., Thim, L., Lawson, D. M., Dodson, G. G., Vantilbeurgh, H., Egloff, M. P. and Cambillau, C. (1995). Relationships between structures and kinetic properties of pancreatic lipases. *Enzyme Engineering,* 750**:** 190-194.

Verger, R. (1984). Pancreatic Lipases. *In:* Borgström, B. and Brockman, H. L. (eds.) *Lipases*, Amsterdam: Elsevier Science.

Verger, R. and de Haas, G. H. (1976). Interfacial enzyme kinetics of lipolysis. *Annual Review of Biophysics and Bioengineering,* 5**:** 77-117.

Verger, R. and de Haas, G. H. (1973). Enzyme reactions in a membrane model. 1. A new technique to study enzyme reactions in monolayers. *Chemistry and Physics of Lipids,* 10**:** 127-136.

Verger, R., Mieras, M. C. E. and de Haas, G. H. (1973). Action of phospholipase A at interfaces. *Journal of Biological Chemistry,* 248**:** 4023-4034.

Ville, E., Carriere, F., Renou, C. and Laugier, R. (2002). Physiological study of pH stability and sensitivity to pepsin of human gastric lipase. *Digestion,* 65**:** 73-81.

Vingerhoeds, M. H., Blijdenstein, T. B. J., Zoet, F. D. and van Aken, G. A. (2005). Emulsion flocculation induced by saliva and mucin. *Food Hydrocolloids,* 19**:** 915-922.

Vors, C., Pineau, G., Gabert, L., Drai, J., Louche-Pelissier, C., Defoort, C., Lairon, D., Desage, M., Danthine, S., Lambert-Porcheron, S., Vidal, H., Laville, M. and Michalski, M. C. (2013). Modulating absorption and postprandial handling of dietary fatty acids by structuring fat in the meal: a randomized crossover clinical trial. *American Journal of Clinical Nutrition,* 97**:** 23-36.

Wainwright, P. E. (2002). Dietary essential fatty acids and brain function: a developmental perspective on mechanisms. *Proceedings of the Nutrition Society,* 61**:** 61-69.

Waldron, K. W., Parker, M. L. and Smith, A. C. (2003). Plant cell walls and food quality. *Comprehensive Reviews in Food Science and Food Safety,* 2**:** 101-119.

Waldron, K. W., Smith, A. C., Parr, A. J., Ng, A. and Parker, M. L. (1997). New approaches to understanding and controlling cell separation in relation to fruit and vegetable texture. *Trends in Food Science & Technology,* 8**:** 213-221.

Wang, Q., Ellis, P. R. and Ross-Murphy, S. B. (2006). Dissolution kinetics of guar gum powders - III. Effect of particle size. *Carbohydrate Polymers,* 64**:** 239-246.

Washington, C. (1992). *Particle Size Analysis in Pharmaceutics and Other Industries,* Chichester: Ellis Horwood.

Weaber, K., Freedman, R. and Eudy, W. W. (1971). Tetracycline inhibition of a lipase from *Corynebacterium acnes*. *Applied Microbiology* 21**:** 639-642.

Werch, S. and Ivy, A. (1941). On the fate of ingested pectin. *American Journal of Digestive Diseases,* 8**:** 101-105.

White, D. A., Fisk, I. D., Makkhun, S. and Gray, D. A. (2009). *In vitro* assessment of the bioaccessibility of tocopherol and fatty acids from sunflower seed oil bodies. *Journal of Agricultural and Food Chemistry,* 57**:** 5720-5726.

Wickham, M., Faulks, R. and Mills, C. (2009). *In vitro* digestion methods for assessing the effect of food structure on allergen breakdown. *Molecular Nutrition & Food Research,* 53**:** 952-958.

Wickham, M. J. S., Faulks, R. M., Mann, J. and Mandalari, G. (2012). The design, operation, and application of a dynamic gastric model. *Dissolution Technologies,* 19**:** 15-22.

Wickham, M. J. S., Garrood, M., Leney, J., Wilson, P. D. G. and Fillery-Travis, A. (1998). Modification of a phospholipid stabilized emulsion interface by bile salt: effect on pancreatic lipase activity. *Journal of Lipid Research,* 39**:** 623-632.

Wiechelman, K. J., Braun, R. D. and Fitzpatrick, J. D. (1988). Investigation of the bicinchoninic acid protein assay: identification of the groups responsible for color formation. *Analytical Biochemistry,* 175**:** 231-237.

Wieloch, T., Borgstrom, B., Pieroni, G., Pattus, F. and Verger, R. (1982). Product activation of pancreatic lipase. Lipolytic enzymes as probes for lipid/water interfaces. *Journal of Biological Chemistry,* 257**:** 11523-11528.

Wilde, P. J. and Chu, B. S. (2011). Interfacial & colloidal aspects of lipid digestion. *Advances in Colloid and Interface Science,* 165**:** 14-22.

Willats, W. G. T., Knox, P. and Mikkelsen, J. D. (2006). Pectin: new insights into an old polymer are starting to gel. *Trends in Food Science & Technology,* 17**:** 97-104.

Willats, W. G. T., Orfila, C., Limberg, G., Buchholt, H. C., van Alebeek, G. J., Voragen, A. G., Marcus, S. E., Christensen, T. M., Mikkelsen, J. D., Murray, B. S. and Knox, J. P. (2001). Modulation of the degree and pattern of methyl-esterification of pectic homogalacturonan in plant cell walls. Implications for pectin methyl esterase action, matrix properties, and cell adhesion. *Journal of Biological Chemistry,* 276**:** 19404-19413.

Winkler, F. K., Darcy, A. and Hunziker, W. (1990). Structure of Human Pancreatic Lipase. *Nature,* 343**:** 771-774.

Winton, A. L. and Winton, K. B. (1932). *The Structure and Composition of Foods. Volume I: Cereals, Starch, Oil Seeds, Nuts, Oils, Forage Plants,* New York: John Wiley & Sons.

Woda, A., Mishellany, A. and Peyron, M. A. (2006a). The regulation of masticatory function and food bolus formation. *Journal of Oral Rehabilitation,* 33**:** 840-849.

Woda, A., Foster, K., Mishellany, A. and Peyron, M. A. (2006b). Adaptation of healthy mastication to factors pertaining to the individual or to the food. *Physiology & Behavior,* 89**:** 28-35.

Wright, H. K., Cleveland, J. C., Tilson, M. D. and Herskovic, T. (1969). Morphology and absorptive capacity of the ileum after ileostomy in man. *American Journal of Surgery,* 117**:** 242-245.

Wu, T., Rayner, C. K., Young, R. L. and Horowitz, M. (2013). Gut motility and enteroendocrine secretion. *Current Opin in Pharmacology,* 13**:** 928-934.

Yada, S., Lapsley, K. and Huang, G. W. (2011). A review of composition studies of cultivated almonds: macronutrients and micronutrients. *Journal of Food Composition and Analysis,* 24**:** 469-480.

Yang, M. H., Chin, Y. W., Yoon, K. D. and Kim, J. (2014). Phenolic compounds with pancreatic lipase inhibitory activity from Korean yam (Dioscorea opposita). *J Enzyme Inhib Med Chem,* 29**:** 1-6.

Yehuda, S., Rabinovitz, S. and Mostofsky, D. I. (1999). Essential fatty acids are mediators of brain biochemistry and cognitive functions. *Journal of Neuroscience Research,* 56**:** 565-570.

Yurkstas, A. A. (1965). The masticatory act. A review. *Journal of Prosthetic Dentistry,* 15**:** 248-262.

Yurkstas, A. A. and Manly, R. S. (1950). Value of different test foods in estimating masticatory ability. *Journal of Applied Physiology,* 3**:** 45-53.

Zhong, R. and Ye, Z.-H. (2009). Secondary Cell Walls. *Encyclopedia of Life Sciences.* Chichester: John Wiley & Sons.

Zhu, X., Ye, A., Verrier, T. and Singh, H. (2013). Free fatty acid profiles of emulsified lipids during *in vitro* digestion with pancreatic lipase. *Food Chemistry,* 139**:** 398-404.

APPENDICES

Appendix A: Gas chromatography parameters used for sugar analysis

Instrument conditions

Instrument:	PerkinElmer Autosystem XL
Column:	ESTEK Rtx-225
Column length:	30 m x 320 µm internal diameter
Carrier gas:	Helium
Flow rate:	2 mL/min
Split ratio:	1:1
Temperature:	Gradient
Injector temperature:	250°C

Notes: Split ratio set to 60:1 at 2 min, and back to 10:1 at 10 min.

Channel parameters

Channel A signal source:	DetA
Analogue output:	INT
Attenuation:	-6
Offset:	5.0 mV
Delay time:	0.00 min
Run time:	78.00 min
Sampling rate:	12.5 pts/s

Autosampler method

Injection volume:	1.0 µL
Sample washes:	2
Injection speed:	NORM
Sample pumps:	6
Viscosity delay:	0
Pre-sequence washes:	0
Waste vial:	1
Solvent A washes:	6

Carrier's parameters

Carrier A control:	PFlow – He
Column A length:	30.00 m
Column A diameter:	320 µm
Vacuum compensation:	OFF
Split control mode:	Ratio
Set point:	0.0:1
Initial set point:	2.0 mL/min
Initial hold:	999 min

Valve configuration and settings

Valve 1:	SPLIT ON
Valves 2-6:	NONE

Detector parameters

Detector A:	FID
Detector B:	NONE
Range:	1
Time constant:	200
Autozero:	ON
Ref gas flow:	250.0 mL/m
MKUp gas flow	25.0 mL/m

Heated zones

Injector A:	PSSI
Injector B:	NONE
Initial set point:	250°C
Injector B setpoint:	OFF
Initial hold:	999.00 min
Detector A:	250°C
Detector B:	0°C
Auxiliary (NONE):	0°C

Oven program

Cryogenics:	OFF
Initial temperature:	140°C
Maximum temperature:	350°C
Initial hold:	5.00 min
Equilibration time:	2.0 min
Ramp 1:	2.5°C/min to 210°C, hold for 45 min
Total run time:	78.00 min

Timed events

SPL1:	set to 60 at 1.00 min
SPL1:	set to 10 at 10.00 min

Real-time plot parameters

Channel A – Pages:	1
Offset:	0.000 mV
Scale:	1000.000 mV

Appendix B: Lipid release according to size as predicted by the mathematical model

The average diameter of the almond cell (d) is ~35 µm. The particle size for which all cells are fractured is ~55 µm (adapted from Grassby *et al.*, 2014).

Equations used for the calculations

Sphere diameter, D (mm)	Volume at diameter (%)	Mass at diameter (%)	Equivalent cubic particle size, p (mm)	d/p	Lipid released, L_R
x	From laser diffraction	$= V \times \frac{m_{almond\ for\ the\ size\ range}}{100}$	$= \sqrt[2]{\frac{4}{3}\pi\left(\frac{D}{2}\right)^3}$	$= \frac{d}{p}$	$= \frac{1}{2}\left(\frac{64}{\pi}\left(\frac{d}{p}\right) - 8\left(\frac{d}{p}\right)^2 + \frac{4}{3}\pi\left(\frac{d}{p}\right)^3\right)$

Where **D** is the specific diameter of a particle (assumed to be spherical), ***r*** is the sphere radius (D/2), ***V*** is the volume measure by the laser diffraction analyser, ***m*** the mass, ***d*** the cell diameter and ***p*** is the average cubic particle size of size fraction. To obtain the lipid release in percentage, L_R has to be multiplied by 100.

Values for lipid release

For reasons of clarity, only the values for the sizes of interest have been presented. By adding the percentage of lipid release based on the volume percentage of particles that have a given size, the predicted lipid release for the whole bolus can be obtained.

Sphere diameter, D (µm)	**d/p**	**Lipid released, L_R (%)**
20	1.802	100
32	1.126	100
63	0.601	93
125	0.288	65
187	0.193	49
250	0.144	39
500	0.072	21
850	0.042	13
1000	0.036	11
1700	0.021	7
2000	0.018	6
3350	0.011	3

Appendix C: Schematic representation of mono- and multicompartmental models adapted from (De Boever *et al.*, 2000; Guerra *et al.*, 2012; Salles *et al.*, 2007)

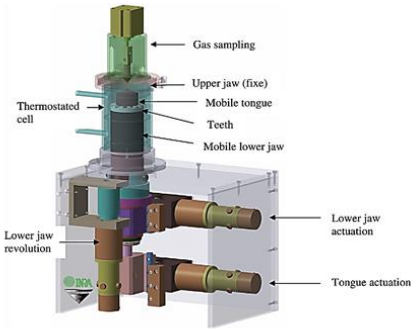

Chewing simulator

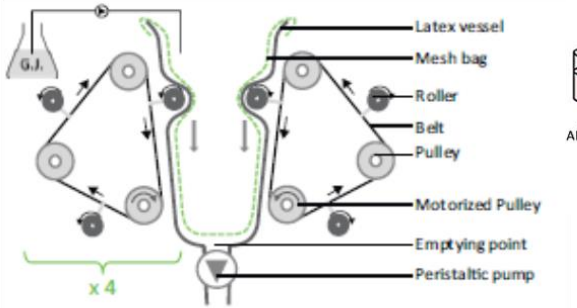

HGS

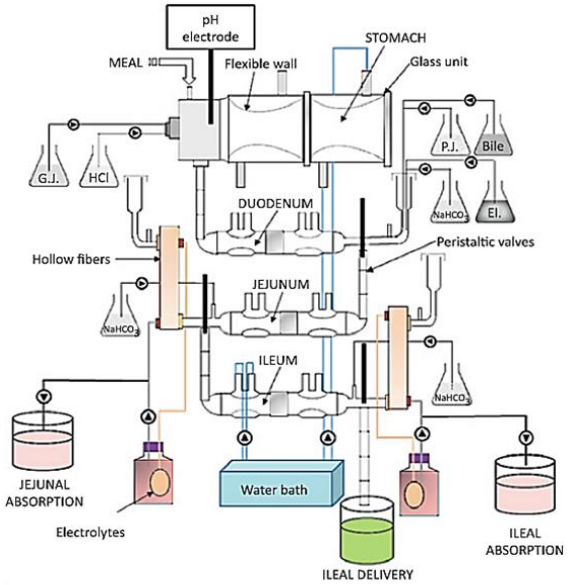

TIM

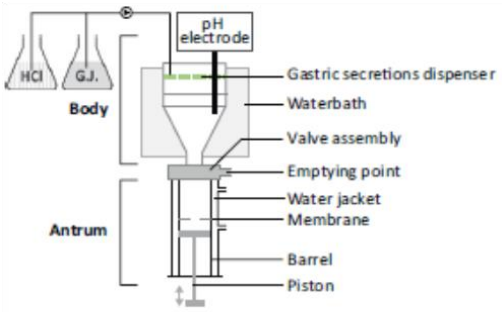

DGM

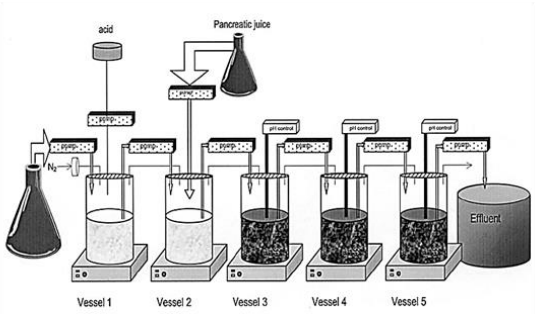

SHIME

Appendix D: Test meals preparation and composition

The ingredients used for the muffins are presented in Table D. The dry ingredients were sifted together twice to ensure that they were thoroughly mixed. The wet ingredients were mixed together in a separate mixing bowl. The dry ingredients were then added to the wet ingredients and stirred gently for about 2 minutes to fully incorporate all the ingredients. The batter was poured into muffin cases and cooked for 20 min Gas 4, 10 min Gas 6 and an additional 3 min Gas 6 recovered with some foil.

Table D Ingredients entering into the composition of almond muffins and their weight.

Ingredients	**Weight (in g)**
Cornflour	10.57
Wheat flour, white, plain	25.00
White sugar	32.59
Baking powder	2.29
Skimmed milk	54.61
Egg white	5.73
Flavouring	4.40
Almond	**85.00**
Custard	80.00
Total without custard	220.19
TOTAL	**300.19**

Appendix E: Participant information sheet

Guy's and St Thomas' NHS
NHS Foundation Trust

KING'S College LONDON

Participant Information Sheet:

BIOGUT

A study of nutrient bioaccessibility

IMPORTANT INFORMATION

We would like to invite you to take part in our research study. Before you decide, we would like you to understand why the research is being done and what it would involve for you. We will be happy to answer any questions you may have before you decide to take part. You may also discuss the study with friends and family. Participation is entirely voluntary and you may withdraw from the study at any time without giving any reason.

What is the study for?

Accumulating evidence shows that the structure and properties of plant foods, particularly of the cell wall component ('dietary fibre'), play an important role in regulating the release (bioaccessibility) of nutrients from plant foods during chewing and digestion. Cell walls may act as a physical barrier to the digestion of carbohydrate and/or fat thus attenuating the blood glucose or lipid response induced. In a meal, fat and/or starch availability can therefore be controlled by modifying the amount of the nutrients encapsulated by cell walls.

Because glucose and lipid responses following the consumption of a meal are associated with reduced risk factors for type 2 diabetes mellitus and cardiovascular disease, this work has implications for the prevention and management of these diseases.

Therefore, we want to understand how much lipid or starch are lost at the terminal ileum after consumption of plant foods, either almonds for lipids or wheat for starch, and relate this to the blood glucose and lipid response generated.

Am I eligible to take part?

We are looking for ileostomy patients, who are not allergic to almonds or any other ingredients incorporated in any of the test meals to participate in this study. To be eligible, you must:

- Be a male or female aged 20-75 years, who previously had proctocolectomy for ulcerative colitis, colon cancer or Crohn's disease (pure colonic form).
- Be stable at least 12 months post-operative
- Have eaten almonds with no adverse effects.

You must not:

- Be allergic to nuts of any kind or gluten
- Have previous case of obstruction of the stoma

These eligibility criteria have been selected to ensure the safety of the study volunteers and researchers involved, and also to produce consistent samples between individuals. We will also record your age, BMI and sex.

What does the study involve?

Once we have checked your eligibility and you have given consent, we will ask you to attend a screening session and five study visits at the Clinical Research Facility of St Thomas' Hospital, Westminster Bridge Road, London SE1 7EH. **Note that the study will take place on Tuesdays and Thursdays ONLY. Furthermore, each visit session will last approximately 13 hours starting at either 8 or 8.30 am and finishing around 9 pm. Therefore, before agreeing to take part, make sure that you can attend these days at these times.**

The study visits are divided into two studies: **Study 1** looking at **fat** release and **Study 2** looking at **starch** release.

During the session (between 13 and 14 hours) you will be given for breakfast **either:**

Study 1: Fat availability (2 visits)

a- a muffin containing almond flour and almond oil with some custard

b- a muffin containing 2 mm almond pieces and some custard

Study 2: Starch availability (2 visits)

a- porridge containing durum wheat flour (77g dry) and 300 mL water

b-. porridge containing 2 mm durum wheat large semolina (77g dry) and 300 mL water.

You will attend Study 2 first and if you wish you could carry on with Study 1. In Study 1, you will have the choice to attend 3 (meals a, b and c) or 2 (meals b and c only) visits depending on how the study goes for you.

Screening visit (lasting about 1h½)**:**

1) You should avoid eating or drinking anything, except water, from 10 pm the previous night.

2) You will arrive at the Clinical Research Facility of St Thomas' Hospital at between 8 and 9.30 am.

3) We will give you a copy of this information sheet, explain to you all the details of the study and answer any questions you have. If you are still happy to take part in the study, you will be asked to sign a consent form.

4) We shall ask you questions about your medical history, your food habits and measure your weight, height, blood pressure and waist and hip circumference.

5) We will need to take a blood sample (approximately 15 mL = 3 x teaspoons).

6) You will try a smaller portion of the almond meals: 4 g of almonds as well as 25 g of muffin containing 2 mm almond particles.

7) You will be asked to chew about 5 g of almonds (four), 5 times, 3 of which will be expectorated.

8) Finally, you will be given a 3 day diet diary to fill up as well as instructions for the day before the study visits.

Study visit:

Day before your visit:

1) You will have eaten for dinner the meal provided.

2) You should avoid eating or drinking anything, except water, from 10 pm the previous night.

Visit day:

3) You will arrive at the Clinical Research Facility of St Thomas' Hospital at 8.00 or 8.30 am.

4) A venous cannula (fixed needle) will be inserted into your arm by an experienced nurse and a fasting blood sample collected.

5) You will eat **the test meal.**

~~6) You will be given a marker, a food colorant dissolved in water (not a licenced medication).~~

7) Effluent will be collected once every 2h up to 12h and at your convenience in the evening and overnight.

8) Blood will be collected (about 200 mL) after the meals at different time intervals up to 8 h for Study 1 and 4 h for Study 2.

9) We will provide you with a meal 4.5 h and 10 h after breakfast.

You will be paid £100 per session completed included screening (£600 in total), which will be paid by cheque or bank transfer after completion of the appropriate form.

What do I have to do?

We would like you to visit the Clinical Research Facility at St Thomas before agreeing to participate so you can see the area where you would stay and meet some of the staff, so we can describe the research in more detail, and so we can answer any questions. On that day we will also process to

the screening as described above. A light breakfast will also be provided before you leave the screening session.

On the day preceding each of the 5 visits, you will be given a ready meal (low in fat or residue) to have for your dinner and asked to drink enough water to avoid dehydration. We will also ask you to fast overnight and avoid eating or drinking anything, except water, after 10 pm. We would then like you to come to the Clinical Research Facility for five study visits on the days and at the time we agree. We would like you to eat the lunch and evening meals that we provide (we would discuss your food preferences before you come, and would try to accommodate them). We would provide drinks when you wish, but these would be free from caffeine. Before you start eating your breakfast and lunch, we will ask you to ingest a marker (a capsule containing small pieces of different shape) to estimate transit time. We would like to collect effluents during your time spent at the Clinical Research Facility as well as overnight at home. We will give you a kit with some explanation on how to store the samples. Overnight effluent may be brought to King's College London (Franklin Wilkins Building, Waterloo Campus, London) the next day or may be collected by a courier (your choice). Each visit will also include blood collection (about 200 mL which corresponds to less than 1/2 pint) as described above. During your visit we would like you to remain within the Clinical Research Facility until around 13 hours after your arrival. For the duration of your visit there will be a room for you to sit and study/work/read in, with a DVD player and a selection of films for your entertainment.

What will happen to my samples?

Your samples will be marked with your participant number, the date, sample type and sample code only, so you will not be identifiable to the researchers studying your samples. The effluent samples produced will be used for nutrient analysis (lipid or starch), microscopy and particle sizing. Glucose and lipid levels will be measure in the collected blood samples.

They will either be analysed immediately or be stored in a freezer in a locked laboratory on a corridor not accessible to the public until October 2014. Also, some of the blood that we will be collecting may be analysed for gut hormones (peptide YY (PYY), cholecystokinin (CCK), glucagon-like peptide-1 (GLP-1) and gastric inhibitory polypeptide (GIP) and may be stored for use in a later study. No genetic tests will be done.

What are the advantages/disadvantages in taking part?

We do not anticipate any direct benefits to volunteers from taking part, but it will help us understand the digestion and absorption of fat and starch from plant foods (almond and wheat).

We believe the risks to participants are minimal as the study involves everyday activities. Our main concern is for individuals who are allergic to nuts, gluten and/or have previously experienced obstruction of the stoma, and we therefore specify that individuals who fall into this category should not take part. There is also a small risk of bruising from blood collection.

What will happen if I wish to withdraw from the study?

You are free to withdraw from the study at any time without giving a reason. However when we ask for your consent at the start of the study, we will also ask you for permission to continue to use any samples you have already provided.

Will my taking part in this study be kept confidential?

We will request your contact details in order to organise sessions. They will be stored on an encrypted pen drive that will be kept in a locked filing cabinet in the private office of the researchers. Only the researchers organising sessions will be authorised to access your details.

Should you wish to find out the results of this study you are welcome to contact either Myriam Grundy or Cathrina Edwards (details below) for a copy of the final report once the study is finished.

Who is organising and funding the study?

The project is organised by researchers from Kings College London and funded by the Biotechnology and Biological Sciences Research Council (BBSRC) under reference BB/H004866/1. The study has also been reviewed and given a favourable opinion by the Research Ethics Committee of South East Coast – Kent (reference no. 12/LO/1016), an independent group who protect the interests of research participants.

What if I have questions/want to make a complaint?

If you have any questions/concerns about any aspect of this study, you should ask to speak to the researchers (020 7848 4345, myriam.grundy@kcl.ac.uk or cathrina.edwards@kcl.ac.uk), who will do their best to answer your questions.

Address: King's College London
Diabetes and Nutritional Sciences Division
4.131 Franklin-Wilkins Building
150 Stamford Street
London
SE1 9NH

If this study has harmed you in any way you can contact KCL using the details below for further advice and information: Dr Peter Ellis, p.ellis@kcl.ac.uk (telephone 020 7848 4238), Nutritional Sciences Division, King's College London, Franklin Wilkins Building, 150 Stamford Street, London SE1 9NH. In the event that something does go wrong and you are harmed during the research, and this is due to someone's negligence then you may have grounds for a legal action for compensation against King's College London, but you may have to pay your legal costs.

Thank you for your interest.

For further information, please contact:

Myriam Grundy or Cathrina Edwards
Diabetes and Nutritional Sciences Division
Tel.: 020 7848 4345
email: biogut@kcl.ac.uk

Appendix F: Volunteers screening and visit procedures

Prior to screening, volunteers were asked to complete pre-screening questionnaires with general questions about their health (e.g., regarding medical conditions, medicines, allergies, smoking and dietary habits). The completed questionnaires were used to assess the volunteers suitability for Study 1 and Study 2. If the volunteers were likely to be eligible for either one of these studies, they were invited to attend a screening visit at the CRF. Invited volunteers were provided with further information about the study, and instructed not to eat any food or drink (except water) for 12 h prior to their screening appointment.

At screening, the study was explained again, and the volunteers had several opportunities to ask questions about the study before written consent was taken.

Following screening, volunteers were asked to attend the CRF on 2 to 4 separate occasions with a gap of at least one week between visits. At each visit, lasting about 13 h, volunteers received one of the 4 test meals for breakfast. On the day preceding the study day, volunteers were given a low-residue and low-fat ready-meal to have for their dinner, asked to fast overnight and instructed to avoid eating or drinking anything, except water, after 8 pm.

When volunteers arrived at the CRF on the visit day a venous cannula was inserted and fasting blood (15 mL) collected. They then consumed the test meal in a manner convenient to them (e.g. taking a bite of muffin with some custard). They were also provided with meals designed not to interfere with the test meals but still providing enough nutrients, at 4.5 h (lunch) and 10 h (dinner) post-breakfast test meal (*Appendix G)*. Venous samples were collected at regular intervals (see *Appendix H* for more details).

Simultaneously, ileal effluent were collected after consumption of the meal every 2 h up to 10 h. After having had their diner the volunteers returned home with a sample collection pack and resume their normal life. Effluent collections continued up to 24 h at their convenience. The pack consisted in a cold bag containing a polystyrene box with cool blocks (Eutectic plates, Phase change material products Ltd., Yaxley, UK) that have been stored at -80°C, a grip bag, Stomacher®bags and gloves (thermal and nitrile) for the volunteers to protect their hands when handling the cool blocks. These overnight collections were brought to the CRF the next day or send to KCL by courier.

Appendix G: Typical intakes of a visit day

Table G Typical nutritional composition of meals served for a visit day.

	Dinner evening before visit		**Breakfast**		**Lunch**		**Dinner**			**Total visit day**
	Ready meal	Yogurt	Muffin	Custard	Müllerlight® yogurt	Banana	Ready meal	Dessert	Soft drink	
Energy (kJ)	1422	366	3161	224	380	646.0	1333	827	399	6970
(kcal)	338	86	742	53	89	152.3	316	196	94	1642
Protein (g)	16.1	6.1	25	0.5	6.8	1.9	25.5	2.0	0.2	61.9
Carbohydrate (g)	45.8	14.8	79	9.5	14.2	37.2	40.0	38.7	22.6	241.5
Total Sugars (g)	8.8	13.9	40	6.4	12.3	33.5	8.0	28.6	22.6	151.4
Starch (g)			28			3.7	32.0			63.7
Fat (g)	**9.0**	**0.1**	**48**	**1.4**	**0.2**	**0.5**	**3.6**	**2.9**		**56.6**
Saturates (g)	5.0	0.1	3	1.4	0.2	0.2	0.4	1.4		6.6
MUFA (g)			25			0.0	2.1			27.1
PUFA (g)			10			0.1	1.1			11.1
Fibre (g)	**4.5**	**0.7**	**10**	**0.1**	**0.9**	**1.8**	**10.8**	**3.5**		**27.1**
Salt (g)							1.22	Trace		1.22
Sodium (g)	0.93	0.09	0.30	0.04	0.20	0.00	0.49	0.10		1.14

The test meal is circled in red.

Appendix H: Protocols for blood analysis

A venous cannula (BD Nexiva 20 GA) was inserted into a vein on the forearm by the nurse appointed to this study. Two fasted blood samples were collected from the cannula with a syringe 15 min apart. Immediately after the fasted blood sample was taken, participants were served the test meal (time = 0) and accompanying drink of water. Bloods were then collected at 15, 30, 45, 60, 90, 120, 150,180, 240 min and thereafter either at 3 and 4 h for glucose, insulin, C-peptide and gut hormones, or hourly up to 8 h for TAG and NEFA. Four mL BD vacutainer® collection tubes were filled at each time point (Table 8a) These were centrifuged, and duplicate aliquots of serum were taken and stored in freezers at -40 °C or -70 °C.

Table H Overview of the blood collection

TUBE	ADDITIVE	ICE	SPIN	ANALYTE	ANALYSIS[1]
GREY	Sodium fluoride (antiglycolytic agent) and Potassium Oxalate (anti-coagulant)	YES	10 min 1300xG 4 °C	GLUCOSE	IL Test™ Glucose (Oxidase)
GOLD	Clotting accelerator and separation gel	NO	10 min 1300xG 4 °C	TAG	IL Test™ Triglycerides
				NEFA	Randox NEFA
GOLD	Clotting accelerator and separation gel	NO	10 min 1300xG 4 °C	INSULIN	Immulite® Insulin Test (Siemens)
				C-PEPTIDE	Immulite® C-peptide Test (Siemens)
LAVENDER	Spray-coated K_2 EDTA (anti-coagulant) added DPPIV- inhibitor* (Merck Millipore)	YES	10 min 1300xG 4 °C	GLP-1	GLP-1 ELISA kit Merck Millipore
				GIP	GIP ELISA kit Merck Millipore
LAVENDER	Spray-coated K_2 EDTA (anti-coagulant) added Aprotinin (10,000 KIU/mL, Nordic Pharma)*	YES	10 min 1300xG 4 °C	PYY	PYY (total) RIA kit Millipore
				CCK	CCK ELISA kit USCN Life Science Inc.

*additives, were added to the vacutainer tubes one day before use.
Abbreviations: TAG, triacylglycerol; NEFA, non-esterified fatty acids; GLP-1, glucagon-like peptide 1 ; GIP, glucose dependent insulinotropic peptide; PYY, Peptide YY; CCK, cholecystokinin.

Glucose, TAG and NEFA were determined at King's College London, UK. Insulin and C-peptide were analysed by GSTS pathology, St Thomas Hospital, London, UK, and gut hormones (PYY, CCK, GLP-1 and GIP) were analysed by GSTS pathology at Denmark Hill, King's College Hospital, UK.

Plasma glucose, TAG and NEFA analysis was performed on an iLab 650 auto-analyzer (Instrumentation Laboratories). Calibrations were carried out before each set of analysis, and quality control standards (i.e. upper and lower end of working range) were run between each sample tray. ReferrIL G (Instrumentation Laboratories) was used as the calibrant for IL Test™ kits, whereas the internal Randox calibrant (Randox Laboratories) was used for NEFA calibrations.

Glucose was determined using a glucose oxidase assay kit (IL Test™), which is based on a two-step reaction in which glucose is first converted to gluconic acid and hydrogen peroxide by glucose oxidase. The hydrogen peroxide then reacts, in the presence of peroxidase, 4-aminophenazone and phenol to produce a red quinoneimine dye. The increase in absorbance as generated by the red dye is proportional to the glucose concentration in the sample. Primary absorbance measurements are taken at 510 nm, and a blank reading is taken at 600 nm on the iLab 650. This assay has a linear working range for serum glucose levels between 0.1 and 28.2 mmol/L.

TAG were determined with an IL Test™ Triglycerides assay kit, which is based on an end-point colorimetric assay. In this assay, TAG are first broken down into glycerol and fatty acids by lipoprotein lipase. The glycerol is then phosphorylated by glycerol kinase, forming glycerol-3-phosphate (G3P), which, in turn is oxidized in a reaction catalysed by glycerolphosphate oxidase to form dihydroxyacetone phosphate and peroxide. The peroxide then reacts, in the presence of aminoantipyrine and 4-chlorophenol to form a red quinoneimine dye. Thus, the increase in absorbance generated by the red dye is proportional to the TAG concentration of the sample. Absorbance measurements are taken at 510 nm. The assay has a linear working range for serum or plasma TAG between 0.02 and 11.4 mmol/L.

NEFA were determined with a Randox NEFA Kit (Randox Laboratories, County Antrim, UK), which is based on a colorimetric end-point reaction in which NEFA is first converted to Acyl Co A by Acyl Co A Synthetase, which is then converted to 2,3,-trans-Enoyl-CoA and peroxide by Acyl CoA Oxidase. Peroxide, in the presence of 4-aminoantipyrine and toluidine, reacts with peroxidase to form a purple adduct. The increase in absorbance as generated by the purple complex is proportional to the NEFA concentration of the sample. Absorbance measurements are taken at 546 nm. This assay has a linear working range for serum or plasma NEFA levels up 0.072 to 2.24 mmol/L.

Insulin and C-peptide concentrations were determined by Immulite® (electro-) chemiluminescence assays with an Immulite 2000 analyser, according to manufacturer specifications (Siemens Medical Solutions, Diagnostics Europe Ltd.). In brief, these assays are both based on a two-site sandwich assay in which C-peptide or Insulin is sandwiched between two antibodies. One antibody is covalently linked to paramagnetic particles, whereas the second antibody is labelled with either acridinium ester (for insulin detection) or with ruthenium (C-peptide). Insulin is detected by the light emitted upon reaction of the complex with horseradish peroxidase (HRP), whereas C-peptide is detected under voltage, which causes emission from ruthenium. Thus, the light intensity measured in a luminometer was proportional to the insulin or C-peptide concentration.

GLP-1 and GIP concentrations were determined by sandwich-ELISA using human GIP and GLP-1 (active) ELISA kits from Merck Millipore Corp. In brief, GLP-1 or GIP are immobilised on a microwell plate, washed to remove unbound materials, and then bound to a biotinylated anti-GLP-1 or anti-GIP monoclonal antibody. Unbound conjugate is then washed off, and HRP-labelled Streptavidin, which binds to the biotinylated antibodies, is added. Free enzyme conjugates are washed off, and the chromogenic substrate 3,3',5,5'-tetramethylbenzidine (TMB) is added. HRP catalyses the oxidation of this substrate in the presence of hydrogen peroxides. The resulting diimine can be quantified spectrophotometrically. The increase in absorbance at 450 nm is directly proportionate to the amount of GLP-1 or GIP in the sample.

CCK was determined using an ELISA kit obtained from USCN Life Science Inc. This kit is based on a competitive inhibition enzyme immunoassay technique. In brief, the microplate is coated with a monoclonal antibody specific to CCK. Biotin-labelled CCK and the sample (contains CCK) are then added to the plate and will competitively bind to the coating. Next, the plate is washed to remove any unbound conjugate. Avidin (a biotin binding protein) conjugated to HRP is then added to each well. This binds to the biotin labelled CCK, and is visualised, after a period of incubation, by the addition of a chromogenic substrate (TMB, as above). Thus, the amount of colour intensity developed on addition of the visualisation substrate (as described above) is reversely proportional to the concentration of CCK in the sample.

PYY was determined using a Human PYY (total) radioimmunoassay kit (Merck Millipore Corp.), which measures both the 1-36 and 3-36 forms of this peptide. This assay kit uses 125I-labeled PYY and a PYY antiserum to determine the concentration of total PYY in serum samples. The 125I-labeled PYY and the sample containing PYY are incubated with PYY antiserum and competitively bind to binding sites on the PYY antibody. Any unbound material is then removed and the amount of radiolabelled antigen is quantified (bound or unbound) using an instrument to count radioactivity.

Appendix I: Blood results, raw data

	AF					AP				
Time (min)	*Glucose (mmol/L)*	*TAG (mmol/L)*	*NEFA (mmol/L)*	*Insulin (pmol/L)*	*C-peptide (pmol/L)*	*Glucose (mmol/L)*	*TAG (mmol/L)*	*NEFA (mmol/L)*	*Insulin (pmol/L)*	*C-peptide (pmol/L)*
0	4.9	1.02	0.84	20	496	5	0.90	0.55	31	523
15	5.2	1.00	0.66	107	825	7.3	0.88	0.25	352	1718
30	5.6	0.89	0.44	94	1137	7.8	0.84	0.23	491	2648
45	5.3	0.94	0.31	170	1468	7.2	0.83	0.06	305	2273
60	5.6	1.02	0.22	136	1486	6.3	0.85	0.03	228	2175
90	6.3	1.11	0.20	196	1765	5.2	0.85	0.02	114	1658
120	6.2	1.33	0.21	180	2015	4.7	0.96	0.03	80	1428
150	6.6	1.65	0.26	178	2035	5.8	1.16	0.08	106	1264
180	6.9	1.55	0.22	239	2076	6	1.20	0.08	75	1063
240	6.7	1.4	0.17	116	1693	5.4	1.32	0.25	43	829
300		1.38	0.1				1.24	0.25		
360		1.22	0.08				1.12	0.1		
420		1.33	0.41				1.04	0.47		
480		1.77	0.65				1.13	0.57		